THESIS

PLATINUM-GOLD-COPPER MINERALIZATION, CENTRAL MEDICINE BOW MOUNTAINS, WYOMING

Submitted by

Robert Ray Loucks

In partial fulfillment of the requirements

for the Degree of Master of Science

Colorado State University

Fort Collins, Colorado

Fall, 1976

COLORADO STATE UNIVERSITY

April 5, 1977

WE HEREBY RECOMMEND THAT THE THESIS PREPARED UNDER OUR SUPERVISION BY ROBERT RAY LOUCKS ENTITLED "PLATINUM-GOLD-COPPER MINERALIZATION, CENTRAL MEDICINE BOW MOUNTAINS, WYOMING" BE ACCEPTED AS FULFILLING IN PART REQUIREMENTS FOR THE DEGREE OF MASTER OF SCIENCE.

Committee on Graduate Work

Tommy B. Thompson

Larry K. Burns

C. H. Warren

M. E. McCallum
Adviser

ABSTRACT OF THESIS

PLATINUM-GOLD-COPPER MINERALIZATION,

CENTRAL MEDICINE BOW MOUNTAINS, WYOMING

A diversified assemblage of platinum-palladium, gold, and base-metal deposits occurs within the Precambrian igneous-metamorphic terrane of the central Medicine Bow Mountains, Wyoming. The mineralized localities investigated lie in a 125-square-mile area adjacent to and structurally disrupted by the Mullen Creek-Nash Fork shear zone, a major Precambrian tectonic discontinuity that splits the Medicine Bow Mountains into two distinct geologic provinces. Investigations of the lithologic and structural associations of sixteen mined deposits and five mineralized prospects and studies of the mineralogical and chemical characteristics of the ores demonstrate that three principal types of deposits are present: 1) an association of platinum-group elements with hydrothermal copper ores in sheared metagabbroic rocks; 2) numerous gold- and copper-bearing quartz-carbonate veins and less commonly lead- and silver-bearing quartz-carbonate veins associated principally with hydrothermally altered mafic rocks; and 3) a highly metamorphosed body of massive and disseminated zinc, copper and lead sulfides in amphibolites and calc-silicate rocks.

Structural, mineralogical, and chemical data of country rocks and hydrothermally altered wallrocks indicate that Pt-Pd-Cu and Au-Cu deposits have formed from fluids of metamorphic origin. Solutions permeating weakly to strongly cataclastic rocks throughout a six to eight mile wide belt south of the Mullen Creek-Nash Fork shear zone have induced pervasive retrograde metamorphic effects. Metamorphic solutions laden with metals, silica, and other dissolved species leached from local country rocks are believed to have diffused into relatively low pressure dilatant zones in shears and fault intersections and there deposited metalliferous veins and sulfide replacement bodies.

Mineralogical and textural characteristics of the Zn-Cu-Pb sulfide body and its lithologic associations point to an origin as a metamorphosed syngenetic exhalative sedimentary massive sulfide deposit.

Robert Ray Loucks
Department of Earth Resources
Colorado State University
Fort Collins, Colorado 80523
Fall, 1976

ACKNOWLEDGMENTS

The study reported here is an aspect of a more extensive investigation by the U. S. Geological Survey of potential mineral resources of the Medicine Bow Mountains. The writer has worked in close cooperation with M. E. McCallum, a principal investigator in the U. S. G. S. Medicine Bow Project. Assistance by the U. S. G. S. in the form of thin and polished section preparation, chemical analyses of ore and wall-rock specimens, partial financial support of field studies, and use of facilities in the electron microprobe laboratory has allowed the scope of this investigation to be broadened substantially beyond that which otherwise would have been attainable. Utilization of excellent photographic facilities of the U. S. Geological Survey assisted in obtaining good quality figures that were essential to depict many of the ore mineral relationships.

Louis Cabri of the Canada Centre for Minerals and Energy Technology generously contributed synthetic platinum and palladium compounds as standards for electron microprobe analysis of platinoid minerals. Standards for the remainder of the microprobe analyses and patient assistance in performing the analyses were provided by G. A. Desborough, U. S. Geological Survey, Denver, Colorado, in whose laboratory the work

was done. R. R. Carlson, E. F. Cooley, and T. A. Doerge of the U. S. Geological Survey, Denver, are thanked for the care with which they performed the many high quality analyses for platinum-group elements and gold.

Portions of the thesis have benefitted from critical readings by G. A. Desborough and B. F. Leonard, U. S. Geological Survey. Professors L. K. Burns, T. B. Thompson, and C. G. Warren served on the writer's graduate committee, and their critical comments have assisted in clarifying the presentation. Most of all, the writer wishes to thank Professor M. E. McCallum for insightful discussions of numerous aspects of this study and especially for his unfailingly inspirational, repeated demonstrations of the rewards of perseverance and hard work.

To Gerald G. Loucks, whose example

and generosity of spirit opened the doors.

TABLE OF CONTENTS

TABLE OF CONTENTS--Continued

TABLE OF CONTENTS--Continued

Page

TABLE OF CONTENTS--Continued

LIST OF FIGURES

LIST OF FIGURES--Continued

LIST OF TABLES

LIST OF TABLES--Continued

INTRODUCTION

A zone of mafic plutonic complexes and orthoamphibolites trends northeastward across the Sierra Madre, Medicine Bow, and Laramie Ranges, broadly coincident with the trend and position of a major Precambrian structural discontinuity transecting the region, the Mullen Creek-Nash Fork shear zone. Within this zone of mafic rocks, gold-bearing quartz veins, high grade pockets of copper sulfides--locally platiniferous--and more rarely nickel and cobalt sulfides have been mined, but these regions have not yet had major production from Precambrian ores.

Most base- and precious-metal mineralization in the central Medicine Bow Mountains consists of Au-Cu-bearing quartz-carbonate veins along southeast-trending faults and cross fractures subsidiary to the Mullen Creek-Nash Fork shear zone. Copper and platinum-palladium mineralization occurs sparsely within the major northeast-trending shear zones as small lenses and pods apparently localized in dilatant zones (McCallum et al., 1976). A gneiss-hosted sulfide deposit not affiliated with the mafic plutonic series or shear zone system is apparently an isolated occurrence of polymetallic massive and disseminated sulfide ores of another genetic class.

PURPOSE AND METHODS OF INVESTIGATION

The purpose of this study has been threefold: to establish major characteristics of the lithologic and structural associations of mineralized localities in the central Medicine Bow Mountains; to ascertain the ore and gangue mineral parageneses and the nature of hydrothermal wallrock alteration; and to characterize physical and chemical aspects of processes by which the mineral deposits formed.

Geologic reconnaissance of lithologic and structural relations in the vicinity of 21 mineralized areas and general surface mapping at five mine sites were done during the summers of 1973 and 1974. Efforts at detailed geologic mapping were hindered by poor bedrock exposure. Several mines are situated in creek bottoms and marshy areas, and the environs of most other deposits are obscured by a veneer of Tertiary gravels, colluvium, or deep soil and heavy vegetation. However, reconnaissance studies have provided sufficient information for characterization of the lithologic and structural settings of the deposits.

The investigation has involved primarily a microscopic, electron microprobe, and X-ray powder diffraction evaluation of several hundred samples of ore and hydrothermally altered and unaltered wallrocks. About 900 samples of ore and associated rocks were collected from sixteen mines and

associated prospects and five isolated mineralized localities during field studies. Two hundred-eighty samples were selected for detailed microscopic study of ore minerals in polished section, and 156 thin sections of country rocks and hydrothermally altered wallrocks were evaluated. One hundred thirty quantitative chemical analyses of minerals have been made using the electron microprobe, and many tentative visual identifications of ore and gangue minerals were confirmed by qualitative analysis using the multi-channel analyzer accessory to the electron microprobe and scanning electron microscope.

Microprobe analyses were made by the writer using an A. R. L. instrument in the laboratory of G. A. Desborough, U. S. Geological Survey. Operating conditions, data correction procedures, and standards employed in the analyses are described in the appendix. Identifications of some minerals by X-ray powder diffraction were made using a Nonius camera and vanadium-filtered Cr K-alpha radiation.

Results of the mineralogical investigation include discovery of at least six previously undescribed ore minerals and identification of several rarely encountered mineral species. At the time of writing, investigations of the new minerals are incomplete, but additional studies are planned

(chiefly structural studies by X-ray diffraction methods and quantitative measurements of optical properties).

PREVIOUS WORK

The geology and mineral deposits of the Medicine Bow Mountains have, since the latter half of the last century, been the subjects of numerous investigations sponsored by the U. S. Geological Survey, U. S. Bureau of Mines, the Geological Survey of Wyoming, and the Geology Department of the University of Wyoming. Houston et al. (1968) present a comprehensive review of published information treating various aspects of the geology and mineral deposits of the district.

During the principal period of active mining and prospecting in the Medicine Bow Mountains between 1870 and 1910, brief geologic investigations of mines and prospects and their immediately adjacent areas were conducted by the Wyoming Territorial and State Geologists. A modest literature treating the history and progress of certain mining operations which generally presents an optimistic view of their potential was compiled by the Territorial Geologist Ricketts (1888, 1890), and by Wyoming State Geologists Beeler (1904-1908) and Jamison (1911). Mineral production in Albany and Carbon Counties and progress of mine development at certain

properties were reviewed annually by the U. S. Bureau of Mines in volumes of Mineral Resources of the U. S.

During and following World War II, the potential of certain mineral properties was re-examined by the Geological Survey of Wyoming (Knight, 1942) and the U. S. Bureau of Mines (U. S. Bureau of Mines, 1942; Kasteler and Frey, 1949). Since the late 1950's, various aspects of the geology and mineral deposits of the Medicine Bow Mountains have been the topics of thesis investigations by students at the University of Wyoming and Colorado State University. Those by McCallum (1964), Curry (1959), and Ramirez (1971) deal with areas within the district studied here. The results of some such studies have been published as Preliminary Reports by the Geological Survey of Wyoming; those by Curry (1965) and by McCallum and Orback (1968), which deal with mineral deposits and general geology in the Keystone and New Rambler areas are relevant. In a comprehensive general review of mineral resources of Wyoming, Osterwald et al. (1966) cite locations and brief descriptions of recorded mines and prospects in the Medicine Bow Mountains, compiled from unpublished as well as published sources. The occurrence of platinum-group elements at the New Rambler mine has been discussed by Theobald and Thompson (1968) and by McCallum, et al. (1975, 1976).

Unpublished geologic maps of the Keystone and Albany 7½ minute quadrangles by M. E. McCallum (scheduled for publication in the U. S. Geological Survey GQ series) have provided needed information concerning the structural fabric of this mineralized district.

GENERAL GEOLOGY

GEOLOGIC SETTING

The metalliferous deposits discussed in this report are scattered through the central part of the Medicine Bow Mountains in portions of T. 13 N. through T. 15 N., R. 78 W. through R. 80 W., Albany and Carbon Counties, Wyoming. The area investigated lies principally within the Albany and Keystone 7½ minute quadrangles.

Physiographically, the region is a low-relief upland surface of conifer-forested rolling hills at elevations ranging from about 8700 to 9700 feet. The area is accessible from June through September via State Highways 130 and 11 to the town of Albany and via State Highway 230 that crosses the mountains south of the study area. A system of gravel roads maintained by the U. S. Forest Service and dirt logging roads provide access from state highways to most of the localities discussed herein.

The Medicine Bow Mountains consist of a complex of Precambrian rocks that comprise the core of a large, asymmetric anticline bounded on the east by west-dipping thrusts. For a detailed discussion of the general geology of the region, the reader is referred to Houston et al. (1968). The central part of the Medicine Bow Mountains is structurally

dominated by a series of northeast-trending shear zones (Fig. 1). The most prominent of these, referred to as the Mullen Creek-Nash Fork shear zone (Houston et al., 1968), constitutes a major Precambrian lineament that splits the Medicine Bow Mountains into two distinct geologic provinces. Rocks northwest of the Mullen Creek-Nash Fork shear zone are a complex of Archean gneisses and igneous rocks overlain by low-grade miogeosynclinal metasedimentary units ranging in age from 1650 m.y. to approximately 2410 m.y. (Hills et al., 1968). Precambrian rocks immediately southeast of the shear zone are continuous with the igneous-metamorphic province of northern and central Colorado. These rocks are predominantly paraschists and paragneisses of felsic-intermediate composition metamorphosed to upper amphibolite grade 1750 m.y. ago (Hedge et al., 1967) and younger Precambrian mafic and granitic intrusives that also have been subjected to varying intensities of metamorphism and cataclasis.

STRUCTURE

The cataclastic history of the central part of the Medicine Bow Range has been complex. The large northeast-trending shear zones appear to have been initiated during the terminal stages of the 1750 m.y. orogeny and were active intermittently through Laramide time. Shear zone rocks comprise a

Fig. 1. Generalized Precambrian outcrop map of the Medicine Bow Mountains, Wyoming (after McCallum et al., 1976, Fig. 1). The area in the box inset is enlarged in Figure 2.

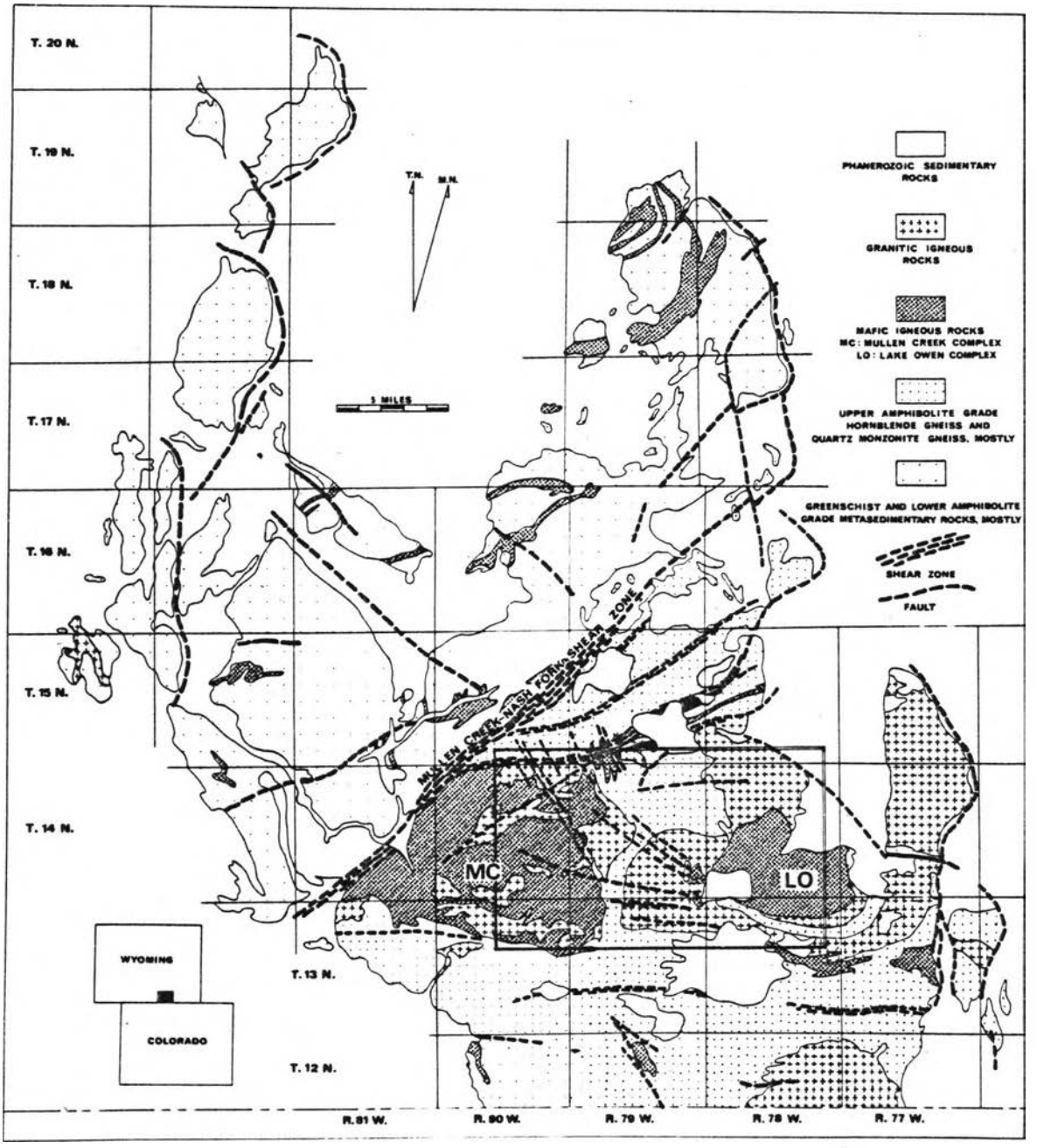
T. 20 N.
T. 19 N.
T. 18 N.
T. 17 N.
T. 16 N.
T. 15 N.
T. 14 N.
T. 13 N.
T. 12 N.
R. 81 W.
R. 80 W.
R. 79 W.
R. 78 W.
R. 77 W.
T.N.
M.N.
5 MILES
PHANEROZOIC SEDIMENTARY ROCKS
GRANITIC IGNEOUS ROCKS
MAFIC IGNEOUS ROCKS
MC: MULLEN CREEK COMPLEX
LO: LAKE OWEN COMPLEX
UPPER AMPHIBOLITE GRADE HORNBLENDE GNEISS AND QUARTZ MONZONITE GNEISS, MOSTLY
GREENSCHIST AND LOWER AMPHIBOLITE GRADE METASEDIMENTARY ROCKS, MOSTLY
SHEAR ZONE
FAULT
MULLEN CREEK-NASH FORK SHEAR ZONE
MC
LO
WYOMING
COLORADO

polymetamorphic assemblage ranging from an early series of blastomylonite gneisses, schists, and layered migmatites of almandine amphibolite facies to regionally retrograded cataclasite and mylonite zones that reflect subsequent translative deformations under epidote amphibolite and greenschist facies conditions; narrow zones of massive breccia, shattered flinty crushrock, and graphitic gouge attest to Laramide movement (McCallum, 1974, p. 473).

A large area south of the Mullen Creek-Nash Fork shear zone is structurally characterized by an extremely complex fault and fracture pattern comprised of small second and higher order shear zones and tensional cross fractures subsidiary to the master shear system (Fig. 2). The most conspicuous set of second order dislocations is a generally southeast-trending, commonly mineralized system whose individual elements are steeply dipping narrow fractures and anastomosing shears with a total width ranging from a few to a few tens of feet in most cases. Movement along these structures has mostly been minor--usually imperceptible--but both right and left lateral oblique offset have been noted, in a few cases amounting to a quarter mile (McCallum, unpub.).

Southeast-trending faults cut a less persistent set of generally east-trending fractures that in a number of cases have exerted obvious influence on localization of

Fig. 2. Generalized geologic map of mineralized area outlined in Figure 1, showing locations of mineral deposits investigated in this study. Geology after Houston et al. (1968, Plate 1), with additional structural detail from McCallum (unpub.). Mineral deposits are numbered on map as follows: 1) Keystone mine; 2) Black mine; 5) Gold Crater mine; 6) Au-Cu prospect; 7) Pt-Pd prospect; 8) Pt-Pd-Cu prospect; 9) Bear mine; 10) Cuprite mine; 11) Albany mine; 12) Douglas mine; 13) New Rambler mine; 14) Blanche mine; 15) Duchess mine; 16) Cu prospect; 17) Pb-Ag-Cu prospect; 18) Sunset mine; 19) Golden Key mine; 20) "Anonymous" mine; 21) Lake Creek mine.

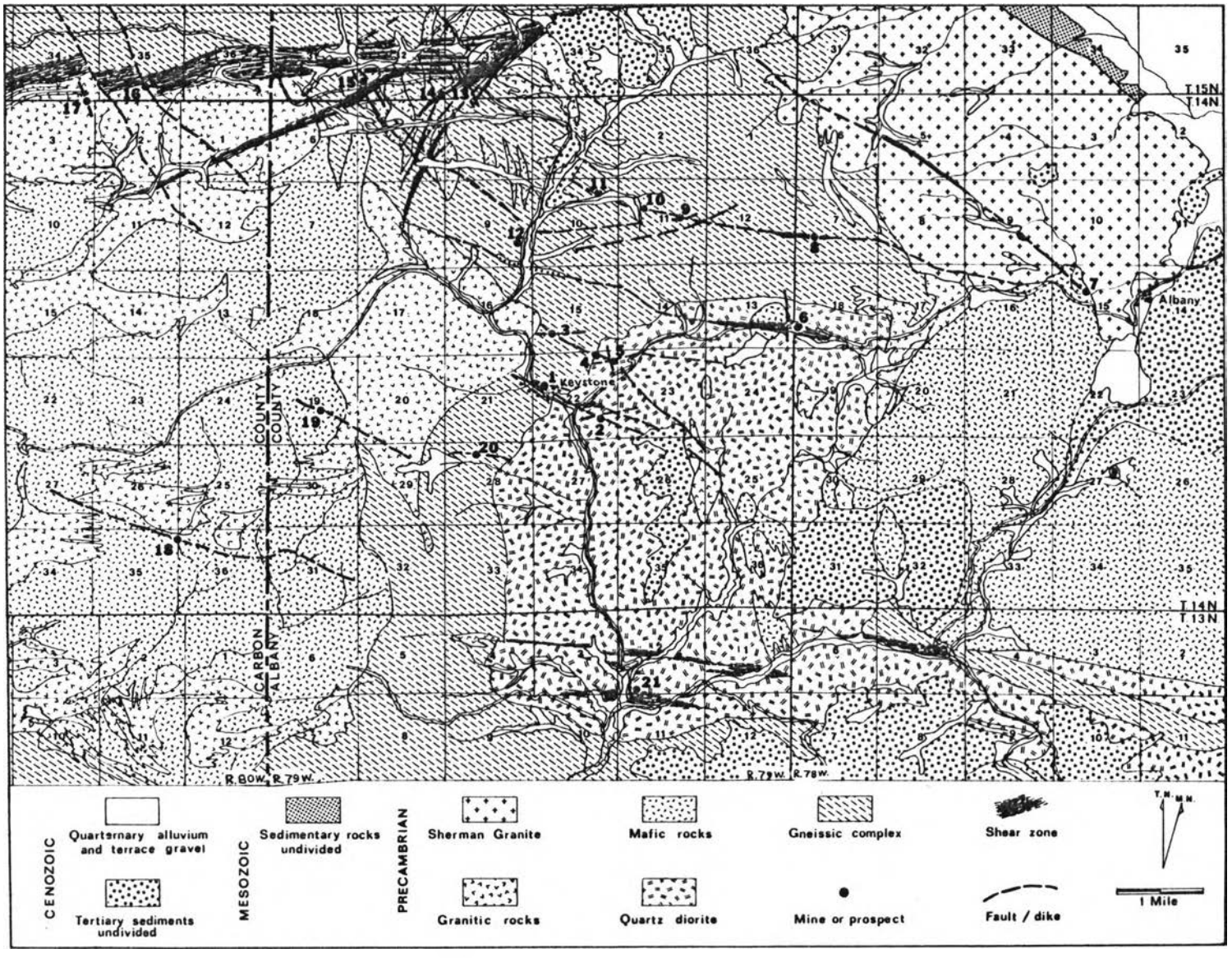
T15N
T14N
T14N
T13N
Albany
Keystone
CARBON COUNTY
ALBANY COUNTY
R.80W.
R.79W.
R.78W.
CENOZOIC
Quaternary alluvium and terrace gravel
Tertiary sediments undivided
MESOZOIC
Sedimentary rocks undivided
PRECAMBRIAN
Sherman Granite
Granitic rocks
Mafic rocks
Quartz diorite
Gneissic complex
Mine or prospect
Shear zone
Fault / dike
T.N.
M.N.
1 Mile

mineralization (McCallum, unpub.). Narrow mafic dikes and discontinuous lenses and pods of mafic rock commonly occupy east- and southeast-trending fractures.

Between the more strongly developed faults are innumerable dislocation surfaces of variable trends along which comminuted zones a few inches wide are healed by epidote and potash feldspar and locally by minor quartz and carbonates Although joint systems appear to be largely influenced by the attitude of local foliation, a southeast-trending joint set is persistent in the Keystone-Douglas Creek vicinity, and these joint planes are typically slickensided and epidotized. Thin sections of rock samples collected hundreds of feet from well expressed faults usually show variable degrees of mortar texture bounding K-feldspar grains, quartz is invariably polygonized, and the mineral assemblages are in most cases retrograded to epidote amphibolite grade and locally to greenschist facies.

Within the area investigated, virtually all rock units within six to eight miles of the Mullen Creek-Nash Fork shear zone have undergone some degree of cataclasis by translation, rotation, and granulation of tectonic units having dimensions from miles to microns. Metasomatic effects and retrograde metamorphism have generally accompanied cataclastic deformation.

LITHOLOGIC UNITS

Major rock types exposed within the area investigated are all Precambrian. They comprise an extremely varied array in lithology and origin, and in many cases intergradation of types makes subdivision for purposes of descriptive classification difficult. However, the Precambrian sequence can be divided roughly into three main groups: 1) older, highly metamorphosed gneisses and schists, 2) younger mafic intrusive rocks, and 3) felsic intrusive rocks. Terminology of lithologic units is largely that of Houston et al. (1968).

Older Gneisses and Schists

This complex assortment of rocks consists mostly of quartzo-feldspathic gneisses and biotite-hornblende-quartz-andesine gneisses and schists that are intercalated with and grade into hornblende gneisses and volumetrically minor calc-silicate gneisses and marbles.

Along the northern part of the area, quartzo-feldspathic gneiss is the dominant rock type (Fig. 2). This unit consists of light gray to pink rocks that vary from layered gneisses to augen gneiss to weakly foliated, nearly massive rocks having a granitoid aspect. Where it was encountered in the vicinity of the Albany and Cuprite mines (see Figure 2 for locations of mines and prospects), the quartzo-feldspathic gneiss unit consists of moderately foliated to locally

granitoid rocks comprised of about equal amounts of quartz and oligoclase, subordinate to equal amounts of microcline, minor epidote, biotite, chlorite, and muscovite, and traces of magnetite, sphene, and apatite. Near the Cuprite mine, the granitoid facies contains pods and dike-like bodies of alaskite and tourmaline (schorl)-bearing pegmatite. Igneous-looking phases grade into well-foliated biotite and hornblende-rich gneisses in which the plagioclase is typically andesine.

Along the northwestern sector of the area shown in Figure 2, in and adjacent to the southern branch of the Mullen Creek-Nash Fork shear zone, rocks of these lithologies have been moderately to strongly sheared. Where encountered in the vicinity of the New Rambler mine and prospects in the northwestern corner of the area, the quartzo-feldspathic unit is mostly a mylonitic gneiss characterized by a notably high epidote content, variable amounts of biotite (often chloritized), and abundant quartz and oligoclase-andesine. The rocks are pink to gray-green, fine- to medium-grained, and moderately to poorly foliated. Mylonitic fabric is expressed mainly by alignment of platy minerals, streaks of epidote, and closely spaced zones of intense comminution.

In the central part of the area, a belt of gneisses and schists trends roughly north-south, sandwiched between the Mullen Creek igneous complex and the Keystone quartz diorite

pluton. Lithologies are variable along this zone. The Douglas mine on Douglas Creek occurs in a mafic-rich series that includes hornblende/cummingtonite-garnet gneiss, biotite-hornblende-quartz-andesine schist, diopside-tremolite gneiss, and foliated, chlorite-bearing tremolite-calcite-epidote marble. These rocks are distinctly foliated, but in mafic and calcic phases, compositional layering at the hand-sample to thin-section scale is poorly developed or absent.

Farther south in the vicinity of Keystone (Fig. 2), well foliated, fine- to medium-grained quartz-andesine-biotite-hornblende-epidote gneisses predominate. Amphibole + biotite-rich layers are interlaminated with quartz + plagioclase $\pm$ muscovite-rich zones, and epidote is usually abundant throughout. Locally, biotite is distributed along cleavages and grain margins of hornblende in a manner indicating appreciable potassium metasomatism (biotization).

South of Keystone, this gneiss-schist belt between the plutonic complexes does not contain notable ore mineralization and was not investigated by the writer. According to Houston et al. (1968, p. 54 and Plate 1), the gneissic complex in this area is predominantly a more mafic phase comprised principally of fine-layered hornblende-plagioclase gneiss, with well layered representatives containing more accessory quartz and less anorthite-rich plagioclase;

hornblende-rich phases are poorly laminated and contain a more calcic plagioclase and little quartz.

The advanced metamorphic grade and highly variable lithology of the gneissic complex make attempts at resolution of its origin largely a matter of speculation. The hornblende- and biotite-rich gneisses have apparently originated by metamorphism and/or metasomatism of a variety of rock types that according to Houston et al. (1968, p. 57) could have included intrusive rocks, flows, and tuffs of mafic to intermediate composition, and calcareous or dolomitic shales, tuffaceous shales, or impure graywackes. As will be discussed in greater detail in a following section, Zn-Cu mineralization associated mainly with mafic gneisses at the Douglas mine is apparently of a syngenetic type that is typically associated with mafic-intermediate volcanic rocks. This lends inconclusive support to an igneous origin of some components of this lithologic assemblage.

Houston et al. (1968, p.65) speculate that the quartzo-feldspathic gneisses are probably derived from rocks of igneous and sedimentary parentage that now show similar mineralogical and textural features. These authors propose a predominantly metasedimentary and metasomatic origin for the quartzo-feldspathic gneiss, with granitoid facies representing locally advanced products of metasomatic granitization.

Intrusive Mafic Rocks

The older gneissic complex is intruded by two large Precambrian plutonic complexes composed in large part of layered mafic rocks. The western portion of the area shown in Figure 2 includes about 35 square miles of the Mullen Creek igneous complex, which is comprised principally of a bimodal association of granitic and tholeiitic gabbroic rocks, although members of intermediate composition are also represented. The southeastern third of the area is occupied by part of a large intrusive complex that includes the Keystone quartz diorite, the Lake Owens mafic complex, and numerous small sills, dikes, and stocks of granitic composition.

The Mullen Creek Mafic Complex

Epigenetic precious- and base-metal mineralization is associated with amphibolitized gabbroic units of the Mullen Creek igneous complex at several localities. These rocks were investigated in the vicinities of the New Rambler, Blanche, Duchess, Sunset, and Golden Key mines, and at the Cu and Pb-Ag-Cu prospects in the northwest corner of the area shown in Figure 2.

In degree of metamorphism, they range from nearly fresh gabbroic rocks with relict ophitic, diabasic, and gabbroic textures to crystalloblastic orthoamphibolites to mylonitic

chlorite schists. Most abundant are medium- to coarse-grained, weakly foliated to non-foliate metagabbro and metadiorite consisting of labradorite or andesine (variably sausseritized) and brownish to bluish green hornblende (commonly chloritized), although uralitized pyroxenes are locally significant, particularly in metagabbro. Common accessory minerals include magnetite, pyrite, ilmenite, epidote and biotite, accompanied by lesser amounts of sphene, allanite, apatite, and garnet. Coarse-grained metapyroxenite encountered at the New Rambler and Blanche mines consists chiefly of hornblende, uralitized orthopyroxene and clinopyroxene, magnetite, and pyrite, with accessory epidote, sphene, apatite, and locally, olivine.

Locally well expressed primary compositional layering consists mostly of cyclic alternation of anorthositic and mafic-rich layers at intervals of a few centimeters to tens of feet or more. Fine-grained, weakly foliated to massive metabasalt or metadiabase units are locally conspicuous, as in the vicinity of the Sunset mine, and appear to be cut by coarse-grained phases of the gabbro. Secondary foliation is often distinct, but except where cataclastic fabrics are developed along shear zones, most of these rocks are not strongly deformed. Where transected by shear zones, the mafic rocks are intensely comminuted and are converted to

submylonites or mylonites in which chlorite, epidote, iron oxides, and sericite or K-feldspar are the main mineral constituents.

The Lake Owens Mafic Complex

Mafic rocks of the main body of the Lake Owens intrusion were encountered in this study only at a small Pt-Pd prospect one half mile west of the village of Albany. The prospect is situated at the intrusive contact of a younger Sherman-type granite pluton with the Lake Owens body, and mafic rocks at the contact are intensely hybridized by metasomatic reaction. The hybrid is compositionally varied, but in general, most closely approximates granodiorite heavily impregnated with iron oxides.

According to Houston et al. (1968, p.75), mafic rocks of the Lake Owens intrusion are generally fresh and unmetamorphosed. The rocks of the mafic complex include troctolite, olivine gabbro, olivine norite, gabbro, and norite. In the sector of the intrusion in the vicinity of the Pt-Pd-REE prospect, gabbro and norite are the dominant facies.

Mafic Dikes, Sills, and Related Bodies

Numerous small bodies of mafic rocks occur throughout the district as narrow dikes and sills and discontinuous cataclastic lenses along sporadically mineralized and barren

faults. Where encountered at mine and prospect workings, they have usually been subjected to cataclasis and hydrothermal alteration of a degree that totally obscures the original composition. In some cases, however, portions of the dikes and related bodies are relatively unaltered at short distances from the centers of mineralization. Fresher representatives range from meta-andesite to metapyroxenite. Since mafic rocks are believed to bear significantly on the localization and origin of mineralization in the district, mafic dikes and related bodies that are associated with mineralization will be described in a following section discussing salient characteristics of individual deposits.

Intrusive Felsic Rocks

Igneous rocks of broadly granitic composition representing several Precambrian intrusive events are widespread throughout the district. Those associated with the Mullen Creek mafic complex include the Rambler granite adjacent to the New Rambler mine and the Horse Creek granodiorite sill bounding the mafic complex southwest of the Douglas mine (Fig. 2); a host of granitic sills, dikes, and small stocks occur near the contact of the Keystone quartz diorite and Lake Owens mafic complex, and a younger Sherman-type granite pluton abuts the Lake Owens complex along its northern margin.

Keystone Quartz Diorite

A large body of quartz diorite has been invaded by the Lake Owens mafic complex, and its outcrop surrounds the mafic intrusion on its east, south, and west sides (Fig. 1). The largest part of the quartz diorite mass occurs on the west side of the mafic complex in the area east and southeast of Keystone (Fig. 2). This portion of the Keystone quartz diorite covers about 34 square miles and occupies about a quarter of the study area. The quartz diorite intrudes the gneissic complex but is older than other major plutonic units in the district (Houston et al., 1968, p.66).

The Keystone quartz diorite is a light to dark gray, medium- to coarse-grained, faintly to strongly foliated rock. Andesine, hornblende, and quartz, generally in that order of abundance, are its major minerals; important accessories are epidote, biotite, potassium feldspar, and sphene; apatite, magnetite, and zircon are present as trace accessories. In the areas where it was investigated near the Florence and Gold Crater mines in the vicinity of Keystone, and along the southern margin of the pluton in the vicinity of the Lake Creek mine, the quartz diorite shows pervasive weak cataclasis and potassium metasomatism, and locally it is strongly sheared.

In the vicinities of the Florence, Gold Crater, and Lake Creek mines, the foliation trends generally east-west, roughly concordant with the intrusive contacts, and approximately parallel to an early set of east-west fractures developed in the district. In these areas, the foliation appears to be cataclastic in origin and is expressed mainly by alignment of secondary biotite that, together with epidote and sphene, partially replaces hornblende. Quartz is invariably polygonized, and margins of K-feldspar grains commonly show mortar texture and recrystallization. In proximity to shear zones, notably those in the vicinity of the Lake Creek mine, cataclastic foliation is strongly developed, and K-metasomatism has altered much of the rock to granodioritic mineralogy by K-feldspathization of plagioclase and biotization of hornblende. In the vicinity of Keystone, strong K-metasomatism is generally prevalent only over a few tens of feet outward from prominent faults; in and adjacent to the faults, the quartz diorite shows strong hydrothermal alteration.

"Granitic" Rocks of the Mullen Creek Igneous Complex

A large number of irregular "granitic" stocks have intruded mafic rocks of the Mullen Creek igneous complex. These were encountered in connection with investigations of ore mineralization at three localities--at the Pb-Ag-Cu

prospect in the northwest corner of the study area and in the vicinities of the Sunset and New Rambler mines.

At the Pb-Ag-Cu prospect, the country rock is a medium-grained, weakly foliated pink granite composed of about equal amounts of quartz and microcline, subordinate sodic oligoclase, a little muscovite and biotite (variably chloritized), and traces of apatite and zircon. Although the granite intrudes the main mass of mafic rocks with little hybridization at the contact, the granite is cut by metagabbroic dikes, which suggests possible penecontemporaneous availability of mafic and felsic magma types.

Medium-grained, weakly foliated pink quartz monzonite was encountered in several small irregular bodies a short distance west of the Sunset mine. The quartz monzonite consists of quartz, microcline, and oligoclase in about equal proportions, with accessory muscovite, chlorite, magnetite, and apatite. Foliation is expressed by weak subparallel orientation of plagioclase.

An irregular granitic stock, about 1.5 square miles in outcrop area, is exposed mainly within metagabbroic rocks a few hundred yards northeast of the New Rambler mine and was encountered in subsurface mine workings. Samples of granite collected from the mine dump are coarse-grained and strongly epidotized. The main body of the granite was not investigated

by the writer, but according to a description provided by McCallum and Orback (1968, p.6), medium-grained equigranular pink granite comprises the bulk of the stock, although quartz monzonitic, aplitic, and pegmatitic facies are also present. In order of decreasing abundance, the principal minerals of the granite are quartz, microcline, albite-oligoclase, biotite, and chlorite, with minor amounts of epidote, hornblende, muscovite, magnetite, and allanite. Lenses and sills of tourmaline-rich granite crop out on the northern margin of the stock. Albite, quartz, microcline schorl, muscovite, and garnet are its major minerals. The granite stock is situated primarily within the Mullen Creek-Nash Fork shear zone, and it is locally mylonitized.

"Granitic" Rocks Associated with the Keystone Quartz Diorite and Lake Owens Igneous Complex

Several small stocks and dikes of granite to quartz monzonite composition intrude the Keystone quartz diorite and the northwest margin of the Lake Owens mafic complex (McCallum, unpub.). In the vicinity of the quartz diorite-mafic complex intrusive contact, innumerable narrow sills of granitic composition are intercalated with gabbroic sills invading the foliated quartz diorite. The sills are too narrow to be shown on the generalized geologic map in Figure 2. There is no notable metallic mineralization associated with these

granitic stocks and sills, and they were not studied in this investigation.

Sherman-Type Granite

Part of a large body of Sherman-type granite is exposed in the northeast corner of the study area near the town of Albany. This granite represents the latest important episode of granitic intrusion in the central Medicine Bows (Houston et al., 1968, p.84). Sherman-type granite was encountered in this study only at its contact with mafic rocks of the Lake Owens complex where hybridized phases are associated with anomalous levels of platinum-group elements, as described earlier. Unhybridized representatives were not investigated by the writer, but according to McCallum and Orback (1968, p.7), the Sherman-type granite consists of pinkish-gray, medium- to coarse-grained granite with quartz monzonitic phases. The principal mineral constituents--potash feldspar, plagioclase, and quartz--occur in variable proportions, along with considerable accessory biotite and hornblende and minor amounts of magnetite, ilmenite, sphene, apatite, allanite, epidote, chlorite, pyrite, and zircon.

THE MINERAL DEPOSITS

Mineralized localities in the central part of the Medicine Bow Mountains in southeastern Wyoming comprise a diversified assemblage of ore types. Principal among them are 1) an association of platinum-group elements and hydrothermal copper ores in and adjacent to a large mafic plutonic complex; 2) a mineralogically varied group of quartz-carbonate-sulfide veins, some with high concentrations of gold and silver, associated with metasedimentary and mafic to felsic metaigneous intrusive rocks; 3) a polymetallic sulfide deposit in which ore minerals are disseminated in amphibolitic and calc-silicate units of a gneissic sequence apparently derived from intercalated basic volcanic and sedimentary rocks.

Occurrences of platinum-group elements (PGE) are now known at several localities in the central Medicine Bow Mountains. Recorded production of PGE has come only from the New Rambler mine, although a small amount of Pt- and Pd-rich copper ore was recovered at the Blanche mine, a quarter mile southwest of the New Rambler (Fig. 2). Minor amounts of platinum metals have been found in the Centennial Ridge district (Hess, 1926) about eight miles northeast of the New Rambler mine. At Centennial Ridge, platinoids and

gold are associated with sulfide or arsenide concentrations occurring as fracture and breccia fillings and lenses where branches of the Mullen Creek-Nash Fork shear zone and related faults cut mafic metaigneous and amphibolitic units (McCallum, 1968). No production of platinoid ore has been reported from this district. In the course of sampling mineralized localities in the central Medicine Bow Mountains, the writer and M. E. McCallum have found high concentrations of PGE (from 1-2 ppm Pt + Pd to 40 ppm Pt and 30 ppm Pd) in copper sulfides and leached gossan material at two small vein occurrences a few miles southeast of the New Rambler mine (localities 7 and 8, Fig. 2).

Vein mineralization containing predominantly gold-, copper-, and more rarely lead-, zinc-, and silver-rich sulfide assemblages are the most widespread of the three principal classes of ore deposits in the district. Although some veins or portions of veins were phenomenally rich, as indicated by reports issued during the period of active mining and by assays made in connection with the present study that show up to 28 ounces Au per ton, only the Keystone and Florence gold mines yielded notable production. A number of the vein deposits investigated have no economic significance, but they share essential features with the larger orebodies and supply information valuable in compiling a composite

character profile of regional vein mineralization that forms the basis for interpretive analysis of vein genesis.

In succeeding sections, descriptive and interpretive accounts of the mineral deposits are presented in the following order: (1) platinum- and palladium-bearing replacement deposits; (2) gold- and copper-dominant vein-type deposits; and (3) a metamorphosed body of massive and disseminated zinc-copper-lead ore.

THE NEW RAMBLER MINE: AN ASSOCIATION OF PLATINUM METALS WITH HYDROTHERMAL COPPER-NICKEL ORES

Introductory Comments

The New Rambler deposit is interpreted as representing a non-magmatic accumulation of platinum-group elements (PGE) and other metals that have been concentrated by processes of hydrothermal leaching of ordinary gabbroic rocks and redeposition of the leached metals along shear zones as palladium- and platinum-rich copper sulfide ore (McCallum et al., 1976).[1] This account documents an instance in which PGE have been mobilized and concentrated to a remarkable degree by hydrothermal fluids at intermediate temperatures.

---

[1] Substantial portions of the following report on the New Rambler mine are taken from the account of McCallum et al. (1976).

Cousins (1973, p.77) noted that "Geochemists appear to have been misled on the geochemistry of platinum group elements by over-emphasis on the chemical inertness of these elements." In their commercial deposits of world significance (except those formed by exogenic processes), PGE are associated with sulfides and/or chromite in or adjacent to mafic igneous complexes. Concentration of ore metals in these deposits traditionally has been attributed mainly to magmatic processes. Recent reports on platinoid deposits have documented evidence of appreciable solubilities of PGE, principally palladium and platinum, leading to their enrichment in magmatic fractions of a volatile-rich, residual character, e.g., the Merensky Reef (Vermak, 1976), at Sudbury (Keays and Crocket, 1970), and Noril'sk (Genkin, 1959, 1968). Stumpfl (1974) has compiled convincing evidence of remobilization and redistribution of platinoids by deuteric or hydrothermal fluids in many important deposits, and it now seems generally accepted that the relatively Pd- and Pt-rich offset deposits at Sudbury and similar vein ores at Noril'sk represent, at least in part, late-stage hydrothermal events in these districts. The known platinum-metal ores of wholly hydrothermal character are of relatively minor economic significance. Examples include the occurrence at the Artonvilla mine, Transvaal (Mihálik et al., 1974) and the

Waterburg lodes, Transvaal (Mertie, 1969). It seems apparent that ore grade concentrations of the PGE collectively span a full spectrum of depositional environments from purely magmatic stratiform segregations, represented by the A chromitite and other occurrences in the Stillwater Complex and the Merensky and UG2 reefs of the Bushveld Complex, to deposits of wholly hydrothermal origin such as that discussed in this report, and a range of intermediate members of composite magmatic-hydrothermal character, exemplified by familiar deposits of the Sudbury and Noril'sk districts and many less well known deposits.

Local Structure and General Features of the New Rambler Orebody

In the vicinity of the New Rambler mine, geologic relationships are obscured by a thin veneer of late Cenozoic boulder and gravel deposits. The principal exposures of bedrock units, all Precambrian, are in prospect pits and mine workings.

All rock units in the area have undergone variable degrees of cataclasis, recrystallization, and chemical reconstitution. An east-trending branch of the Mullen Creek-Nash

Fork shear zone is the dominant structural feature in the vicinity of the mine. The New Rambler orebody was localized near the intersection of a poorly defined northeast-trending mylonite zone with this east-west mile-wide belt of intensely sheared rocks and a set of four close-spaced northwest-trending fractures (Fig. 2) (McCallum, et al., 1976). The four small cross faults are not exposed at the surface, but old mine reports indicate that well developed fault planes were present at depth, dipping about 40 degrees to the northeast. Orback (1958) states that some copper mineralization and considerable fault gouge were encountered along these planes in the mine workings.

Inasmuch as the New Rambler mine workings are caved and inaccessible, and nearly all mine records were destroyed in a fire that terminated the mining operation in 1918, the following account of the geometry and structural control of the orebody is necessarily tenuous because it relies heavily on a few brief and sketchy reports published by early visitors to the active mine.

Kemp (1904) gives the most detailed description of the orebody, and the general outlines of his account are corroborated by subsequent reports. The mine's entire production[1]

---

[1]Approximately 6000-7000 tons of ore concentrates were shipped, but platinoids were extracted only from a small fraction owing to belated recognition of their presence. Payment was received for 451 oz Pd and 170 oz Pt (U. S. Bureau of Mines, 1942).

apparently came from three irregular pods of ore enclosed in decomposed metadiorite and metagabbro. Diamond drilling has shown that these units grade at shallow depth into "pyroxenite" and "peridotite," although the depths at which these transitions were encountered is highly erratic, due presumably to complex faulting (Kasteler and Frey, 1949).

The upper ore pod was described as a dome-shaped body extending from 30 to 70 feet below the ground surface and having a horizontal diameter of about 40 feet (Kemp, 1904, p.248). The upper part of this body was a gossan of iron oxides from which the copper had been extensively leached. The lower part of the oxidized pod was heavily impregnated with copper carbonates, sulfates, and oxides, chrysocolla, and native copper, with minor sulfides near the base.

About 50 feet southeast of the oxidized ore pod, a separate pocket of sulfide ore "of no definite outline" was encountered at a depth of 100 feet. This ore mass was about 25 feet high and extended 30 feet north-south and 50 feet east-west. A few tens of feet west of this pod, another large irregular ore shoot was opened up on the same level. Kemp (1904) reports that the part of the ore mass stoped out at that time was 40 feet north-south, 25 feet high, and 12 to 25 feet wide. He found it remarkable that "the usual vein minerals of the gangue, such as quartz, calcite, etc. are

lacking. Instead we have over an area of nearly a hundred feet east and west and the same distance north and south... the decomposition products of an eruptive dike [sic] in place" (p.249). Actually, minor quartz is present, although the predominant gangue is gray to yellow cryptocrystalline jasperoid. The mafic rocks containing the ore are not "dikes" but are tectonically translated blocks and projections of the Mullen Creek layered mafic intrusive complex.

However, several tens of feet east of the three irregular ore pods, subsequent underground development encountered quartz-carbonate fissure veins related to the four small northwest-trending faults mentioned previously. A report by the U. S. Bureau of Mines (1942, p.4) states that a map of the property, prepared in 1918 just prior to the fire, indicates that most of the underground development in the previous decade was on fissure veins. This development work was done on the assumption that the orebody was along fissures and that by following fissures other ore shoots might be found. Other than the three orebodies just discussed, no ore was disclosed by the rather extensive underground explorations. Bureau of Mines engineers (1942, p.4) believed the ore to be "independent of fissure veins."

In summary, the disconnected reports on the New Rambler orebody suggest that it consisted of three large ore pockets

of irregular outline. If the geometry of the stopes at the time of Kemp's (1904) visit can be taken as representing the distribution of ore in the deposit, the pods lacked a consistent trend. The ore was entirely in decomposed, sheared, mafic metaigneous rocks and was situated near the intersection of a northeast-trending mylonite zone and closely spaced northwest-trending faults with an east-trending branch of the Mullen Creek-Nash Fork shear zone. The nature of the affiliation, if any, between the orebodies and the cross faults is obscure; however, the intersecting shear zones may have generated zones of dilatancy in which ore deposition was localized (McCallum et al., 1976).

Mineralization

Methods of Investigation

Two hundred specimens of sulfide ore (variably oxidized) and altered metagabbroic host rock collected from the New Rambler mine dump were evaluated. Eighty-seven ore- and gangue-mineral separates and bulk samples of ore and host rock were analyzed quantitatively for PGE and Au by a combined fire assay-emission spectographic method described in detail by Cooley et al. (1976) (analysts, R. R. Carlson, T. A. Doerge, E. F. Cooley, U. S. G. S.). Osmium cannot be determined by this method and was not sought. Ag and Cu in all 87 samples and Au, Ni, Co, Zn, As, and Te in some specimens were

determined by atomic absorption analysis (analysts, U. S. G. S. chemists).[1] Other trace element characteristics of the 85 samples were determined by semiquantitative emission spectrographic analysis for 30 elements (analysts, U. S. G. S. chemists). One hundred forty-three polished ore specimens and 14 thin sections of altered host rock were examined microscopically. Mineral identifications were made by optical means, X-ray powder diffraction analysis, and quantitative and semiquantitative electron microprobe analysis. The paragenetic sequence outlined in Figure 3 is based on interpretation of ore and gangue mineral intergrowths.

Wallrock Alteration

Owing to poor bedrock exposure in the vicinity of the mine and inaccessibility of the mine workings, most samples studied for effects of hydrothermal alteration were collected from the mine dump. Silicate rocks on the dump exhibit varying intensities of silicification, sericitization, chloritization, and sausseritization.

Propylitic alteration All rock units have been chloritized and sausseritized to a variable extent along the shear zones. Although greenschist/propylitic alteration has affected to some extent the country rocks over a broad area, development of the chlorite-epidote/clinozoisite-albite-

[1] Chemists are credited individually in tables presenting assay data.

Fig. 3. Paragenetic sequence, New Rambler deposit. Queried minerals are those whose identities have not been verified unequivocally (Cu-Ni thiospinel) or whose former presence is inferred ("cubanite"). "Cubanite" is intermediate solid solution of cubanite composition; "exsoln" is exsolution; and "incl. blaubl." following covellite means including blaubleibender covellite.

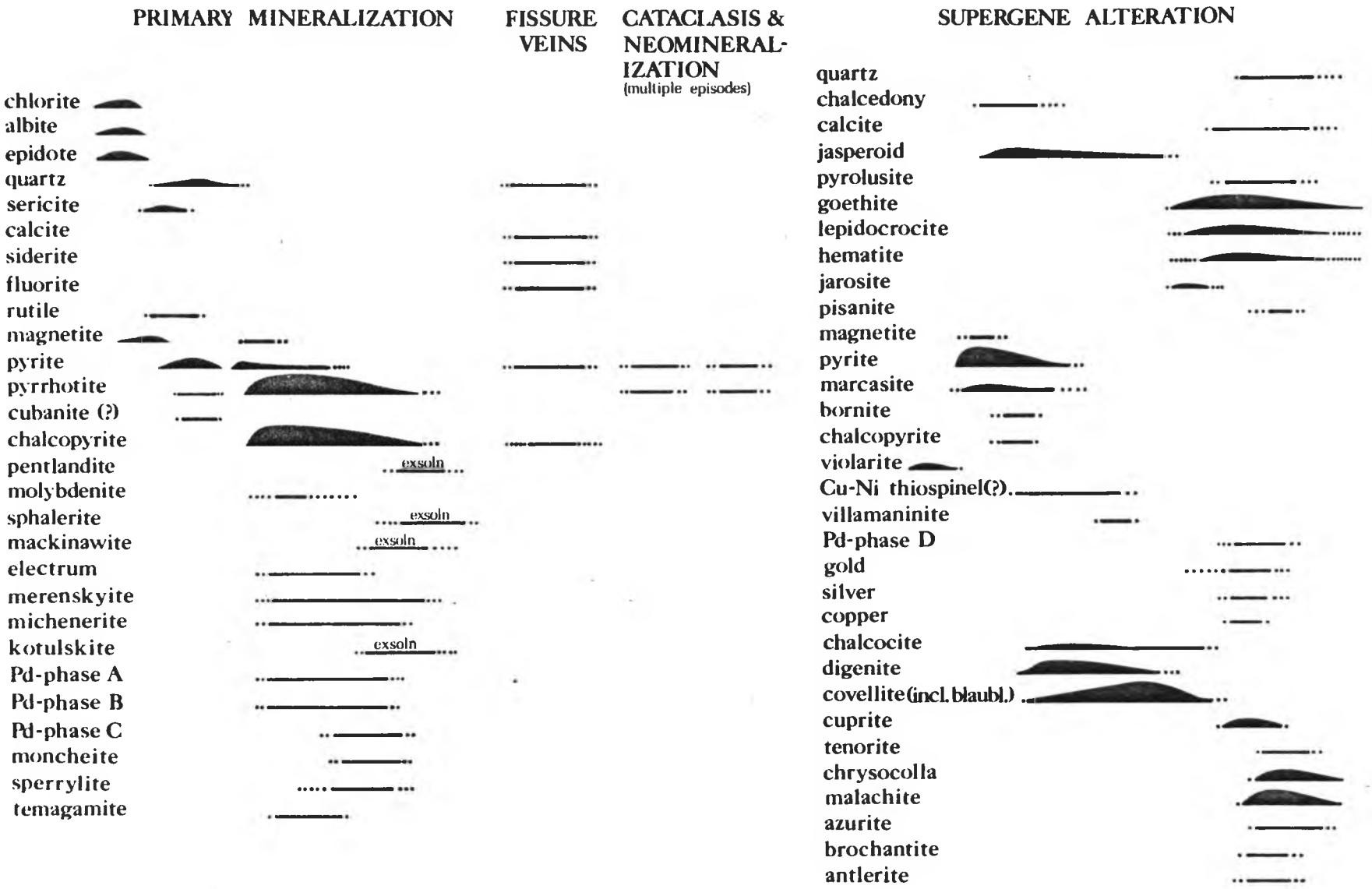
PRIMARY MINERALIZATION
FISSURE VEINS
CATACLASIS & NEOMINERALIZATION
(multiple episodes)
SUPERGENE ALTERATION
chlorite
albite
epidote
quartz
sericite
calcite
siderite
fluorite
rutile
magnetite
pyrite
pyrrhotite
cubanite (?)
chalcopyrite
pentlandite
molybdenite
sphalerite
mackinawite
electrum
merenskyite
michenerite
kotulskite
Pd-phase A
Pd-phase B
Pd-phase C
moncheite
sperrylite
temagamite
exsoln
quartz
chalcedony
calcite
jasperoid
pyrolusite
goethite
lepidocrocite
hematite
jarosite
pisanite
magnetite
pyrite
marcasite
bornite
chalcopyrite
violarite
Cu-Ni thiospinel(?)
villamaninite
Pd-phase D
gold
silver
copper
chalcocite
digenite
covellite (incl. blaubl.)
cuprite
tenorite
chrysocolla
malachite
azurite
brochantite
antlerite

magnetite (-pyrite) assemblage shows notable intensification with proximity to the orebodies. In most propylitized samples from the dump, the alteration is quite incomplete; much hornblende and lesser calcic plagioclase survive as corroded relics, and biotite is largely unaffected. Magnetite and epidote veinlets are abundant.

Quartz-sericite-pyrite alteration With further progress of wallrock hydrolysis, relict plagioclase and albite are strongly replaced by sericite and quartz, and in turn the remaining hornblende, biotite, and chlorite are attacked. Pyrite is conspicuous as veinlets and disseminated grains and locally as overgrowths on magnetite. Reticulated nets of rutile platelets have developed along partings in decomposed hornblende. Minor amounts of glassy, fine- to coarse-grained quartz may express locally intense hydrothermal silicification, but much of this material is difficult to distinguish from the products of pervasive supergene silicification, discussed below. In addition to pyrite, sparse disseminations of chalcopyrite occur in quartz-sericite gangue, but in general it appears that zones of silicification and quartz-sericite alteration constitute nearly barren zones developed locally along the walls of fluid channels in the general vicinity of ore mineralization.

Jasperoid With the exception of subordinate amounts of pyrite associated with quartz + sericite, the sulfide ore is enclosed in turbid microcrystalline or cryptocrystalline

silica of supergene replacement origin, referred to in following discussions as jasperoid. Varieties of this secondary silica include massive microcrystalline quartz; large volumes of porous, crumbly, gray to white jasperoid composed of minute colloform silica grains and argillaceous-looking material shown by powder diffraction to be amorphous; dense, massive, slightly opaline translucent silica with a gel-like appearance; and masses of turbid, cryptocrystalline jasperoid that preserves with variable degrees of clarity relict textural features of the original metagabbroic rock, viz., the granular fabric and relict cleavages of hornblende and chlorite. The latter type of jasperoid also typically contains nets and parallel sets of rutile platelets formerly disposed along cleavage partings of hornblende and biotite (Fig. 4A) and similar net-like arrays, sets of parallel platelets, and irregular wisps of sulfides that also were originally distributed along cleavages and grain boundaries of silicate minerals (notably hornblende) in the variably hydrolytically altered metagabbroic rocks (Fig. 4B).

The presence of ferruginous and weakly copper-stained patches in some jasperoid and the gel-like appearance of much of it point to derivation by supergene decomposition of metagabbroic rocks enclosing the weathering ore masses under the influence of $Fe_3(SO_4)_2$- and H_2SO_4-bearing meteoric solutions.

Fig. 4. A. Rutile lamellae (white) pseudomorphous after ilmenite exsolved along octahedral planes in former magnetite that has been replaced by supergene amorphous silica (mottled, dark gray). A grain of chalcopyrite (white, lower right) is largely replaced by supergene digenite (pale gray). Matrix is amorphous supergene silica that has replaced metagabbroic silicates. Disseminated ore. Sample MR-83A. X160. Reflected light.

B. Supergene digenite (light gray) that has pseudomorphously replaced chalcopyrite distributed along cleavages in hornblende. Metagabbroic silicates are entirely decomposed to supergene jasperoid (mottled gray). Sample MR-83A. X250. Reflected light.

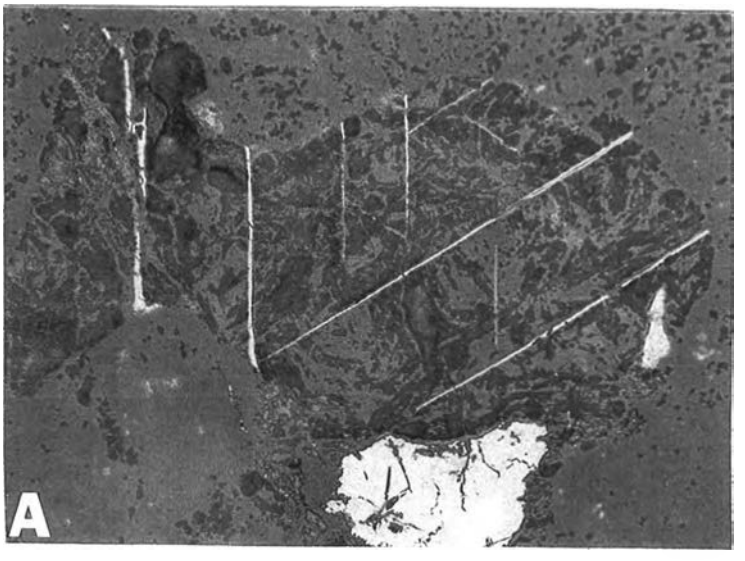

Figure 4

Early published reports indicate that all the ore occurred as huge "bunches" and streaks in "highly decomposed diorite [that] in its extreme form...is a white kaolinized mass of the consistency of soft clay but often retaining something of the original granular structure of the rock. Near the orebodies covellite grains are so uniformly distributed through it as to give the appearance at a little distance of basic silicates in a white feldspathic rock" (Emmons, 1903, p.97). No kaolin or other clay has been identified in this investigation, but much of the friable jasperoid fits that description. The account of abundant disseminated sulfides "near the orebodies" clearly implies that what was considered to constitute an orebody was essentially (or actually) massive sulfide. Ore specimens collected from the mine dump during this investigation are principally chunks of massive sulfide ore as much as a foot in diameter and irregular nodules of sulfide several inches across in jasperoid (formerly metagabbro) matrix; less abundant are jasperoid disseminations in sulfide matrix (matrix ore) and jasperoid with granular disseminations of fine-grained ore minerals (disseminated ore).

Mineral Associations in the Ore

All ore specimens available exhibit some degree (usually intense) of supergene alteration. Published reports indicate

that no fresh ore was mined. Ore specimens from the least oxidized portion of the alteration profile are affected by moderate to extensive replacement of primary ore minerals by supergene sulfides, by incipient limonitic oxidation, and by complete supergene silicification of the metagabbroic rock matrix. The least weathered examples of the various ore types provide the basis for this descriptive account. The mineralogy of the oxide zone, although interestingly varied, is for the most part peripheral to the focus of this report and is not discussed in detail. Because of total obliteration of some primary minerals by supergene processes, an account of the hypogene mineral assemblages necessarily must be interpretive in part. The sulfide ore can be classified into three distinct associations of primary ore minerals:

(1) an assemblage consisting principally of pyrite, with magnetite as a major accessory, and traces of chalcopyrite, pyrrhotite, and pentlandite, occurring as massive sulfide and as disseminations in the quartz-sericite wallrock alteration facies;

(2) an association of chalcopyrite and pyrrhotite with minor pyrite and numerous trace accessories, including sphalerite, mackinawite, pentlandite, electrum, and six hypogene Pd and Pt minerals, occurring as massive sulfide and as nodular and granular disseminations in metagabbroic rock;

(3) an association identical to (2) in major ore mineralogy and matrix material, but with a distinctive accessory base- and precious-mineral suite consisting of sphalerite, magnetite, pentlandite, electrum, and seven platinoid minerals.

Assemblage 1

About 5 percent of the ore collection belongs to this association. Medium-grained magnetite occurs abundantly in most specimens as euhedral to anhedral, corrosively rounded, extensively martitized and goethitized grains enclosed in nearly fresh pyrite. Semiquantitative emission spectrographic trace-element analyses of magnetite separates reveal Mn contents in the 500-700 ppm range, and low contents of Cr (~20 ppm), Ti (less than 20 ppm), and V (~150 ppm).

Euhedral to anhedral pyrite, the principal sulfide in this assemblage, typically occurs as very coarse-grained, polycrystalline massive sulfide and as disseminations in jasperoid and quartz-sericite matrix. The smooth polish and whiter brilliance distinguish this hypogene pyrite from the generally pitted, ragged, fine-grained, and slightly darker supergene pyrite that has replaced pyrrhotite of assemblages 2 and 3 (Fig. 5A). Spectrographic trace element analyses show that pyrite of assemblage 1 is relatively cobaltiferous (up to 3000 ppm Co) and usually contains less than 1500 ppm Ni, but disseminated pyrite contains up to 1

Fig. 5. A. Corrosively rounded and embayed primary pyrite (smooth, near white) with incorporated small chalcopyrite-pyrrhotite and pyrrhotite-pentlandite blebs (light gray); the primary pyrite is intergrown with secondary pyrite that has replaced medium- to coarse-grained pyrrhotite. The rough appearance and traces of relict pyrrhotite (001) parting distinguish supergene pyrite from hypogene pyrite. (Ore transitional between assemblages 1 and 2). Sample MR-72E. X80. Reflected light.

B. Chalcopyrite (darker medium-gray) and pyrrotite (lighter medium-gray) as inclusions in primary pyrite (light gray matrix). Six of the inclusions are visibly bi-mineralic. Assemblage 1. Sample MR-56. X400. Reflected light.

C. Pentlandite (light gray) as a feathery exsolution in pyrrhotite (darker gray) enclosed by primary pyrite. Assemblage 1. Sample MR-56. X400. Reflected light.

D. Chalcopyrite (light gray) with elongate star-shaped bodies of exsolved sphalerite (dark gray) and faintly visible minute rods or platelets of exsolved mackinawite (medium gray, abundant). Large black areas are voids. Assemblage 2. Sample MR-60. X400. Reflected light. Oil imm.

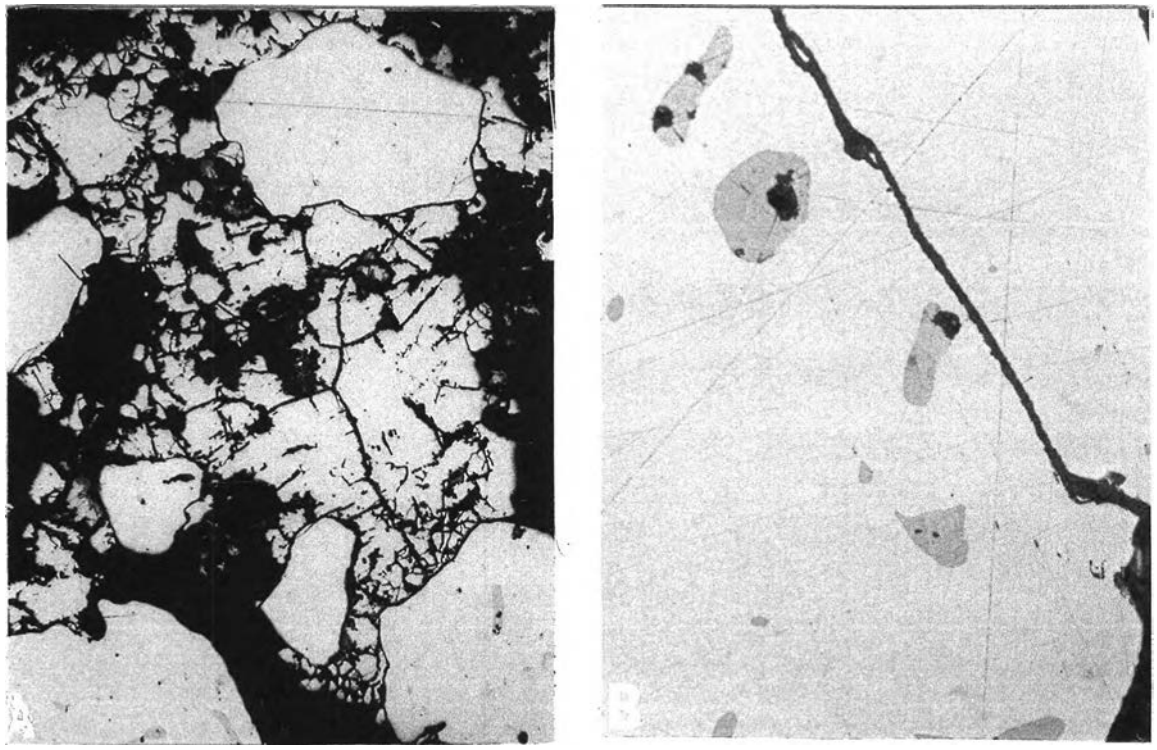

FIGURE 5

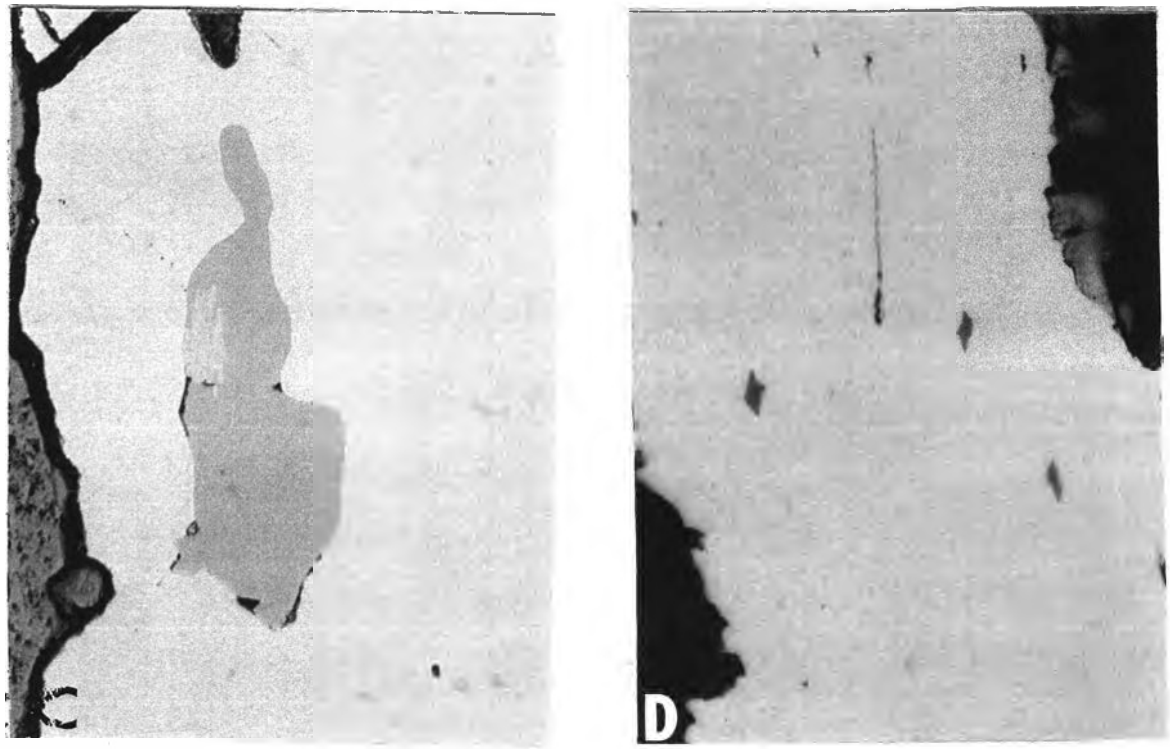

wt percent Ni occurring mainly as inclusions of nickeliferous pyrrhotite + pentlandite.

An interesting feature of this assemblage is the occurrence within pyrite of tiny inclusions (typically 10-50 microns across) of pyrrhotite and chalcopyrite, mostly as visibly composite ovoid blebs (Figs. 5A and 5B). These are locally so abundant as to constitute an emulsion in pyrite. Pentlandite (Fig. 5C), identified by microprobe analysis, is recognized in fewer than 1 percent of the inclusions (principally the largest ones), sometimes in clearly tri-mineralic blebs.

Assemblage 2

This mineral association is common to about 80 percent of the ore samples collected. All samples have been strongly affected by supergene processes and consist principally of chalcopyrite, pyrite, covellite, and goethitic limonite. Most specimens are devoid of gangue, but in some larger samples, ore minerals occur as fist-size and smaller corroded sulfide nodules in jasperoid matrix and in some cases as granular disseminations in silica.

Chalcopyrite This mineral was the most abundant sulfide in primary ore. Coarse- to very coarse-grained, complexly twinned chalcopyrite contains a variety of other minerals as inclusions. Sparse small globules of pyrrhotite

in chalcopyrite are conspicuous in some samples of nodular and massive ore. Mackinawite occurs, commonly in profusion, as exsolved, minute, discontinuous lamellae and crystallographically oriented specks. Sphalerite is present in chalcopyrite as tiny stars, isolated blebs and rods (Fig. 5D), and as discontinuous lamellae. The coalescence of rods to form discontinuous lamellae manifests control by octahedral planes of the chalcopyrite structure and suggests that these minute sphalerite inclusions have originated by exsolution from chalcopyrite. Larger, equant sphalerite grains (up to 0.1 mm across) of apparent non-exsolution origin are very rare.

Spectrographic trace element analyses of chalcopyrite of assemblage 2 show Zn contents typically in the range 1000-1500 ppm. Zn contents of other major sulfide minerals are low. Statistical analysis of the associations of metallic trace and major elements in massive sulfide ore reveals a high correlation coefficient between Cu and Zn--0.786 at the .001 significance level--indicating that chalcopyrite contains virtually all the zinc in the deposit, principally as exsolved sphalerite inclusions.

Chalcopyrite usually shows variable degrees of replacement by a grid of tapering covellite lamellae, in part of the <u>blaubleibender</u> (blue-remaining) variety; digenite and,

more rarely, chalcocite replace chalcopyrite of assemblage 2 in some disseminated ore.

Villamaninite Another supergene metasome of chalcopyrite in this suite occurs sparsely in most samples (abundantly in a few) as tiny, bronze-pink, isotropic cubes, aggregates of cubes, and anhedral grains always enclosed in covellite and commonly as rim overgrowths on tiny (5-15 microns) granules and rods of secondary pyrite that in part is derived from replacement of mackinawite (Figs. 6A and B). Electron microprobe analysis shows it to be a sulfide of Cu, Ni, and Co, in that order of abundance, having a metal: sulfur ratio closely approximating 1:2. It is identified on the basis of chemical composition and optical properties as villamaninite, $(Cu,Ni,Co)S_2$, a very rare mineral with pyrite structure. Microprobe analyses of two villamaninite grains are shown in Table 1. The analytical conditions and standards used in the microprobe analyses are described in the appendix.

Pyrite, Marcasite, and Pyrrhotite The massive sulfide ore contains hypogene pyrite as a minor accessory disseminated in chalcopyrite. The primary pyrite occurs as small cubes, usually 50-150 microns across, that are distinctly whiter than secondary pyrite of the same assemblage, owing probably to the effects of dissimilar Co and Ni contents in the two varieties.

Fig. 6. A. Supergene covellite (dark gray matrix and light gray laths, tone varying with optical orientation) after chalcopyrite encloses abundant disseminated cubes, aggregates of cubes, and irregular grains of villamaninite (near white). A few small relics of chalcopyrite (white, bottom and left) survive in covellite. Assemblage 2 supergene enriched ore. Sample MR-78J. X400. Reflected light.

B. Supergene covellite (large areas in various shades of gray) after chalcopyrite encloses lamellae and specks of secondary pyrite (white) after mackinawite lamellae exsolved from chalcopyrite. Pyrite lamellae are overgrown by villamaninite (medium gray). Supergene enriched assemblage 2 ore. Sample MR-78J.

C. Supergene pyrite (white) after pyrrhotite partially encloses a subhedral grain of Cu-Ni thiospinel(?) (light lamellae in cross hatch) after pentlandite. (The medium-gray material in crosshatch intergrowth is unidentified.) The fringe-textured phase around the main pentlandite replacement aggregate is Cu-Ni thiospinel(?) after pyrrhotite. Most of the fringe phase is replaced by digenite (dark gray). Veinlet pyrite occupies a shrinkage crack (right side of photo) along the former pentlandite-pyrrhotite grain contact. Assemblage 2. Sample MR-18. X400. Reflected light.

D. Subhedral grain of Cu-Ni thiospinel(?) (light gray) partially replaced in its upper half by digenite (dark gray). Larger masses of digenite and blaubleibender covellite (mottled) have replaced chalcopyrite (top and lower left). White is supergene pyrite. Black is supergene jasperoid. Assemblage 2 disseminated ore. Sample MR-18. X400. Reflected light.

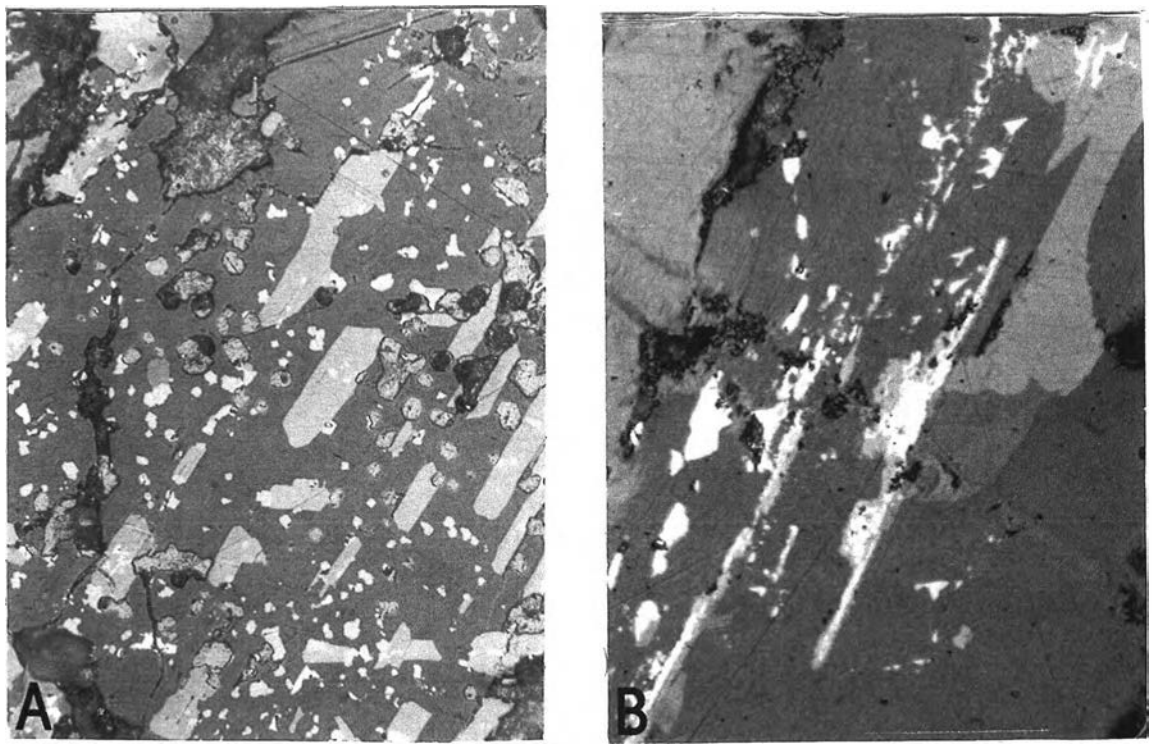

FIGURE 6

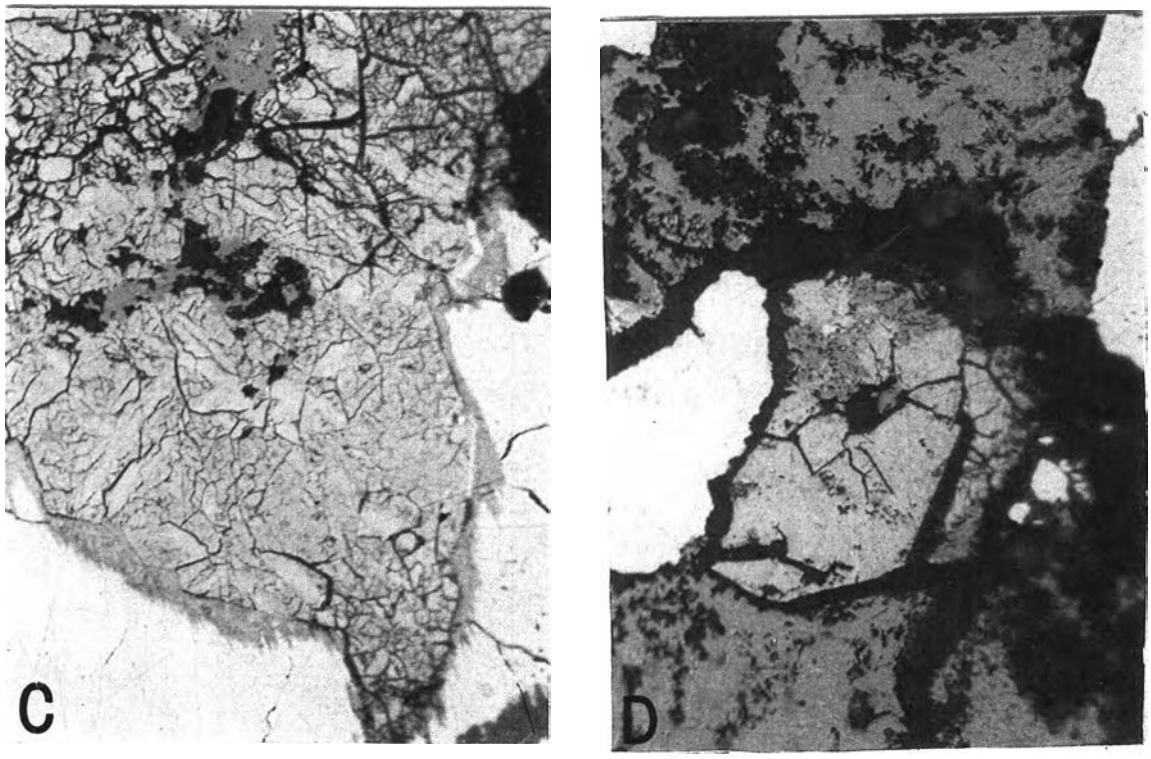

Most secondary pyrite of this suite has a pitted and rather ragged appearance (Fig. 5A). It occurs typically as large, compact, granular masses of fine- to very fine-grained pyrite with or without intergrown marcasite. Granoblastic masses of pyrite and marcasite often display conspicuously the inherited relict basal parting of medium- to coarse-grained pyrrhotite and contain sparse, tiny, ragged inclusions of relict pyrrhotite. The granoblastic masses of secondary pyrite and marcasite usually also contain disseminations (sometimes emulsions) of co-genetic minute magnetite granules, most of which do not exceed 5 microns in diameter. Also typical of supergene pyrrhotite replacement is the occurrence of extremely fine-grained melinkovite pyrite and marcasite as porous, sandy-looking, sieve-textured masses disposed in large concentric shells and making up the walls of coarse, cellular boxworks.

In summary, pyrrhotite was originally a major primary mineral that, together with chalcopyrite, constituted the bulk of assemblage 2 ore. Pyrrhotite has survived only as sparse minute shreds in secondary iron disulfides and as small globules armored by chalcopyrite.

Spectrographic trace element analyses of secondary pyrite (ex-pyrrhotite) separates from assemblage 2 ore reveal a relatively Ni-rich, Co-poor chemical signature (Ni greater

than 5000 ppm, Co less than 700 ppm) distinct from that of primary pyrite of assemblage 1 (Ni < 1500 ppm, Co up to 3000 ppm). Quantitative electron microprobe analysis shows that the Ni content of secondary pyrite is inhomogeneously distributed, commonly ranging from less than 0.5 to more than 2 wt percent within a 2 mm^2 area of fine-grained pyrite. Watmuff (1974, p. 206-208) has documented similar contrasts in Ni and Co contents of hypogene and supergene pyrite in a study of the weathered profile at the Mt. Windarra nickel deposit, Western Australia.

Violarite Secondary pyrite encloses very sparse blebs of violarite that have replaced pentlandite originally disposed as exsolved rods or lamellae in pyrrhotite. An electron microprobe analysis of violarite (Table 1) reveals an unusually Fe-rich composition and a metal:sulfur ratio closer to the 9:11 stoichiometry suggested by Desborough and Czamanske (1973) to be more typical of violarites than 3:4 stoichiometry.

Cu-Ni Thiospinel(?) A most interesting mineralogical feature of some samples of disseminated sulfide ore is a pale, neutral gray-white, optically isotropic mineral enclosed in and scattered along the margins of granoblastic secondary pyrite-marcasite masses. This mineral (Figs. 6C and D) comprises up to about 2 modal percent of some specimens. Electron microprobe analysis of several grains shows it to

Table 1. Electron microprobe analyses of minerals with Cu-Ni-Fe-Co-S compositions, New Rambler mine. Values in wt percent.

	Fe	Co	Ni	Cu	S	Total	Formula
Villamaninite							
grain 1	0.6	2.8	8.5	40.6	48.7	101.0	$(Cu_{.81}Ni_{.18}Co_{.06}Fe_{.01})_{1.07}S_{1.93}$
grain 2	0.5	2.5	8.9	38.9	49.1	99.9	$(Cu_{.78}Ni_{.19}Co_{.05}Fe_{.01})_{1.04}S_{1.96}$
Violarite	32.3	9.1	17.4	0.3	41.2	100.3	$(Fe_{4.98}Ni_{2.56}Co_{1.33}Cu_{.04})_{8.91}S_{11.08}$
Cu-Ni-thiospinel							
grain 1	9.1	4.3	18.7	30,2	38.1	100.4	$(Cu_{2.78}Ni_{1.86}Fe_{.96}Co_{.43})_{6.03}S_{6.97}$
grain 2	8.0	4.7	18.4	31.3	38.2	100.5	$(Cu_{2.88}Ni_{1.84}Fe_{.84}Co_{.46})_{6.02}S_{6.98}$
grain 3	8.7	4.0	18.1	30.6	38.1	99.4	$(Cu_{2.85}Ni_{1.82}Fe_{.92}Co_{.40})_{5.98}S_{7.02}$
grain 4	8.6	4.1	17.3	31.8	38.2	100.0	$(Cu_{2.95}Ni_{1.73}Fe_{.90}Co_{.41})_{5.99}S_{7.01}$
Cu-Ni Phase A							
grain 1	20.2	3.1	16.6	24.5	35.7	100.1	$(Cu_{.70}Fe_{.66}Ni_{.51}Co_{.10})_{1.97}S_{2.03}$
grain 2	22.6	4.5	12.2	25.7	35.5	100.4	$(Cu_{.74}Fe_{.74}Ni_{.38}Co_{.14})_{1.99}S_{2.01}$
grain 3	20.0	1.6	17.9	24.6	35.8	99.8	$(Cu_{.71}Fe_{.65}Ni_{.55}Co_{.05})_{1.97}S_{2.03}$

be a sulfide of Cu, Ni, Fe, and Co, in that order of abundance, yielding a stoichiometry very near $(Cu,Ni,Fe,Co)_6S_7$. X-ray structural studies will be done on this mineral after optical and physical investigations are completed on the three single-phase grains so far discovered. The stoichiometry and optical and textural characteristics of this mineral suggest it may be a metal-rich thiospinel. The tendency to non-stoichiometric, metal-rich compositions in low-temperature Ni-thiospinels has been discussed by Desborough and Czamanske (1973).

Characteristic textural features of the Cu-Ni thiospinel(?) include an orthogonal crosshatch intergrowth with variable amounts of a slightly darker, compositionally heterogeneous, but more Cu-rich material of the same qualitative composition (Fig. 6C). Also characteristic is the presence of a few large cracks that are usually also in an orthogonal arrangement, but rotated 45^{o} relative to the cross-hatching. Grain margins typically have cockscomb or fringe-like rims of the same phase, but the fringe generally is preferentially replaced by digenite or covellite (Fig. 6C). Secondary Cu sulfides also replace the main mass of the Cu-Ni thiospinel(?). Thin veinlets of pyrite may intervene between the fringed rims and the grains (Fig. 6C), and veinlet pyrite commonly occupies orthogonal cracks within

grains. The disposition of Cu-Ni thiospinel(?) in secondary pyrite is texturally reminiscent of typical pentlandite-pyrrhotite intergrowths in ores of some other deposits.

Watmuff (1974), in a discussion of supergene alteration of the Mt. Windarra nickel deposit of Western Australia, describes textural features identical to those reported above. By his account, Ni^{2+} released during violaritization of pentlandite migrates to the margins of adjacent pyrrhotite grains and displaces Fe, producing in the pyrrhotite thin tapering lamellae of violarite which in time coalesce to form continuous comb-structured margins around the pyrrhotite. Upon completion of pentlandite replacement by violarite, release of Ni^{2+} stops, and the remaining unreplaced pyrrhotite is abruptly replaced by nickeliferous pyrite + marcasite $\pm$ magnetite. Secondary pyrite appears as fillings along slightly parted ex-pyrrhotite and ex-pentlandite grain boundaries and occupies the large octahedral contraction cracks in violarite that were developed along pentlandite cleavage planes. When pyrrhotite replacement by supergene pyrite and marcasite is concluded, chalcopyrite is electrochemically destabilized, and copper is released in solution. Watmuff (1974, p.212) reports that violarite shows increasing enrichment in copper toward the top of the secondary enrichment zone. Close to the water table, some of the violarite,

particularly the comb- or fringe-structured violarite after pyrrhotite, shows varying degrees of replacement by secondary copper sulfides. In view of the strong similarity between the features just recounted and those of the Cu-Ni thiospinel(?) of the New Rambler ore, it is concluded that this phase originated from pentlandite, possibly via alteration of normal violarite, either through gradual Cu metasomatism of violarite or by direct replacement of violarite by a distinctly different Cu-Ni sulfide phase.

Other grains of Cu-Ni thiospinel(?) in supergene jasperoid matrix (Fig. 6D) lack the grid texture and compositional heterogeneity that characterizes complex grains of the type seen in Figure 6C. The simple-type grains may be products of direct supergene precipitation in sites of decomposing silicates rather than replacements of pentlandite. The microprobe analyses of Cu-Ni thiospinel(?) in Table 1 are for simple, unaltered grains of the type seen in Figure 6D.

No mineral of a chemical composition approaching $(Cu,Ni)_6S_7$ has previously been reported. Phase relations in the synthetic Cu-Ni-S system have been studied at high temperatures under dry conditions by Kullerud et al. (1969). In that investigation, villamaninite appeared below 503°, and is the only known ternary compound in the Cu-Ni-S system. Watmuff (1974, p.214) presents a microprobe analyses of an

incompletely described gray-white, optically isotropic Ni-Cu-Fe-Co-S mineral containing 39.4 to 41.1 wt percent S, 45.3 to 51.8 wt percent Ni, and up to 14.7 wt percent Cu, with minor Fe and Co. This mineral, which occurs as a supergene metasome of chalcopyrite in the Ni-rich Mt. Windarra deposit, approximates M_9S_{11} stoichiometry and may be a compositional variant of the Cu-Ni thiospinel(?) described here.

Merenskyite and related minerals Identifications of platinum and palladium minerals have been made on the basis of optical properties and quantitative electron microprobe analyses. Compositional data and qualitative optical characteristics indicate that at least one and possibly several Pd minerals of assemblage 2 constitute new mineral species. (Quantitative determinations of the structural and optical characteristics of the platinoid minerals are in progress.)

The hypogene platinoid mineral suite of assemblage 2 consists of sperrylite [$(Pd,Rh)As_2$], merenskyite [$(Pd,Pt)(Te,Bi)_2$], kotulskite [Pd(Te,Bi,Sb)], michenerite [(Pd,Pt)(Bi,Sb)Te], temagamite (Pd_3HgTe_3), and an unidentified mineral of composition $PdTe_2$. The palladium minerals occur as anhedral grains, usually 75-250 microns across, but occasionally exceeding 600 microns, enclosed in chalcopyrite or its derivative covellite and limonite (Figs. 7A and B, 8B), in secondary pyrite-marcasite-limonite masses (ex-pyrrhotite) (Figs. 7D,

8A and C), and in supergene silica that replaced metagabbroic silicates (Figs. 7C and 8D). As many as 15 aggregates of merenskyite-kotulskite-michenerite have been encountered in a single polished surface of less than 2 cm diameter. No palladium minerals have been seen in strongly oxidized ore from upper levels of the weathered zone.

The most abundant of these species is merenskyite, and it accompanies most occurrences of other platinoid minerals. In polished section, merenskyite is bright pure white. Under crossed nicols it shows moderate anisotropy with pinkish or bluish medium gray to dark gray-brown polarization colors. From microprobe analyses of nearly two dozen merenskyite grains from assemblage 2, a selection of eight representing the compositional average and range is presented in Table 2.

A mineral of composition $PdTe_2$ (Table 2) occurs as granular intergrowths with Bi-rich merenskyite (Fig. 7D and 8A). This mineral is provisionally termed Pd-phase C. According to Cabri (1972, p.11), $PdTe_2$ is the end member composition of merenskyite. However, the sharp grain boundary relations of Pd-phase C with Bi-rich merenskyite indicate that this $PdTe_2$ mineral is structurally as well as compositionally distinct. Unlike merenskyite, Pd-phase C has slightly lower reflectivity (Fig. 8A), is cream-colored, and in the three grains encountered, anisotropic effects under crossed nicols are weak.

Table 2. Electron microprobe analyses of merenskyite, moncheite, and Pd-phase C. Sample MR-83A is from assemblage 3; all others belong to assemblage 2. Values in weight percent. ND = analyzed, but not detected.

	Pt	Pd	Bi	Sb	Te	Total	Formula
Pd-phase C ($PdTe_2$)							
MR-18	ND	28.90	1.58	ND	69.67	100.15	$Pd_{.99}(Te_{1.99}Bi_{.02})_{2.01}$
MR-116	ND	27.67	4.66	ND	67.92	100.24	$Pd_{.96}(Te_{1.96}Bi_{.08})_{2.04}$
MR-132	ND	29.35	0.86	ND	70.35	100.57	$Pd_{1.00}(Te_{1.99}Bi_{.01})_{2.00}$
Merenskyite [$Pd(Te,Bi)_2$]							
MR-17	ND	27.22	17.89	ND	55.02	100.13	$Pd_{.99}(Te_{1.68}Bi_{.33})_{2.01}$
MR-18 grain 1	ND	27.09	17.70	ND	55.36	100.15	$Pd_{.99}(Te_{1.68}Bi_{.33})_{2.01}$
grain 2	ND	26.44	18.25	ND	55.24	99.93	$Pd_{.97}(Te_{1.69}Bi_{.34})_{2.03}$
grain 3*	0.73	27.72	24.79	ND	45.47	99.08	$(Pd_{1.05}Pt_{.02})_{1.07}(Te_{1.44}Bi_{.49})_{1.93}$
MR-60 grain 1	ND	28.06	12.47	0.23	59.39	100.15	$Pd_{1.00}(Te_{1.77}Bi_{.22}Sb_{.01})_{2.00}$
grain 2	3.86	24.39	18.75	0.36	52.88	100.23	$(Pd_{.91}Pt_{.08})_{.99}(Te_{1.64}Bi_{.36}Sb_{.01})_{2.01}$
MR-116*	ND	27.45	26.02	1.88	44.85	100.19	$Pd_{1.03}(Te_{1.41}Bi_{.50}Sb_{.06})_{1.97}$
MR-132*	ND	27.40	26.40	1.48	44.27	99.55	$Pd_{1.04}(Te_{1.40}Bi_{.51}Sb_{.05})_{1.96}$
MR-83A grain 1	19.90	13.49	17.23	ND	49.89	100.50	$(Pd_{.54}Pt_{.44})_{.98}(Te_{1.67}Bi_{.35})_{2.02}$
grain 2	21.67	12.25	19.71	ND	46.39	100.02	$(Pd_{.50}Pt_{.49})_{.99}(Te_{1.59}Bi_{.42})_{2.01}$
Moncheite [$Pt(Te,Bi)_2$]							
MR-83A grain 1	36.42	2.83	11.66	0.60	48.72	100.22	$(Pt_{.86}Pd_{.12})_{.98}(Te_{1.75}Bi_{.25}Sb_{.02})_{2.02}$
grain 2	36.45	2.82	11.68	ND	49.69	100.64	$(Pt_{.85}Pd_{.12})_{.97}(Te_{1.77}Bi_{.26})_{2.03}$

*These Bi-rich merenskyite compositions occur as granular intergrowths with Pd-phase C grains whose compositions are listed at the top of the table.

Fig. 7. A. Merenskyite (light gray) with kotulskite (darker gray) as lamellae exsolved along merenskyite (0001) cleavage (dark lines near top and bottom of grain; white is a scratch) and as exsolved partial rim (lower right). Matrix is chalcopyrite and secondary covellite (lower left) and supergene jasperoid (upper right). Assemblage 2. Sample MR-31X. X600. Reflected light, crossed nicols.

B. Complex intergrowth of Pd minerals. Dominand phase is Pt-bearing, Bi-rich merenskyite that includes several bodies of slightly whiter Bi-poor, Pt-absent "merenskyite" (top and along right side of aggregate). Dark gray round splotches are michenerite. Light gray irregular lamellae are exsolved kotulskite. Matrix is covellite (black) with a few relics of chalcopyrite (gray). Assemblage 2 massive chalcopyrite ore. Sample MR-60. X600. Reflected light. Oil imm. (Contrasts greatly enhanced photographically.)

C. Large rectangular grain of michenerite with a partial rim of sperrylite (upper left) and inclusions of kotulskite (bottom). Irregular white mass in lower left is merenskyite. Matrix (black) is supergene silica after metagabbro. Assemblage 2 disseminated ore. Sample MR-32B. X600. Reflected light.

D. Large elongate grain of michenerite (light gray) with attached merenskyite (white). A small grain of Pd-phase C ($PdTe_2$) within merenskyite is outlined by dots (upper right). Gray speck in michererite (center) is chalcopyrite. Gray porous masses in the upper left and lower right are supergene marcasite after pyrrhotite. Black is limonite and void. Blaubleibender covellite after chalcopyrite along lower right margin (dark gray, mottled). Assemblage 2. Sample MR-116. X160. Reflected light.

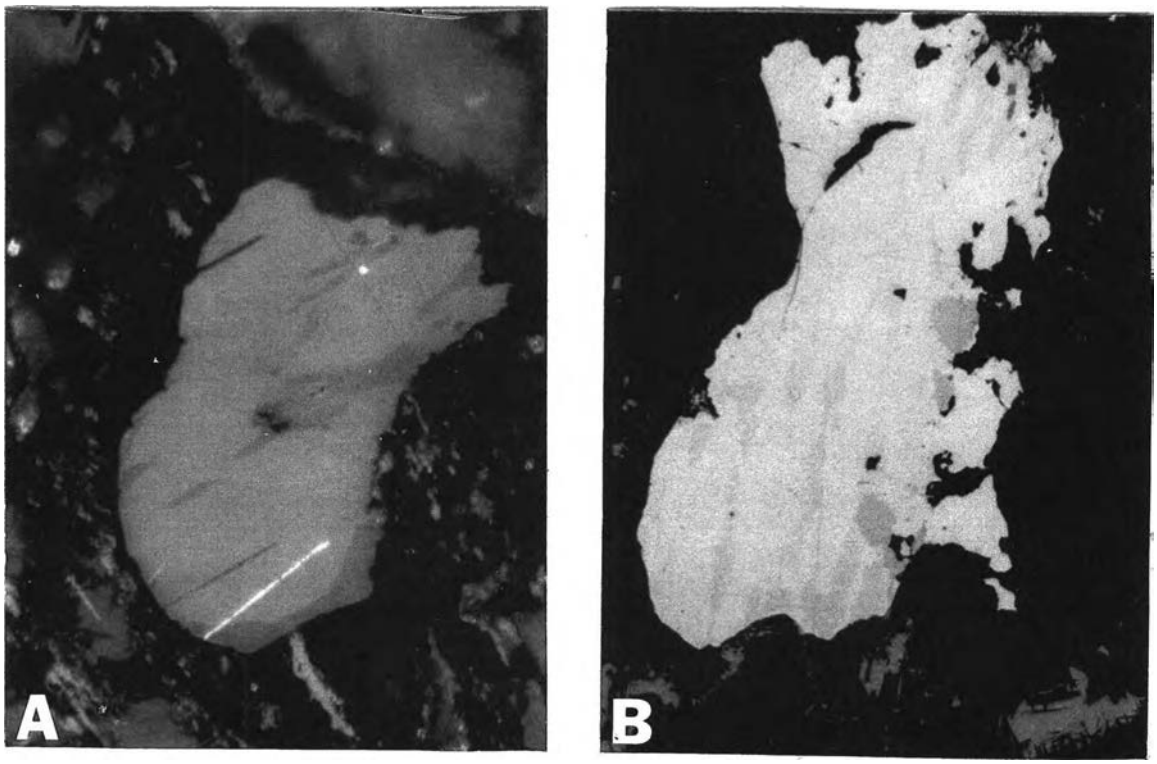

FIGURE 7

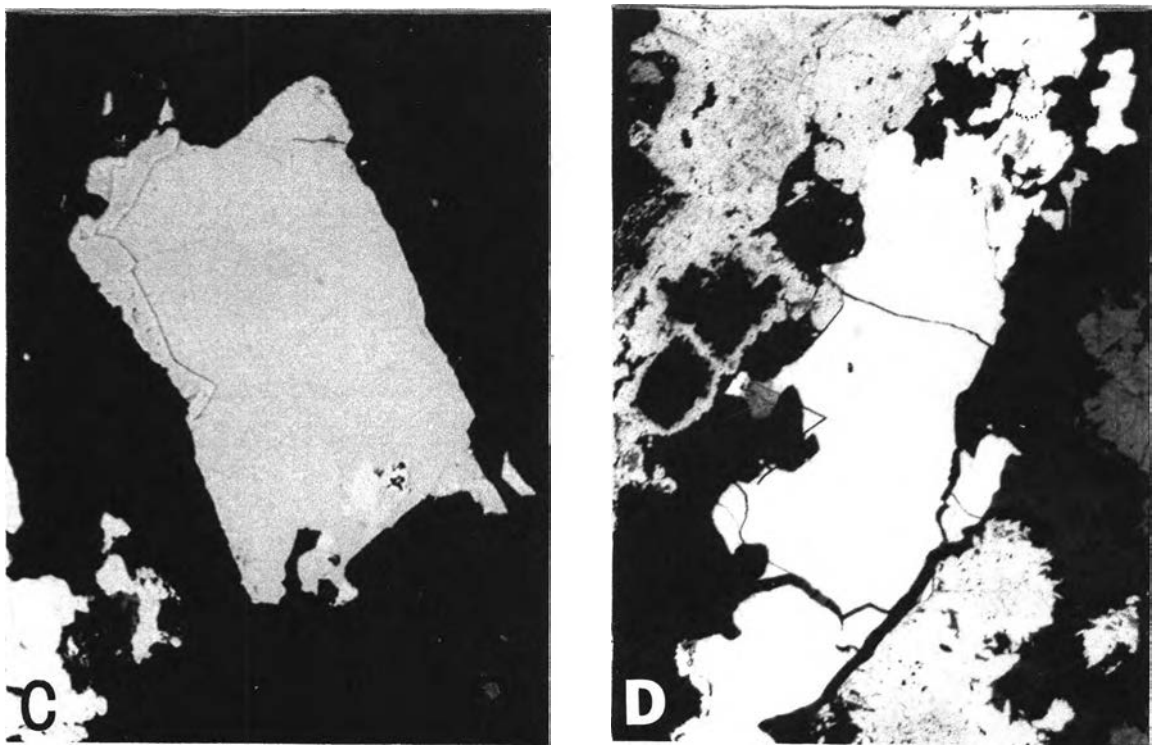

During microprobe analyses of the complex aggregate of Pd minerals in Figure 7B, it was found that the major phase is Pt-bearing merenskyite with a "normal" Bi content (i.e., about 18 wt percent) whereas the very white phase is a Pt-absent, relatively Bi-poor variant, which, judging from its very sharp grain contacts, is also structurally distinct from "normal" merenskyite. The composition of the Bi-poor phase is shown in Table 2, MR-60 grain 1. The available evidence from microprobe and optical data indicate that "merenskyite" is not a single mineral, but a complex family of minerals in the manner of "pyrrhotite."

Kotulskite Merenskyite almost invariably appears intergrown with subordinate but variable amounts of kotulskite. The latter is cream-white in color and has strong anisotropic effects under crossed nicols, with polarization colors similar to but somewhat brighter than merenskyite. Kotulskite commonly occurs as discontinuous lamellae oriented parallel to the excellent (0001) cleavage of merenskyite. The manner of this intergrowth is clearly indicative of kotulskite exsolution from a merenskyite host (Fig. 7A). Irregular corrugation lamellae of kotulskite in merenskyite (Fig. 7B) and kotulskite partial rims on merenskyite (Fig. 8B) are also interpreted as derived by exsolution. An experimental investigation of phase relations in the Pd-Bi-Te

system by Hoffman and MacLean (1976) has established that between $575^{\circ} \pm 10^{\circ}$ and $710^{\circ} \pm 10^{\circ}$C, solid solution between merenskyite and kotulskite is complete. The extent of the solid solution field at lower temperatures has not been defined. Five selected electron microprobe analyses of kotulskite grains, all from assemblage 2, are presented in Table 3.

Michenerite This mineral is a common associate of merenskyite and kotulskite, with which it occurs as granular intergrowths suggestive of independent penecontemporaneous deposition (Figs. 7B, C, D, and 8C). Michenerite (PdBiTe) is distinguished from other Pd-Bi-Te minerals by its lower reflectivity, gray-white tone, and optical isotropy. All the michenerite analyses (Table 3) indicate slight substitution of Te for Bi and Pd. Similar trends in the crystal chemistry of michenerite were found by Hoffman and MacLean (1976) in their investigation of the Pd-Bi-Te system. Pt-bearing michenerite was noted only in association with Pt-rich merenskyite or moncheite.

Pd-Phase D In moderately oxidized limonitic sulfide ore, michenerite is not uncommonly altered along grain margins to extremely fine-grained aggregates of a light coffee-brown mineral (Fig. 8C) that has reflectivity only slightly greater than goethite. In plane light it is weakly bireflectant from yellowish tan to pinkish tan,

Table 3. Electron microprobe analyses of temagamite, kotulskite, michenerite, and Pd-phase D. Values in weight percent. ND = not detected. Sample MR-83A is from assemblage 3; all others, assemblage 2.

		Pt	Pd	Bi	Sb	Te	Hg	Total	Formula
Temagamite	(Pd_3HgTe_3)								
MR-116		ND	34.56	ND	ND	41.65	22.73	98.94	$Pd_{2.97}Hg_{1.04}Te_{2.99}$
Kotulskite	[Pd(Te,Bi)]								
MR-18		ND	35.32	23.35	2.53	39.30		100.51	$Pd_{.86}(Te_{.80}Bi_{.29}Sb_{.05})_{1.14}$
MR-31G		ND	36.41	22.01	5.40	35.40		99.21	$Pd_{.89}(Te_{.72}Bi_{.27}Sb_{.12})_{1.11}$
MR-32B		ND	34.65	22.10	2.72	39.85		99.31	$Pd_{.85}(Te_{.81}Bi_{.28}Sb_{.06})_{1.15}$
MR-116		ND	37.12	24.33	0.83	38.02		100.30	$Pd_{.91}(Te_{.77}Bi_{.30}Sb_{.02})_{1.09}$
MR-132		ND	36.28	23.46	0.99	38.52		99.25	$Pd_{.89}(Te_{.79}Bi_{.30}Sb_{.02})_{1.11}$
Michenerite	(PdBiTe)								
MR-18		ND	24.19	41.13	0.69	33.81		99.82	$Pd_{.98}(Bi_{.85}Sb_{.02})_{.87}Te_{1.14}$
MR-25B		0.46	23.73	42.16	0.30	32.94		99.74	$(Pd_{.97}Pt_{.02})_{.99}(Bi_{.88}Sb_{.01})Te_{1.14}$
MR-32B		ND	24.25	40.17	0.78	34.85		100.05	$Pd_{.98}(Bi_{.82}Sb_{.03})_{.85}Te_{1.17}$
MR-60		ND	24.74	42.07	0.83	32.58		100.22	$Pd_{1.00}(Bi_{.87}Sb_{.03})_{.90}Te_{1.10}$
MR-83A	grain 1	1.76	23.17	43.97	0.60	30.87		100.37	$(Pd_{.95}Pt_{.04})_{.99}(Bi_{.92}Sb_{.02})Te_{1.06}$
	grain 2	1.63	23.35	39.95	2.56	32.115		99.59	$(Pd_{.94}Pt_{.04})_{.98}(Bi_{.82}Sb_{.09})_{.91}Te_{1.08}$
MR-116		ND	24.57	41.52	0.41	33.34		99.85	$Pd_{1.00}(Bi_{.86}Sb_{.01})_{.87}Te_{1.13}$
MR-132		ND	24.70	40.22	0.23	34.99		100.14	$Pd_{.99}(Bi_{.82}Sb_{.01})Te_{1.17}$
Pd-phase D	[$Pd(Te,Bi)O_3$] (?)						Oxygen	w/o oxygen	
MR-25B*		1.59	27.20	36.36	ND	20.20	14.38	85.62	$(Pd_{.85}Pt_{.03})_{.88}(Bi_{.59}Te_{.53})_{1.12}O_{3.00}$
MR-31E		1.17	30.13	32.92	ND	20.95	14.83	85.17	$(Pd_{.92}Pt_{.03})_{.95}(Te_{.53}Bi_{.51})_{1.04}O_{3.01}$

*This example occurs as an alteration rim on the analyzed michenerite of MR-25B listed above.

Fig. 8. A. Idioblastic supergene pyrite after pyrrhotite (medium gray) encloses a complex intergrowth of sperrylite (subhedral gray lath), merenskyite (near white), and Pd-phase C ($PdTe_2$) (slightly darker gray patches in merenskyite on either side of sperrylite). Black is supergene silica. Assemblage 2 disseminated ore. Sample MR-18. X600. Reflected light.

B. Merenskyite (white) with cleavage cracks is mantled by a thick rim of kotulskite (slightly grayer). The light gray knob at the upper left corner of the aggregate is temagamite. Matrix is chalcopyrite (gray) extensively replaced by digenite (dark gray) and limonite (black). Assemblage 2. Sample MR-116. X600. Reflected light.

C. Merenskyite (white) as a corrosively weathered grain intergrown with michenerite (slightly grayer, lower third of aggregate). Michenerite has a medium gray partial rim of Pd-phase D. Spongy limonite (dark gray) replaces secondary pyrite (light gray, top and right). Sample MR-25B. X160. Reflected light.

D. Merenskyite (near white) with irregular lamellae and specks of exsolved kotulskite (gray). Merenskyite encloses a small grain of electrum (white, adjacent to black hole). Matrix is jasperoid after metagabbro. Assemblage 2 disseminated ore. Sample MR-31K. X600. Reflected light.

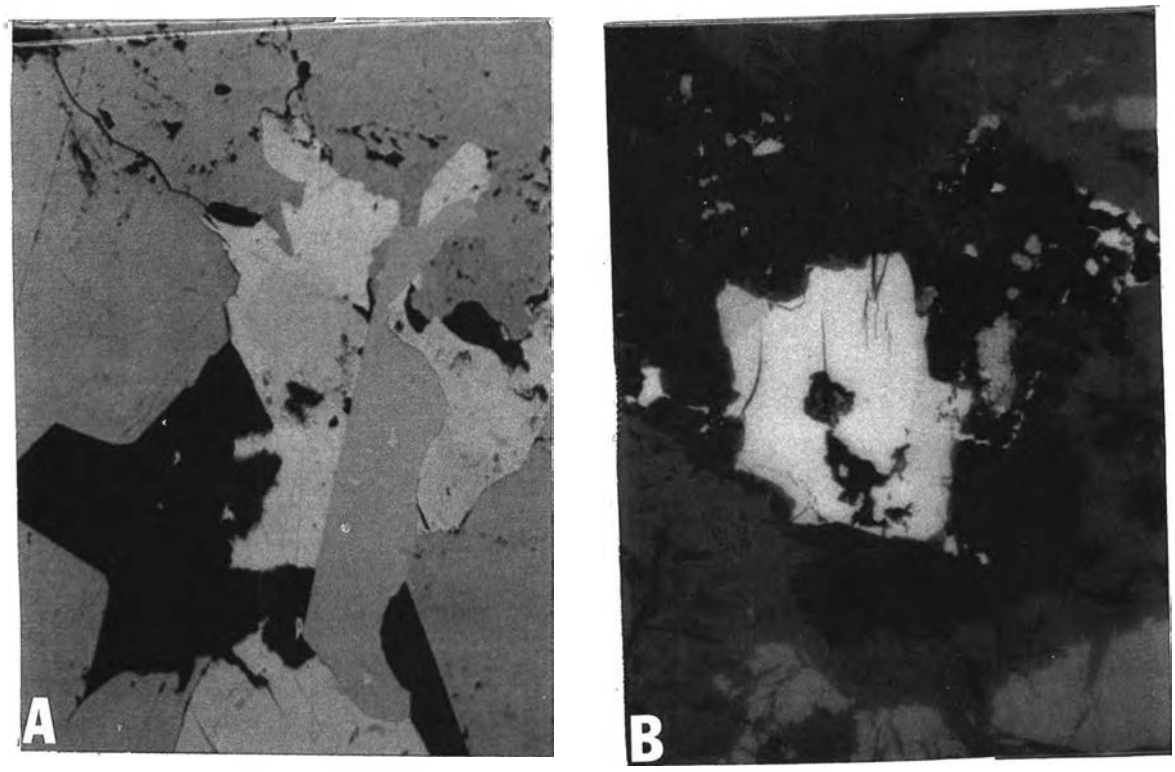

FIGURE 8

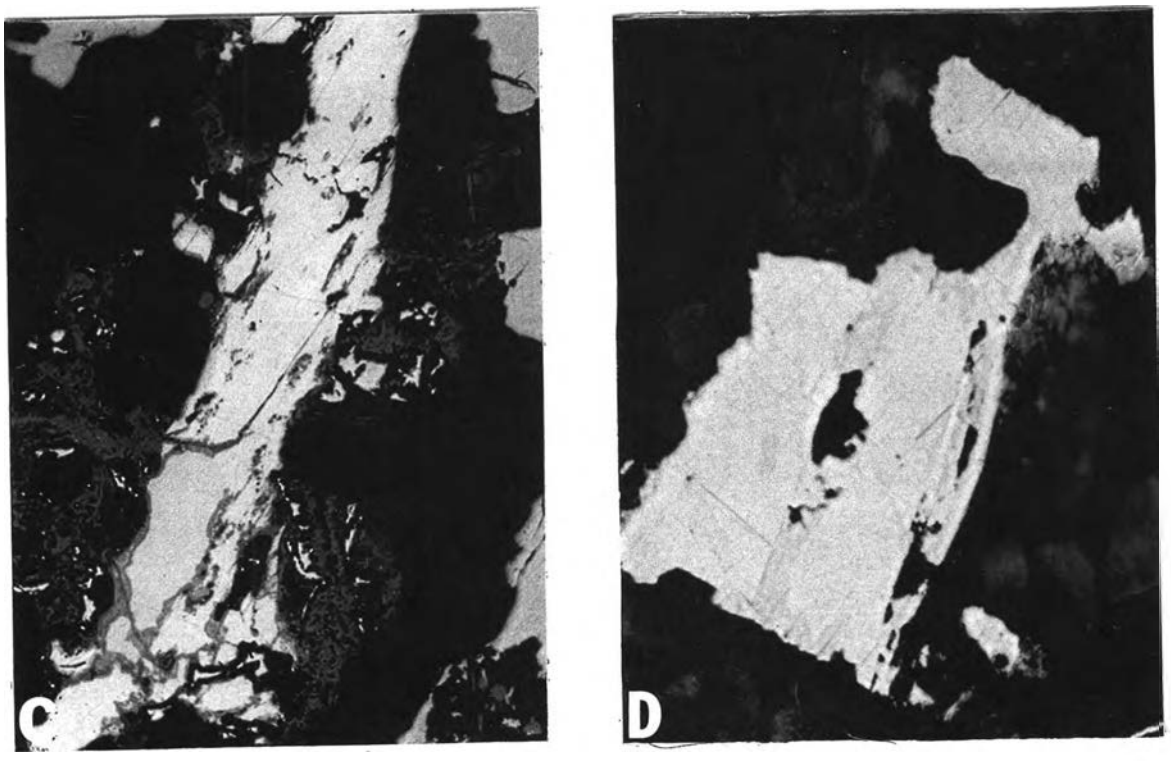

and anisotropic effects under crossed nicols are extreme, with bright yellow to dark blue and black polarization colors. The mineral has not been X-rayed, but optical properties suggest a layer-lattice structure similar to molybdenite, graphite, and covellite, which exhibit comparable extreme optical anisotropy. The rims of this phase on michenerite are in most cases too thin to yield reliable microprobe analyses, and the material shows variable degrees of crystallinity, as indicated by strength of anisotropic effects. Several of the larger, better crystallized aggregates of this mineral were analyzed by electron microprobe. Qualitative analysis on the multi-channel analyzer accessory to the electron probe showed only Pd, Bi, and Te. In most cases, quantitative analysis of Pd-phase D was preceded or followed directly by analysis of associated michenerite, and in each case the michenerite grains yield satisfactory analyses, whereas totals for analyses of Pd-phase D are consistently very low. Such low totals cannot be attributable to porosity of grains, but must be due to the presence of an unanalyzed element. The paragenesis of the mineral and its low reflectivity imply the missing element is oxygen. The energy of oxygen X-radiation is too low to permit detection by microprobe with available diffraction crystals. The most reliable analyses of the largest well crystallized

aggregates of Pd-phase D are presented in Table 3, and formulas are calculated on the assumption that the deficiency in the analysis is wholly attributable to oxygen in combination with Te and Bi, a simplistic assumption that does not consider the likelihood that the mineral is hydrated, in which case a stoichiometry akin to $(Pd,Pt)_2BiTeO_4 \cdot 2H_2O$ could be accommodated by microprobe data. No tellurites or tellurates of Pd have been reported previously, but a hydrated tellurate of Bi, montanite $[(BiO)_2(TeO_4) \cdot 2H_2O]$, is known as an alteration product of tetradymite (Bi_2Te_2S).

Temagamite A single 15 micron-wide grain of temagamite (Pd_3HgTe_3) occurs as an intergrowth with kotulskite and merenskyite (Fig. 8B). Relative to the latter minerals, temagamite has slightly lower reflectivity and is pale rose-tan with an orange cast. Anisotropic effects under crossed nicols are very weak in tones of gray. A microprobe analysis of temagamite is presented in Table 3. It is the only Hg mineral identified in New Rambler ores. Temagamite is known previously only from the Temagami copper deposit, Ontario, and was described initially by Cabri and La Flamme (1973).

Sperrylite Of the nine sperrylite grains encountered in 128 polished sections of sulfide ore examined, four grains

occur with assemblage 2--two intergrown complexly with merenskyite in massive sulfide ore (Fig. 8A), one as a partial rim on michenerite in supergene jasperoid (Fig. 7C), and another also in disseminated sulfide ore as an isolated grain in weathered metagabbroic matrix. Table 4 presents electron microprobe analyses of six sperrylite grains from the New Rambler deposit.

Electrum[1] Small grains of electrum, 10-100 microns across, are present as a rare trace accessory in assemblage 2, enclosed in jasperoid, sulfides, and merenskyite (Fig. 8D). Electrum in three samples of New Rambler ore was analyzed by electron microprobe (Table 5). Au, Ag, and Pd were sought in the analyses, but Pd was not detected in any of these samples. Ag values are homogeneously distributed in the grains. Optical examination of a grain in thoroughly oxidized ore showed a thin, porous partial rim of distinctly yellower gold over a pale embayed electrum grain.

Summary of Deposition Sequence in Assemblage 2 Textures of assemblage 2 ore mineral intergrowths suggest penecontemporaneous deposition of pyrite, pyrrhotite (or locally, Fe-Ni monosulfide solid solution--mss), chalcopyrite ss, electrum, michenerite, merenskyite ss, Pd-phase C, and

---

[1] Nomenclature of Hurlbut (1971, p.225) for Au-Ag alloys is employed; those containing more than 20 wt percent Ag are termed electrum.

Table 4. Electron microprobe analyses of sperrylite. Samples ABK-3 and MR-83A are from assemblage 3; others are from assemblage 2. Values in weight percent. ND = analyzed, but not detected.

		Pt	Rh	Pd	As	Sb	Te	Total	Formula
MR-18		53.68	0.13	0.95	44.31	ND	ND	99.08	$(Pt_{.94}Pd_{.03}Rh_{.004})_{.98}As_{2.02}$
MR-32B		54.61	0.31	ND	44.48	ND	ND	99.40	$(Pt_{.96}Rh_{.01})_{.97}As_{2.03}$
MR-83A	grain 1	55.64	0.09	ND	44.58	ND	ND	100.32	$(Pt_{.97}Rh_{.003})_{.97}As_{2.03}$
	grain 2	55.04	ND	ND	42.82	ND	1.73	99.59	$Pt_{.98}(As_{1.98}Te_{.05})_{2.03}$
	grain 3	55.79	0.18	ND	41.77	0.30	1.24	100.28	$(Pt_{1.01}Rh_{.006})_{1.02}(As_{1.94}Te_{.03}Sb_{.01})_{1.98}$
ABK-3		56.05	ND	ND	43.16	ND	ND	99.21	$Pt_{1.00}As_{2.00}$

Table 5. Electron microprobe analyses of electrum from New Rambler mine. Values in weight percent. Formula expressed as decimal fractions.

Sample	Au	Ag	Total	Formula
MR-31K (assemb. 2)	71.7	27.8	99.5	$Au_{.59}$ $Ag_{.41}$
MR-61 (assemb. 2)	71.3	28.9	100.2	$Au_{.57}$ $Ag_{.43}$
MR-83A (assemb. 3)	65.9	32.2	97.1 (porous grain)	$Au_{.53}$ $Ag_{.47}$

sperrylite, followed at lower temperatures by exsolution of kotulskite from merenskyite ss, of mackinawite and sphalerite from chalcopyrite ss, and, in disseminated and matrix ores, of pentlandite from mss (Fig. 2).

Some assemblage 2 ore is cataclastic and is veined by supergene pyrite, marcasite, and silica, but there is no evidence of primary sulfide recrystallization or hydrothermal neomineralization, the lack of which suggests the cataclastic effects may be relatively young--Laramide or Tertiary.

Assemblage 3

Samples belonging to this suite comprise about 15 percent of the ore collection. Although the major mineralogy of this assemblage is identical to that of assemblage 2, the accessory minerals, textural features, and weathering characteristics are distinctive.

Chalcopyrite Chalcopyrite shows extremely complex twinning. It is devoid of exsolved mackinawite, but sphalerite inclusions are as abundant as in assemblage 2, occurring in chalcopyrite as isolated tiny rods typically consistent in crystallographic orientation. Slightly larger equant grains of primary (non-exsolved) sphalerite are very rare. In addition, chalcopyrite of this suite typically contains Ni-bearing minerals as sparsely scattered specks, delicate filamentous bodies, lamellae (oriented parallel to sphalerite

rods), and complex, extremely fine-grained polymineralic inclusions, few of which exceed 75 microns in length.

Cu-Ni Phase A One sample of assemblage 3 massive chalcopyrite ore contains numerous irregular grains and wisps of a mineral (Fig. 9D) shown by electron microprobe analysis to be a sulfide of Cu, Fe, Ni, and Co. This mineral does not correspond to a known species and is provisionally referred to as Cu-Ni-phase A. Microprobe analyses of the three largest ($\pm$ 60 microns across) unaltered grains yet encountered are presented in Table 1. Analytical conditions and standards are described in the appendix. Cu-Ni-phase A is bright yellow with a weak apricot cast. Reflectivity in air is very similar to chalcopyrite but lowered somewhat in oil, and in oil the pinkish tone is enhanced. Polishing hardness is indistinguishable from chalcopyrite. The minute, irregular, commonly filamentous bodies are often located in the interiors of chalcopyrite grains and do not have a distribution along cracks or chalcopyrite grain margins suggestive of supergene origin, although the chalcopyrite host does show slight supergene replacement by digenite, chalcocite, and porous goethite containing calcite and native silver. An origin by hypogene exsolution seems possible.

In most occurrences, Cu-Ni phase A is intergrown with variable amounts of chalcocite, marcasite, and violarite(?)

Fig. 9. A. Electrum (white) as rim on chalcopyrite (light gray) and supergene digenite (medium gray) and as disseminated specks in supergene jasperoid (dark gray). Assemblage 3 disseminated ore. Sample MR-83A. X400. Reflected light.

B. Supergene native silver (white), that, together with supergene calcite (dark gray) occupies a solution cavity in oxidized ore of assemblage 3. Gray spherules in calcite are orbicular goethite. Goethite and chalcocite (both gray) replace chalcopyrite (light gray). Sample MR-89. X120. Reflected light.

C. Chalcopyrite (medium gray) encloses a complex aggregate of minerals including Cu-Ni-phase A (gray, about same shade as chalcopyrite, violarite(?) and chalcocite (both dark gray) and marcasite (lightest gray). Assemblage 3 massive chalcopyrite ore. Sample ABK-10A. X600. Reflected light. Oil imm.

D. Cu-Ni phase A (darker gray) as irregular partly filamentous mass in chalcopyrite (lighter gray). Black is void. Dark gray in upper right is digenite replacing chalcopyrite along a fracture. Assemblage 3 massive chalcopyrite ore. Sample ABK-10A. X800. Reflected light. Oil imm.

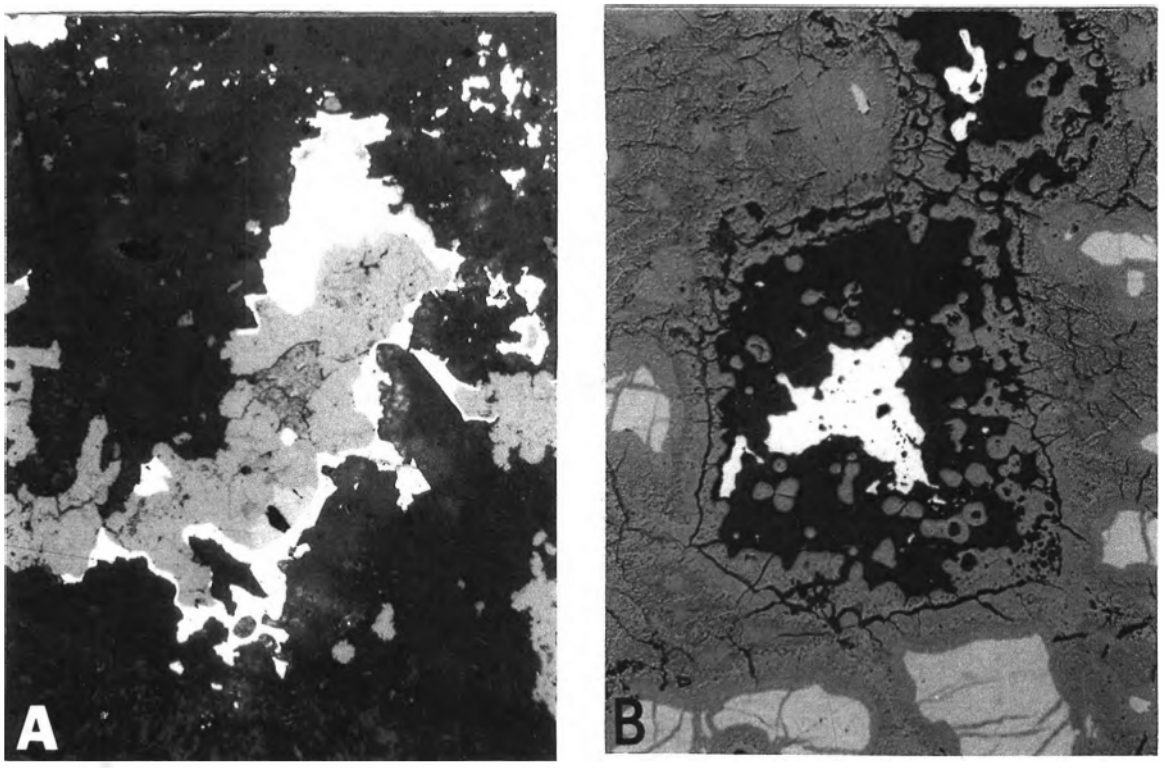

Figure 9

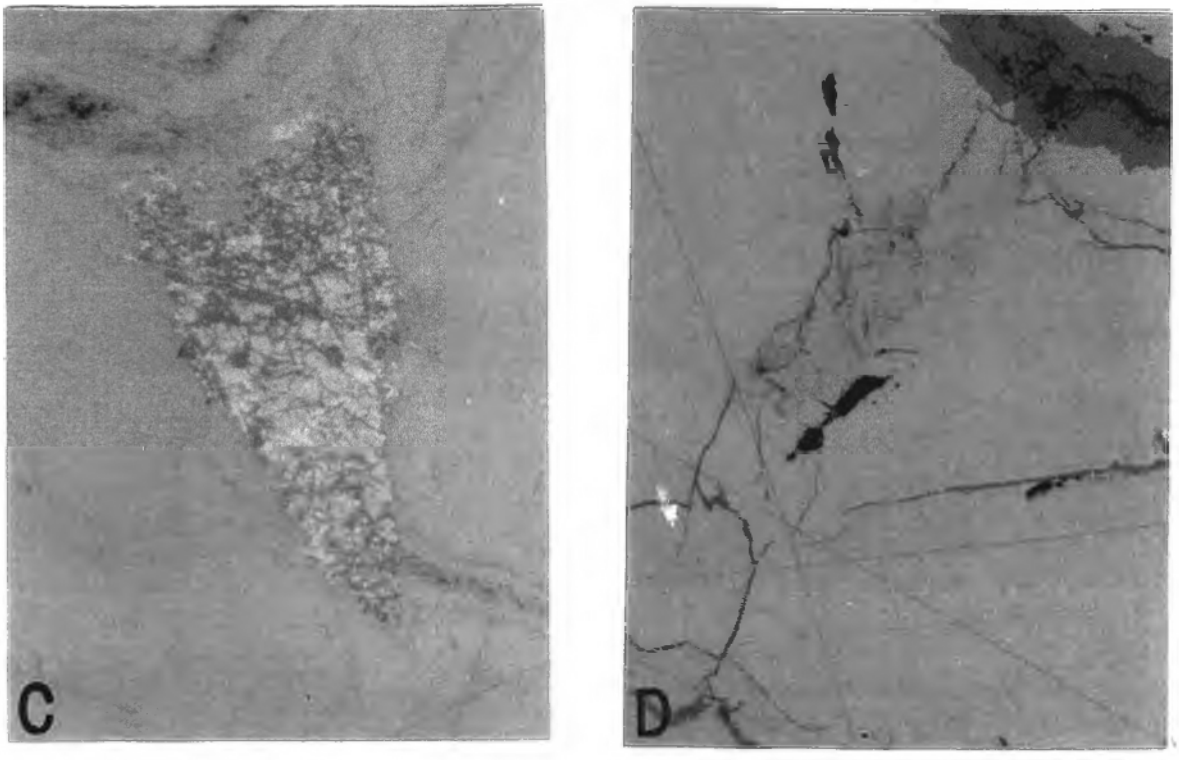

that are possibly its decomposition products (Fig. 9C). The dark material in Figure 9C is mostly a composite of bluish chalcocite and a violet-reddish brown phase shown by microprobe to be Ni-rich, but the intergrowths are invariably too fine-grained to resolve in quantitative analysis. Its color and apparent optical isotropy and the compositional and paragenetic considerations suggest the violet-brown mineral is violarite.

Hypogene Fe Minerals Other accessory minerals enclosed in chalcopyrite of assemblage 3 are magnetite as fresh to slightly martitized euhedra and primary pyrite as rare small euhedral to anhedral grains.

Secondary pyrite and marcasite with textural characteristics similar to those discussed previously for assemblage 2 are major constituents of assemblage 3. In many samples of this ore type, pyrrhotite has been replaced not only by marcasite and pyrite but by a variety of supergene Cu sulfides as well, including covellite, digenite, bornite, and chalcopyrite. These occur mostly as very fine-grained, porous, concentrically shelled, polymineralic "melinkovite" masses. Cu-Ni thiospinel(?) has replaced sparse pentlandite exsolved from pyrrhotite in assemblage 3 disseminated ore.

Silver Native silver is commonly visible in partially oxidized samples of assemblage 3. It occurs as fine flakes

dispersed sparsely through more or less well crystallized limonite and as larger grains enclosed in secondary calcite in supergene solution cavities (Fig. 9B). Microprobe scans of native silver show a small arsenic content but no trace of PGE, Au, or other metals.

The only hypogene silver mineral recognized in New Rambler ore is silver-poor electrum, which is far less abundant in assemblage 3 than native silver. Probably most of the Ag from which supergene native silver formed was liberated from solid solution in weathering chalcopyrite. The average Ag content of chalcopyrite, as determined by atomic absorption analyses of five chalcopyrite separates, is 62 ppm (J. Viets and J. Roybal, analysts, U. S. G. S.). Tests of Ag correlations with other elements in chalcopyrite-secondary pyrite ore yield the strongest correlation coefficient with Cu (r_s[Ag-Cu]=.668), indicating that chalcopyrite carried most of the Ag in primary ore.

Electrum Electrum is seen more frequently in assemblage 3 than in assemblage 2, usually intergrown with chalcopyrite or its Cu sulfide replacements (Fig. 9A). The mean Au content of 7 analyzed assemblage 3 bulk ore samples is 10 ppm; the mean Au content of 13 bulk samples of assemblage 2 ore is 1 ppm, as determined by combined fire assay-emission spectrographic analysis (R. R. Carlson and E. Cooley, analysts,

U. S. G. S.). Microprobe analysis of one electrum grain from assemblage 3 is shown in Table 5.

Pd-Phase A Two platinum and five palladium minerals constitute the platinoid suite of assemblage 3. By far the predominant platinoid mineral of this assemblage is an apparently new Pd-Pt-Te-Bi-Sb material provisionally termed Pd-phase A (Fig. 10A and B.) Representative electron microprobe analyses are presented in Table 6. Although its stoichiometry is similar to kotulskite, unlike other analyzed kotulskites, Pd-phase A is more metal-rich, it invariably contains Pt, and its optical and textural properties and weathering habit are distinctive. Pd-phase A is bright apricot-cream, with a reflectivity estimated visually at about 55-60 percent. A single cleavage is frequently visible, and the mineral shows parallel extinction. Anisotropy under crossed nicols is strong, with bright blue to medium olive-brown polarization colors. Pd-phase A occurs as small anhedral grains, typically 50-250 microns across, enclosed in massive chalcopyrite and in supergene replacements of chalcopyrite and pyrrhotite. A spongey texture is rather characteristic of Pd-phase A (Fig. 10B). The texture may be a primary feature or may be due to supergene leaching. Pd-phase A generally shows supergene alteration of variable degree to a dull gray-brown substance (the darker mottling

Fig. 10. A. Fresh Pd-phase A (long near-white grain) and weathered Pd-phase A (mottled). Dissolution of chalcopyrite host has left the Pd-phase A grains stranded in a solution cavity subsequently occupied by supergene calcite (dark gray) and native silver (white). Chalcopyrite (light gray, lower left margin) is rimmed by chalcocite (medium gray) and in turn a thicker rim of goethite limonite (slightly darker gray) that borders the calcite cavity and fringes the Pd-phase A grains. Assemblage 3 massive sulfide ore. Sample MR-89. X160. Reflected light.

B. Spongy mass of weathered Pd-phase A (light gray) that contains wisps and irregular bodies of Pd-phase B (darker gray). Black is void and a little limonite. Assemblage 3 massive chalcopyrite ore. Sample ABK-10A. X600. Reflected light. Oil imm.

C. Pd-phase B (white) as a corroded remnant of a formerly large subhedral grain enclosed in chalcopyrite. Limonite (dark gray) occupies part of solution cavity. Chalcopyrite (light gray) is extensively altered to supergene chalcocite (medium gray). Sample MR-89. X400. Reflected light.

D. Michenerite (medium gray) sandwiched between two grains of moncheite (near white). Jasperoid matrix. Assemblage 3 disseminated ore. Sample MR-83A. X400. Reflected light.

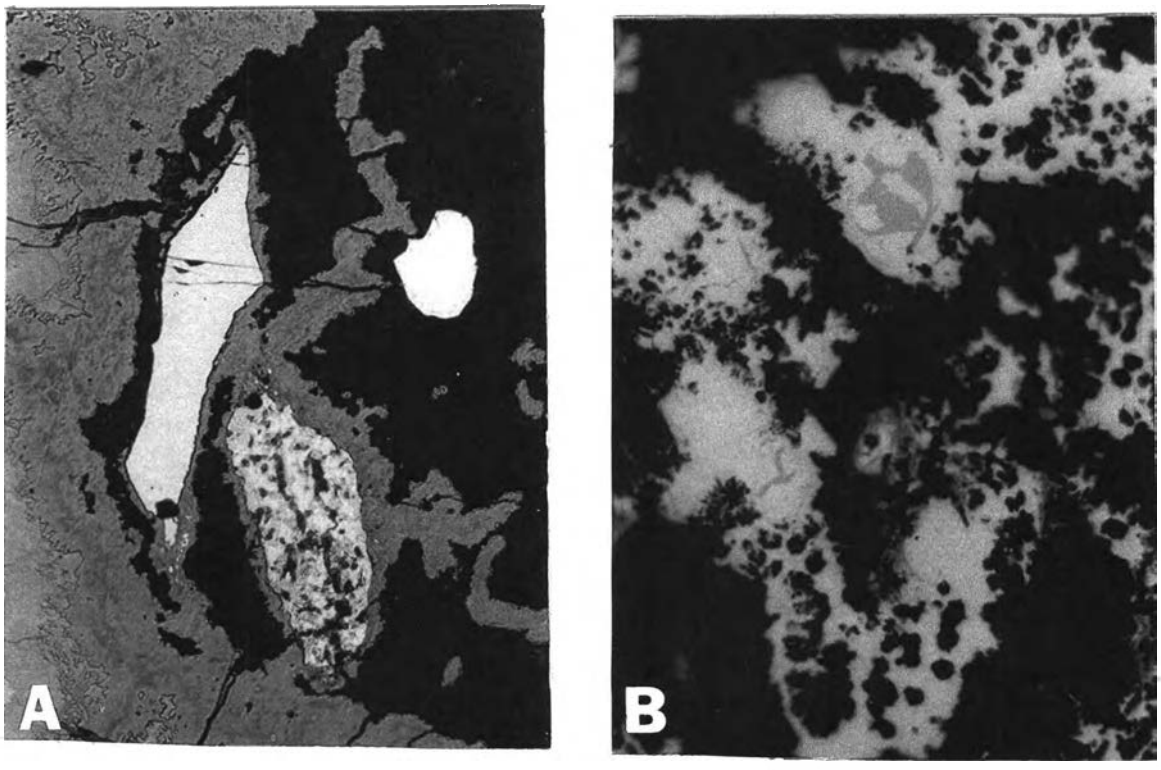

FIGURE 10

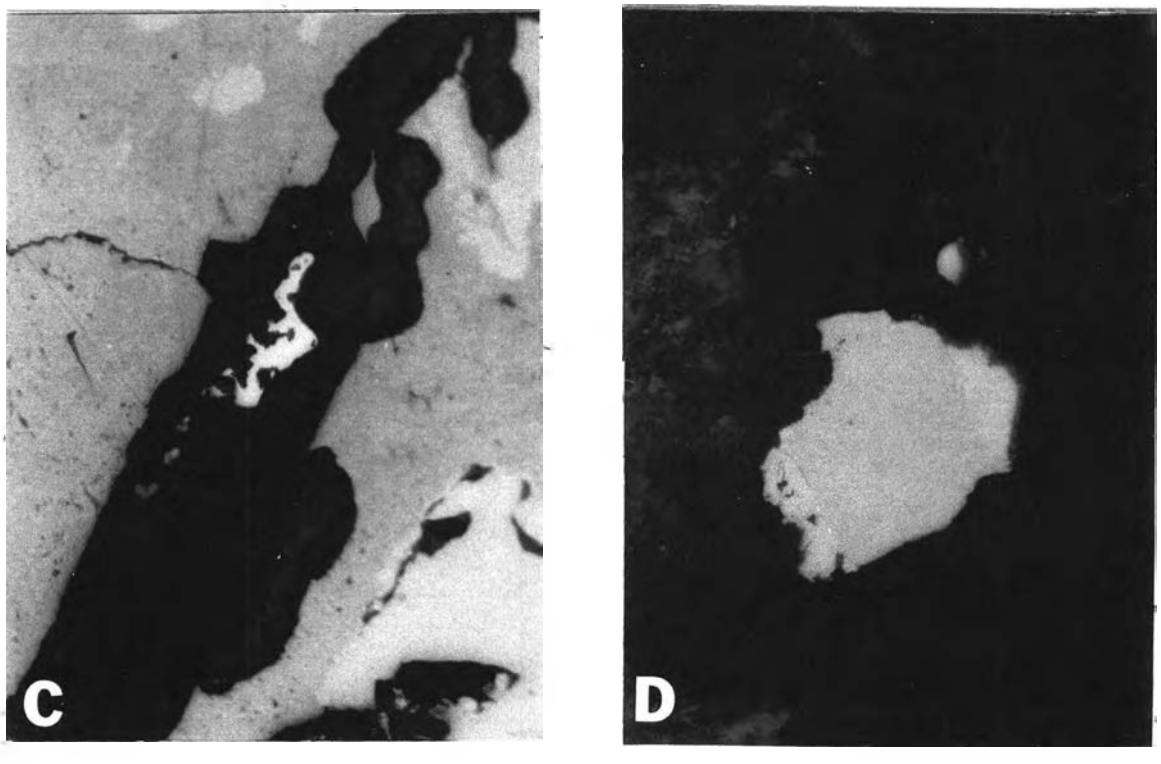

Table 6. Electron microprobe analyses of Pd-phase A and Pd-phase B. Values in weight percent. ND = not detected.

	Pt	Pd	Bi	Sb	Te	Total	Formula
Pd-phase A [Pd(Te,Bi)]							
MR-89	0.30	40.66	20.54	5.47	33.55	100.51	$(Pd_{.97}Pt_{.004})_{.97}(Te_{.67}Bi_{.25}Sb_{.11})_{1.03}$
ABK-10A	6.85	37.09	16.02	ND	40.76	100.05	$(Pd_{.90}Pt_{.08})_{.98}(Te_{.82}Bi_{.20})_{1.02}$
Pd-phase B $[Pd_5(Te,Bi)_2]$							
MR-89	ND	63.22	15.27	2.32	18.61	99.42	$Pd_{5.00}(Te_{1.23}Bi_{.61}Sb_{.17})_{2.00}$
ABK-10A	0.84	63.40	13.51	2.16	19.14	99.05	$(Pd_{5.01}Pt_{.04})_{5.04}(Te_{1.26}Bi_{.54}Sb_{.15})_{1.95}$

material in Figure 10A) that microprobe analysis shows to be an inhomogeneous, compositionally complex material containing appreciable Pd, Bi, and Te, but also much Cu and Fe. Microscopic inspection suggests that the alteration material is either amorphous or a mixture of several minerals with grain size below the limits of optical resolution.

Pd-Phase B Some Pd-phase A contains tiny inclusions of a slightly darker peach-buff-colored new Pd-Te-Bi-Sb mineral referred to as Pd-phase B. Microprobe analyses (Table 6) indicate the stoichiometry $Pd_5(Te,Bi,Sb)_2$, suggesting it may be the Te-Bi analogue of stibiopalladinite (Pd_5Sb_2). The mineral has been identified in four samples, in three cases as minute intergrowths with Pd-phase A in a texture suggestive of unmixing (Fig. 10B). The fourth occurrence is apparently a weathered relic of what was originally a large subhedral grain of that phase (Fig. 10C). Except where seen in direct contact, Pd-phase B is virtually indistinguishable from Pd-phase A. Both have similar color and optical properties, although anisotropic effects in Pd-phase B are less conspicuous.

Michenerite and Merenskyite-Moncheite Michenerite, merenskyite, and kotulskite, the most common Pd minerals of assemblage 2, are relatively rare in assemblage 3. Pt-bearing michenerite occurs in this assemblage in association

Fig. 11. A. Grains of compositionally intermediate moncheite-merenskyite (large white grain and about half the white specks) and grains of michenerite (also white) disseminated in supergene digenite (light gray) and blaubleibender covellite (medium gray). Dark gray is jasperoid after metagabbroic silicates. Assemblage 3 disseminated ore. Sample MR-83A. X160. Reflected light.

B. Euhedral sperrylite in supergene jasperoid (mottled dark gray). An irregular mass of supergene blaubleibender covellite (various shades of medium gray) has replaced chalcopyrite. Sample MR-83A. X400. Reflected light.

C. Scanning electron micrograph of sperrylite crystal showing well developed octahedron and cube faces. Assemblage 3. X1400.

D. Scanning electron micrograph of sperrylite crystal showing typical distorted octahedron form. X2400.

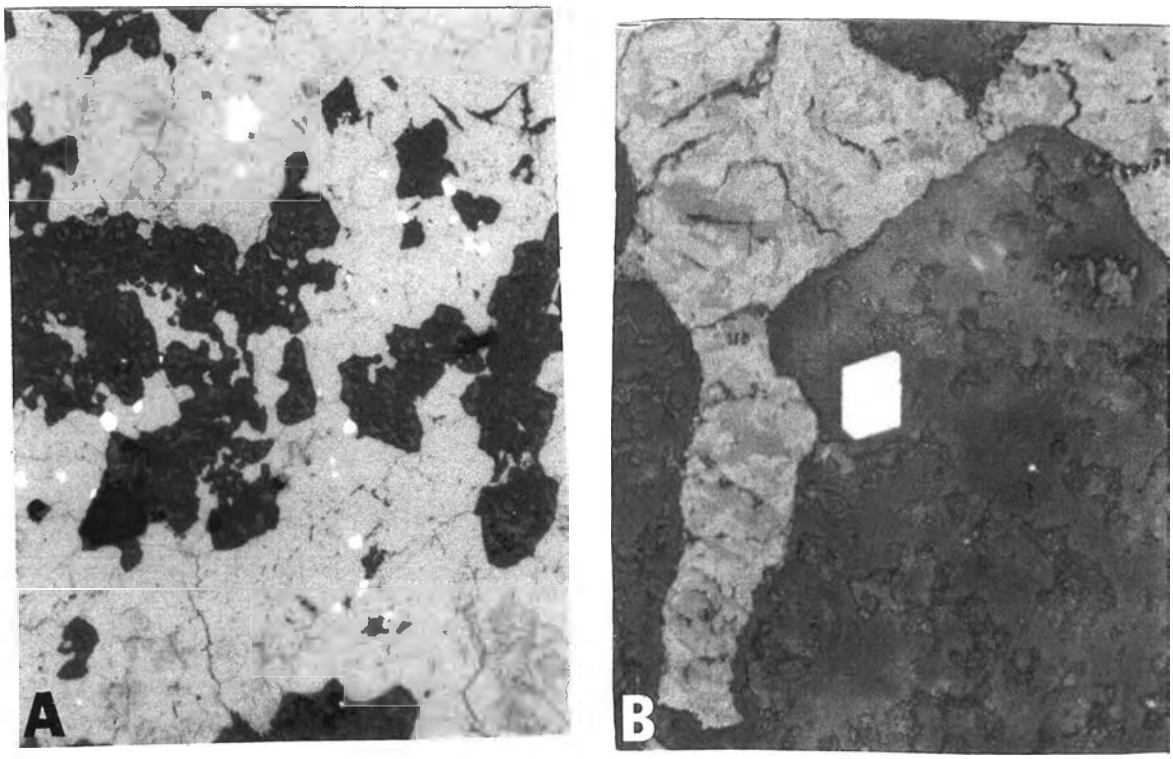

Figure 11

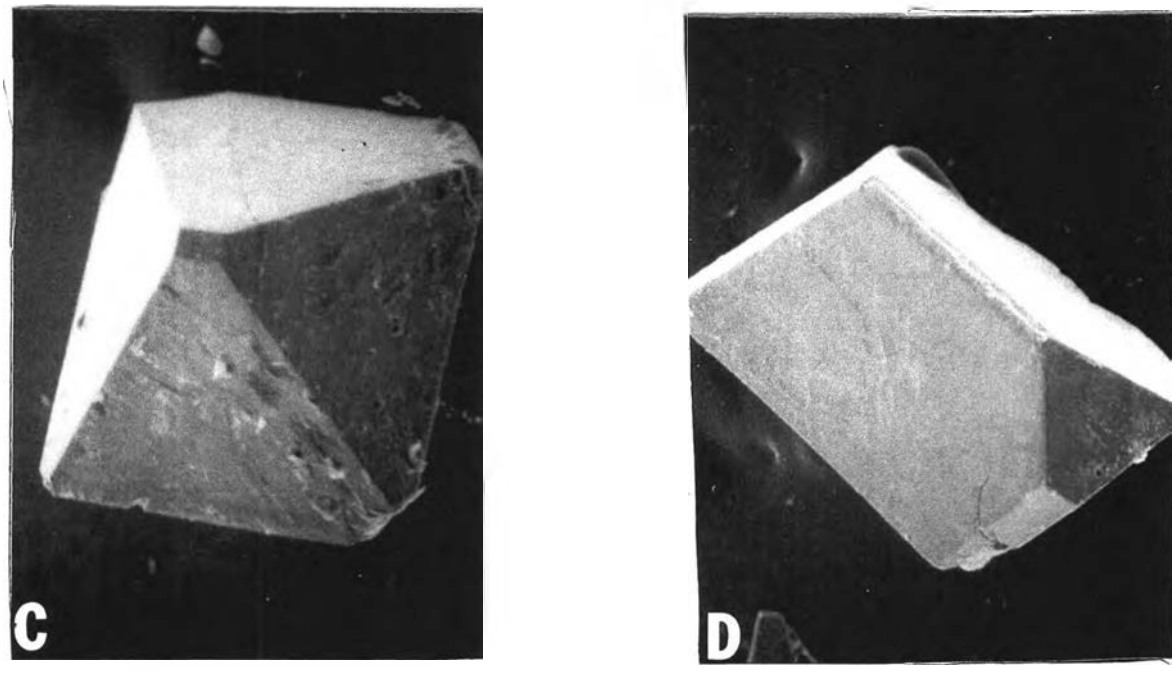

with Pt-rich merenskyite (Fig. 11A) and moncheite [$Pt(Te,Bi)_2$] (Fig. 10D).

Kingston (1969, p.829) has suggested on the basis of structural similarity and compositional data of natural minerals that a solid solution series extends from merenskyite to moncheite. Phase relations have apparently not been investigated in the synthetic Pt-Pd-Te(-Bi) system, but microprobe analyses of merenskyite and moncheite from one sample of assemblage 3 disseminated ore confirm extensive solid solution between the two minerals.

Moncheite is pure white and optically indistinguishable from merenskyite. Like merenskyite, it was encountered in assemblage 3 ore as isolated anhedral grains disseminated in supergene jasperoid (texturally pseudomorphous after metagabbro), as intergrowths with platinian michenerite (Fig. 10D), and as disseminations in supergene digenite-covellite aggregates that have replaced the primary chalcopyrite matrix.

Sperrylite Subhedral-euhedral sperrylite occurs as inclusions in Pd-phase A and more commonly as sparse disseminations in supergene jasperoid (Fig. 11B). Te-bearing sperrylites (analyses in Table 4) occur as single euhedra isolated in jasperoid matrix, without intergrown telluride minerals. The crystal forms of sperrylite grains obtained by acid digestion of ore are shown in scanning electron micrographs

in Figure 11C and D. Far more typical than the well developed octahedron-cube form of Figure 11C are distorted octahedra of the type seen in Figure 11D.

Molybdenite A single grain of molybdenite (MoS_2) was seen complexly intergrown with merenskyite in assemblage 3 massive chalcopyrite ore (identity of molybdenite confirmed by microprobe), and a few tiny flakes of molybdenite were identified by X-ray powder diffraction in otherwise totally oxidized assemblage 3 ore. Most ore samples analyzed (by U. S. G. S. chemists) contain less than 20 ppm Mo (100 ppm maximum).

Summary of Assemblage 3 Paragenetic Relations The deposition sequence of hypogene minerals of assemblage 3 appears to be (1) magnetite and pyrite; (2) penecontemporaneous formation of chalcopyrite ss, pyrrhotite or mss, electrum, sperrylite, moncheite, merenskyite ss, michenerite, Pd-phase A ss, and Pd-phase B; and (3) exsolution of pentlandite from mss, of sphalerite and Cu-Ni phase A from chalcopyrite ss, of kotulskite from merenskyite ss, and Pd-phase B from Pd-phase A ss. The available specimens of this assemblage have not been affected by cataclasis. The noncataclastic state and the distinctive accessory mineral suite and weathering characteristics of assemblage 3 ore suggest

that it may have come from a different ore shoot than assemblage 2.

Quartz-Carbonate Fissure Veins

Several tens of feet east of the ore pods, fissure veins were encountered in the mine workings. Material from the fissure veins collected on the mine dump consists principally of milky quartz (mostly massive but some with crystal druses), abundant calcite and siderite, traces of purple fluorite, and limonite probably derived from pyrite. A report by the U. S. Bureau of Mines (1942) states that little ore was encountered along fissure veins. The paragenetic relation of the fissure veins to the main mineralization event is unresolved.

Temperatures of Ore Deposition

Most standard geothermometry techniques are inapplicable to New Rambler ore because of the complex ore history. Hydrothermal quartz is unsuitable for fluid inclusion studies due to very fine grain size or cataclastic effects. Pervasive weathering effects preclude sulfur isotope thermometry. However, applications of thermochemical data on conditions of ore mineral compatibilities permit meaningful inferences to be drawn regarding the general range of ore deposition temperatures in this deposit.

Of particular interest in this regard are the bi-mineralic pyrrhotite-chalcopyrite inclusions in primary pyrite of assemblage 1 (Fig. 5B).[1] Pyrrhotite is about as abundant in the inclusions as chalcopyrite. The fact that the majority of the inclusions are visibly composite implies that most of the remainder are also bi-mineralic in the third dimension, which strongly suggests that the chalcopyrite and pyrrhotite in these inclusions are the disproportionation products of a once homogeneous phase poikilitically included in the pyrite. Heating experiments were not applicable to New Rambler ore samples due to the prevalence of limonitic oxidation of pyrrhotite in these inclusions (black spots in Fig. 5B). However, in heating experiments conducted by Won Park (pers. comm., 1975) of Kennecott Corporation on similar chalcopyrite-pyrrhotite blebs in hydrothermal pyrite, the chalcopyrite + pyrrhotite homogenized near 325°C.

Examination of phase stability diagrams for the Cu-Fe-S system (Yund and Kullerud, 1966; Craig and Scott, 1974; Sugaki et al., 1975) at temperatures below 500°C (as required by the wallrock alteration mineral assemblages) reveals

---

[1] A few larger pyrrhotite inclusions containing pentlandite, usually without associated chalcopyrite (Fig. 5C), apparently represent traces of mss included poikilitically in the pyrite as a co-precipitated phase.

Fig. 12. A. Phase relations in a selected portion of the Cu-Fe-S system at 350°C (after Sugaki et al., 1975, Fig. 3). At this temperature pyrite coexists stably with iss of cubanite composition. Abbreviations: chalcopyrite, cp; intermediate solid solution, iss; cubanite, cb; pyrrhotite, po; pyrite, py.

B. Phase relations in the same portion of the Cu-Fe-S system at 300°C (after Sugaki et al., 1975, Fig. 7). Stable coexistence of pyrrhotite with iron-rich chalcopyrite is permitted at this temperature by replacement of the py-iss(cb) tie line of Figure 6A by the cp-mpo tie line. Abbreviations: monoclinic pyrrhotite, mpo; hexagonal pyrrhotite, hpo.

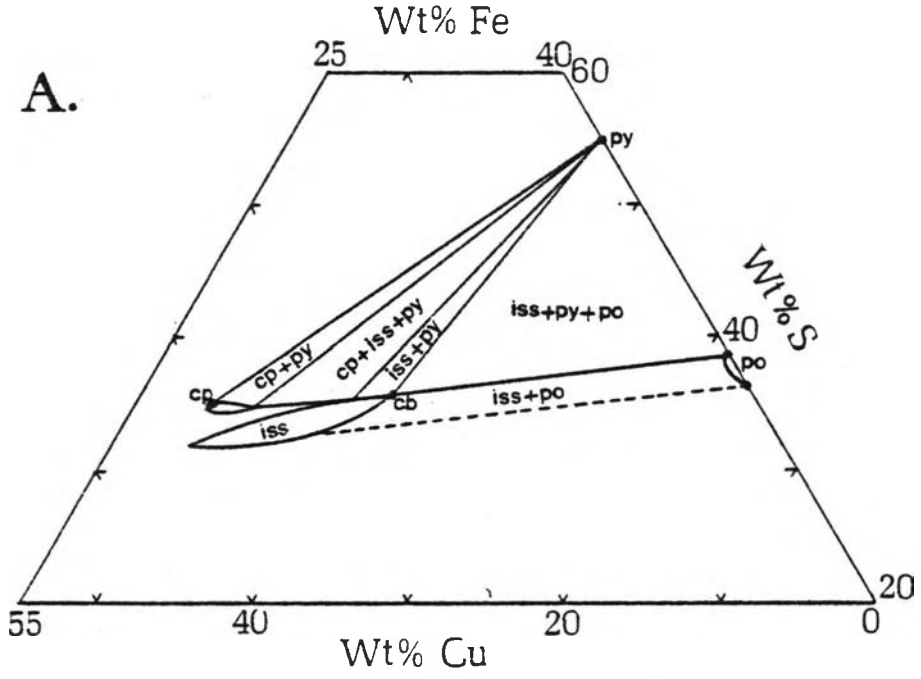
A.
Wt% Fe
25
40
60
py
Wt% S
40
20
cp+py
cp+iss+py
iss+py
iss+py+po
cp
cb
po
iss+po
iss
55
40
20
0
Wt% Cu

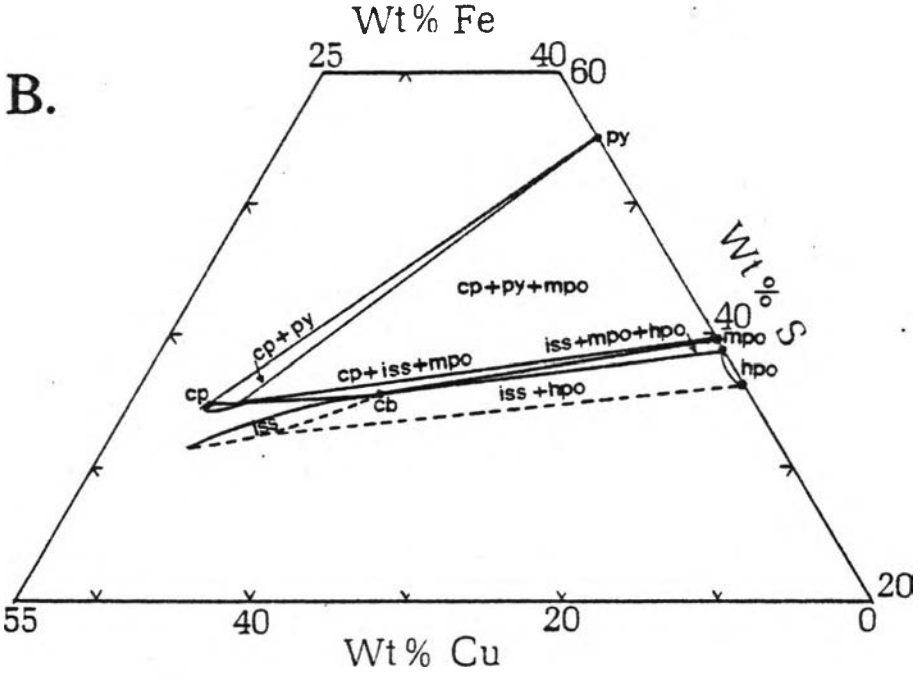
B.
Wt% Fe
25
40
60
py
Wt% S
40
20
cp+py+mpo
cp+py
iss+mpo+hpo
mpo
cp+iss+mpo
hpo
cp
cb
iss+hpo
iss
55
40
20
0
Wt% Cu

that the only phase that coexists stably with pyrite and is compositionally intermediate between chalcopyrite and pyrrhotite is the cubic intermediate solid solution (iss) phase present in the central portion of the system Cu-Fe-S at intermediate to high temperatures. Experimental studies by Yund and Kullerud (1966) and Kullerud et al. (1969) have shown that at temperatures from 743°C to 334°C pyrite coexists stably with cubic iss of composition very near that of cubanite (Fig. 12A). The tie line between these two phases precludes stable coexistence of pyrrhotite and chalcopyrite compositions in the 743°-334°C temperature interval. At 334° ± 15°C the tie line between pyrite and cubic iss of cubanite composition is broken, and chalcopyrite + pyrrhotite becomes a stable assemblage (Yund and Kullerud, 1966, p.476), (Fig. 12B). Additional, although inconclusive, data presented by Yund and Kullerud (1966, p.476) place this tie line change at 328° ± 5°C.

Therefore, if the bi-mineralic inclusions in pyrite of assemblage 1 are the disproportionation products of a homogeneous phase, as indicated by results of heating experiments cited above, then cubic iss of cubanite composition is the only reasonable parental candidate. (Orthorhombic cubanite exists stably only at temperatures below 200°-215°C--Cabri et al., 1973). These inferences require that:

(1) sulfide assemblage 1, consisting of magnetite (relict) + pyrite + mss + iss of cubanite composition, was deposited at temperatures above ~334°C; (2) the iss inclusions in pyrite disproportionated to chalcopyrite + pyrrhotite at or below that temperature; (3) the medium- to coarse-grained chalcopyrite-pyrrhotite (-pyrite-platinoid) ore of assemblages 2 and 3 was deposited below ~334°C.

The strong corrosional rounding and embayment of assemblage 1 pyrite (with abundant bi-mineralic inclusions) enclosed by secondary pyrite (ex-pyrrhotite) in an ore sample mineralogically transitional between assemblages 1 and 2 (Fig. 5A) can be accounted for by one of two alternative hypotheses: (1) an interval of sulfide dissolution intervened between deposition of the highly pyritic sulfide assemblage 1 and the chalcopyrite-pyrrhotite ore of paragenetically younger assemblages; or (2) the corrosion of the pyrite is due to solid state reactions following sulfide deposition.

The likelihood of the latter alternative is supported by considerations regarding distribution of accessory hypogene pyrite of a later generation (without inclusions) in typical ore of assemblage 2. Small, euhedral pyrite grains are present enclosed in chalcopyrite of assemblage 2 in amounts commonly exceeding 1 modal percent, but a

determined search failed to disclose any hypogene pyrite grains in secondary pyrite (ex-pyrrhotite) of this assemblage. Hypogene and supergene pyrite are easily distinguishable where seen in contact in the association transitional between assemblages 1 and 2 (Fig. 5A). Mutual inclusion and intergrowth relationships indicate that chalcopyrite and pyrrhotite of assemblage 2 are paragenetically contemporaneous. It is suspected that pyrite cubes of the type enclosed in chalcopyrite were initially enclosed within paragenetically contemporaneous pyrrhotite as well, but that they were resorbed (at least beyond recognition, if not entirely) by pyrrhotite upon transformation from a hexagonal to a monoclinic structure.

With decreasing temperature, the composition of hexagonal pyrrhotite in equilibrium with pyrite assumes increasingly iron-rich, sulfur-poor compositions, reaching a maximum Fe:S ratio near the temperature of the hexagonal-monoclinic transformation. (See Craig and Scott, 1974, for a summary of data pertaining to the pyrite-pyrrhotite solvus.) The composition of monoclinic pyrrhotite in equilibrium with pyrite is more sulfur-rich, and on transformation from hexagonal to monoclinic structure, pyrrhotite may adjust its composition by reaction with pyrite (Kullerud et al., 1969, p.357). These authors suggest that this reaction may be

responsible for corrosion of pyrite associated with monoclinic pyrrhotite in Sudbury ores. The temperature of the hexagonal-monoclinic transformation has been subject to considerable uncertainty, but Taylor (1969) found that this transformation was reversible at $292^{\circ} \pm 4^{\circ}C$ for pyrrhotite of composition Fe_7S_8, and Sugaki et al. (1975) have synthesized monoclinic pyrrhotite coexisting with pyrite at $300^{\circ}C$ in hydrothermal experiments believed by them to represent equilibrium conditions. These lines of evidence suggest that pyrrhotite in massive sulfide ore of assemblage 2 was probably deposited as hexagonal pyrrhotite at temperatures between $\sim 300^{\circ}$ and $\sim 334^{\circ}C$. (Similar considerations should apply to sulfide assemblage 3 as well, but oxidation of pyrite in that assemblage has destroyed most of the evidence for this argument.) Primary pyrite is sparse to absent from Cu-Ni thiospinel (ex-pentlandite)-bearing specimens of disseminated ore, and chalcopyrite of this association is markedly impoverished in sphalerite and particularly in mackinawite exsolution bodies. These features suggest dwindling deposition of pyrite with diminishing temperature.

In conclusion, thermochemical data applicable to the mineral association magnetite (relict) + pyrite + mss + iss of cubanite composition in assemblage 1 indicate development of this assemblage at temperatures somewhat (but probably

not far) above ~334°C; similar considerations require that the hypogene assemblage chalcopyrite ss + Ni-bearing pyrrhotite + accessory pyrite + platinoid minerals of assemblages 2 and 3 were deposited below ~334°C, but probably above ~300°C. Disseminated and matrix ore of assemblages 2 and 3 (mss + chalcopyrite ss + accessory platinoid minerals) may have been deposited within or below this ~334°-300°C temperature interval. Naldrett et al. (1967) showed that at temperatures as low as 300°C pyrrhotite readily accepts in excess of 15 wt percent Ni into solid solution; Ewers (1972, p.24) has demonstrated that nickel is taken up by pyrrhotite at temperatures above 200°C. Thus, initial Ni contents of 3-5 wt percent in mss of some ore samples cannot be taken as an indication of relatively high deposition temperature.

Considerations Regarding Genesis of the New Rambler Deposit

Two hypotheses regarding formation of the deposit deserve consideration: (1) The deposit is solely the product of hydrothermal processes. The metal content of the deposit has been derived by hydrothermal leaching of a large volume of cataclastic mafic rock where part of the Mullen Creek mafic igneous complex is intensely sheared along an east-west belt nearly a mile wide. The ore was deposited as fissure filling and metasomatic replacement of mafic rock

within dilatant zones or other similarly favorable loci at the intersection of the east-west shear zone with a subsidiary northeast-trending mylonite zone. Northwest-trending cross faults adjacent to the deposit do not seem to have been the main conduits for introduction of metals. (2) The orebody represents portions of a magmatic sulfide deposit tectonically translated into their present positions in the shear zone and hyrothermally reworked by fluids introduced along avenues in the shear zone or cross faults.

Evidence for an Exclusively Hydrothermal Genetic Process

Lines of evidence supporting a strictly hydrothermal origin for the deposit include the structural setting, the general spatial coincidence of ore and hydrothermal alteration, textures of ore and silicate matrix intergrowths, and, most significantly, the predominance of the more readily soluble PGE, Pd and Pt, and the relative unimportance of the more chemically refractory platinoids Ir, Os, Ru, and Rh (McCallum et al., 1976).

Ore textures No textural evidence of magmatic origin of the sulfides has been recognized, e.g., sulfides as rounded or droplet forms in silicate matrix, or sulfides as interstitial granular intergrowths with magmatic silicates. Rather, sulfides and magnetite occur as fracture fillings and fine granular dispersions within silicate grains, as invasions

along grain boundaries and cleavages of silicate minerals (notably hornblende), and as angular, polycrystalline sulfide aggregates whose regular, granular-textured distribution in metasomatic supergene jasperoid suggests preferential replacement of certain (unrecognizable) minerals of the metagabbroic rock. Because hornblende is easily recognized as a mineral strongly affected by ore mineral replacements (Fig. 4B), it is apparent that sulfide crystallization followed (possibly closely) the diaphthoresis to epidote-amphibolite (and locally lower) grade of the gabbroic host and other rocks throughout the district during the period of major cataclastic activity along the Mullen Creek-Nash Fork shear system.

Hydrothermal alteration The distribution of ore in the deposit correlated rather closely with the volume of mafic rock affected by intensified hydration to chlorite-rich assemblages and locally developed intense hydrolysis producing the quartz-sericite assemblage that is clearly of hydrothermal origin. Diamond drill hole logs (Kasteler and Frey, 1949) and published descriptions of mine workings (Emmons, 1903; Kemp, 1904) indicate that the nature of host rock alteration consists only of a weak propylitic-greenschist type downward within a hundred feet or less from the orebody. The only sulfide encountered in this alteration facies is pyrite, which occurs as local stringer enrichments. Rather strong

hydrothermal alteration extends laterally outward from the orebodies for at least a few hundred feet.

PGE ratios Strong evidence that the ore metals have been concentrated by hydrothermal processes is seen in the ratios of platinum-group elements. The ratio of Pd:Pt in New Rambler sulfide ore is near 18:1, and the ratio Pd:Pt: minor PGE is estimated to be on the order of 1800:100:1 (analytical data for the concentrations of PGE and other elements in the ore are presented in a following section). Table 7 provides a comparative compilation of platinoid ratios from available published data for other significant occurrences of platinoid ores. The tabulated data indicate that the New Rambler deposit shows remarkable relative enrichment in palladium--the most soluble of the platinum-group elements. The deposit is singularly poor in Ru, Rh, Os, and Ir, the least soluble platinoids, in comparison to all other deposits for which data could be located (McCallum et al., 1976).

The ratio of Pd:Pt in mafic rocks in the vicinity of the New Rambler mine averages about 1:1 (Table 8). Palladium is enriched in New Rambler sulfide ore relative to enclosing fresh metagabbroic rocks by a factor of about 7500, and platinum by about 400. Ginzburg and Rogover (1961, p.925) have determined partition ratios for base and precious metals between sulfide samples and mafic silicate host rock in the

Table 7. Comparison of ratios of Pt, Pd, and minor PGE in New Rambler ore and other PGE deposits. Platinoid occurrences in placers and in alpine-type and alkaline ultramafic intrusions are not considered. The deposits are classified in three general categories, distinguished as follows: (I) Platinoid concentrations formed by magmatic processes, associated mainly with sulfide and in some cases chromite segregations in mafic-ultramafic intrusions of diverse characters, including komatiitic intrusions (Ungava, Shangani), peridotite-pyroxenite intrusions of tholeiitic affinity (Pechenga, Monchegorsk, Thomsom River), large stratified tholeiitic complexes (Bushveld, Great Dyke, Stillwater, Sudbury), and picritic intrusions (Noril'sk, Talnakh). Many deposits of this group overlap class II in character--Cu- and PGE-enriched portions of the deposits have formed at a late stage of the paragenetic sequences under volatile-rich and hydrothermal conditions. (II) PGE concentrations formed by hydrothermal processes at intermediate temperatures, with or without an obvious link to igneous activity. (III) Dunite pegmatoids of the eastern Bushveld Complex. Cameron and Desborough (1964) consider the Driekop, Mooihoek, and Onverwacht pipes to be of post-magmatic, high-temperature "hydrothermal" replacement origin. (N.D.=no data)

Deposit	Class of Deposit	Pd:Pt	Pd:Pt:Σminor PGE	Literature Source
A chromitite, Stillwater Complex	I	2.3:1	N.D.[1]	Page et al., 1972
Merensky Reef (Rustenburg), Bushveld	I	0.3:1	5:19:1	Mertie, 1969
Merensky Reef, avg. E.& W.compartments	I	0.4:1	2:4.6:1	Cousins & Vermaak, 1976
UG2 chromitite, Bushveld Complex	I	0.8:1	1.4:1.7:1	do.
Vlakfontein pipes, W. Bushveld Complex	I	2.6:1	1.8:0.7:1	do.
Ungava, Quebec	I	0.3:1 to 1.4:1	N.D.	Naldrett & Cabri, 1976
Pechenga, Kola Peninsula, USSR	I	1.7:1	N.D.	Yushko-Zakharova et al., 1967
Monchegorsk, Kola Peninsula, USSR	I,II	~2:1	N.D.	do.
Hitura, Finland	I,II	1.8:1	N.D.	Hakli et al., 1976
Noril'sk district, W. Siberia	I,II	3:1[2]	N.D.	Yushko-Zakharova et al., 1967
Sudbury district, Ontario	I,II	1:1[3]	2:2:1	Stumpfl, 1974
Shangani, Rhodesia	I,II	1.2:1	1:0.8:1	Viljoen et al., 1976
Thomson River, Victoria, Australia	I,II	1.7:1	N.D.	Keays & Kirkland, 1972
Artonvilla, Messina, Transvaal	II	4.8:1	22:4.5:1	Mihálik et al., 1974
New Rambler, Wyoming	II	18:1	~1800:100:1	-----
Waterburg district, Transvaal	II	0.1:1 to 0.6:1	N.D.	Mertie, 1969
Driekop & Onverwacht pipes, E.Bushveld	III	0.04:1	1:23:1	Cousins & Vermaak, 1976
Mooihoek pipe, E. Bushveld	III	0.2:1	N.D.	est. fr. Crocket, 1969

[1]Pd:Pt:Rh in the A chromitite is 9.3:4:1 (Page et al., 1972).

[2]Ginzburg and Rogover (1961) give a figure of 6 as the ratio Pd/Pt in PGE-rich sulfide ores at Noril'sk; Pd/Pt reaches 8 to 10 in late hydrothermal chalcopyrite-millerite veins (Yushko-Zakharova et al., 1967).

[3]Data given by Mertie (1969) for a paragenetically late offset deposit are Pd:Pt, 2:1 and Pd:Pt:Rh, 13:6.6:1.

Noril'sk deposit. Enrichment factors in sulfide samples relative to silicate samples at Noril'sk are Pd, 32; Pt, 9. The Noril'sk deposit is believed to be a magmatic sulfide deposit reworked to some extent by late-stage hydrothermal activity (Genkin, 1968, 1959; Stumpfl, 1974). If the partition factors for Noril'sk are presumed to reflect principally magmatic partitioning, as implied by Ginzburg and Rogover, then the enormous difference with Pd and Pt enrichment factors in New Rambler ore suggests that the process which accomplished this partitioning was not magmatic, but some other enrichment mechanism that was far more effective.

Cousins and Vermaak (1976, p.299) have noted, with particular reference to evidence from the Sudbury and Noril'sk districts, a general tendency to progressive enrichment of Pd relative to Pt in ore paragenetic sequences. According to these authors, Pd tends preferentially to form solution complexes with volatile elements, e.g., As, Sb, Te, S, that fractionate to a low-temperature milieu. The exceptionally high ratio of Pd/Pt (~18) in New Rambler sulfide ore supports the hypothesis that this deposit has had a relatively low-temperature thermal history from beginning to end, compared to other Cu-Ni sulfide ores listed in Table 7, most of which have a wholly magmatic or dual magmatic-hydrothermal history. The Pd-rich post-magmatic hydrothermal copper ores at Messina,

Table 8. Average concentrations of some trace metals (in ppm) in sheared and unsheared mafic rocks of the Mullen Creek Igneous Complex in the vicinity of the New Rambler mine. (The numbers in parentheses indicate the number of samples analyzed in each group.) (R. R. Carlson, E. Cooley, R. T. Hopkins, analysts, U.S.G.S.) (after McCallum et al., 1976).

	Pt	Pd	Cu	Ni	Co	Cr	V
Metaleucogabbro (5)	0.020	0.020	61	53	23	200	149
Metagabbro (13)	0.008	0.002	46	151	59	428	177
Sheared metagabbro (5)	0.008	0.020	63	268	68	1250	213
Metapyroxenite (5)	0.028	0.026	23	468	81	1175	120
Sheared metapyroxenite (3)	0.120	0.113	68	283	58	150	73

Transvaal (Pd/Pt, 4.8) are considered to have been deposited within the temperature interval 270°-400°C (Mihalik et al., 1974, p.260).

The low Pd:Pt (1:13 to 1:1.6) in the platiniferous quartz veins of the Waterburg district, Transvaal might be taken to represent an exception to the trend outlined above. These lodes occur within felsic rocks of the Epicrustal series of the Bushveld Complex, and Mertie (1969, p.44) has suggested that the occurrence of Pt and chromiferous chlorite in these veins points to derivation of at least some of their metal content from mafic rocks of the underlying Layered Sequence. The mafic rocks of the Bushveld Complex seem to have a relatively low Pd:Pt ratio in general, and Cousins and Vermaak (1976, p.297) note a trend to relative enrichment of Pt over Pd upward in the Complex. Thus, it seems likely that subjacent portions of the Layered Sequence that contributed metals to the Waterburg lodes may have had even lower Pd/Pt, and the general trend to relative Pd enrichment with mobilization of PGE might hold even in this case.

Other geochemical evidence for hydrothermal origin

Comparison of selected geochemical characteristics of the New Rambler deposit with a number of Au-Cu-bearing quartz-carbonate veins in the district yields significant information. Similarities in structural control and mesothermal

character of many of the deposits suggest the New Rambler deposit formed during the mineralization episode that affected the rest of the district. The Au-Cu veins are in each case spatially associated with small, hydrothermally carbonatized mafic (dioritic or hornblenditic) dikes and lenses in metamorphosed felsic rocks and weakly faulted, carbonatized mafic plutonic rocks, but of the known mineralized localities in the central Medicine Bow Mountains, only the New Rambler deposit occurs enclosed in a large volume of non-carbonatized cataclastic mafic rocks. The influence of CO_2 on the solubility of PGE is obscure, but as will be evident from ensuing discussions, it apparently represses platinoid mineralization.

Figures 13 and 14 compare Ni and Ag contents, elements typically enriched in mafic rocks, in the two types of deposits. New Rambler ores are substantially enriched in both Ni and Ag relative to other ores in the district. Co does not show a significant relative enrichment pattern. Higher concentrations of Ni and Ag in New Rambler ores are taken to reflect important contributions of metals from the mafic host rock to the hydrothermal ore fluids (McCallum et al.,

1976). The locally intensified hydrothermal alteration clearly supports this inference.[1]

To test this hypothesis further, contents of selected trace metals were compared for sheared versus unsheared mafic rocks from the general area of the mine (McCallum et al., 1976). These data are shown in Table 8. Sheared metagabbros are significantly enriched in palladium and base metals relative to their unsheared counterparts. All metals are mobilized in sheared metapyroxenites, and Pt, Pd, and Cu are appreciably upgraded. Sheared metaleucogabbros were not encountered, so no chemical data are available for them; however, the high platinoid and copper contents of unsheared metaleucogabbros (which, significantly, are somewhat more pyritic) suggest that sheared leucocratic mafic rocks may have been important contributors of Cu and PGE to the deposit.

A similar hypothesis has been invoked to explain genesis of metamorphic Cu-Ni-Fe sulfide ores in the Allarechensk region, USSR. Zak and Proskuryakov (1971) have proposed formation of this deposit by (1) leaching of Ni, Fe, and Cu from hyperbasites, and (2) contemporaneous with tectonic activity, deposition of sulfides of these metals.

---

[1]In a series of hydrothermal experiments on natural rocks, Ellis (1968) was able to leach 0.2-4 ppm Cu from andesite in the temperature range 360°-500°C with solutions in the salinity range 2-4 m NaCl, 1500 bars pressure. The concentration is well within the range known to be capable of depositing economic copper deposits (Wedepohl, 1972, p.29-F-2).

13. Comparison of ratios of Ni to Fe in New Rambler ore samples (triangles) with those in samples from Au-Cu-quartz-carbonate veins of the district (circles). Regression lines reflect the systematic character of the Fe:Ni variation. (Log scale)

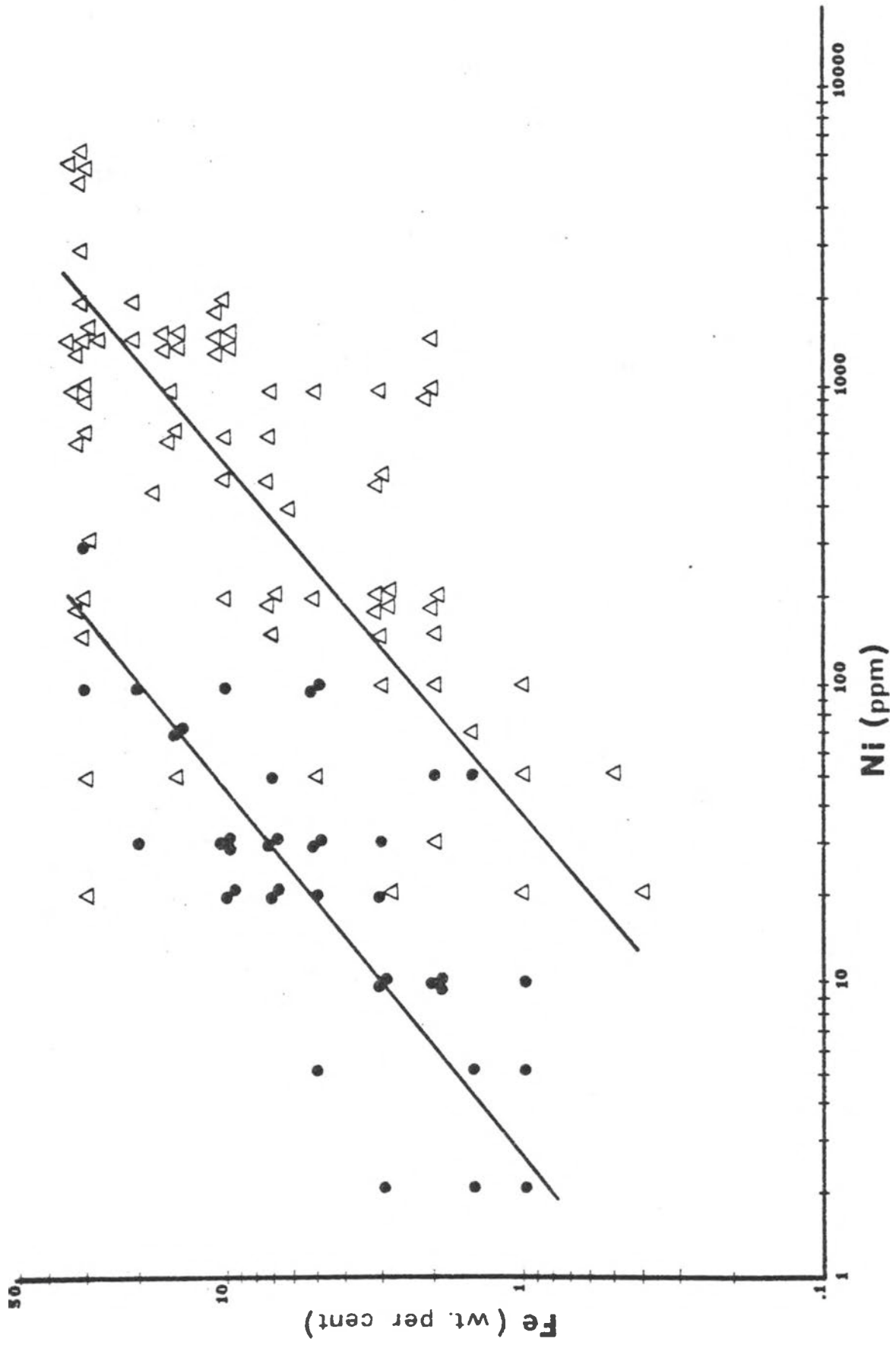
Fe (wt. per cent)
50
10
1
.1
1
10
100
1000
10000
Ni (ppm)

Fig. 14. Comparison of ratios of Ag to Fe in New Rambler ore samples (triangles) with those in ore samples from Au-Cu-quartz-carbonate veins of the district (circles). The average Fe:Ag value for each type deposit is shown by corresponding large symbols. (Log scale)

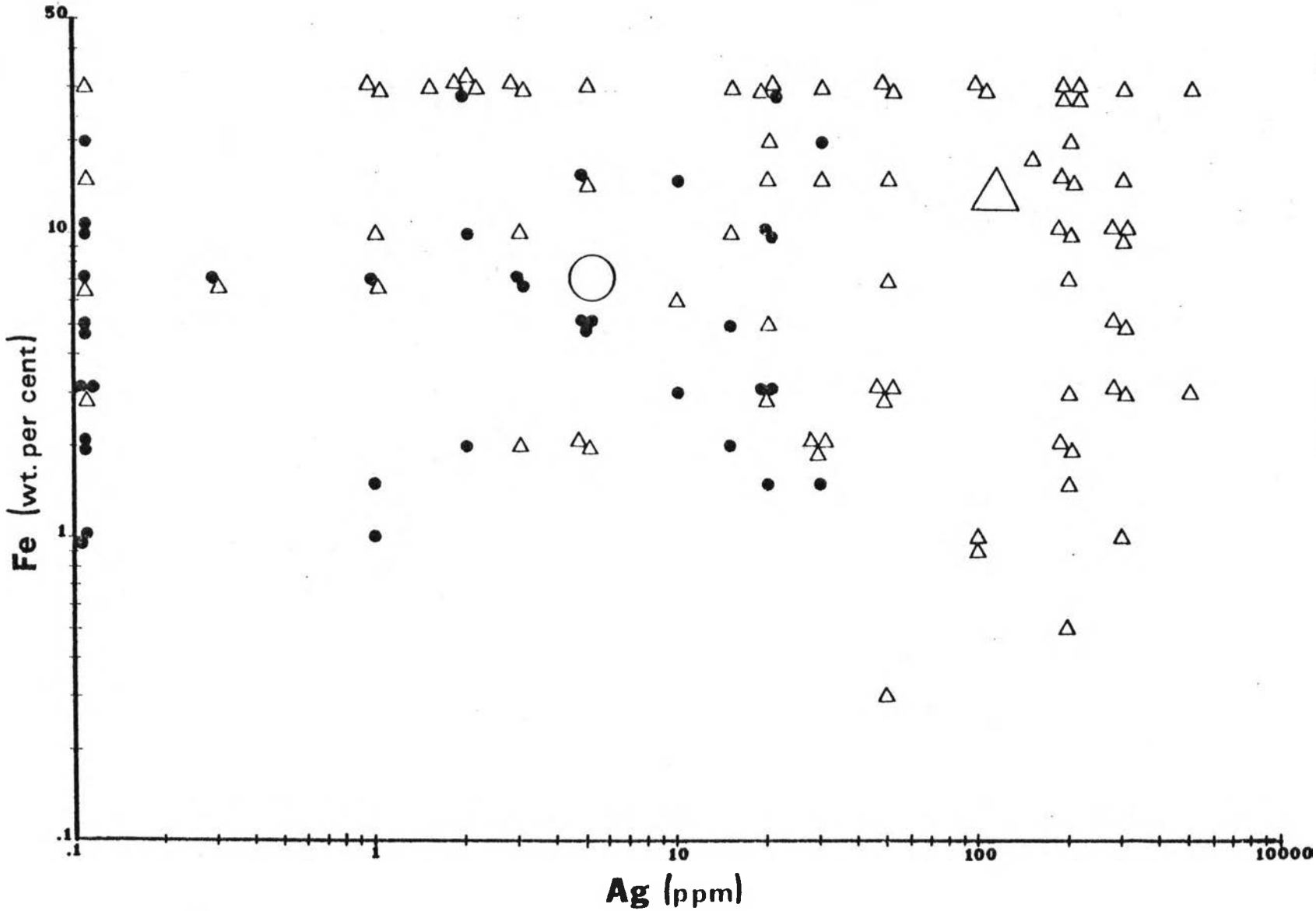
50
10
1
.1
Fe (wt. per cent)
.1
1
10
100
10000
Ag (ppm)

Evidence for a Principally Magmatic Origin of the Deposit

Keays and Kirkland (1972) studied the Thompson River orebody in Victoria, Australia, a deposit with some salient features in common with the New Rambler deposit, viz., a platiniferous Cu-Ni-Fe sulfide paragenesis in hydrothermally altered mafic rock. Keays and Kirkland have convincingly demonstrated that the Thomson River mineralization reflects metamorphism and hydrothermal reworking of a magmatic deposit. Some features of the New Rambler occurrence suggest that consideration should be given to a similar genetic process.

The association of platiniferous chalcopyrite-pentlandite-pyrrhotite ore within a layered mafic igneous complex might be taken ipso facto by some workers as evidence for a predominently magmatic origin of the metal concentrations. However, the implicitly assumed similarities with well known deposits of analogous associations are not well substantiated on closer inspection of the deposit. Textures of the ore lend no support to a magmatic origin. If the ore ever had magmatic textures, they have been obliterated by complete recrystallization. The distribution of the ore--disseminated stringers and large irregular pods of massive sulfide, up to tens of feet in thickness and enclosed predominantly in leucocratic facies of the intrusive--has little in common with magmatic deposits at Noril'sk and Sudbury, where immiscibly

segregated massive sulfide ore occurs at the floors of the mafic intrusions, or with the thin, widespread ore seam in the pyroxenitic Merensky Reef. No magmatic sulfide segregations have been observed in the extensive outcrop area of mafic complexes in the central Medicine Bows.

Based on the structural, textural, and chemical evidence presented, it is concluded that the New Rambler deposit has formed entirely from hydrothermally introduced constituents, and not by in situ reworking of earlier magmatic ores.

Discussion

Although evaluation of variations in mineralization within a deposit as functions of time, space, temperature, pressure, and chemical parameters of the hydrothermal system is a difficult task at best, and major limitations were imposed on this investigation by inaccessibility of the deposit and pervasive supergene alteration, a few meaningful inferences regarding the origin of the deposit can be summarized from evidence presented to this point.

As mafic rocks throughout the district show evidence of significant redistribution of ore-forming metals during retrograde metamorphism that accompanied major cataclastic activity along the shear system, it seems likely that the ore metals present in the New Rambler orebody were mobilized from gabbroic rocks during the peak of diaphthoresis and tectonism

and were later redeposited during waning stages of the same tectonic-metamorphic event.

Intensified hydration of mafic rocks to greenschist/propylitic assemblages and the quartz-sericite-pyrite alteration of wallrocks (including local appearance of lensatic and stringer-like concentrations of pyrite, represented by sulfide assemblage 1) typify effects developed along walls of flow channels in shear zones throughout the district. The apparent local intensification of these effects in the vicinity of the New Rambler mine is attributable to enhanced permeability at this intersection of shear zones and faults. The principal effect of these hydrolytic alteration processes was base cation leaching, and it appears that these phenomena contributed to significant upgrading of the fluids in concentrations of dissolved metals, notably Cu and PGE. The somewhat higher contents of Cu, Pd, and Pt in the slightly more pyritic metaleucogabbroic facies of the mafic complex (Table 2) suggest that these rocks may have been particularly favorable contributors of sulfur and ore metals to the metamorphic-hydrothermal solutions.

Localization of the ore at the complex intersection of faults and shear zones (McCallum et al., 1976) suggests that zones of dilatancy in the fluid path may have been influential

in focussing activity of the mineralizing solutions. Intensified brecciation characterizes dilatant zones along multiplane faults (Mitchum, 1974, p.412), and the resulting enhancement of permeability should promote hydrothermal replacement. Constrictions along the flow passage might induce locally intense pressure gradients and throttling. Adiabatic expansion of ore fluids is suspected to be an effective cause of ore deposition (Toulmin and Clark, 1967; Barnes and Czamanske, 1967, p.374).

Replacement of gabbroic rocks by chloritic and sericitic mineral assemblages indicates moderate acidity of the altering solutions (Meyer and Hemley, 1976). The available evidence indicates that Cu and Pd (and to a lesser extent Pt) are most effectively transported in acidic aqueous solutions as chloride complexes (Helgeson, 1969; Fuchs and Rose, 1974). The chemical response to decompression of such ore fluids on passing into dilatant zones should be a shift toward increased association of dissociated dissolved species--viz., the strongest electrolytes, HCl and alkali chlorides--at the expense of chloride complexes of ore-forming metals. Dechlorination of metal complexes diminishes metal solubilities and could be expected to induce rather rapid ore deposition. As Fe^{2+}, Ni^{2+}, and Co^{2+} do not associate significantly with chloride or sulfide ions to form aqueous

solution complexes (Cotton and Wilkinson, 1972, p.596; Helgeson, 1970, p.176), and Pt^{2+} associates to a moderate extent only with chloride (Fuchs and Rose, 1974), the solubilities of these metals should respond less dramatically to decompression. These considerations regarding the influence of pressure changes on the stabilities of metal solution complexes do much to account for the anomalous metal ratios and near absence of a mineral deposition sequence in main-stage ore. As shown in Table 9, main-stage ore, which comprises about 95 percent of the deposit, is exceptionally rich in Cu and Pd, contains moderate Pt, and has relatively low Fe, Ni, and Co, compared to metal ratios in sulfide assemblage 1 and in mafic source rocks.

Mode of Occurrence of Platinum, Palladium, and Rhodium in Sulfide Ore

Nine hypogene platinoid minerals have been encountered in New Rambler ores in this investigation. These are sperrylite and eight tellurides of Pd and Pt. The tendency of Pd and Pt to appear as compounds with Te and Bi late in the paragenetic sequence has been noted at Pechenga, Monchegorsk, and Sudbury (Yushko-Zakharova et al., 1976, p.1110), at Noril'sk and Talnakh (Genkin, 1968, p.144; Genkin et al., 1973, p.1008), and in the Merensky Reef (Kingston, 1976, p.821). Thus, the predominance of bismutho-tellurides

Table 9. Contents of some precious and base metals in New Rambler sulfide ores (in ppm, except as noted). Data of assemblage 1 are for 3 samples of nearly fresh massive hypogene pyrite ore and 3 sulfide separates (virtually all pyrite) from the disseminated pyrite-quartz-sericite association. Analyzed bulk samples of sulfide assemblages 2 and 3 main stage ore include 24 samples of massive chalcopyrite-secondary pyrite (ex-pyrrhotite) ore with variable but subordinate amounts of jasperoid matrix and 5 samples of disseminated ore of the same mineral assemblage. The upper determination limit for Fe by spectrographic analysis was 20 wt percent. For samples in which Fe exceeded the determination limit, Fe was estimated from the specimen mode. Pt, Pd, Rh, Au by fire assay-spectroscopy--analysts: R.R. Carlson, E.F. Cooley, T.A. Doerge; Ag, Cu, Au by atomic absorption--analysts: R.B. Carten, C.A. Curtis, J.G. Frisken, J. Mitchell, R.M. O'Leary, J.A. Roybol, J. Sharkey, J.G. Viets; Co, Fe, Ni, Pb, Zn by semiquantitative D.C. arc spectroscopy--analysts: R. Babcock, L.B. Breeden, E.F. Cooley, K.J. Curry, G.W. Day, J. Domenico, W.D. Goss, D.J. Grimes, J. Haffty, R. Hopkins, L.B. Riley, D. Siems.

	Assemblage 1		Assemblages 2 and 3	
	mean	std. dev.	mean	std. dev.
Ag	2.3	1.3	58	57
Au	0.44	0.45	4.3	10
Co	1850	1150	160	182
Cu	0.5%	0.5%	21%	14%
Fe	46%	0.7%	27%	18%
Ni	4000	3333	1662	2173
Pb	14	7	12	9
Pd	24	23	76	70
Pt	0.98	0.87	4.4	9.2
Rh[1]	0.06	0.06	0.02	0.06
Zn	not detected		453	540

[1]Rh was detected in 4 of 6 samples of sulfide assemblage 1; the mean of detected values is 0.09 ppm.

[2]Rh was detected in 15 of 29 samples of assemblages 2 and 3 ore; the mean of detected values is 0.05 ppm, with the analytical detection limit averaging 0.015 ppm. For purposes of estimating mean Rh, cases in which Rh was not detected were assigned at estimated value of 0.002 ppm.

in the New Rambler paragenesis is consistent with its apparent hydrothermal origin.

A study of the distribution of palladium minerals has shown that chalcopyrite is most commonly the host in chalcopyrite-secondary pyrite (ex-pyrrhotite) ore. Since the Pd minerals show no visible sign of instability in the zone of pyritization of pyrrhotite deep in the supergene alteration profile, the relative frequency with which Pd minerals are seen in chalcopyrite and secondary pyrite is believed to represent their distribution in primary chalcopyrite-pyrrhotite ore (Fig. 15). Although Pd minerals are more commonly observed enclosed in chalcopyrite than in secondary pyrite by a factor of nearly 3:1, consideration of the fact that the ratio chalcopyrite:pyrrhotite in main stage ore is on the order of 6:1 indicates that pyrrhotite was actually a preferred associate of Pd minerals. A substantial proportion of the merenskyite and michenerite grains considered in Fig. 15 as hosted by chalcopyrite are intergrown complexly with very small amounts of secondary pyrite and marcasite after pyrrhotite (Figs. 7D and 8A), and the polymineralic aggregate is enclosed in more or less massive chalcopyrite. The proportion of Pd minerals enclosed in major sulfide minerals exceeds the proportion enclosed in supergene jasperoid (formerly metagabbroic silicate matrix) by a factor

Fig. 15. Relative frequency with which major constituents of the primary ore contain the three most abundant palladium minerals. Numbers in parentheses indicate the number of occurrences on which the frequency distribution is based. Abbreviations: pyrrhotite, po; chalcopyrite, cp; metagabbroic silicate matrix, si.

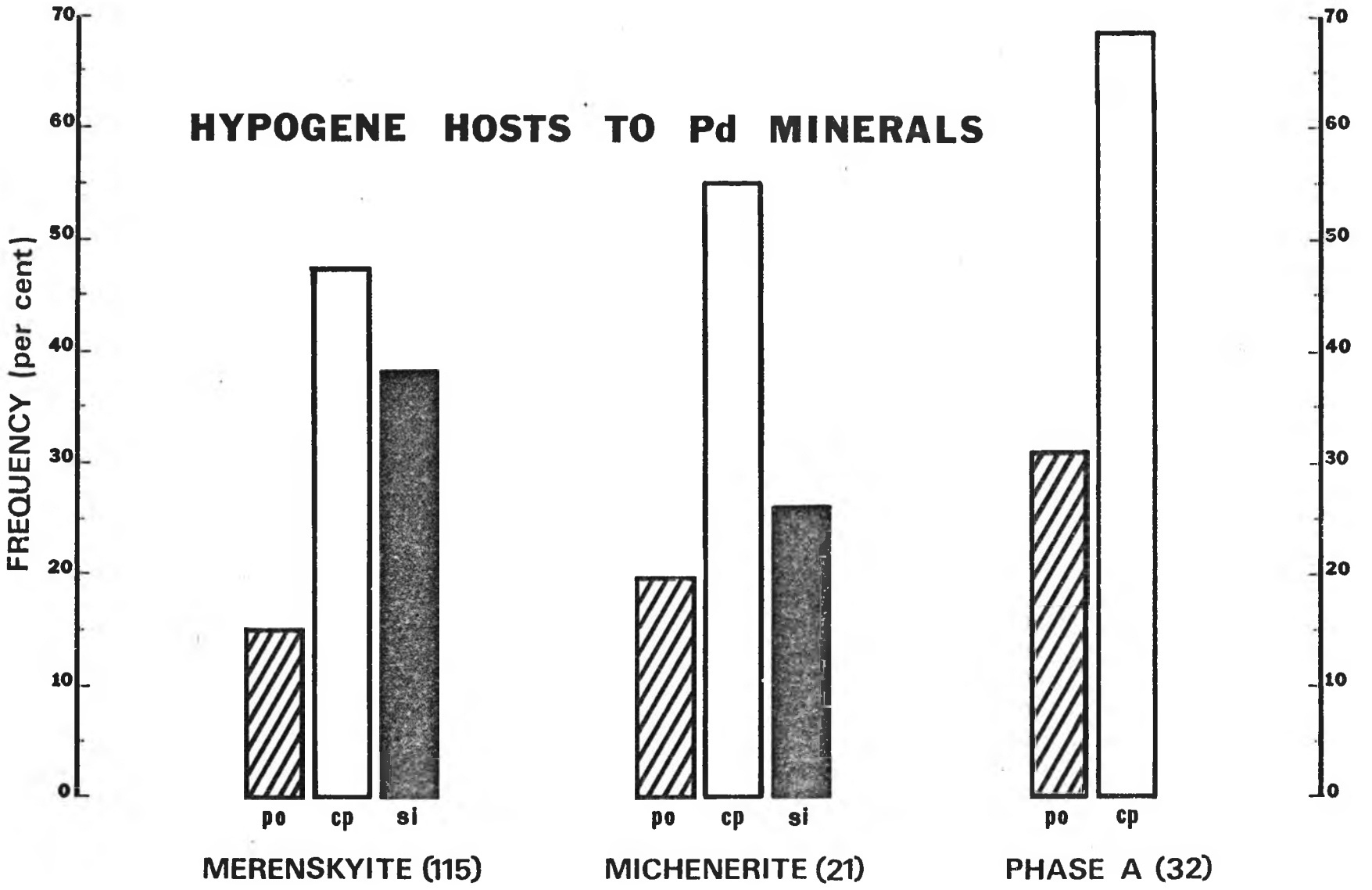
HYPOGENE HOSTS TO Pd MINERALS
FREQUENCY (per cent)
0
10
20
30
40
50
60
70
po
cp
si
MERENSKYITE (115)
MICHENERITE (21)
PHASE A (32)

of about 4:1, which underscores the rather strong chalcophile preference of Pd. As documented in a following discussion, the preferred associations of Pt minerals are essentially the reverse of those of Pd minerals.

To further investigate characteristics of the distribution and associations of ore metals, chemical data of ore samples were evaluated statistically. Sixty-six ore samples were analyzed quantitatively for PGE and Au by fire-assay emission spectrography (R. R. Carlson, E. F. Cooley, and T. A. Doerge, analysts, U. S. G. S.). Osmium cannot be determined by this method and was not analyzed. Ag and Cu in all 66 samples and Au, Ni, Co, Zn, As, and Te in some specimens were determined by atomic absorption analysis, and each of the samples was also analyzed for 30 elements by a semi-quantitative spectrographic method (analyses by U. S. G. S. technicians). Analyzed samples were divided into four approximately homogeneous groups representing four distinct zones or chemical regimes in the weathered profile of the deposit. The first group consists of the freshest samples of massive to moderately siliceous chalcopyrite-(ex-)pyrrhotite ore of assemblages 2 and 3. Chalcopyrite and secondary pyrite are the predominant constituents of most samples, but a few percent of secondary Cu sulfides and limonite are present in some cases, and jasperoid is an important constituent of

some specimens. The second group is comprised of ore from the zone of secondary copper sulfide enrichment. Covellite, digenite, chalcocite, and variable amounts of non-siliceous earthy goethitic limonite comprise the bulk of these samples. Oxidized copper ore comprising the third group consists mainly of malachite, cuprite, antlerite, brochantite, chrysocolla, and more or less siliceous limonite. The fourth class is silicified iron oxide material from the surface gossan.

The chemical data for each group of ore samples was analyzed statistically for the data means and standard deviations, and precious metals were tested for significant correlations in their associations with each other and with other trace and major elements. Histograms of element concentrations in many cases show a non-normal distribution; furthermore, the detection limit cutoffs for several trace elements (e.g., Rh, Cr, Bi, Pb) and upper determination limits for major elements (Fe and Cu) have resulted in censored concentration-frequency distributions. Therefore, the data were tested for element correlations using Spearman's non-parametric correlation coefficient, r_s, since the data do not satisfy the assumption of a bivariate normal distribution (Till, 1974). Student's t tests were used to determine the levels of significance of correlation coefficients. Results of these analyses are shown in Table 10.

Table 10. Mean concentrations and standard deviations (in ppm, except where indicated otherwise) of important major and trace elements in four zones of the weathered profile, and correlation coefficient matrices for each of the four zones. In some zones certain elements were detected in too few instances to provide significant information, and were omitted from tabulations for those zones. The significance indicator, given in parentheses for each correlation coefficient, represents the probability of obtaining a correlation of that degree by chance, e.g., a significance level of .005 represents a probability of 5/1000 of obtaining such an extreme correlation by chance selection of an unrepresentative sample suite from a population in which the correlation is really nil. (See Table 9 for analysts.)

I Massive and disseminated chalcopyrite-secondary pyrite ore of assemblages 2 and 3.

Ag	Au	Pd	Pt	Rh		Number of Det'ns	Mean	Std Dev
----	.134 (.275)	.202 (.147)	-.050 (.400)	-.174 (.184)	Ag	29	58	57
.054 (.431)	.175 (.284)	.086 (.391)	.437 (.068)	.188 (.270)	As	13	22	26
.134 (.275)	----	-.129 (.289)	.055 (.406)	.361 (.055)	Au	21	4.3	10.5
.048 (.403)	.267 (.122)	-.577 (.001)	.366 (.026)	.481 (.005)	Ba	29	233	566
-.125 (.260)	-.297 (.096)	.200 (.150)	.104 (.297)	-.127 (.257)	Bi	29	11	13
.155 (.211)	.041 (.431)	.335 (.039)	.249 (.097)	.095 (.313)	Co	29	160	182
.015 (.470)	.426 (.028)	-.428 (.011)	.044 (.410)	.366 (.026)	Cr	29	26	58
.668 (.001)	.077 (.371)	.194 (.158)	-.180 (.175)	-.230 (.115)	Cu	29	21%	14%
.198 (.152)	-.210 (.182)	.581 (.001)	.009 (.482)	-.400 (.016)	Fe	29	21%	14%
.297 (.059)	.229 (.159)	-.413 (.014)	-.106 (.293)	.033 (.433)	Mn	29	54	60
.145 (.228)	-.024 (.459)	.416 (.013)	.419 (.012)	.267 (.082)	Ni	29	1662	2173
-.331 (.040)	.116 (.309)	-.328 (.041)	.194 (.157)	.029 (.442)	Pb	29	11	9
.202 (.147)	-.129 (.289)	----	.211 (.136)	.189 (.164)	Pd	29	76	70
-.050 (.400)	.055 (.406)	.211 (.136)	----	.449 (.008)	Pt	29	4.4	9.2
-.174 (.184)	.361 (.055)	-.189 (.164)	.449 (.008)	----	Rh*	29	0.02	0.06
-.402 (.016)	.244 (.144)	-.346 (.033)	.006 (.487)	.389 (.019)	Ti	29	1084	2237
-.510 (.003)	.104 (.328)	-.343 (.035)	.409 (.014)	.406 (.015)	V	29	30	43
.299 (.089)	.002 (.497)	.514 (.008)	-.215 (.169)	-.461 (.016)	Zn	22	453	540

*Rh was detected in only 12 of 25 analyses. The mean of detected values is 0.038, with the analytical detection limit averaging 0.015 ppm. It was deemed important to consider in these computations the instances in which Rh was low, so for these purposes, cases in which Rh was undetectable were assigned an estimated average Rh value of 0.002 ppm. This might have resulted in slight underestimation of the mean Rh in sulfide ore and slight enhancement of Rh correlation coefficients, but conclusions regarding preferred element associations of Rh in the ore would not be affected.

Table 10 (cont'd.)

II. Massive ore of the Cu sulfide enrichment zone. Rh was detected in only 5 of 21 analyses.

Ag	Au	Pd	Pt	Rh		Number of Det'ns	Mean	Std Dev
----	.283 (.154)	.030 (.449)	-.047 (.420)		Ag	21	161	106
.414 (.178)	.255 (.291)	-.378 (.202)	.451 (.156)		As	7	106	176
.283 (.154)	----	.330 (.116)	.586 (.011)		Au	15	3.5	5.8
-.161 (.243)	.059 (.418)	-.413 (.032)	-.258 (.130)		Ba	21	314	1080
.055 (.407)	-.076 (.394)	.568 (.004)	.080 (.365)		Bi	21	52	126
-.444 (.022)	-.074 (.398)	-.418 (.030)	-.196 (.198)		Co	21	129	147
.058 (.402)	.184 (.257)	-.099 (.335)	-.036 (.440)		Cu	21	38%	27%
0 (.500)	-.090 (.376)	-.253 (.134)	-.188 (.207)		Fe	21	19%	21%
-.123 (.299)	.235 (.200)	-.451 (.021)	.166 (.237)		Mn	21	89	96
-.286 (.105)	-.520 (.024)	-.267 (.121)	-.375 (.047)		Ni	21	783	620
-.117 (.307)	-.261 (.175)	.148 (.262)	-.215 (.176)		Pb	21	10	10
.030 (.449)	.330 (.116)	----	.425 (.028)		Pd	21	72	130
-.047 (.420)	.586 (.011)	.425 (.028)	----		Pt	21	4.5	7.4
.156 (.250)	-.015 (.479)	.244 (.144)	.095 (.342)		Tl	21	79	166
-.025 (.457)	.230 (.206)	-.382 (.044)	-.112 (.315)		V	21	45	50
.346 (.224)	0 (.500)	-.255 (.291)	0 (.500)		Zn	7	100	87

III. Massive ore of the oxide zone. Bi determinable in only 4 of 8 analyses. Rh detected in 7 of 8 analyses; the N.D. case was estimated at 0.002 ppm Rh.

----	.321 (.242)	-.203 (.315)	-.429 (.145)	.071 (.434)	Ag	8	11	11
-.211 (.395)	.211 (.395)	-.056 (.473)	.211 (.395)	- 211 (.395)	As	4	85	47
.321 (.242)	----	-.180 (.350)	.107 (.410)	-.429 (.169)	Au	7	0.67	0.66
.520 (.094)	.039 (.467)	.160 (.353)	-.786 (.011)	-.406 (.160)	Ba	8	69	40
.036 (.467)	-.162 (.365)	.283 (.249)	-.383 (.175)	-.180 (.336)	Co	8	205	327
.795 (.010)	.218 (.320)	-.436 (.140)	-.325 (.216)	.217 (.303)	Cu	8	21%	7%
.374 (.182)	.236 (.305)	.261 (.267)	-.349 (.199)	-.349 (.199)	Fe	8	21%	16%
.146 (.365)	.630 (.065)	.344 (.203)	.122 (.387)	-.512 (.098)	Mn	8	280	500
-.036 (.467)	-.107 (.410)	.325 (.216)	-.359 (.192)	-.192 (.325)	Ni	8	993	761
-.154 (.358)	-.777 (.020)	-.116 (.392)	-.617 (.052)	-.077 (.428)	Pb	8	5	3
-.204 (.315)	-.180 (.350)	----	.383 (.175)	.395 (.169)	Pd	8	30	21
-.429 (.145)	.107 (.410)	.383 (.175)	----	.238 (.286)	Pt	8	9.7	6.6
.071 (.434)	-.429 (.169)	.395 (.167)	.238 (.286)	----	Rh	8	0.14	0.20
.198 (.320)	.265 (.284)	.367 (.186)	.432 (.143)	.346 (.201)	Tl	8	45	46
.098 (.410)	.147 (.377)	.589 (.063)	.781 (.012)	.098 (.410)	V	8	163	103
-.100 (.437)	1.000 (.001)	.359 (.277)	0 (.500)	-.900 (.019)	Zn	8	90	61

Table 10 (cont'd.)

IV. Gossan. Bi was above the determination limit (10 ppm) in only 1 of 8 analyses. As and Zn were not determined.

Ag	Au	Pd	Pt	Rh
----	0 (.500)	-.378 (.178)	-.222 (.299)	-.013 (.488)
0 (.500)	----	-.319 (.269)	.858 (.015)	-.232 (.330)
.706 (.026)	-.418 (.205)	-.233 (.290)	-.249 (.277)	.037 (.466)
0 (.500)	-.882 (.010)	.469 (.121)	-.331 (.212	.102 (.406)
.055 (.449)	-.693 (.064)	.200 (.318)	.053 (.451)	.250 (.275)
-.249 (.276)	-.493 (.161)	.659 (.038)	-.038 (.465)	-.192 (.325)
-.185 (.331)	-.882 (.010)	.301 (.285)	-.340 (.205)	.386 (.173)
-.026 (.476)	-.448 (.187)	-.542 (.083)	-.828 (.006)	-.265 (.263)
.370 (.184)	-.971 (.001)	.048 (.455)	-.417 (.152)	.133 (.378)
-.062 (.443)	.105 (.422)	-.056 (.448)	.360 (.191)	.056 (.448)
-.378 (.178)	-.319 (.269)	----	.545 (.082)	-.119 (.390)
-.222 (.299)	.858 (.015)	.545 (.082)	----	.178 (.337)
-.013 (.488)	-.232 (.330)	-.119 (.390)	.178 (.337)	----
-.223 (.298)	-.870 (.013)	-.240 (.284)	-.772 (.013)	.120 (.389)
-.581 (.066)	-.500 (.157)	.843 (.005)	.186 (.330)	-.012 (.489)

	Number of Det'ns	Mean	Std Dev
Ag	8	1.1	1.6
Au	6	0.28	0.22
Ba	8	98	57
Co	8	210	147
Cr	8	58	101
Cu	8	1.6%	2.2%
Fe	8	45%	15%
Mn	8	359	321
Ni	8	1550	834
Pb	8	4	5
Pd	8	16	16
Pt	8	5.9	5.9
Rh	8	0.18	0.24
Tl	8	126	70
V	8	190	166

If only correlation coefficients greater than .500 are considered significant, then data for the freshest sulfide ore (Table 10-I) indicate that Ag associates significantly only with Cu in chalcopyrite (r_s[Ag-Cu]=.668) and is notably antipathetic to V, which is tied up in jasperoid after metagabbroic silicates. The lack of strong correlations for Au is consistent with the mineragraphically observed promiscuous distribution of electrum in (ex-)pyrrhotite, chalcopyrite, merenskyite, and secondary jasperoid (ex-metagabbro). In the freshest ore, Pd shows a weak tendency to chalcophile affiliations, those with Fe and Zn being most notable, and antipathy to Ba, which is concentrated in the jasperoid phase. The general trend to chalcophile preferences for Pd is corroborated by mineragraphic data summarized in Figure 15.

The low correlation between Pd and Bi (r_s[Pd-Bi]=.200) and the very low ratio of mean Bi:Pd (11:76 ppm) in analyzed sulfide samples (compared with Bi:Pd $\simeq$ 0.8:1 in palladium minerals, overall) might be taken as an indication that the largest part of the Pd content of the primary ore occurs in a form other than Pd-Bi-Te minerals. However, Pd minerals are microscopically visible in virtually every square inch of every polished sample of main-stage sulfide ore, and from the writer's experience in microscopic examination of assayed siliceous gold and platinum ores in which the precious metal values are known to occur in mineral rather than solid

solution form, it can be stated with certainty that the visibility of Pd minerals in main-stage ore does not correspond to that expectable from 12-15 ppm Pd occurring as Pd-Bi-Te minerals, as implied by Bi assay values. Although the possibility of some Pd solid solution in major ore minerals cannot be dismissed, the semiquantitative Bi determinations must be considered suspect and an unreliable guide.

An attempt was made to evaluate by microprobe analysis the possibility of Pd solid solution in major minerals of the ore. Since the statistical data of Table 10-I show that Pd correlates most strongly with Fe (r_s[Pd-Fe]=.581) and the correlation with Cu is very weak (r_s[Pd-Cu]=.194), pyrite was considered to be the most promising target in these analyses. Furthermore, intensive microscopic scrutiny of five polished slabs of assemblage 1 massive hypogene pyrite assaying 60 ppm Pd failed to disclose a single platinoid mineral grain, although Pd minerals are usually visible in Cu-rich main-stage ore carrying as little as 20-30 ppm Pd. A sample of this primary pyrite was analyzed for Pd by electron microprobe, operated at 15 KV with a constant beam current of 50 nanoamperes. A counting interval of 100 seconds was used for each point analysis in order to obtain maximum consistency of results. The zero concentration standard employed was analyzed natural pyrite from a sedimentary geode occurrence.

No standard of suitably low Pd concentration was available for quantitative determination of the Pd content of analyzed pyrite. However, the microprobe data do indicate the presence of a small content of Pd dissolved in hypogene pyrite. The "background" Pd counts in the blank pyrite standard averaged 661 counts with a standard deviation of 19 for twenty-four 100-second point analyses. Twenty-four comparable point analyses of assemblage 1 pyrite averaged 701 counts per 100 seconds with a standard deviation of 18.5. The Pd counts in primary pyrite are more than 2 sigma above background, which appears to confirm the presence of a small amount of Pd in solid solution. Similar analyses of supergene pyrite after pyrrhotite in three samples of typical assemblage 2 massive sulfide ore from which pyrite concentrates (~96-97 percent pure) assayed 180-250 ppm Pd did not yield Pd counts above the blank standard. It may be concluded that if Pd does occur in solid solution in secondary pyrite, the influence of solid solution on the overall distribution of Pd is minor relative to the proportion of Pd occurring visibly as its own minerals in these same samples.

Most moncheite and sperrylite grains seen in New Rambler ore were enclosed in supergene jasperoid in a single exceptionally Pt-rich sample of assemblage 3 disseminated ore. If this sample, which also contains unusually Pt-rich merenskyite and michenerite, is momentarily eliminated from consideration as

abnormal, then it is possible to estimate the distribution of Pt in "average" New Rambler ore. The weighted average Pt content of 34 grains of merenskyite, michenerite, and Pd-phase A analyzed by electron microprobe is 0.6 wt percent (range, <0.2--6.9 wt percent), from which it can be estimated, on the basis of the ratios of Pd to Pt in these minerals and in the ore (76:4.4 ppm), that 35-40 percent of the Pt content of main-stage ore occurs in solid solution in Pd minerals.

The observed heterogeneous distribution of Pt in the ore--as sperrylite and moncheite in siliceous disseminated ore and in massive sulfide ore as sperrylite and as a minor substituent in Pd minerals--is consistent with the lack of strong preferred element associations as reflected by correlation data of Table 10-I.

Little is known of the distribution and mode of occurrence of Rh except that it has been detected by microprobe analyses as a trace substituent in sperrylite (Table 4). The correlation coefficient data of Table 10-I are not particularly revealing, but the low correlations with Pt and As suggest that sperrylite may not be the only residence of Rh.

Geochemical Behavior of Precious Metals in the Weathering Zone

Table 10 and Figure 16 summarize analytical data relating to the distribution of precious metals in four levels of the

weathered profile of the deposit. The metal concentrations shown in the four zones of Figure 16 are the data means of Table 10-I, -II, -III, and -IV.

When silicification of metagabbro, decomposition of pentlandite, and pyritization of pyrrhotite were nearly complete in the lowermost alteration zone, chalcopyrite was electrochemically destabilized, and chalcopyrite and any surviving pyrrhotite were replaced by chalcocite (Cu_2S), digenite (Cu_9S_5), and covellite (CuS), with or without accompanying formation of a little pyrite or marcasite. In the upper part of this zone, relict chalcopyrite oxidized to covellite + goethite limonite, without net Cu enrichment, and pyrite was simultaneously replaced by limonite. As the oxidation zone descended onto secondary Cu sulfide ore, the sulfides were altered to Cu oxides, carbonates, sulfates, and chrysocolla. These were in turn dissolved by descending groundwaters, leaving at the surface of the deposit a leached gossan of silicified iron oxides.

Mineragraphic observations show that in the zone of supergene Cu sulfide enrichment, primary Pd minerals are stable, and the mean Pd content of this zone (Table 10-II) does not differ significantly from that in underlying chalcopyrite-(ex-)pyrrhotite ore. (The fact that decomposition of primary major sulfides has not accomplished a noticeable effect on the Pd content of the ore is further evidence that solid solution

of Pd in chalcopyrite and pyrite is not an important mode of its occurrence in the ore.) Correlation coefficient data for secondary Cu sulfide ore (Table 10-II) indicate that Pd associates significantly only with Bi.

Pd minerals are rapidly destabilized with the onset of limonitic oxidation (Figs. 8C, 10A), and Pd minerals have not been observed in strongly oxidized ore from the upper levels of the deposit. The sudden drops in mean Pd contents of oxide ore (30 ppm Pd) and the gossan (16 ppm) (Fig. 16) indicate that most of the Pd is being flushed from the system. According to Table 10-III, in oxide ore Pd associates significantly only with vanadium (r_s[Pd-V]=.589). Vanadium is undergoing residual enrichment in successively higher weathering zones, so similarities in the geochemical behavior of Pd and V are not remarkable, and the meaning of the Pd-V correlation in this environment is obscure. One might doubt the significance of the correlation on the strength of only eight analyses, but the correlation is more striking in gossan material (r_s[Pd-V]=.843). It is tempting to speculate that vanadates or vanadiferous clays may be significant Pd collectors in a highly oxidized environment. The concentration of V in this surface horizon is several times that of Pd, and the ease with which V can be spectrochemically analyzed may lend it promise as a tracer in geochemical prospecting for Pd in this region.

In oxide ore, Pt shows a similar strong correlation with vanadium (r_s[Pt-V]=.781), but for unknown reasons, this correlation breaks down in gossan material (r_s[Pt-V]=.186), and in the gossan Pt correlates significantly only with Au (r_s[Pt-Au]=.858) (Table 10-IV); the number of analyses are too few to draw reliable conclusions regarding associations of Pt in the oxidized horizons. The most significant feature of the chemical data for Pt in the weathered profile is the abrupt rise in Pt content in the oxide ore horizon (Table 10-III and Fig. 16). Pt is also higher in gossan material than in sulfide ore. On the basis of only 8 analyses each for the oxide ore and gossan, one might hesitate to speculate on the possible significance of the apparent Pt increase, but corroborative evidence comes from results of solution experiments on the ore.

Since no discrete minerals of the minor PGE were detected in polished sections, 7 oxide ore samples (1.3 kg total) and 14 primary and secondary sulfide ore samples (1.14 kg total), including assayed samples with the highest Rh, Ir, Ru, and usually high Pt contents, were digested by boiling in $H_2C_2O_4$ + HF and then aqua regia with the hope of obtaining minerals of the minor PGE in the insoluble residue. Although one unusual metallic crystal obtained by this procedure was lost, no minor PGE minerals have been recognized. However, 54 sperrylite grains were obtained (the identity of each

Fig. 16. Schematic section of the New Rambler deposit showing variation of average precious metal contents (in ppm) between horizons of the weathered profile. (Log scale)

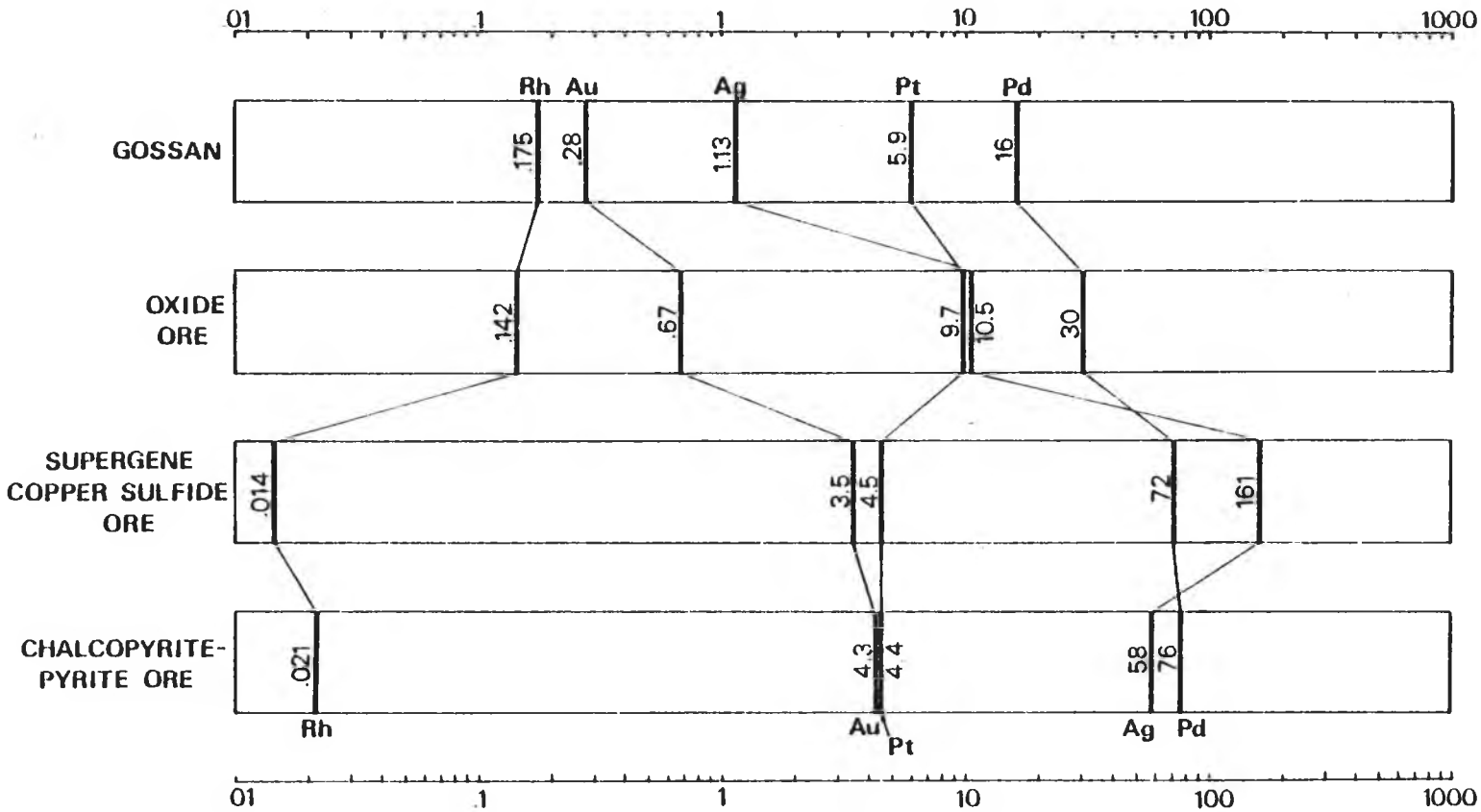
.01
.1
1
10
100
1000
Rh
Au
Ag
Pt
Pd
GOSSAN
.175
.28
1.13
5.9
16
OXIDE ORE
.142
.67
9.7
10.5
30
SUPERGENE COPPER SULFIDE ORE
.014
3.5
4.5
72
161
CHALCOPYRITE-PYRITE ORE
.021
4.3
4.4
58
76
Rh
Au
Pt
Ag
Pd
.01
.1
1
10
100
1000

sperrylite grain was established by qualitative microprobe analysis). An interesting feature of the distribution of sperrylite emerged: the mean content of sperrylite grains in 14 samples of sulfide ore was 0.43 grains/100 g sample, with a standard deviation of 0.61; the oxide ore yielded 2.12 grains/100 g sample, standard deviation 1.6. The grain size was equivalent in both groups (30-100 microns).

Thus, there are suggestions that Pt may be undergoing substantial secondary enrichment in the oxidized ore horizon by a solution-redeposition process, possibly by reprecipitation of Pt liberated from solid solution in decomposing Pd-Bi-Te minerals. But the alternative hypothesis that this sperrylite distribution is a relict feature of the primary ore cannot be discounted, and this interesting topic invites more attention.

Like Pt, the Rh content leaps dramatically in the oxidized levels of the deposit. Rh-Pt correlation coefficients are low in oxide ore and gossan (.238 and .178, respectively). The residence of Rh in the oxidized horizons is not known, but available evidence suggests it is not sperrylite.

Iridium and ruthenium were rarely detected in the ore (detection limit 0.5 ppm for each). It is no doubt significant that Ir was detected in only 1 of 45 sulfide samples and Ru not detected in any, whereas Ir or Ru was detected in 3 of 8 gossan samples. Travis et al. (1976) report that

retention of Ir in gossans of nickel sulfide deposits in Western Australia is exploited in geochemical prospecting for these nickel ores.

Considering the low Au values in the ore, the frequency with which electrum has been seen suggests that Au occurs in the ore mainly in the metallic state. Yellower color and greater resistance to dissolution in acid digestion experiments indicates that gold grains in oxide ore have undergone preferential leaching of alloyed Ag. Data of Figure 16 suggest that some Au is also undergoing solution in the oxidized levels of the deposit, but the evidence does not reflect secondary enrichment of Au in underlying horizons.

On the other hand, Ag originally liberated by decomposition of chalcopyrite has undergone dramatic secondary enrichment by a cycle of repeated leaching from the oxidized ore horizons and redeposition in the secondary Cu sulfide zone (Fig. 16). The Ag in enriched ore occurs in covellite (mean 119 ppm Ag, 6 mineral separates), in chalcocite (mean 162 ppm Ag, 4 separates), and in "deep-zone" non-siliceous, earthy limonite associated with abundant sulfides (mean 212 ppm Ag, 5 separates--analysts, J. G. Viets and J. A. Roybol, U. S. G. S.).

In oxide ore, Ag is tied up mainly in cuprite (mean 250 ppm Ag, 2 mineral separates), and in earthy limonite.

These data of mineral separates are corroborated by a high Ag-Cu correlation coefficient (.795) in oxide ore and by significant correlations with Ba (r_s[Ag-Ba]=.520 and .706 in oxide ore and gossan, respectively -- Table 10-III and -IV). Ba is concentrated in limonite in amounts of a few hundred to 5000 ppm, and ordinarily does not exceed a few ppm in Cu minerals, except sulfates and chrysocolla.

The only secondary Ag mineral recognized in New Rambler ore is native silver in partially oxidized assemblage 3 ore specimens, occurring in calcite-filled supergene solution cavities (Figs. 9B and 10A) and as small leaves and grains in deep zone limonite.

Summary of Major Features of the New Rambler Deposit

The New Rambler deposit is of hydrothermal origin and occurs in metagabbroic rocks at the intersection of a major shear zone with a subsidiary mylonite zone and several closely spaced faults.

Three principal mineral assemblages have been defined in the hypogene ore paragenesis: (1) an early assemblage consisting mainly of pyrite, with magnetite, pyrrhotite, pentlandite, and chalcopyrite as accessories; (2) and (3) copper-rich assemblages representing the main stage of ore deposition and consisting principally of chalcopyrite +

pyrrhotite but differing in accessory platinoid- and base-metal minerals. Thermochemical data on mineral compatibilities suggest deposition of assemblage 1 at temperatures in the vicinity of 335°C or somewhat higher, and the principal mineralization with deposition of copper- and platinoid-rich assemblages at temperatures somewhat below 335°C. Ten platinum and palladium minerals are recognized in the ore, nine of which contain essential Te. Pt and Pd apparently occur in the ore principally as platinoid minerals.

A comparative study of the distribution and geochemical behavior of the precious metals Pt, Pd, Rh, Au, and Ag in the weathered portions of the deposit has shown that Pt and Rh are substantially enriched in the strongly oxidized ore horizons, possibly due to supergene processes. Pd and Ag have been extensively mobilized from the upper levels during weathering. Ag has undergone dramatic enrichment in the supergene sulfide zone, but Pd apparently has been removed from the systems.

OTHER OCCURRENCES OF PLATINUM-GROUP ELEMENTS

High concentrations of PGE are known from three other localities within the area studied. A copper-rich quartz vein containing high concentrations of platinoids is closely related in type to the Au-Cu-bearing quartz veins, and is discussed along with them. Anomalous levels of PGE are present in a fault-controlled occurrence near the town of Albany, and a small deposit resembling the New Rambler is situated immediately southwest of that mine.

The Blanche Mine

This property is located in the SE¼ Sec 32, T.14N, R.79W., a quarter mile southwest of the New Rambler mine. Bedrock exposures are non-existent in the immediate vicinity of the mine, and details of the structural influences localizing the deposit are unknown, but according to McCallum and Orback (1968, Plate 1) the northeast-trending mylonite zone that in part localizes the New Rambler ore bodies is known to pass through the Blanche property (Fig. 2). Rock types exposed on the small mine dump are mostly fresh to chloritized metapyroxenite and metagabbro with a small amount of mylonitic felsic gneiss. Beeler (1902, p.2) reports that the principal mineralization encountered to that date was associated with a lens of white quartz 8 inches to 8 feet wide having a "honey-combed" structure filled with iron oxide. "Soft

clay-like gouge matter" adjacent to the quartz lens was described as "highly mineralized." Beeler (1906, p.45) states that a shaft had been sunk to a depth of 160 feet, and at a depth of 120 feet copper carbonates and sulfides were found. There is no record of production, if any, from the Blanche property.

Mineralized material is very sparse on the dump, but two fist-size samples collected were comprised of banded massive ochreous yellow and red limonite with abundant disseminated malachite, a little cuprite, and traces of chalcocite and sperrylite. No silicate gangue was present, and these specimens are replacement-type ore indistinguishable from typical oxide ore of the New Rambler deposit. Sperrylite seen in section was a large euhedral crystal (about 0.5 mm across) enclosed in yellow limonite. Twelve additional grains of sperrylite and a few irregular fragments of gold (or electrum) were obtained by acid digestion of 366 grams of the oxide ore samples. Assays of the two samples from the Blanche mine gave 6 and 17 ppm Pt, 30 and 20 ppm Pd, .002 and .060 ppm Rh, .06 and .02 ppm Au, and 20 and 17 percent Cu.

Too little is known of the mineralogy and distribution of ore in the Blanche deposit to evaluate the origin of this deposit, but the resemblance of specimens examined to New Rambler ore and the similar lithologic environment suggest a similar origin.

Prospect, Sec. 15, T.14N, R.78W.

A short prospect trench has explored limonitic fault breccia within a gabbroic xenolith in Sherman granite adjacent to its contact with the Lake Owen mafic complex (McCallum, pers. comm. 1976). Where cut by the fault, the gabbro is mostly strongly metasomatized to rock of more or less granodioritic character. No quartz or other typical vein gangue was noted along the fault, but magnetite and spongey brown limonite of indeterminate parentage are very abundant in fault material in the prospect trench. An assay of a magnetite concentrate (about 95 percent pure) showed more than 1 wt percent Ti, 1000 ppm Cr, 5000 ppm V, 0.020 ppm Pt, and 0.035 ppm Pd. Limonite concentrates averaged 0.058 ppm Pt (0.120 maximum), 1.2 ppm Pd (1.4 ppm maximum) and contained up to 500 ppm Mo, 700 ppm Pb, and 1500 ppm Zn (R. R. Carlson and E. F. Cooley, analysts). Values of the other metals were very low.

This PGE occurrence was given only cursory inspection due to the low grade of ore metals, and little is known of the mineralogy or origin of the deposit. However, the chemical data of the magnetite sample unequivocally point to very high temperature origin (i.e., not hydrothermal in the ordinary sense of the term), and it seems likely that heat derived from the Sherman granite intrusion may have induced diffusion of relatively mobile elements of the metagabbro (and to a lesser extent of the granite) into the fault zone.

VEIN DEPOSITS

Introductory Comments

The deposits discussed in this section are mineralogically diverse and occur in a variety of host rocks, but all share one characteristic: the ore mineralization is confined in quartz and/or carbonate shoots along faults and tension fractures subsidiary to the Mullen Creek-Nash Fork shear zone. The overwhelming majority are associated with mafic metaigneous bodies that range in dimension from major plutons to narrow dikes and dike-like lenses a few hundred feet or less in length. It is believed that mafic rocks played a significant, though possibly non-essential role in genesis of metallic vein mineralization.

Features such as possible large scale zoning of mineral distribution in veins and possible intimate relations between mineral distribution and lithologic and structural controls in the deposits could not be studied in detail due to inaccessibility of subsurface workings at all mined deposits and poor to non-existent outcrop exposure of mineralized segments of the vein-fault systems. Hand-sample size fragments of mineralized vein material and hydrothermally altered wallrock were collected from waste dumps of mines and prospect pits, and in a few cases it was possible to collect from outcrops a series of progressively altered wallrock samples traversing weakly mineralized segments of faults.

One hundred twenty-four polished ore specimens from the vein deposits were examined microscopically, and 136 thin sections of country rocks and altered wallrocks were evaluated. Several dozen quantitative and qualitative analyses of vein minerals were made using the electron microprobe. Representative analyses of all minerals analyzed quantitatively are presented. Concentrations of minor and trace elements in vein, wallrock, and country rock samples were determined semiquantitatively by emission spectrographic analysis by chemists with U. S. Geological Survey, and U. S. G. S. chemists provided quantitative determinations of Au, Ag, and Cu by atomic absorption analysis, and of PGE and Au by a combined fire assay emission spectrographic method. Significant information from these assays is presented.

The typically Cu-Au-rich (locally Cu-Ag-Pb-rich and rarely platinoid-bearing) vein deposits are interpreted to have been derived by concentration in faults and fissures of metals, silica, and other constituents mobilized during retrograde hydration, carbonatization, and desilication metamorphic-hydrothermal reactions that accompanied regional cataclasis on the Mullen Creek-Nash Fork shear zone and its complex system of secondary fractures. The Au-Cu deposits share a number of general features--mineralogy, lithologic milieu, and structural setting--with well known gold-producing districts elsewhere in the world, notably the Yellowknife district,

Northwest Territories (Boyle, 1960); the Mother Lode district, California (Knopf, 1929); the Kalgoorlie Goldfields, Western Australia (Lindgren, 1905; Simpson and Gibson, 1911); and numerous deposits in the greenstone terranes of the Rhodesian and Kapvaal cratons, southern Africa (Anhaeusser, 1976).

General Characteristics of the Mines and Prospects

In this section, a brief account is given of lithologic and structural associations of individual vein deposits, the character of the veins is described briefly, and a summary of mine development and production is provided in cases for which information is available. Several deposits having no economic significance share essential features with the larger orebodies and supply information valuable in compiling a composite character profile of regional vein mineralization.

The Keystone Mine

The Keystone mine is located in Sec.22, T.14 N., R.79 W., adjacent to the small resort settlement of the same name. The deposit occurs in the southeast-trending Keystone-Florence wrench fault which locally is a splayed shear system up to 300 feet wide but converges along most of its length to a narrow, steeply dipping planar shear six to ten feet wide. The main oreshoot in the Keystone deposit was over 300 feet long and two to six feet wide (Anonymous, 1896, p.9). The

vein is along a metadiorite-metadiabase dike that intrudes generally intermediate-composition biotite-hornblende-quartz-andesine gneisses of the older metasedimentary-metavolcanic complex. Most of the dike is intensely sheared, and where exposed in prospect pits along the Keystone-Florence fault, it consists of narrow lenses a few tens of feet long of chlorite-sericite-carbonate-albite-quartz blastomylonite and mylonite schist, referred to as "talc" by the miners. Samples of weakly foliated and non-foliated, fine-grained, nearly fresh metadiorite-metadiabase collected on the mine dump consist of about 45 percent blue-green hornblende (some with fairly abundant small quartz inclusions suggesting former clinopyroxene), moderately epidotized zoned calcic andesine, 2 to 3 percent biotite (secondary in part), minor sphene, traces of pyrite, and occasionally a little chlorite.

The Keystone vein was developed by a 365-foot deep shaft and about a mile of drifts (Beeler, 1906, p.49). The ore was processed by one ten-stamp and one twenty-stamp mill and four concentrators. Full-scale operations ceased in 1893, by which time the mine had yielded about $96,000 of its approximately $98,000 in gold production (Curry, 1959, p.56). The ore reportedly averaged $23.50 per ton in gold (1896 prices), about 55 percent of the gold being free-milling (Anonymous, 1896, p.9).

Pyrite, chalcopyrite, and gold are the only hypogene ore minerals present in quantity, but a variety of other primary metallic minerals are present in minor to trace amounts. Supergene copper sulfides and oxidized copper minerals are major vein constituents. Gold occurs as relatively coarse isolated or clustered grains and specks disseminated in quartz and to a lesser extent in chalcopyrite. Much of the gold has been remobilized into microfractures in quartz where it occurs as fine flakes. Metal values in eight assayed vein samples collected from the waste dump are shown in Table 11.

The Florence Mine

The Florence mine is situated about 0.75 mile southeast of Keystone on the Keystone-Florence shear. Auriferous pyrite seams occur in and along quartz-ankerite veins associated with cataclastic-metadiabase lenses that are enclosed in sheared quartz diorite. The metadiabase pods are pervasively altered to chlorite-sericite-calcite-albite quartz mylonite schist, and quartz diorite is converted to a locally strongly foliated assemblage of quartz, microcline, sericite, calcite, and chlorite. The oreshoot was from three to five feet wide and was developed by a 160-foot shaft and about 200 feet of drifts (Anonymous, 1896, p.9; Knight, 1942, p.12). The mine's $50,000 gold production came from seams of auriferous pyrite one to eighteen inches wide that ran from $155 to $1000 per

Table 11. Contents of some precious and base metals in mineralized vein samples from 17 deposits. Number in parentheses below name of locality indicates the number of samples analyzed from that deposit. Values in ppm, except Cu and Fe. Au, Pd, and Pt by fire assay-emission spectrography--analysts: R.R. Carlson, E.F. Cooley, T.A. Doerge; Ag, Au, Cu, Pb, Zn by atomic absorption--analysts: R.B. Carten, C.A. Curtis, J.G. Frisken, J. Mitchell, R.M. O'Leary, J.A. Roybol, J. Sharkey, J.G. Viets; As and Mo by color spot--analysts: W. Cary and R.B. Carten, respectively; Bi, Co, Fe, Ni, Pb, Sb by semiquantitative D.C. arc spectroscopy--analysts: R. Babcock, L.B. Breeden, E.F. Cooley, K.J. Curry, G.W. Day, J. Domenico, W.D. Goss, D.J. Grimes, J. Haffty, R. Hopkins, L.B. Riley, D. Siems, all of U.S. Geological Survey. Abbreviations: ND(100) = not detected at detection limit of 100 ppm; ——(2/5) = mean not computed, element detected in only 2 of 5 samples analyzed.

		Albany Mine	"Anonymous" Mine	Bear Mine	Black Mine	Cuprite Mine	Duchess Mine	Florence Mine	Gold Crater Mine	Golden Key Mine
		(8)	(3)	(2)	(7)	(3)	(1)	(7)	(2)	(3)
Ag	mean	10	5.0	ND (0.5)	12	4.0	720	12	29	7.1
	range	0.2-30	0.1-10		0.1-50	1.0-5.0		0.1-30	24-34	0.5-20
As	mean	18	ND (200)		——(2/7)	350	1000	159	ND (200)	——(1/3)
	range	10-20		<200-500	<200-300	20-1000		50-500		<200-1000
Au	mean	5.0	53	.77	15	.15	8	292	5.3	33
	range	.05-20	.06-110	.04-1.5	.04-100	.05-.35		2.0-800	3.5-7.0	0.2-75
Bi	mean	ND (10)	ND (10)	ND (10)	——(2/7)	——(1/3)	50	17	160	ND (10)
	range				10-300	<10-20		2-30	20-300	
Co	mean	7	12	50	429	307	15	348	30	72
	range	~3-20	5-20	30-70	50-1000	70-700		15-700	10-50	15-150
Cu	mean	9.3%	.04%	6.1%	.55%	.04%	8.8%	.05%	3.6%	1.1%
	range	.64-21%	.002-.11%	3.2-9.0%	.001-2.3%	.02-.12%		.003-.2%	.5-6.6%	.1-3.0%
Fe	mean	4.3%	7.3%	13%	8.6%	24%	10%	11%	7.5%	13%
	range	1.5-7%	5-10%	5-20%	3-15%	5-60%		5-20%	5-10%	3-20%
Mo	mean	11	ND (5)	51	——(1/7)	——(1/3)	ND (5)	ND (5)	ND (5)	8.7
	range	3-20		1-100	<1-2	<1-1.0				1-15
Ni	mean	15	12	3	44	123	30	40	12	233
	range	2-30	7-20	3-3	20-150	20-300		15-100	3-20	50-500
Pb	mean	34	5.3	28	458	13	150	8.1	325	14
	range	10-100	1-10	5-50	1-3000	10-20		1-20	150-500	1-30
Pd	mean*	.011 (6/8)	.005	.005	.009 (4/7)	.012 (2/3)	.010	.014	——(1/2)	.034
	range	<.001-.025	.005-.006	.002-.008	<.001-.045	<.004-.020		.001-.050	<.001-.010	.002-.070
Pt	mean*	.007 (5/8)	.008	.014	——(1/7)	.013	.014	.012 (5/7)	——(1/2)	.022
	range	<.002-.035	.005-.010	.008-.020	<.002-.080	<.002-.025		<.002-.050	<.002-.004	.007-.050
Sb	mean	ND (100)	ND (100)	ND (100)	ND (100)	ND (100)	3000	ND (100)	ND (100)	ND (100)
	range									
Zn	mean	13	ND (200)	ND (200)	318	53	300	ND (200)	ND (200)	ND (200)
	range	10-20			75-1000	40-70				

Table 11 (cont'd.).

		Independence Mine	Keystone Mine	Lake Creek Mine	Prospect, Sec.7, T.14 N., R.78 W.	Prospect, Sec.18, T.14 N., R.78 W.	Prospect, Sec.34, T.15 N., R.80 W.	Prospect, Sec.35, T.15 N., R.80 W.	Sunset Mine
		(9)	(8)	(5)	(2)	(4)	(9)	(3)	(11)
Ag	mean	9.7	10	27	56	9.5	784	.3	1.4
	range	.1-50	1.0-20	1.5-84	2.5-110	1.0-28	2.5-2000	.2-.5	.1-5.5
As	mean	500	---(1/8)	---(1/5)	---(1/2)	250	4556	ND (200)	15
	range	100-1000	200-200	200-500	200-1000	75-700	200-12500		5-20
Au	mean	3.2	117	.17	1.6	1.7	2.6	.40	.83
	range	.15-14	6.5-300	.004-.60	.60-2.5	.25-5.0	.30-5.0	.15-.45	.05-7.0
Bi	mean	---(1/9)	339	ND (10)	---(1/2)	---(1/4)	196	ND (10)	ND (10)
	range	10-10	10-1000		10-15	10-20	10-500		
Co	mean	242	37	134	25	18	ND (5)	12	43
	range	1-700	3-150	10-500	20-30	20-200		5-20	~1-200
Cu	mean	3.2%	2.3%	12%	41%	5.9%	.72%	5.2%	3.1%
	range	.02-8.0%	2.8-30%	3.5-47%	.01-16.5%	.01-16.5%	.15-2.5%	2.0-8.0%	.36-9.0%
Fe	mean	17%	3.1%	14%	4%	19%	2.3%	7%	3.5%
	range	5-45%	1-5%	7-20%	1-7%	10-30%	0.5-5%	5-10%	1.5-10%
Mo	mean	22	---(1/8)	ND (5)	17	95	24	ND (5)	14
	range	1-150	5-7		3-30	30-200	10-50		1-50
Ni	mean	121	31	76	250	88	7	43	25
	range	15-300	10-50	10-150	200-300	50-200	2-20	10-70	10-100
Pb	mean	6.4	---(3/8)	61	35	21	134800	48	---(3/11)
	range	1-20	10-30	5-200	20-50	5-30	46000-190000	40-55	5-20
Pd	mean	.006 (6/9)	.004 (6/8)	.028	16	.004	.022	.002	---(5/11)
	range	.002-.020	.002-.010	.004-.040	1.2-30	.002-.006	.006-.060	.001-.002	.002-.070
Pt	mean	---(4/9)	---(4/8)	.060	23	---(1/4)	ND (.005)	ND (.004)	ND (.002)
	range	.002-.040	.002-.014	.001-.250	5.5-40	.002-.007			
Sb	mean	ND (100)	ND (100)	ND (100)	ND (100)	ND (100)	5189	ND (100)	ND (100)
	range						700-15000		
Zn	mean	ND (200)	15	ND (200)	ND (200)	---(1/4)	1457	72	53
	range		10-25			200-500	110-3000	45-90	20-80

*For deposits in which Pd or Pt was detected in more than half the analyzed samples, the mean of analyses was estimated by assigning an arbitrary concentration of 0.0005 ppm to samples in which Pd or Pt was not detected. Fraction in parentheses is (number in which detected/number of samples analyzed). Average detection limits are 0.002 ppm Pd, 0.003 ppm Pt.

ton in gold (Anonymous, 1896, p.10). Chalcopyrite is uncommon in the vein, and all the value was in gold. Most of the gold occurs in pyrite and its derivative limonite as disseminated specks a few microns in diameter and as thin veinlets healing fractures in brecciated pyrite and quartz. Seven ore samples from the Florence mine were assayed in the present investigation (Table 11).

The Independence Mine

The Independence Mine is located in Sec.15, T.14 N., R.79 W., about a mile north of Keystone. The deposit is situated at the intersection of the east-trending Monarch fault and the southeast-trending Mammoth shear; the latter is a persistent structure traceable for about four miles southeastward from the Independence mine. At the intersection, both faults are occupied by large quartz veins six to twenty feet wide that contain disseminated pyrite, chalcopyrite, a little gold, and locally abundant ankerite. The deposit is enclosed in a series of intermediate-composition gneisses. The southeast-trending shear contains pods of blastomylonitic mafic rock in the vicinity of the mine, and this material is common on the mine dump. The oxidized, near-surface portion of the Mammoth vein carried "low-grade" disseminated Cu-Au mineralization reportedly assaying $3 to $3.50 per ton in Au and Ag and 13.5 percent Cu in "average specimens" (Anonymous, 1900, p.11).

However, principal interest focused on a "large number of small rich veins on each side of this ledge [i.e., master vein] dipping and running into it, varying in width from six to eighteen inches and carrying from $10 to $300 gold per ton" (Anonymous, 1896, p.10). Few samples approaching the indicated grades are presently in evidence on the mine dump. Metal values in assayed dump samples are shown in Table 11. Gold seen infrequently in polished section occurs as micron-size specks in Co- and As-rich, massive, medium-grained pyrite that is present on the dump in fist-size and larger chunks.

The Independence deposit was developed by an 80-foot shaft with 100 feet of crosscuts on the Mammoth vein, and about 0.1 mile to the west, a 125-foot adit driven eastward on the Monarch vein. The value of production is not recorded.

The Black Mine

This property is located 0.5 mile southeast of the Independence mine and is situated at the intersection of the Mammoth shear with an east-trending fault occupied by an andesite dike that runs for about two miles eastward from the Black mine (McCallum, unpub.). The faults intersect adjacent to the contact of the gneiss-schist complex and the Keystone quartz diorite pluton (Fig. 2). A shaft was sunk on the fault intersection within quartz diorite, and a few hundred feet to the west in gneisses and schists, an adit was driven northwestward

on the Mammoth vein. Sparse fragments of vein quartz impregnated with chalcopyrite and appreciable electrum may be found on the mine dump, but the bulk of the sulfide mineralization occurs as very abundant small lenses and streaks of pyrite in hydrothermally altered schists. Locally, minor amounts of sphalerite and galena and traces of chalcopyrite and electrum accompany pyrite in the schists. Assays of seven samples from the Black mine are presented in Table 11.

The hydrothermal alteration includes quartz-sericite-chlorite-carbonate replacement, but much of the alteration is an atypical, apparently higher temperature type comprised of a phlogopite-quartz-calcite-albite-tourmaline-sulfide assemblage. (The character of hydrothermal alteration is discussed in fuller detail in a following section.)

The Gold Crater Mine

A quarter mile east of the Black mine on the east-trending, andesite dike-bearing fault is the Gold Crater mine (Fig. 2). The deposit occurs in quartz diorite country rocks. According to Beeler (1905), initial development on the property was a shaft sunk into a large quartz vein within the andesite dike. Beeler (1905, p.3) notes that in either direction from the mine, the dike and fault trend east-west, but the mineralized segment into which the shaft was sunk trends southeasterly--indicating the mineralization is localized at a flexure in the

fault. Another shaft was sunk about 400 feet southwest of the first, and a drift connecting the shafts encountered a mineralized lensatic quartz seam trending northeast along the drift. This oreshoot was three to eighteen inches wide, approximately 35 feet long, and was stoped updip over an unreported interval, but it pinched out a number of feet short of connecting with the main east-west vein. Beeler's account of the oreshoot apparently describes a mineralized tear fault splaying from the east-west vein-fault. Judging from the attention it received, it apparently carried substantially higher grade ore than the larger main vein. Beeler (1905, p.4) characterized the splay as averaging "one foot of $20 ore," with some "phenomenally rich ore" being taken out locally, apparently from pyrite- and chalcopyrite-rich portions. Only a trace of sulfide was seen in dump material and no gold.

About 400 feet west of the Gold Crater shafts, the east-west dike-fault is cut by a small fracture trending N.10°W. The crossfault is occupied by a quartz seam five to eighteen inches wide that carries abundant ankerite and a high concentration of chalcopyrite, bornite, and a little electrum.

Two ore samples from the Gold Crater group were assayed (Table 11). One is a moderately oxidized chalcopyrite-bearing vein specimen with attached selvage from the dump of the main shaft, and the other is a Cu-rich vein sample from the cross

fracture west of the mine; the latter has a chalcopyrite-bornite-pyrite-hematite assemblage with traces of galena and electrum.

Prospects, Sec.13, T.14 N., R.79 W. and Adjacent Sec.18, T.14 N., R.78 W.

This small group of Cu-Au prospects is situated in a generally east-trending 200- to 300-foot wide shear zone near its intersection with a younger north-trending fault (Fig. 2). Immediately west of the prospects, the shear zone cuts a small gabbroic stock emplaced in Keystone quartz diorite, and east of the prospects, the shear zone intersects a number of closely spaced diabasic and granitic sills and dikes concentrically bounding the Lake Owens mafic complex (McCallum, unpub.). The main body of the mafic complex crops out 0.75 mile southeast of the Au-Cu prospects.

Small mineralized quartz veins along the margin of the shear zone have been explored by a shaft and two adits. The veins are enclosed in sheared, K-metasomatized, and hydrothermally retrograded quartz diorite. Chalcopyrite, pyrite, and a little gold are the important metallic constituents of the veins. Adjacent to the prospects, a tributary of Indian Creek flows across the shear zone, and the gravel bed has been worked as a small placer operation for a short distance downstream.

The Albany Mine

The Albany mine is located in Sec.10, T.14 N., R.79 W., about 2.5 miles north of Keystone. The vein is along the Albany-Cuprite fault, a relatively simple, steeply dipping wrench fault that carries sporadic mineralization along its length for at least 2.5 miles in a southeasterly direction from the Albany mine. The country rocks are felsic quartz-oligoclase-microcline-biotite gneisses that are intensely to moderately sheared over an interval 30 to 50 feet wide along the fault in the vicinity of the mine. The mineralized fault is occupied by an intensely sheared mafic dike four to six feet wide that is hydrothermally decomposed to chlorite-sericite-calcite-albite-quartz mylonite schist. A quarter mile northeast of the main mine shaft, a flexure in the dike consists of non-foliated, fine-grained metadiorite comprised mainly of hornblende and sodic andesine, with subordinate subhedral epidote, and a little chlorite and sericite derived from hornblende and plagioclase.

There are no available physical descriptions of the ore-body. Beeler (1906, p.45) reports that a 360-foot shaft was sunk on low grade copper ore, and drifts were run on the vein. A report by operators of the mine stated a "large" body of ore containing covellite was encountered at a depth of 150 feet (Curry, 1959, p.51).

Vein material on the mine dump consists of milky quartz (some comb-structured) containing abundant ankerite, calcite, chalcopyrite and its supergene derivatives, lesser pyrite and specular hematite, and variable amounts of electrum. The latter occurs mainly as sparse irregular disseminations in quartz. Metal contents of assayed vein samples are shown in Table 11.

The earliest gold discovery in the region was a placer located in Moore's Gulch a few hundred yards downstream from the site of the Albany mine. The total value of placer gold recovered along Douglas Creek and its tributaries has been calculated by Curry (1959, p.60) from various records as about $73,000. Moore's Gulch contributed about $8000 (1868 prices) in the first few months following its discovery.

The Cuprite Mine

The Cuprite mine is located about 0.75 mile southeast of the Albany mine on the same fault. The country rocks are mainly felsic gneisses varying from granitoid-textured rocks of granitic mineralogy to well foliated quartzo-feldspathic gneisses with substantial amounts of biotite; biotite-rich gneisses grade into minor hornblende-rich gneisses. At the Cuprite mine, the Albany-Cuprite fault contains a mafic dike that is poorly exposed at the surface, but is approximately three to eight feet wide. Relatively unaltered portions of the dike vary lithologically from pegmatitic hornblendite to hornblende

andesine-epidote pegmatite--locally with foot-wide segregations of pegmatitic salmon-pink andesine--to weakly foliated, medium-grained metagabbro comprised of hornblende, calcic andesine, abundant epidote, and a little apatite, sphene, biotite, and magnetite. The hornblendite and other pegmatitic portions of the dike appear to be derived from gabbroic dike rock that recrystallized under volatile-rich conditions at high temperature. Some dike components migrated into a short splay diverging southwestward from the main fault. The diverging arm is occupied by pegmatitic andesine-oligoclase and a little quartz and K-feldspar. Portions of the dike are intensely sheared and are retrograded to lower temperature hydrothermal assemblages comprised mainly of very fine-grained chlorite, carbonate, sericite, and quartz. A few small quartz lenses containing specular hematite are exposed in surface outcrops.

Beeler (1906, p.45) reports that a 945-foot long adit driven eastward along the fault cut a number of bodies of ore. The miners left little evidence of their discoveries on the mine dump. The few small samples of vein material to be found on the dump consist mainly of medium- to coarse-grained microcline and epidote containing variable amounts of oxidized pyrite and occasionally a little quartz. The pyrite is frequently accompanied by variable amounts of martitized magnetite and bladed specular hematite, the latter derived in part

from late hypogene decomposition of ankerite or siderite. Occasionally pyrite is intergrown with prisms of black tourmaline several millimeters long.

Curry (1965, p.8) states that a 1903 review of its properties by the Medicine Bow Mines Company, operators of the Albany, Cuprite, Douglas, Gold Crater, and Lake Creek mines, reported that the mineralized zones in the Cuprite mine contained native copper, cuprite, pyrite, chalcopyrite, chalcocite, and values in Au and Ag. Assays reportedly ranged: Cu, 3 to 28 percent; Au, a trace to 2.56 fine ounces per ton; and Ag, a trace to 2 ounces per ton. The ore reportedly carried values in Co and Cr. Cr was not detected in any of three vein samples assayed for this study, and values of precious metals are very low (Table 11). A composite assay sample of about 25 small fragments of strongly oxidized pyrite yielded 0.35 ppm Au, 2 ppm Ag, and 600 ppm and 1000 ppm Co and As, respectively, the latter two elements being substantially enriched relative to ordinary pyrite (R. R. Carlson and E. F. Cooley, analysts).

The Bear Mine

About 0.5 mile southeast of the Curpite mine, a shaft has been sunk into a small Cu- and Au-bearing quartz vein enclosed in blastomylonitic, carbonated mafic rock. At this point, the Albany-Cuprite fault cuts and offsets laterally a northeast-trending phacolith-like lens of metagabbro about a quarter mile

long and up to 200 feet wide, intruded into apparently unfaulted quartzo-feldspathic gneiss (McCallum, unpub.). A narrow quartz-carbonate vein along this segment of the fault contains abundant chalcopyrite, traces of gold, and a little molybdenite. No descriptive account of the property or its production, if any, is available. Table 11 shows assay data for two chalcopyrite- and malachite-rich vein samples from the Bear mine.

Platinum-Bearing Prospect, Sec.7, T.14 N., R.78 W.

Near the eastward termination of the Albany-Cuprite fault, a gentle swerve in the fault trend is accompanied by broadening of the shear to form a lens of sub-mylonitic to mylonitic quartzo-feldspathic gneiss approximately 100 feet wide and a quarter mile long. In surface exposures, the sheared lens is developed entirely within quartzo-feldspathic gneiss. Prospect pits along the eastern end of the sheared lens have exposed several small, weakly mineralized quartz seams. A few samples comprised mainly of secondary Cu sulfides, malachite, limonite, and a little pyrite were collected from one of the prospect pits. Two samples were assayed and yielded extraordinary concentrations of Pt and Pd, high Rh, Ag, and As, and significant amounts of Au and Ni (Table 11). The occurrence of this metal assemblage in a felsic lithologic milieu is perplexing. The nearest known exposure of mafic rocks is a northeast-trending

gabbroic dike that is cut by the shear zone approximately 0.75 mile west of the prospects and another small diabase dike about 0.25 mile southeast of the prospects that does not appear to reach the fault (McCallum, unpub.). One is tempted to speculate that mafic rocks are cut at depth by the shear.

The Duchess Mine

The Duchess is located in Sec.32, T.15 N., R.79 W., one mile west of the New Rambler mine. The deposit is situated within the Mullen Creek-Nash Fork shear zone and is enclosed in mylonitized metagabbro and metadiorite of the Mullen Creek mafic complex. Three exploratory shafts were sunk where the shear zone is cut by two southeast-trending, closely spaced faults (McCallum, unpub.). The cross-faults have very poor surface exposure within the shear zone. Dump material and vein exposures in prospect pits indicate the mineralization occurred as sizable ankerite- and siderite-rich quartz veins with local concentrations of chalcopyrite, Ag-bearing tetrahedrite, gold, hematite, and pyrite; the latter occurs mainly in wallrock at the vein selvage. This property is given only passing mention in early accounts of mining activity in the region, and apparently it yielded no notable ore production.

Copper Prospect, Sec.35, T.15 N., R.80 W.

About 3.5 miles west of the New Rambler mine, a group of shallow shafts, prospect pits, and trenches explores minor amounts of Cu mineralization in mylonitized quartzo-feldspathic gneiss and metagabbroic units of the Mullen Creek igneous complex. In this general area, the southern branch of the Mullen Creek-Nash Fork shear zone is cut by two large southeast-trending faults that offset the shear belt by right lateral movement of up to a quarter mile (McCallum, unpub.) (Fig. 2). The eastern member of the pair is in turn offset slightly by a small east-southeast-trending fault within the shear zone. Vein quartz containing disseminated hematite, chalcopyrite, pyrite, and their weathering products occupies the intersection, and a large vein of barren bull quartz continues eastward along the younger fault for several hundred yards before wedging out. The mineralization explored by these prospects is economically insignificant. The deposit was investigated because of the resemblance of its lithologic and structural associations to those of the New Rambler deposit. Assay data (Table 11) show no evidence of anomalous concentrations of PGE.

Lead-Silver-Copper Prospect, Sec.34, T.15 N., R.80 W.

Less than a mile west of the Cu prospects just described, a string of prospect pits have exposed a small vein of rich Ag mineralization. Here, a metadiabase dike eight to ten feet

wide intrudes a granitic stock of the Mullen Creek igneous complex. The fault occupied by the dike has been reactivated, and both granite and diabase are sheared; K-metasomatism of the mafic dike is pronounced. A quartz vein a few inches to about a foot in width occurs along the sheared margin of the diabase dike at its contact with granite. The vein is richly impregnated with siderite, specular hematite, fibrous to prismatic hypogene goethite, and abundant coarse-grained argentiferous galena; subordinate amounts of fine-grained bournonite, friebergite, sphalerite, chalcopyrite, and pyrite accompany the galena, and oxidized weathering products of the sulfides are prolific in variety and amount.

The Sunset Mine

The Sunset mine (originally located as the Hamilton) is located on Devil Gate Creek at the boundary of Secs.35 and 36, T.14 N., R.80 W., a little over four miles southwest of Keystone. The vein occurs within a persistent east-southeast-trending fault of little offset that can be followed in discontinuous bedrock exposures over a strike length of about four miles (McCallum, unpub.). The Sunset deposit is situated entirely within cataclastic metagabbro and metadiorite of the Mullen Creek igneous complex, but in this area, metagabbroic units of the complex are intruded by numerous small lenses, pods, and irregular bodies of granitic rocks.

The Sunset fault is occupied by a relatively persistent quartz vein that ranges from a few inches to three feet in width and contains sporadic Cu mineralization and associated traces of gold that are prospected intermittently for over a mile westward from the Sunset mine. The ore exploited by the mine occurs in the main fault immediately east of a splay from the master vein. The weakly mineralized splay has been prospected for a hundred feet or so southeastward from its point of divergence. The main vein pinches out about 700 feet east of the mine.

The Sunset mine workings are comprised of a 95-foot shaft with a few crosscuts along the vein (Beeler, 1907, p.2) and two adits into vein outcrops on either side of the creek. Hypogene ore minerals include local rich concentrations of chalcopyrite and pyrite, subordinate hematite and bornite, and traces of molybdenite and gold. Au values are generally low in assayed samples (Table 11). The higher Au values occur in chalcopyrite-rich pyrite-bearing ore; values are very low in chalcopyrite-bornite-hematite ore. The apparent absence of hypogene carbonates in the vein and wallrocks of the Sunset deposit and adjacent prospects is atypical of mined Cu-Au-bearing veins in the central Medicine Bow Mountains, and their absence may bear significantly on the low gold:sulfide ratio in the vein. No production figures from the Sunset Deposit are available.

The Golden Key Mine

The Golden Key mine is located three miles west of Keystone in Sec.10, T.14 N., R.79 W. A small gold-bearing pyritic quartz vein occurs in a southeast-trending fault along which movement has apparently had a strong vertical component (McCallum, unpub.). The deposit is enclosed in metagabbroic rocks of the Mullen Creek complex.

Vein workings evident at the surface are several prospect pits, two shafts, and a small dump. The quartz vein contained abundant strongly oxidized pyrite, traces of oxidized chalcopyrite, limonite with rhombohedral parting implying derivation from ankerite or siderite, and moderate amounts of gold. Where visible, the gold occurs mainly enclosed in quartz as disseminated grains and as leaves along microfractures in sulfide-rich portions of the vein. No reports on the deposit or its production are available.

"Anonmyous" Mine, Sec.28, T.14 N., R.79 W.

This mine, located about a mile southwest of Keystone, has several collapsed buildings, a relatively large dump, and some fairly high-grade gold ore, but no account of the deposit has been found in published literature or in reports held by the Wyoming Geological Survey.

The deposit is situated along a curved, generally east- to southeast-trending fault that is exposed only for about a

quarter mile west and southeast from the mine, but the position of the arm west of the mine suggests possible continuity with the Golden Key fault (McCallum, unpub.). Vein mineralization occurs within biotite- and hornblende-rich gneisses that are intensely altered to generally non-foliated, very fine-grained, hornfelsic-textured carbonate-sericite-quartz-albite rock. This material encloses a quartz vein or lens less than a foot wide in prospect pit exposures. The only mineralization seen in the quartz vein is magnetite. However, intense hydrothermal alteration of brecciated gneisses extends laterally outward for several feet on either side of the quartz vein. Breccia fractures in altered schist are healed by randomly crisscrossing ankerite and calcite veins mostly two inches or less in width that carry subordinate amounts of cobaltite and a little gold and gersdorffite. Two features of this deposit that deviate conspicuously from the general pattern of vein mineralization in the district are the apparent absence of mafic igneous rocks in the immediate vicinity and the occurence of the bulk of the metallic mineralization within carbonate rather than quartz veins.

The Lake Creek Mine

A wide shear zone trends east-west across the southern margin of the area shown in Figure 2. The Lake Creek mine is located within this shear zone in Sec.2, T.13 N., R.79 W. The

principal vein is along a metapyroxenite dike within sheared, K-metasomatized, carbonated Keystone quartz diorite. Most of the dike consists of chlorite-sericite-carbonate mylonite schist. Samples of unsheared fresh metapyroxenite are composed of distinctly foliated, medium-grained, pale pargasitic amphibole with irregular greenish splotches developed without regard to grain boundaries, and minute traces of magnetite and plagioclase(?).

Curry (1965, p.9) reports that underground workings included a 75-foot shaft with 715 feet of crosscuts and drifts and an adit 335 feet in length. A contemporary account (Anonymous, 1900, p.14-16) reported that the most promising vein being developed at that time was "not less than ten feet in width," and was considered a "high grade gold and copper proposition;" Beeler (1906, p.51) states that drifting going on at that time was "showing some fine ore," but no supportive assay figures are provided by either of these accounts.

Vein material on the mine dump consists of coarse-grained quartz and microcline containing abundant chalcopyrite and secondary copper minerals, a little pyrite, chlorite, and minor barite. No gold was seen in four Cu-rich vein samples examined microscopically, and Au values are low in assayed samples (Table 11). Ag values range from 10 ppm to 84 ppm, and a sample containing abundant malachite and chrysocolla in quartz assayed 0.25 ppm Pt, 0.04 ppm Pd, and 0.006 ppm Rh. A sample

of unsheared, weakly carbonated and sericitized metapyroxenite dike rock assayed 0.12 ppm Pt, 0.12 ppm Pd, and 0.014 ppm Rh (R. R. Carlson and E. F. Cooley, analysts).

Structural Controls on Localization of Mineralization and the Morphology of the Veins

It is worthwhile to survey briefly some features of the morphology and megascopic textural characteristics of a few veins and the spatial relations of oreshoots to the associated principal structural elements. The information available is meager due to the present inaccessibility of most veins to observation, but in a few instances, useful inferences can be drawn from sketchy accounts in contemporaneous reports and from observations of sparse vein outcrops and of vein material from mine dumps.

The Keystone vein was clearly complex. As noted earlier, the main oreshoot was reportedly 300 feet long and lay along the axis of the Keystone-Florence shear. Vein material on the Keystone dump includes quartz-ankerite-calcite-chlorite veins one to three inches wide, bounded sharply on either side by mylonite schist. The quartz in many of these narrow veins, particularly those rich in carbonates, is a clear white, medium- to coarse-grained, commonly showing crystal faces against carbonates and chlorite, and rarely having small scale comb-structure. However, much of the ore-bearing material is derived

from somewhat larger veins with more or less well expressed irregular banding (but not crustification texture) that is in some instances sufficiently pronounced to yield strongly laminated white to gray-green ribbon quartz. Ore minerals occur as thin seams a few millimeters thick parallel to and accentuating the banding. The laminated veins pass laterally through gradational intervals in which thin quartz seams, lenses, and wedging tails are intercalated with streaks, seams, and narrow zones of blastomylonitic sericite-carbonate schist. With increase in the amount of interbanded schist, the veins grade into wallrock. The Keystone oreshoot may thus be visualized as a compound body of simple and laminated veins and lenses passing along the shear zone as multiple pinching and swelling slabs separated by schist bands of varying thickness, the composite oreshoot being two to six feet wide. Although megascopic relations between the simple and laminated veins could not be observed in dump material, more than one stage and process of vein formation in the Keystone deposit is implied.

Consideration of the character of the fault suggests that two principal processes, with varying degrees of relative influence, may account for observed textural features in the veins. These are open-space filling and replacement. Since open space implies net increase in volume, the influence of open-space filling depends partly on whether or not the open

space can be made available. In its conceptually simplest form, planar shearing should not produce open spaces, but in natural occurrences, shear surfaces are more or less curved or irregular, so that movement along them produces an alternative of open and closed intervals. Open intervals ranging from narrow cracks to long gashes were sites of low pressure and low chemical potential into which mineral matter migrated and was deposited. From the abundance of residual seams of sericite schist one might conclude that the laminated lenses were formed by replacement of the shear zone; the presence of some grayish, inclusion-ridden quartz in banded veins suggests this origin. However, much of the quartz in laminated veins is clear white and semi-translucent. The main process in formation of the thin quartz lenses that comprise the laminae of ribbon quartz veins appears to have been repeated formation of incipient openings during translation, with repeated warping, dragging, and recrystallization of the quartz lenses already present, so that successive generations of quartz lenses were accreted to form composite, irregularly banded veins. This process, together with some replacement silicification, tended to obliterate the intervening patches and seams of sericite schist, and segregate the ore minerals into foliated seams. However, the not uncommon association of sulfides with gray-green diffuse slivers of sericite schist within the quartz may indicate

replacement deposition of some sulfide as well as some quartz. The banded vein material in both the Keystone and Florence deposits typically is weakly brecciated, and gold and less commonly chalcopyrite were remobilized late in the paragenetic sequence to heal microfractures in quartz and pyrite.

Late-stage, sulfide-poor, quartz-ankerite-calcite-chlorite veins are seldom brecciated in the Keystone deposit. Preservation of euhedral quartz, locally with comb structure, in intergrowths with coarse-grained carbonates points to open-space filling. Whether these veins were deposited in late fractures subparallel to the main vein or in diverging tear faults that escaped reactivation is not known.

The available data suggest that mineralization along the Mammoth fault at the Independence mine has had a somewhat simpler history, and rather different structural controls on localization of ore are in evidence. In the earlier discussion of the Independence mine, a contemporaneous account (Anonymous, 1900, p.11) was cited which indicated that the richest metal values were concentrated in numerous short divergent splays from the master fault-vein. Vein material on the Independence mine dump cannot be correlated confidently with either type of vein, but all the vein material examined consists of more or less massive coarse- to medium-grained milky quartz with irregular disseminations of sulfide that show no propensity to

clearly defined banded structure of the Keystone type, although sulfides often do exhibit a tendency to occur in diffuse zonal concentrations in the available larger samples. Quartz typically displays euhedral form against chalcopyrite and, in sulfide-poor samples, against ankerite. These textural features imply vein formation by open space filling. According to Anonymous (1900, p.11), the intersection of the Monarch and Mammoth faults was occupied by large quartz veins developed outward on three arms. The vein was up to twenty feet wide on the southeast arm of the Mammoth fault, and six to eight feet wide on the west arm of the Monarch fault. Large scale tensional opening at the intersection is indicated. The Mammoth vein has undergone minor localized post-depositional brecciation and recrystallization of less refractory vein constituents.

Beeler's (1905) account of the Gold Crater deposit implies yet another type of structural influence on localization of mineralization. The presence of higher grade ore on what apparently was a divergent splay was noted earlier, but the feature of present interest is a "huge ledge of quartz, heavily mineralized, lying in the band of [meta-andesite[1]].... having a generally easterly and westerly trend but at the shaft trends south-easterly and north-westerly with a strong dip to

---

[1]Beeler terms all dark rocks "diorite" or "quartz diorite" and refers to the Keystone quartz diorite pluton as "granite."

the northeast of about 45°" (Beeler, 1905, p.3). The east-west Gold Crater fault is fairly well exposed in the hillside on which the mine is located, except in the immediate vicinity of the mine, where it is obscured by waste dump debris. No quartz vein is in evidence in surface exposures adjacent to the mine workings, so it must be inferred that the "huge ledge of quartz" was strictly localized at the implied flexure in the fault. McKinstry (1948, p.316) notes that, where associated with mineralization, such swerves in fault trend typically enclose in the third dimension a lensoid, pipe-like oreshoot shaped like a cam, and advises that development of such lensoid bodies is so common that it should be suspected wherever a vein swings perceptibly.

The three examples described in this section appear to span the spectrum of vein types in the group of deposits investigated. The Florence, Lake Creek, and Cuprite veins most closely resemble those of the Keystone deposit. They are weakly banded, compound shear zone veins in which the ore minerals mostly occur in distinct segregation seams of partial replacement origin, albeit somewhat coarser than ore seams in the Keystone banded veins. Vein material from the Albany, Black, Duchess, and Sunset mines is similar in appearance to that from the Independence mine, and at least the last three deposits are localized in rather large fissures in or near variably

dilatant fault intersections and splays. Details of structural control at the Albany deposit are obscured by very poor surface exposure and lack of contemporaneous records.

Mineralogy of the Vein Deposits

Fifty-two vein minerals have been identified by standard microscopy techniques, electron microprobe analysis, and X-ray powder diffraction. Occurrences of 33 hypogene metallic and gangue minerals are compiled according to locality and means of identification in Table 12. (Supergene mineral assemblages in the veins are discussed briefly at the end of this section.) With few exceptions, the vein deposits show a fairly persistent pattern in major mineral parageneses. Occurrences of minor and rare metallic minerals are discussed with emphasis on their specific associations. Quantitative electron microprobe analyses of minor and rare minerals are presented in tables accompanying descriptive accounts.

Silicates

Quartz The character of quartz in the veins has been discussed in the preceding section. Gray to milky quartz is the principal gangue mineral in all deposits except the Cuprite and "Anonymous" mines. (Microcline and epidote predominate at the Cuprite, and at the "Anonymous" mine, carbonate veins are the principal ore-bearers.)

Microcline Medium- to very coarse-grained microcline is present in variable amounts in many veins. Potash feldspar

Table 12. Hypogene minerals of the vein deposits. Symbols as follows: O, identified optically by standard microscopic techniques; P, identified by electron microprobe analysis; X, identified by X-ray powder diffraction; R, reported and reasonably inferred to be present; A, presence inferred from assay data.

	Albany Mine	"Anonymous" Mine	Bear Mine	Black Mine	Cuprite Mine	Duchess Mine	Florence Mine	Gold Crater Mine	Golden Key Mine	Independence Mine	Keystone Mine	Lake Creek Mine	Prospect, Sec.7, T.14 N., R.78 W.	Prospect, Sec.18, T.14 N., R.78 W.	Prospect, Sec.34, T.15 N., R.80 W.	Prospect, Sec.35, T.15 N., R.80 W.	Sunset Mine
Quartz	O	O	O	O	O	O	O	O	O	O	O	O	O	O	O	O	O
Microcline		O	O	O	O		O				O	O		O		O	
Tourmaline	O		A	O	O		O		A		O						
Epidote					O												
Chlorite	O		O		O		O			O	O	O					O
Barite											A	O					
Calcite	P	P	O	O	O	O	O	O		O	O	O					
Ankerite	P	P			O	O	O	O	O	O	O				O		
Siderite	O					O									O		
Magnetite	O	O			O		O	O									
Hematite	X	O	O		O	O	O	O		O	O	O		O	O	O	O
Goethite		O						O			O						
Pyrrhotite											R						
Pyrite	O	P	O	P	O	O	O	O	O	P	O	O	P	O	O	O	O
Marcasite							O										
Chalcopyrite	X	O	O	O	R	O	O	O	O	O	O	O	O	O	O	O	O
Bornite	X		O				O	O		O	O	O					O
Idaite*								P									
Sphalerite	O	O		O			O	O		O	O	O			O		
Molybdenite			A							A				O			X
Cobaltite		P		P	R					O							
Gersdorffite		P															
Sperrylite													P				
Emplecite											P						
Wittichenite											P						
Bournonite															P		
Tetrahedrite						P											
Friebergite															P		
Electrum	P	P		P		A		P		O				A	A		A
Gold					R		P		P		P	R					
Bismuth											P						
Fe-Cr-Ni				P													

*May be supergene

was not X-rayed, but grid twinning in the examples of vein K-feldspar examined indicates microcline rather than adularia. Those veins in which microcline is abundant, viz., the Florence, Black, Gold Crater, and Lake Creek deposits, are associated with felsic country rocks. In these deposits, much of the microcline replaces wallrock lenses and fragments within the veins; it is mostly fine- to medium-grained and clouded with chlorite and other inclusions. However, these veins also carry coarse- to very coarse-grained clear pink, anhedral to euhedral microcline whose common associations with tourmaline and magnetite and in some cases with epidote, phlogopite, and auriferous pyrite are qualitative indications of a somewhat higher temperature origin than most carbonate-bearing veins or portions of veins. Boudinage structure of microcline-rich ore-bearing veins at the "Anonymous" mine implies that they are earlier than associated undeformed carbonate-rich veins.

Penninite Irregular clots of black-green chlorite up to five centimeters across and other less conspicuous aggregates are common components of carbonate-rich veins at most deposits. In thin section, fine- to medium-grained penninite occurs as bright green, irregular, sheaf-like aggregates that show extremely anomalous blue and maroon-brown interference colors. The optical properties of penninite in quartz-carbonate veins and in strongly carbonated wallrocks contrasts markedly with

the pale color, weak pleochroism, and normal birefringence of finely disseminated chlorite in non-carbonated sericitic alteration zones adjacent to veins in some deposits. Vein penninite rarely is associated with ore minerals *per se*, but it is commonly accompanied by specular hematite and less often by pyrite and magnetite. Chlorite-bearing, carbonate-rich veins typically exhibit late-stage hypogene oxidizing effects (viz., martitization of magnetite and oxidation of ankerite and siderite to specular hematite ± calcite) that point to a generally late position of chlorite in the vein parageneses.

Tourmaline Small amounts of black tourmaline have been noted in veins and advanced wallrock alteration facies at most of the more thoroughly investigated deposits. In localized instances, tourmaline may comprise 5 percent or more of a small vein, but in its typical occurrences, it is disseminated as a trace accessory (Fig. 35). It is common as a vein constituent only at the Cuprite mine and the Gold Crater vein west of the main Gold Crater mine workings. Tourmaline is a common associate of replacement sulfide ores in phlogipitic schists at the Black mine. Its position in the paragenetic sequence is not precisely defined, but its most typical occurrences seem to be in early-intermediate small shear zone veins of partial replacement origin and in mylonitic sericitized wallrocks immediately adjacent to these veins. Tourmaline has

not been found as a central-vein constituent in the large fissure-filling veins of the Independence-Sunset type.

Epidote Large amounts of coarse-grained, locally euhedral epidote accompany pyrite, microcline, quartz, and tourmaline in quartz- and carbonate-poor veins or portions of veins at the Cuprite mine. Disseminated fine- to medium-grained epidote occurs with calcite in the gangue associated with pyrite-sphalerite-galena replacement mineralization in schists at the Black mine. Elsewhere, it is common in wallrock alteration facies at some distance from the veins and is not an immediate associate of ore minerals.

Sulfate and Carbonates

Barite Barite has been seen only at the Lake Creek mine, where it is locally an abundant gangue component. Barite occurs as coarse granular intergrowths with quartz and microcline, associated with the metallic mineral assemblage chalcopyrite + bornite + hematite. Four of five assayed ore samples from the Lake Creek mine show more than 5000 ppm Ba (E. F. Cooley, analyst). (The upper determination limit for Ba is 5000 ppm in semiquantitative emission spectrographic assays.) An assayed sample from a prospect on the Keystone-Florence fault contained more than 5000 ppm Ba, implying the presence of barite.

Fig. 17 A. Tourmaline (dark gray, upper center) with pyrite (black) in carbonated and sericitized quartz-biotite-andesine gneiss (left and upper right). A calcite veinlet. Keystone mine, sample MK-1ZZ10. X40, transmitted light.

B. Bladed specularite (white) with interstitial quartz (dark gray) accompanies an irregular mass of chalcopyrite (near white) that contains a few small hematite inclusions. Chalcopyrite has undergone rim replacement and veining by bornite (medium gray), and bornite is in turn partially replaced by a rim of supergene chalcocite (light gray). Lake Creek mine, sample MLC-10. X160, reflected light.

C. Hematite (near white) with included magnetite as disseminated specks (medium gray). Aggregates of granular and prismatic hypogene goethite (medium gray, right) occur as encrustations on hematite. Matrix is calcite. "Anonymous" mine, sample MW-3. X160, reflected light.

D. Pyrite (white) with cataclastically induced cleavage that is invaded by chalcopyrite (light gray) remobilized from a partly visible mass of enclosing chalcopyrite (right). Chalcopyrite is moderately replaced by supergene covellite and goethite (both dark gray). Independence mine, sample MI-1I. X210, reflected light.

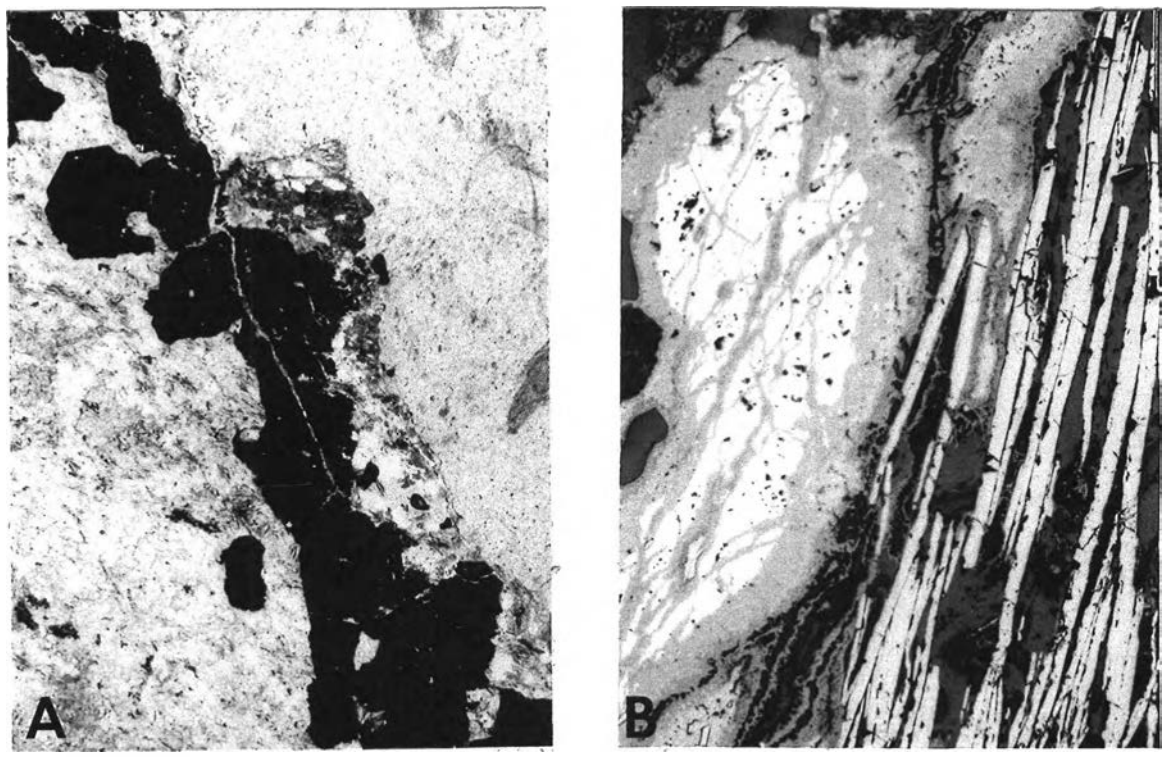

FIGURE 17

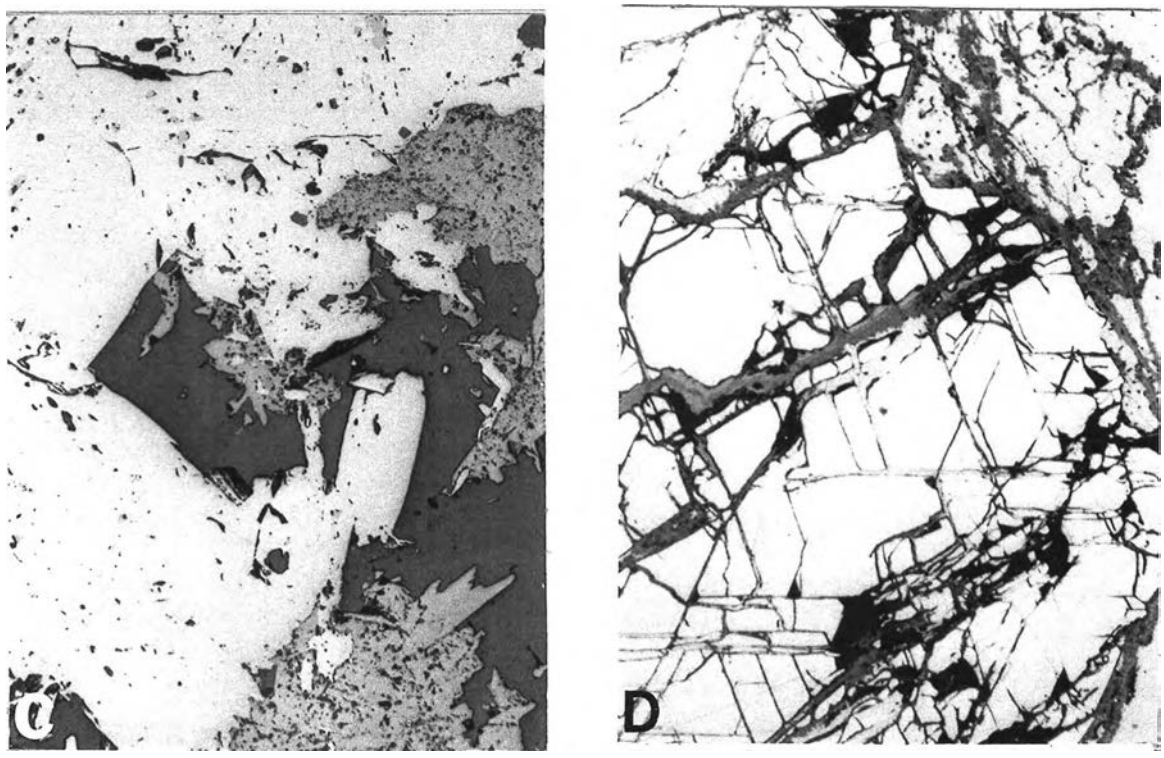

Calcite, Ankerite, and Siderite Calcite is abundant or predominant in veins at several deposits and is the only carbonate recognized in altered wallrocks. Moderate to strong supergene oxidation of most vein deposits has led to early decomposition of the Fe-bearing carbonates, which makes them easily distinguishable from calcite. Fresh carbonates were available at the Albany and "Anonymous" mines, and selected samples of vein and wallrock carbonate were analyzed using the multi-channel analyzer accessory to the electron microprobe. Ca, Mg, Mn, and Fe were sought in vein and wall-carbonates; Mg and Mn were not detected in any samples, and Fe is minor to absent in wallrock carbonates examined from the two deposits. The analyses confirmed the identity of cream-white ankerite [$CaFe(CO_3)_2$], a common mineral in veins at both the Albany and "Anonymous" mines, as well as in other deposits.

Calcite is the dominant constituent of numerous small veins in many deposits (Fig. 17A). It also occurs as medium- to very coarse-grained granular intergrowths with fissure-vein quartz that is usually idiomorphic against calcite, although the reverse relation has been noted at the Albany mine.

Ankerite is a common to major component of paragenetically intermediate- to late-stage veins at the Keystone, Florence, Independence, Gold Crater, Albany, Cuprite, and

Duchess mines, to name the more conspicuous occurrences. Siderite ($FeCO_3$) is important in quartz veins at the Albany and Duchess mines and at the Pb-Ag-Cu prospect. Ankerite and siderite are mostly very coarse-grained and are usually later than quartz of the same veins. Late hypogene oxidation of ankerite and siderite to bladed specular hematite $\pm$ calcite is a common feature, and most of the remaining ankerite and siderite have been oxidized to goethitic limonite $\pm$ calcite by supergene processes. Supergene solutions may eventually leach much or all of the calcite from decomposed ankerite, leaving a porous limonite mass with relict rhombohedral cleavage. Weathering of siderite yields dense brown goethite without in situ secondary calcite. At the Albany mine, attractive pseudomorphous rhombohedral aggregates of cuprite + native copper have been produced by activity of the Cu^{2+}-Fe^{2+} redox couple on contact of supergene solutions with Fe-bearing carbonates.

Oxides

Magnetite Magnetite is a principal associate of sulfides at the Florence, Gold Crater, Albany, Cuprite, and "Anonymous" mines. At the Florence, Cuprite, and "Anonymous" mines, magnetite occurs in granular intergrowths with pyrite and is usually martitized to varying degrees. When extensively or completely martitized, it is usually accompanied by coarse, bladed hematite. At the Cuprite and Florence mines, fine-grained magnetite is

also common in advanced facies of hydrothermal wallrock alteration. It gives way to pyrite in advanced facies at other deposits. At the Albany, "Anonymous," and Gold Crater mines, magnetite commonly occurs as fine-grained, euhedral to anhedral, occasionally martitized inclusions in paragenetically intermediate- to late-stage chalcopyrite. Early chalcopyrite contains pyrite inclusions, and late chalcopyrite in many deposits encloses hematite.

Hematite Hematite is present as a paragenetically late replacement of magnetite (i.e., martite), as a replacement of ankerite and siderite, and as a direct precipitate from hydrothermal solution. It occurs as euhedral to anhedral equant grains and sheafed plates (Fig. 17B and C). Small equant grains of hematite occur abundantly as inclusions in intermediate- to late-stage chalcopyrite at the Gold Crater, Albany, Sunset, and Lake Creek mines, and at the Au-Cu prospect in Sec.18, T.14 N., R.78 W. near the Lake Owens complex. Variable amounts of bornite usually accompany and replace chalcopyrite in hematite-bearing assemblages (Fig. 17B). Specular hematite is a major vein constituent at the Pb-Ag-Cu prospect. Here, hematite paragenetically follows pyrite and chalcopyrite, overlaps and follows galena, sulfosalts, and siderite, and is in turn succeeded by hypogene goethite.

Goethite Hydrothermal goethite ($HFeO_2$) occurs as granular and prismatic to fibrous aggregates in the latest stage of the hypogene vein parageneses at the "Anonymous," Gold Crater, and Keystone mines and at the Pb-Ag-Cu prospect. At the Keystone mine, traces of primary goethite replace ankerite. The goethite appears to be the latest mineral in an assemblage that includes wittichenite (Cu_3BiS_3), native bismuth, and hematite. At the Pb-Ag-Cu prospect and at the "Anonymous" and Gold Crater mines, hypogene goethite is abundant as encrustations on specular hematite (Fig. 17C).

Sulfides

Pyrrhotite Pyrrhotite was not encountered in any vein deposits in this investigation, but it is reported by Curry (1965, p.9) to have been present in the Keystone mine "in a mylonite selvage adjacent to the quartz." The available ore samples from all vein deposits, except the "Anonymous" and Black mines, show moderate to strong supergene oxidation, and, as pyrrhotite is the most susceptible of the common sulfides to weathering, there is little likelihood that pyrrhotite would have survived in the samples examined even if it had been present. The characteristic spongey, porous texture of supergene pyrite developed after pyrrhotite was not seen in any of the samples examined.

Pyrite and Marcasite In all but a few relatively oxide-rich deposits, pyrite is an abundant mineral in the veins and is usually a common constituent in the near-vein wallrock alteration assemblages as well. In all the vein deposits studied, pyrite appears early in the vein deposition sequence. In some cases, several generations are present, though probably not widely separated in time. For example, at the Florence mine, disseminations and dense swarms of very fine-grained euhedral pyrite cemented by interstitial murky gray quartz have formed locally by wallrock replacement. In numerous instances, a later generation of anhedral, medium- to coarse-grained auriferous pyrite has overgrown the perimeter of such a swarm of small euhedra and for some distance inward has replaced the interstitial quartz, producing interlocking granular masses of coarse pyrite that enclose an early generation of minute euhedra (recognizable by subtle differences in relief and anomalous optical anisotropy) disseminated within coarse pyrite grains. The aggregate thus represents a multi-stage auriferous replacement of wallrocks. At the Keystone mine, a second generation of pyrite and chalcopyrite locally heals brecciated quartz that is impregnated with disseminated pyrite and chalcopyrite.

Fine- to very fine-grained pyrite is very common as inclusions in chalcopyrite. In some chalcopyrite-rich, pyrite

poor veins (notably the Albany and Gold Crater veins), this is its only observed mode of occurrence, although wallrocks contain disseminated discrete pyrite. In pyrite-rich deposits, the reverse inclusion relationship is also common, and substantial overlap of the paragenetic positions of pyrite and chalcopyrite is usually apparent.

Pyrite is brittle and the most refractory of the common vein minerals, so clues to the post-depositional tectonic history of the veins are often reflected in pyrite, whereas recrystallization has often obliterated the evidence in other vein minerals (Fig. 17D).

Electron microprobe scans of vein pyrite from the "Anonymous," Black and Independence mines have shown that the pyrite in these deposits is locally enriched in Co, Ni, and As. The distribution of such enrichments tends to be erratic within pyrite grains, and no regular zonation is evident. A representative analysis of Co-, Ni-, and As-rich pyrite from the "Anonymous" mine is presented in Table 13 (page 194).

Marcasite has been seen only in ores of the Florence mine. Here, it occurs in trace amounts in a very late-stage assemblage with magnetite, chalcopyrite, bornite, and sphalerite in calcite gangue.

Chalcopyrite The most abundant hypogene Cu mineral in the vein deposits is chalcopyrite, and in a number of veins

formed from relatively oxidized and/or sulfur-poor ore fluids, it is the principal primary sulfide, viz., at the Albany, Black, Duchess, and Lake Creek mines and at the Au-Cu prospect in Sec.18, T.14 N., R.78 W. near the Lake Owens complex. In the later, more oxidized stages of vein parageneses, chalcopyrite is typically accompanied by and replaced by bornite, and these are associated with more or less abundant Fe oxides, mainly hematite. This assemblage comprises the bulk of the metallic mineralization in many veins. Evidence of multiple stages of chalcopyrite deposition within a vein is rare, but an example at the Keystone mine was noted earlier. Here, the association with veinlet pyrite in breccia fractures indicates a separate depositional event, as opposed to short-distance remobilization of chalcopyrite during deformational recrystallization which occurs easily at temperatures of about 150°C and above (Ramdohr, 1969, p.65) and has been observed in ore of the Independence deposit (Fig. 17D).

Weathering of the ores has yielded abundant secondary Cu sulfides replacing chalcopyrite, usually accompanied by abundant limonite, and without notable supergene enrichment.

Bornite Bornite (Cu_5FeS_4) makes an appearance in intermediate to late stages of the vein parageneses and has been found, usually in small amounts, in most of the more intensively investigated deposits. Its most characteristic habit

is as replacement rims on chalcopyrite aggregates (Fig. 17B) and as slender flames penetrating chalcopyrite masses along their perimeters. The rims are in turn succeeded by chalcocite rims that are of virtually certain supergene origin in every case, so the possibility that some bornite may be of supergene origin cannot be dismissed. However, most bornite is clearly of hypogene origin, as evidenced by granular intergrowths with chalcopyrite and pyrite (Fig. 18A) and the not uncommon occurrence of exsolved chalcopyrite lamellae in bornite from the Gold Crater, Lake Creek, and Sunset mines (Fig. 18B). Every observed occurrence of bornite in the veins is accompanied by hematite and/or magnetite in the same assemblage, and pyrite is usually absent from bornite-bearing associations. The bornite replacement rims on chalcopyrite are thus attributable to redox expulsion of Fe^{2+} in chalcopyrite by Cu^{2+} during late-stage oxidation and cooling of ore fluids.

Idaite Idaite ($Cu_{11}Fe_2S_{13}$) was recognized in several ore specimens from the Gold Crater vein west of the main mine workings. In polished section, it is peach-tan in color, shows characteristic strong absorption pleochroism and extreme anisotropy, with pale cream-white or greenish white to dark gray polarization colors. It occurs in exceedingly fine-grained matted aggregates similar to the texture of some fine sericite

Fig. 18 A. Uncommon association of bornite (dark gray) with pyrite (near white) in chalcopyrite matrix. Sunset mine, sample MS-100D. X800.

B. Bornite (dark gray) with exsolved lamellae of chalcopyrite (light gray) in chalcopyrite matrix. Supergene digenite (medium gray) replaces the exsolution intergrowth along its margins and occurs as veinlets in chalcopyrite. Sunset mine, sample M-693E. X800, reflected light.

C. Extremely fine-grained felted mass of idaite with relict chalcopyrite lamellae. Idaite has replaced bornite of a bornite-chalcopyrite exsolution intergrowth of the type shown in Figure 18B. Quartz matrix. Gold Crater mine, sample MGC-1B. X1300, reflected light.

D. Chalcopyrite (white) surrounds and replaces earlier sphalerite. Matrix is calcite (medium gray, similar in tone to sphalerite). "Anonymous" mine, sample MW-20A. X400, reflected light.

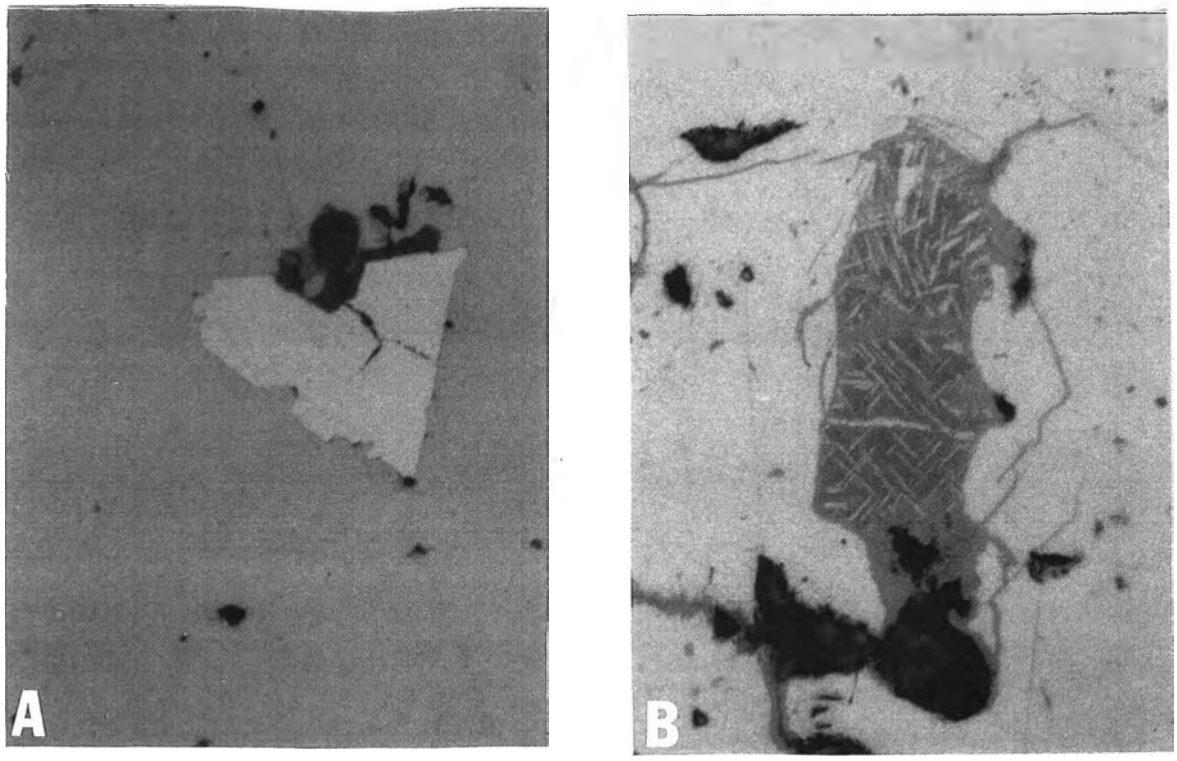

Figure 18

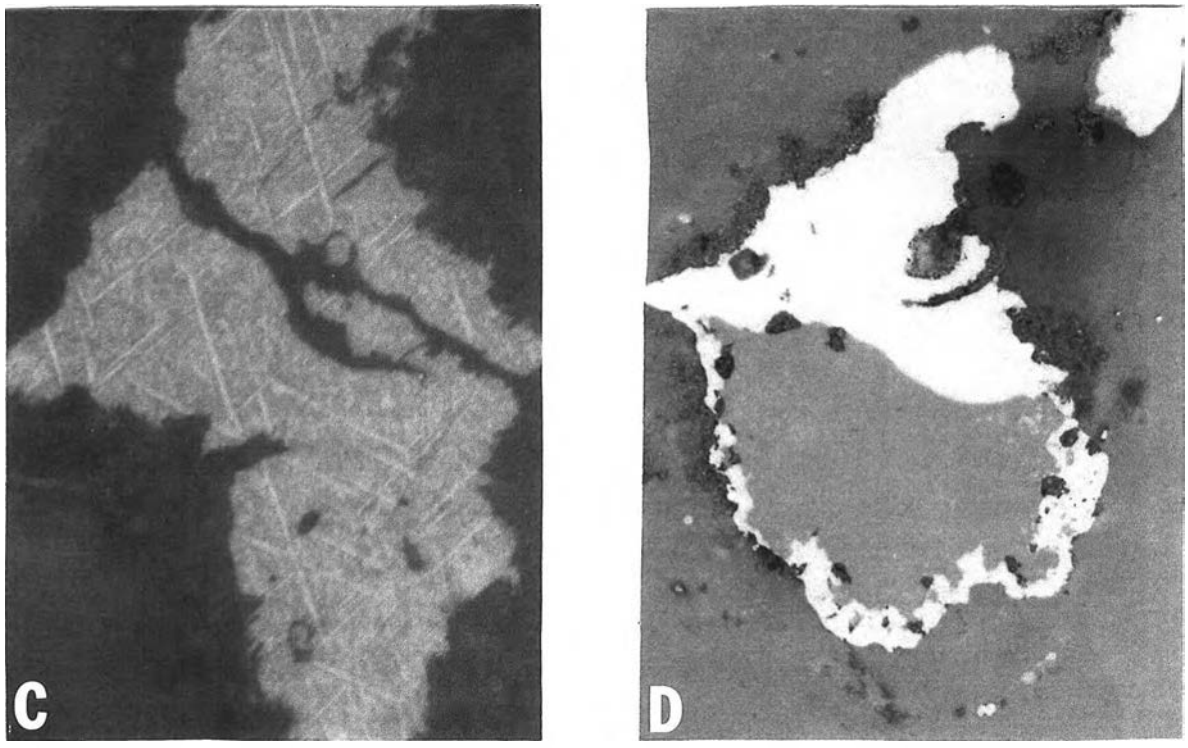

or clay aggregates. A typical "grain" was analyzed by electron microprobe and was found to contain only Cu, Fe, and S, but showed considerable variation in the proportion of these constituents from one point to another. The average stoichiometry calculated from this analysis failed to correspond to a known phase, yielding a composition between idaite and chalcopyrite. Re-examination of several grains at very high magnifications revealed a lace of chalcopyrite lamellae within the idaite (Fig. 18C). According to Ramdohr (1969, p.682), idaite typically forms by decomposition of bornite in chalcopyrite-bornite exsolution intergrowths, not uncommonly during supergene alteration. The paragenetic position of idaite cannot be resolved with certainty in this instance, but primary bornite and chalcopyrite in the same ore samples have undergone moderate supergene replacements by Cu sulfides, so a supergene origin is possible.

Sphalerite This mineral has been found as a trace constituent in most of the vein deposits examined intensively, and it is likely to have escaped notice in a few prospects and mines given less thorough attention. At the "Anonymous" mine, sparse amounts of sphalerite [(ZnFe)S] are intergrown granularly with pyrite and are replaced by chalcopyrite (Fig. 18D). More typical is its appearance in minute amounts as a very late phase in the paragenetic sequence as partial overgrowths on or replacements of chalcopyrite (Fig. 19A) and as small inclusions

in late chalcopyrite. Pale sphalerite is relatively abundant at the Black mine, where it occurs as overgrowths on galena and pyrite (Fig. 19B) in replacement ores in phlogopite-calcite-quartz-albite-tourmaline schists. Sparse weathered relics of once abundant sphalerite occur at the Pb-Ag-Cu prospect, associated with decomposed galena and sulfosalts. The strongly weathered condition of sphalerite at this prospect and the paragenetic diachronism of unweathered sphalerite and galena at the Black mine make these occurrences unsuitable for sphalerite-galena sulfur isotope thermometry, which initially was planned as a phase of this investigation.

Galena Only five veins are known to contain galena (Pbs), and Pb assay values at other deposits are generally very low (Table 11). Traces of galena are disseminated in late bornite at the Gold Crater mine and in quartz with chalcopyrite at the Lake Creek and Duchess mines. Moderate amounts of fine- to medium-grained galena occur at the Black mine, as noted above (Fig. 19B). Coarse-grained galena is the principal sulfide at the Pb-Ag-Cu prospect. Here, galena occurs in quartz intergrown mainly with sphalerite and friebergite (an Ag-rich member of the tetrahedrite family), and galena contains inclusions of bournonite and friebergite, the latter in part as lamellae exsolved along octahedral and cubic lattice planes. Galena-rich samples at the Pb-Ag-Cu prospect assay up to 500 ppm Bi (E. F.

Cooley, analyst). Since independent Bi minerals have not been recognized, and Ag^{+}-Bi^{3+} coupled substitution for $2Pb^{2+}$ is very common in galena (Ramdohr, 1969, p.646), it seems likely that a subordinate but possibly significant proportion of the Ag content of the ore is present in solution in galena.

Molybdenite Traces of molybdenite (MoS_2) were encountered in chalcopyrite-rich vein samples from the Sunset mine and Au-Cu prospect in Sec.18, T.14 N., R.78 W. As the solubility of Mo in pyrite and chalcopyrite is very low, and concentrations of 50 ppm Mo or less in assayed samples are known to correlate with visible molybdenite, it is reasonable to infer the presence of unseen molybdenite in vein material from the Bear and Independence mines that assay 100 ppm or more Mo (Table 11).

Sulfarsenides and Arsenide

Cobalite Cobalite [(Co,Fe,Ni)AsS] is not uncommon in Au- and Cu-rich vein ores at the "Anonymous," Independence, and Black mines, and assay data for pyritized schists at the Black mine suggest that cobaltite of replacement origin may be present as well. The observed cobaltite at the Black mine occurs as subhedral to anhedral grains disseminated in quartz that also encloses abundant chalcopyrite intergrown with an alloy or intermetallic compound of Fe, Cr, Ni, and Co. At the "Anonymous" mine, cobaltite occurs commonly as overgrowths on pyrite (Fig.

Fig. 19 A. Texturally unusual replacement of chalcopyrite (near white) by sphalerite lamellae (light gray) oriented along (111) planes of chalcopyrite. The habit of sphalerite is mimicked by supergene digenite (medium gray, slightly darker than sphalerite) that replaces both sphalerite and chalcopyrite. Formation of marcasite granules (bright white) probably accompanied destruction of chalcopyrite. Carbonate matrix (dark gray). Late ore, Florence mine, sample MF-1ZY. X200, reflected light.

B. Sphalerite (medium gray) overgrown on galena (near white, with cleavage pits) and to a slight extent on pyrite (bright white, upper and lower center). Matrix is quartz-albite-phlogopite-epidote-calcite schist. Replacement ore, Black mine, sample MB-1R. X135, reflected light.

C. Subhedral cobaltite as overgrown on pyrite (near white, scratched). Matrix is chalcopyrite (light gray) and calcite (black, lower right). Ore in carbonate veinlets, "Anonymous" mine, sample MW-20A. X200, reflected light.

D. Cobaltite (near white) as small euhedra in chalcopyrite (light gray) and as a larger euhedral grain in upper right with a partial rim of gersdorffite (medium gray). Irregular grain in upper left is pyrite. Carbonate gangue (dark gray). "Anonymous" mine, sample MW-21. X200, reflected light.

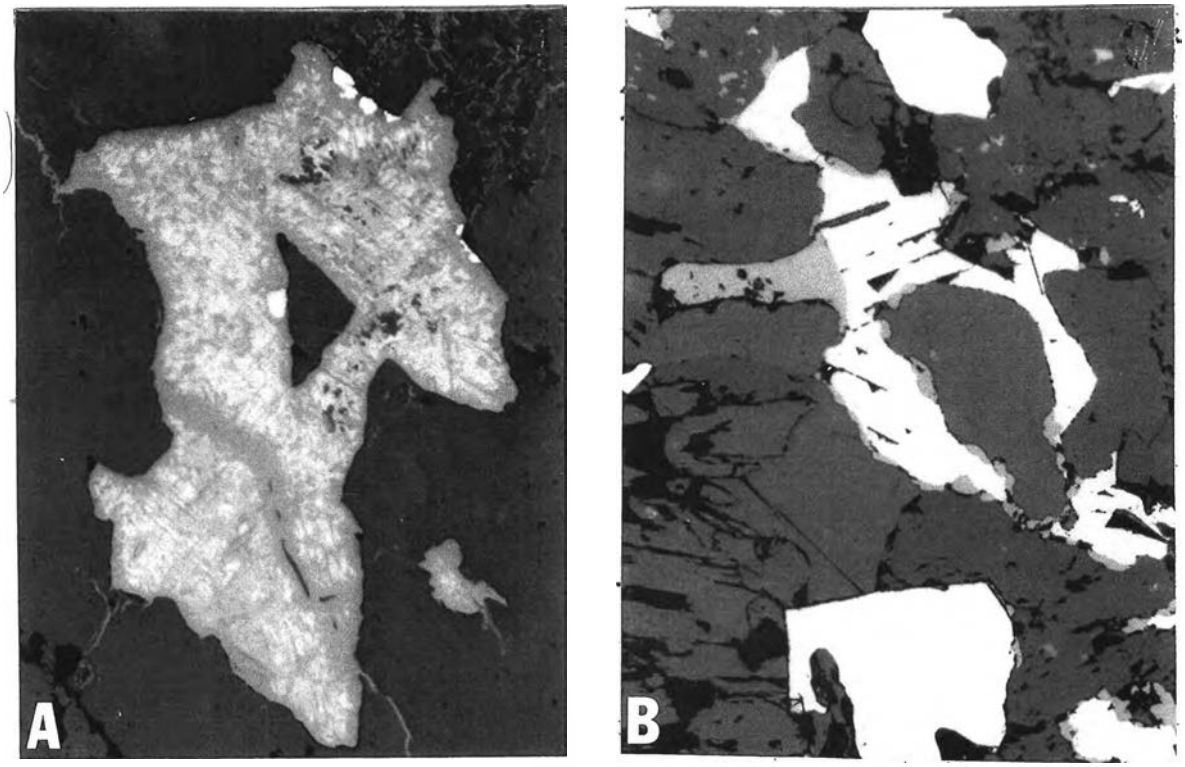

Figure 19

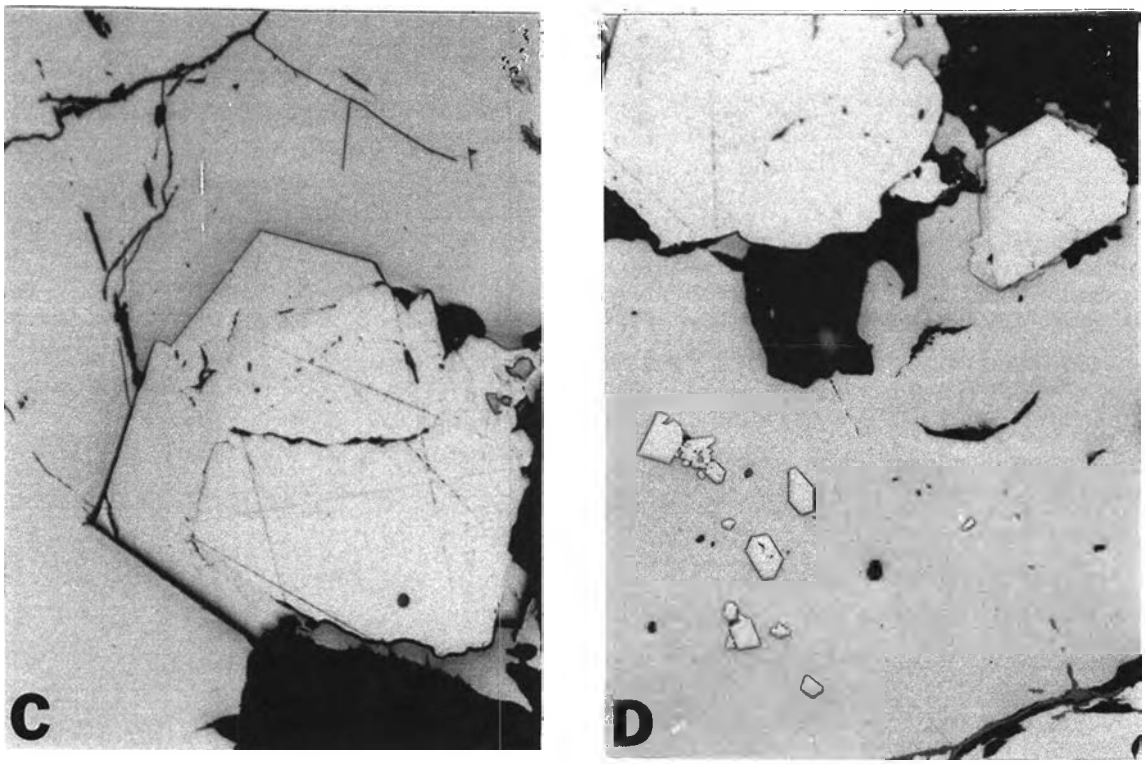

19C) and as disseminated euhedra in microcline, quartz, and carbonate gangue and in chalcopyrite (Fig. 19D). At the Independence mine, minute specks of cobaltite are disseminated sparsely throughout medium-grained, massive pyrite. "Values in cobalt" are reported from the Cuprite mine (Curry, 1965, p.8), and its occurrence as cobaltite is suggested by the presence of 1000 ppm As and 700 ppm Co in assayed limonite.

Electron microprobe analyses of cobaltite from the "Anonymous" and Black mines show rather Fe-poor, Ni-rich compositions (Table 13), and some associated pyrite contains small amounts of Ni, Co, and As (Table 13). The reasons for the high totals of these analyses are undetermined, but the data are of value in underscoring the presence of small but significant contents of Co and Ni in the ores, a feature held to be of some genetic consequence in view of the typical association of mafic rocks with mineral deposits in the central Medicine Bow Mountains.

Gersdorffite A single grain of an isotropic, galena-white mineral with polishing hardness greater than chalcopyrite was encountered as an overgrowth on cobaltite at the "Anonymous" mine (Fig. 19D). An analysis by electron microprobe (Table 13) established its identity as the rather rare mineral gersdorffite (NiAsS). Ramdohr (1969, p.823) reports that its principal occurrences are in "vein deposits of medium

Table 13. Electron microprobe analyses of Co-Ni-Fe-As-S minerals from the Black and "Anonymous" mines. Values in weight percent. N.D. = not detected.

	Fe	Co	Ni	As	S	Total	Mineral Formula
Cobaltite Black mine	6.9	21.7	8.7	44.7	20.4	102.4	$(Co_{.59}Ni_{.24}Fe_{.20})_{1.03}As_{.96}S_{1.01}$
Cobaltite "Anonymous" mine	5.9	21.6	9.2	44.5	20.9	102.1	$(Co_{.59}Ni_{.25}Fe_{.17})_{1.01}As_{.95}S_{1.04}$
Gersdorffite "Anonymous" mine	3.1	1.7	31.2	45.2	21.0	102.2	$(Ni_{.85}Fe_{.09}Co_{.05})_{.98}As_{.97}S_{1.05}$
Pyrite* "Anonymous" mine	43.4	0.7	2.7	2.3	52.6	101.7	$(Fe_{.93}Ni_{.06}Co_{.01})_{1.00}(S_{1.96}As_{.04})_{2.00}$
Pyrite** "Anonymous" mine	46.5	0.04	0.09	N.D.	53.7	100.4	$Fe_{1.00}S_{2.00}$

*Portion of grain rim

**Interior of same pyrite grain

temperature, e.g., in certain siderite veins, or locally in the Cobalt district [Ontario], and in the hydrothermal end phase of the nickel-pyrrhotite paragenesis of Sudbury."

Sperrylite Several grains of sperrylite ($PtAs_2$) were observed in material from a peculiar, small, Cu-rich quartz vein along the Albany-Cuprite fault in Sec.7, T.14 N., R.78 W. A walnut-size sample comprised mainly of supergene digenite, covellite, and chalcocite, with traces of relict pyrite, and another thumbnail-size piece of malachite with limonite were submitted to the U. S. Geological Survey for routine assay. The analyses revealed extraordinary concentrations of Pt and Pd, and appreciable Rh (Table 11). Examination of several polished sections of the sulfide sample showed the Pt to be present as small grains of sperrylite (Fig. 20A), but the residence of Pd could not be ascertained. Electron microprobe analyses of two sperrylite grains from this occurrence are shown in Table 14. Analyzed natural sperrylite from Sudbury was used as standards for Pt and As, and synthetic Pt-Rh and Ir-Rh alloys for Rh.

Sulfosalts

Bournonite Small amounts of bournonite ($PbCuSbS_3$) were seen as isolated granules and composite inclusions in galena at the Pb-Ag-Cu prospect in Sec.34, T.15 N., R.80 W. A composite inclusion with friebergite in galena is shown in Figure

Table 14. Electron microprobe analyses of sperrylite from the PGE-Cu prospect in Sec.7, T.14 N., R.78 W. Values in weight percent.

	Pt	Rh	As	Total	Formula
Grain 1	55.5	0.3	43.3	99.1	$(Pt_{.99}Rh_{.01})_{1.00}As_{2.00}$
Grain 2	55.3	0.6	43.2	99.1	$(Pt_{.98}Rh_{.02})_{1.00}As_{2.00}$

Fig. 20 A. Subhedral sperrylite (white) in supergene digenite (medium gray) and covellite (darker gray specks and patches), with quartz gangue (dark gray, upper left). PGE-rich quartz vein, Sec.7, T.14 N., R.78 W., sample MN-1A. X800, reflected light.

B. Friebergite (dark gray) as an irregular composite inclusion with bournonite (medium gray) in galena. Exsolved blebs of friebergite are visible in lower right. Pb-Ag-Cu prospect, sample MG-6. X270, reflected light.

C. Friebergite rods and specks exsolved along (100) and (111) planes of galena. (100) cleavage of galena visible in lower right. Pb-Ag-Cu prospect, sample MG-6. X610, reflected light.

D. Relatively coarse granules of gold (white) in pyrite. Dark gray is goethitic limonite. Early ore, Florence mine, sample MF-1I. X610, reflected light.

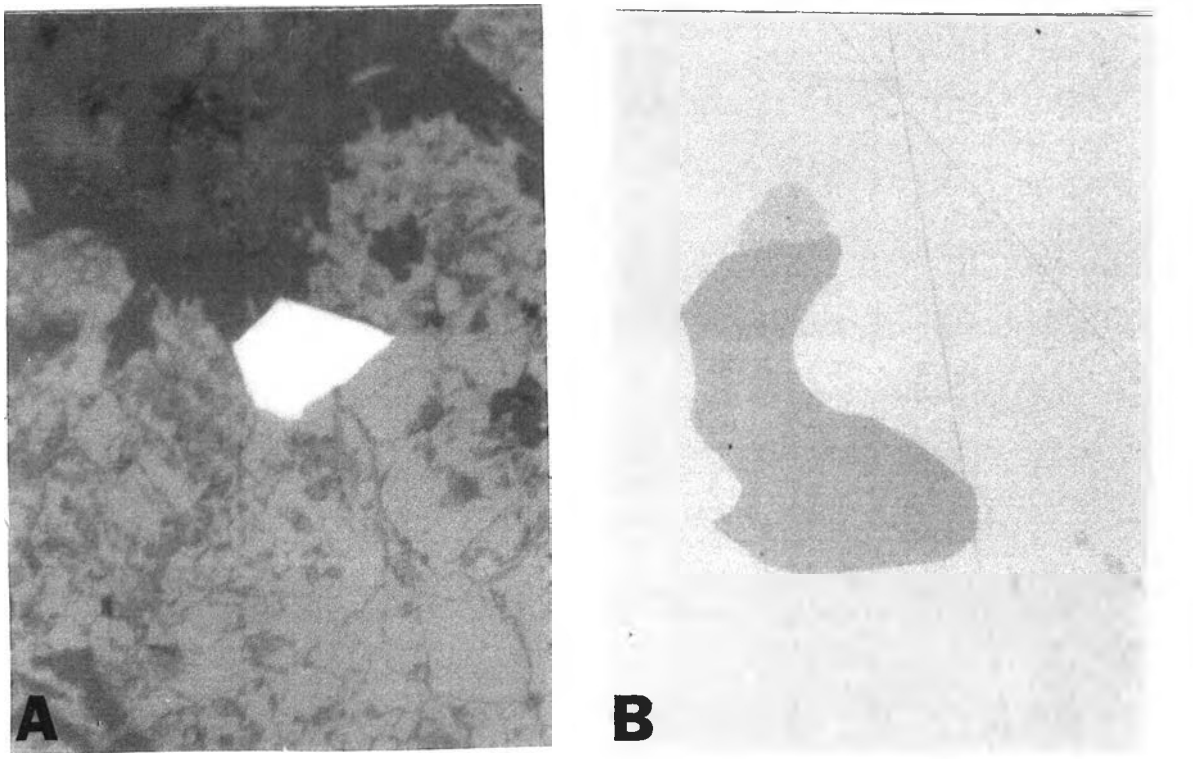

Figure 20

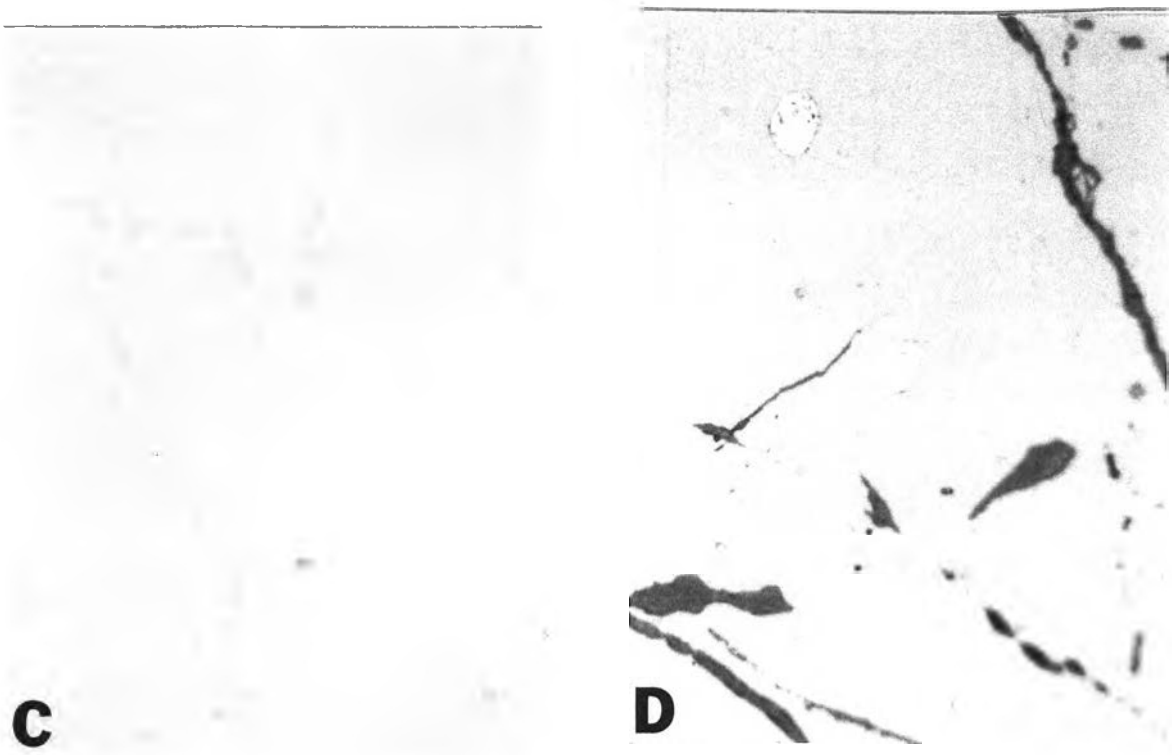

20B, and an analysis by electron microprobe using synthetic bournonite as a standard is presented in Table 15.

Tetrahedrite and Friebergite Ag-bearing tetrahedrite [$(Cu,Fe,Zn,Ag)_{12}(Sb,As)_4S_{13}$] is present as isolated small equant, weathered grains in chalcopyrite-rich quartz vein samples from the Duchess mine. A tetrahedrite-bearing vein sample assayed 26 ounces Ag per ton (Table 11) (J. Viets, analyst).

Friebergite, the Ag-rich member of the tetrahedrite family, is the principal hypogene Cu mineral at the Pb-Ag-Cu prospect, and it appears to be the principal and possibly only Ag carrier in the primary ore, although the possibility of Ag-Bi solution in galena was appraised earlier. Friebergite occurs as isolated grains and polycrystalline aggregates in quartz and as granular intergrowths with galena and sphalerite (Fig. 20B). In polished section, variable amounts (locally prodigious quantities) of exsolved friebergite lamellae are visible along (100) and (111) planes of galena (Fig. 20C). The Ag contents of assayed galena samples vary sympathetically with the visibility of friebergite inclusions.

Electron microprobe analyses of tetrahedrite and friebergite from the Duchess mine and Pb-Ag-Cu prospect are shown in Table 15. (Analytical methods are described in the appendix.) The friebergite grains analyzed are relatively large accidental

Table 15. Electron microprobe analyses of bournonite, friebergite, and tetrahedrite from the Pb-Ag-Cu prospect, Sec.34, T.15 N., R.80 W. and from the Duchess mine. Values in weight percent. ND = not detected.

	Zn	Fe	Cu	Ag	Pb	Sb	As	S	Total	
Bournonite Pb-Ag-Cu Prospect	ND	ND	12.9	ND	43.3	24.6	ND	19.8	100.6	$Pb_{1.02}Cu_{.99}Sb_{.98}S_{3.01}$
Friebergite, grain 1 Pb-Ag-Cu Prospect	1.4	3.8	29.4	13.6	ND	27.6	0.2	23.7	99.7	$(Cu_{8.14}Ag_{2.21}Fe_{1.22}Zn_{.38})_{11.94}$ $(Sb_{3.98}As_{.04})_{4.02}S_{13.04}$
Friebergite, grain 2 Pb-Ag-Cu Prospect	1.3	4.3	28.7	14.1	ND	27.8	0.1	23.7	100.0	$(Cu_{7.95}Ag_{2.30}Fe_{1.36}Zn_{.36})_{11.97}$ $(Sb_{4.01}As_{.02})_{4.03}S_{13.00}$
Friebergite, grain 3 Pb-Ag-Cu Prospect	2.4	3.1	30.5	13.2	ND	27.4	0.1	23.8	100.5	$(Cu_{8.39}Ag_{2.30}Fe_{.97}Zn_{.64})_{12.13}$ $(Sb_{3.92}As_{.02})_{3.94}S_{12.93}$
Tetrahedrite, grain 1 Duchess Mine	4.0	2.9	39.1	1.8	ND	20.1	5.3	25.6	98.8	$(Cu_{10.01}Zn_{1.00}Fe_{.86}Ag_{.27})_{12.14}$ $(Sb_{2.69}As_{1.16})_{3.85}S_{13.01}$
Tetrahedrite, grain 2 Duchess Mine	1.9	4.0	38.4	1.7	ND	26.0	1.4	25.1	98.5	$(Cu_{10.01}Fe_{1.21}Zn_{.48}Ag_{.26})_{12.05}$ $(Sb_{3.57}As_{.32})_{3.89}S_{13.07}$

inclusions in galena (of the type shown in Figure 20B); exsolution lamellae are too small to analyze quantitatively, but qualitative analysis on the multi-channel analyzer disclosed substantial Ag contents in the lamellae.

Wittichenite and Emplecite Several irregular, small weathered grains resembling tetrahedrite were encountered in three samples from the Keystone mine. In polished section, the mineral is creamy gray-white and moderately anisotropic, with dark blue-green to dull grayish yellow polarization colors. It was identified by electron microprobe analysis as wittichenite, Cu_3BiS_3. In two samples it is enclosed in quartz in a chalcopyrite-pyrite-gold paragenesis (Fig. 21A). In the third occurrence, wittichenite is part of a diachronous assemblage composed of an earlier association of euhedral-subhedral quartz, with intergrown pyrite, chalcopyrite, and gold. The quartz containing sulfides and gold is corrosively embayed and surrounded by an assemblage of ankerite, wittichenite, and metallic bismuth. Late hypogene oxidation led to partial replacement of chalcopyrite by bornite and of ankerite by specular hematite and goethite.

Electron microprobe analyses of wittichenite in two samples from the Keystone mine are presented in Table 16. One suspected wittichenite grain analyzed by microprobe showed unexpectedly large deviations in the ratios of Cu, Bi, and S,

Table 16. Electron microprobe analyses of wittichenite from the Keystone mine. Values in weight percent.

	Cu	Bi	S	Total	Formula
Grain 1	37.9	42.7	19.9	100.5	$Cu_{2.94}Bi_{1.01}S_{3.05}$
Grain 2	41.1	39.6	19.6	100.3	$Cu_{3.13}Bi_{.92}S_{2.96}$

and, on average, a more Bi- and S-rich composition than wittichenite (i.e., on the basis of a seven-atom molecule, $Cu_{2.54}Bi_{1.25}S_{3.21}$; analysis total, 98.2 percent). Subsequent microscopic scrutiny at 800X magnification disclosed a number of barely perceptible but slightly lighter, weakly anisotropic, micron-size specks of another phase in the wittichenite, which accounts for the irregularities in the microprobe analysis. The chemical evidence and paragenetic considerations suggest the admixed phase is emplecite, $CuBiS_2$, the most familiar and widespread of the Cu-Bi-S minerals. The optical properties of the specks do not accord with the rare mineral klaprothite, $Cu_6Bi_4S_9$, the only other known mineral in this system.

Wittichenite is replaced to varying degrees by supergene Cu sulfides, mainly digenite, and locally by a complicated brownish mixture of extremely fine-grained unidentified materials containing much Bi.

Native Elements and Alloys

Bismuth Half a dozen small, equant, bright cream-white, moderately anisotropic grains of native bismuth about 75 to 200 microns across were identified in a wittichenite-bearing sample from the Keystone mine. The bismuth occurs as isolated grains in paragenetically late ankerite gangue, as discussed earlier. Identification was confirmed by qualitative microprobe analysis on the multi-channel analyzer. No elements other than Bi were discerned in the X-ray spectrum.

Gold and Electrum These metals are the minerals of principal economic importance in most of the vein deposits, and they were recognized during microscopic investigations in samples from eight vein Deposits (Table 12). Although gold or electrum was not observed in samples from four other deposits that assay more than 5 ppm Au, the fact that gold or electrum has been seen (exceptionally) in samples that assay as little as 0.3 to 4 ppm suggests that the unseen Au values occur in these ores as sparsely disseminated metal grains rather than in solid solution in sulfides.

At the Florence, Independence, and "Anonymous" mines, the visible gold occurs mainly in pyrite as minute inclusions ranging in size from the limits of normal microscopic resolution (less than 2 microns) up to about 75 microns (Fig. 20 D). At the Florence mine, gold commonly occurs as intergranular

Fig. 21 A. Wittichenite (light gray) with abundant inclusions of gold (white). Wittichenite is weathered to digenite (lighter medium gray) along grain margins and fractures, and digenite is intergrown with a darker unidentified Bi-rich weathering product. Quartz matrix. Intermediate-late stage ore, Keystone mine, sample MK-1ZN. X200, reflected light.

B. Gold (white) as irregular specks and interstitial masses in goethite limonite after pyrite. Gold is extensively remobilized along microfractures in (ex-)pyrite. Dark gray is quartz. Florence mine, sample FM-1U. X160, reflected light.

C. Metallic Fe-Cr-Ni (white) as weathered relics in a large body of goethite limonite (lower right) and along margin of a goethite mass near upper edge of photo. Irregular relics of chalcopyrite (near white) are largely replaced by finely intergrown supergene covellite and limonite. Black areas are cavities. Ore in quartz fissure vein, Black mine, sample MB-1D. X210, reflected light.

D. Chalcopyrite (near white) and sphalerite (medium gray, lower half of photo) interstitial to euhedral-subhedral tremolite (dark gray) in a tremolite-epidote-oligoclase gneiss. Large sphalerite grain contains minute specks of exsolved chalcopyrite. Digenite replaces chalcopyrite along grain margins. Rounded white grain in lower left, adjacent to chalcopyrite and sphalerite, is supergene pyrite that has replaced pyrrhotite. Metamorphosed ore, Douglas mine, sample MD-25. X80, reflected light.

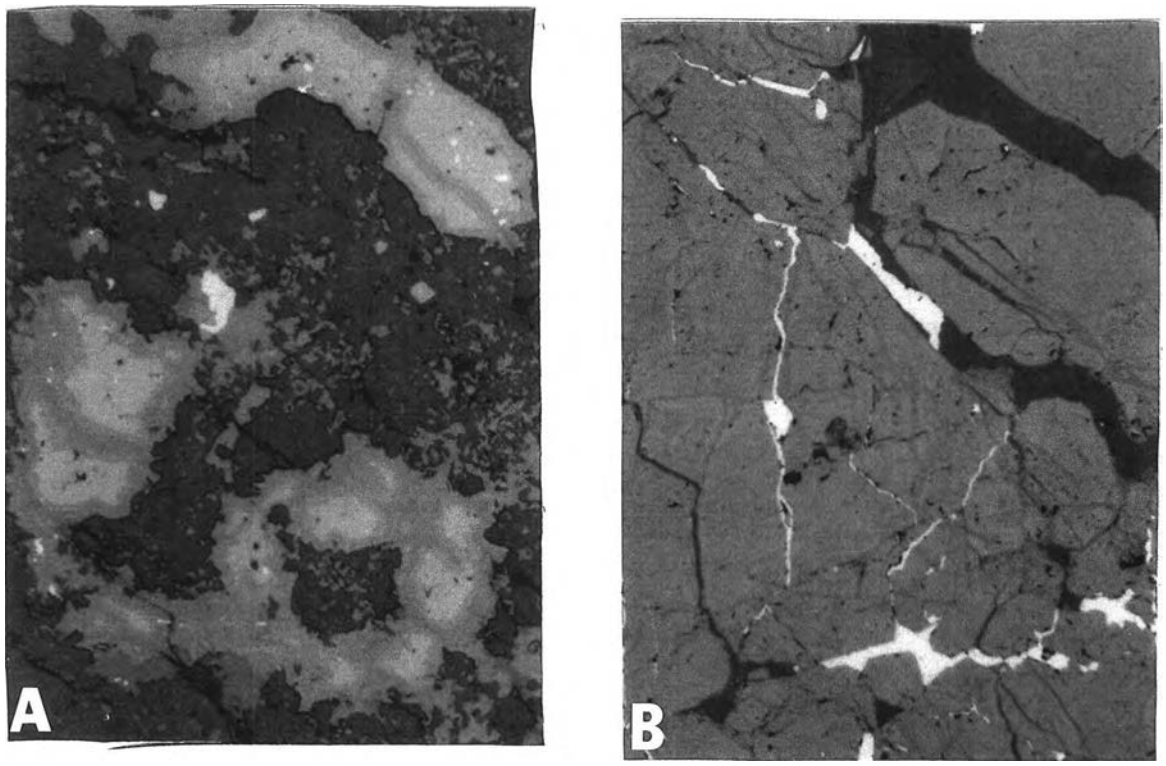

Figure 21

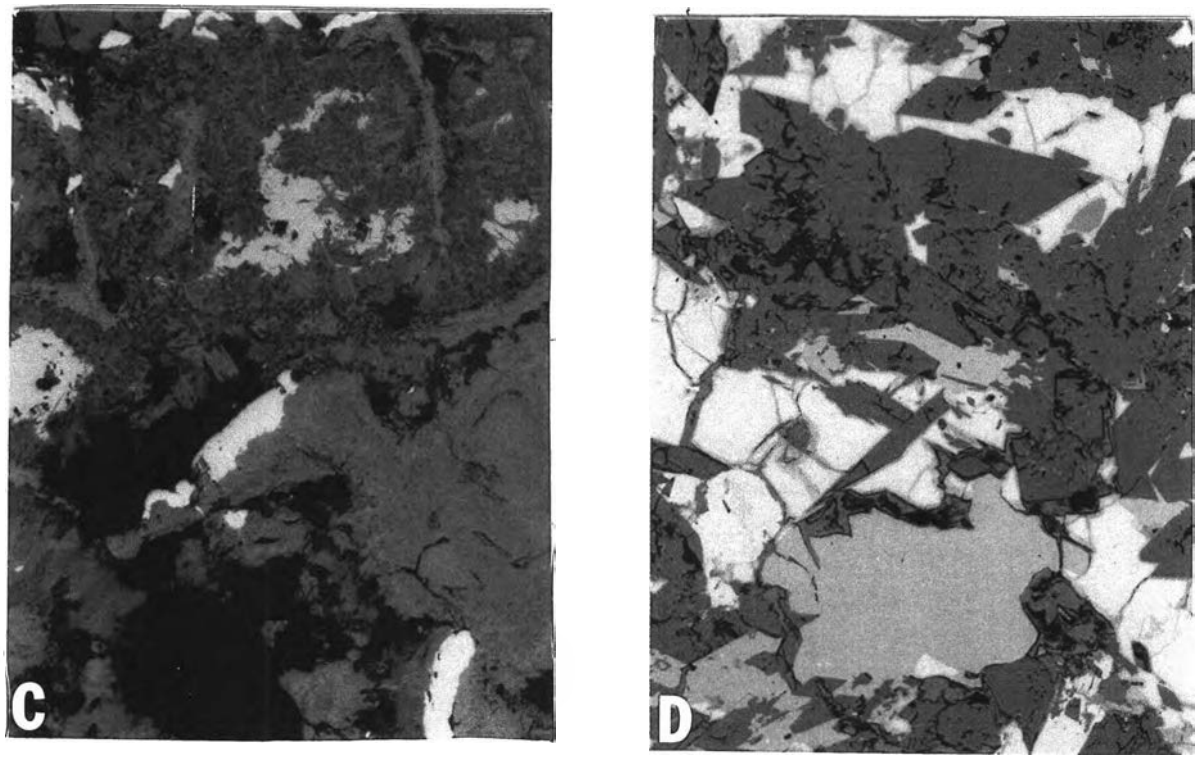

films and larger irregular interstitial patches in massive pyrite lenses, and much of this paragenetically early gold has been remobilized along cataclastic fractures in pyrite and quartz (Fig. 21B). It seems significant that at the Florence, which has the richest gold ore and relatively little Ag alloyed in the gold, the metal has an early position in the paragenetic sequence, following one generation of wallrock-replacement pyrite, but earlier than most chalcopyrite, and earlier than all magnetite, sphalerite, bornite, and hematite. Of fourteen vein samples from the Florence mine examined in polished section, seven have the assemblage gold + pyrite ± chalcopyrite; six have pyrite + martitized magnetite ± chalcopyrite, without gold; one contains pyrite + magnetite + gold, in which the single grain of gold occurs in pyrite developed idiomorphically against magnetite. At the "Anonymous" mine, gold in much lower grade ores has been seen in pyrite- and chalcopyrite-rich, magnetite-bearing assemblages.

At the Keystone, Black, Gold Crater, Golden Key, and Albany mines, gold or electrum occurs mainly in quartz and in chalcopyrite of chalcopyrite-pyrite assemblages. The gold/electrum is often relatively coarse, with grains up to a millimeter across seen in material from the Keystone mine. The Keystone deposit has had a relatively complex cataclastic history, and much of the gold occurs in microfractures in quartz.

Au-Ag alloys from seven mined deposits were analyzed by electron microprobe using synthetic Au-Ag-Cu alloys as standards. The results of these analyses are presented in Table 17. The X-ray spectra of analyzed grains were checked on the multichannel analyzer for traces of other metals, especially Cu, Ni, and PGE. With the exception of Cu-bearing electrum from the Black mine, foreign metals are not present in detectable amounts in the Au-Ag alloys analyzed. The occurrence of Cu in electrum at the Black mine seems significant in view of the fact that this deposit also contains a new alloy or intermetallic compound of Fe, Cr, Ni, and Co. The analyzed electrum at the Black mine occurs in narrow veinlets with chalcopyrite in non-foliate sericite-quartz-albite-pyrite rock.

Electrum from the Albany mine is compositionally heterogeneous, but systematic microprobe traverses across heterogeneous grains showed that the compositional deviations are erratic rather than zonally distributed.

Duplicate samples from the Albany and Florence mines in which Au-Ag alloys were analyzed appear to be paragenetically contemporaneous, but the two analyzed samples from the Keystone mine are paragenetically diachronous. Disseminated equant grains of gold in quartz of an early pyrite-chalcopyrite-quartz assemblage (sample MK-1K) have distinctly higher Au-Ag ratios than gold included in paragenetically

Table 17. Electron microprobe analyses of Au-Ag-Cu alloys from some vein deposits. Values in weight percent. ND = not detected. Formula expressed as atomic ratio in decimal fractions.

Mine and Sample Number	Au	Ag	Cu	Total	Formula
Albany Mine					
MA-9Z11	63.6	36.7	ND	100.3	$Au_{.49}Ag_{.51}$
MA-9Z12 (mean of grain)	60.8	38.5	ND	99.3	$Au_{.46}Ag_{.54}$
MA-9Z12 (high Ag part)	53.9	46.8	ND	100.7	$Au_{.39}Ag_{.61}$
MA-9Z12 (low Ag part)	65.9	34.1	ND	100.0	$Au_{.51}Ag_{.49}$
"Anonymous" Mine					
MW-6	74.4	24.5	ND	98.9*	$Au_{.63}Ag_{.37}$
Black Mine					
MB-1Q (grain 1, mean)	66.3	32.7	0.5	99.5	$Au_{.52}Ag_{.47}Cu_{.01}$
MB-1Q (grain 1, Cu-rich part)	64.9	33.8	1.4	100.1	$Au_{.50}Ag_{.47}Cu_{.03}$
MB-1Q (grain 2, mean)	68.7	30.7	0.4	99.8	$Au_{.55}Ag_{.44}Cu_{.01}$
Florence Mine					
MF-1I (grain 1)	92.3	7.9	ND	100.2	$Au_{.86}Ag_{.14}$
MF-1I (grain 2)	91.5	8.6	ND	100.1	$Au_{.85}Ag_{.15}$
MF-1U	88.8	11.0	ND	99.8	$Au_{.82}Ag_{.18}$
Gold Crater Mine					
MGC-1B	75.4	23.0	ND	98.4**	$Au_{.64}Ag_{.36}$
Golden Key Mine					
M-459D	89.4	10.3	ND	99.7	$Au_{.83}Ag_{.17}$
Keystone Mine					
MK-1K (early gold)	87.0	12.8	ND	99.8	$Au_{.79}Ag_{.21}$
MK-1ZN (grain 1, late gold)	83.7	16.5	ND	100.2	$Au_{.74}Ag_{.26}$
MK-1ZN (grain 2, late gold)	81.7	17.5	ND	99.2	$Au_{.72}Ag_{.28}$

*Low total due to porosity of grain.
**Low total due to small grain size (~5μm) and matrix interference.

intermediate- to late-stage wittichenite (sample MK-1ZN, Fig. 21A). Although data are sparse, comparison of the Au contents in assayed samples from each deposit (Table 11) and the electron microprobe data (Table 17) suggests that gold tends to be Ag-poor in higher grade Au ores and relatively Ag-rich in lower grade veins. Where there is sufficient paragenetic control from polished section studies, it appears that the Ag-poor gold of richer deposits tends to occupy an earlier position in the vein deposition sequence than do Ag-rich alloys of lower grade veins. Gold is definitely early in the Florence deposit, mostly early-intermediate in the Keystone deposit; electrum occupies a late-intermediate position in the Albany vein and is very late at the Gold Crater mine.

In a similar line of investigation of four gold mines in southern Rhodesia, Eales (1961) demonstrated that in the same orebody, high grade ore contains Ag-poor gold, and low-grade ore contains Ag-rich gold, a relationship also found by Anhaeusser (1976, p.58) in some mines in the Barberton Mountain Land, South Africa. However, Eales (1961, p.72) also showed that the composition of gold in the Rhodesian mines tended to change from Ag-rich in the early stages of ore deposition to Ag-poor in late stages of the paragenetic sequence.

Fe-Cr-Ni Mineral A polished section of vein material from the Black mine contains numerous grains of a previously undescribed alloy of intermetallic compound of Fe, Cr, and Ni. Several grains of the metal were analyzed quantitatively by electron microprobe, following qualitative analysis on the multi-channel analyzer. Analyses of four grains are presented in Table 18. The new mineral occurs enclosed in weathered chalcopyrite in a chalcopyrite-cobaltite-pyrite-electrum paragenesis in milky vein quartz. Several dozen grains or weathered relics of grains of the metal range from about 200 to less than 10 microns in length, but the size of limonite masses enclosing the relics suggest some grains were originally at least 400 microns across (Fig. 21C). Although the primary textural relations are obscured by weathering effects, the distribution of the Fe-Cr-Ni metal and its derivative goethitic limonite indicate it originally occurred as granular intergrowths with chalcopyrite and also as crosscutting veinlets or stringer-like inclusions and strings of inclusions in chalcopyrite. In many cases it is difficult to distinguish limonite that has replaced elongate bodies of the metal from limonite developed after chalcopyrite along grain bodies and fractures.

The investigation of the Fe-Cr-Ni mineral is incomplete, and only qualitative characteristics of its optical and physical

Table 18. Electron microprobe analyses of metallic Fe-Cr-Ni from the Black mine. Values in weight percent. Formula expressed as atomic decimal fractions.

	Fe	Cr	Ni	Co	Total	Formula
Grain 1	70.3	19.5	10.4	0.2	100.4	$Fe_{.69}Cr_{.21}Ni_{.10}Co_{.002}$
Grain 2	70.1	19.9	10.6	0.1	100.7	$Fe_{.69}Cr_{.21}Ni_{.10}Co_{.002}$
Grain 3	69.7	19.5	10.5	0.2	99.9	$Fe_{.69}Cr_{.21}Ni_{.10}Co_{.002}$
Grain 4	69.5	19.0	10.5	0.3	99.3	$Fe_{.69}Cr_{.20}Ni_{.10}Co_{.002}$

properties can be reported here. The metal is pure white and optically isotropic, with reflectivity in air estimated visually (relative to pyrite and cobaltite) as about 60 percent. It was initially distinguished from small grains of cobaltite in the same assemblage by its negative polishing relief against goethite limonite and by the relative ease with which it is scratched by a steel needle. Quantitative measurements of reflectivity and hardness and studies of the crystalline structure are planned as future investigations. Whether it is an alloy or an intermetallic compound of restricted stoichiometry is not known. If it is an intermetallic compound, the stoichiometry $(Fe,Co)_7Cr_2Ni$ is most compatible with the microprobe data.

This metal must surely rank as one of the more peculiar species ever reported from a hydrothermal mineral deposit. It is the only known terrestrial mineral containing metallic Cr as a significant constituent,[1] and apparently the first reported occurrence of an Fe-dominant metal from a natural hydrothermal system, although native iron, awaruite (Ni_3Fe), and

---

[1] A single grain of Fe-Cr metal containing 17 wt percent Cr and 81 percent Fe is reported by Goldstein et al. (1972, p.1056) in a lunar soil sample returned by the Apollo 14 mission. Its status as a mineral is in doubt, however, as the authors suggest it may be an accidentally introduced artificial contaminant in the soil sample.

wairauite (CoFe) are rare minerals of a serpentinite paragenesis (Ramdohr, 1969).

Intermetallic compounds of Fe and Ni with rather broad compositional ranges are well known from meteorites, but with the possible exception of iron of the serpentinite association (for which chemical data are apparently lacking), terrestrial occurrences of metallic iron do not contain significant amounts of Ni or Co (Ramdohr, 1969, p.356, 360). Trace element data on meteorite minerals are scant, but Mason and Graham (1970, p.6) report that the nickel-iron phase of analyzed chondrites contains less than 10 ppm Cr. However, chondrites studied by Mason and Graham are chromite-bearing.

El Gorsey and Kullerud (1969) have discussed the mineralogy of the Cr-Fe-S system with reference to meteorites. Three sulfides containing essential Cr are known, and troilite of iron meteorites contains up to 1.6 weight percent Cr. Synthetic phase relations in the system Cr-Fe-S were investigated by El Gorsey and Kullerud (1969) by reconnaissance in the temperature range 300° to 1900°C, and in detail in the interval 600°-700° C. They report (p.640) that complete solid solution between Fe and Cr is interrupted by miscibility gaps appearing in the Cr-rich and Fe-rich portions of the Fe-Cr system between 820° and 700°C. Below 600°C, sulfur-saturated bulk compositions in the Cr-Fe-S system (i.e., using

FeS + CrS $\pm$ S as reactants) yield three solid phases: $(Fe,Cr)_{1-x}S$ ("chromian pyrrhotite"), Cr_2FeS_4 (daubreelite), and alpha $FeCr_{ss}$. In sulfur-saturated systems, Cr is strongly partitioned to the sulfide phases, and at 600°C, the metal phase in equilibrium with "chromian pyrrhotite" and daubreelite contains less than 1 weight percent Cr, and solubility of Cr in this metallic phase diminishes rapidly with decreasing temperature.

At the Black mine, pyrite occurs in the quartz veins and is exceedingly abundant in the wallrocks adjacent to the veins (i.e., several percent pyrite, on the average); magnetite or other hypogene oxide minerals have not been seen in veins or pyritized wallrocks. Thus, there can be little doubt that the hydrothermal system was sulfur-saturated with respect to the content of dissolved chalcophile metals, so the data of El Gorsey and Kullerud (1969) shed scant light on the origin of this unusual metal.

As the formation of metallic Cr implies an extreme reducing environment, its occurrence in the earth's crust would arouse curiosity in any case, but its appearance in a hydrothermal system in association with pyrite (rather than pyrrhotite, the Fe-S mineral stable under strong reducing conditions) is thoroughly baffling. The associated pyrite (shown by microprobe analysis to be normal stoichiometric pyrite without

detectable Ni or Co) occurs as very sparse minute grains isolated in milky quartz that encloses chalcopyrite and its included Fe-Cr-Ni metal, but the spatial association implies that the conditions of formation of pyrite and the metal were probably not radically different. It must therefore be concluded from the extreme disequilibrium shown by this assemblage that the Fe-Cr-Ni mineral formed metastably, and its survival is probably attributable to its chalcopyrite armor.

Supergene Alteration of Vein Deposits

All available specimens from all the vein deposits show some degree of supergene alteration, but as the weathering processes have been destructive rather than constructive in terms of impact on commercial value of the deposits, the supergene effects are peripheral to the focus of this study and will not be reviewed in detail.

Evidence of supergene enrichment of Au and Ag by chemical processes has not been noted in any of the deposits. The possibility of *in situ* mechanical residual concentration of gold cannot be evaluated from inspection of dump samples or from the limited amount of assay data from individual deposits. Microprobe analyses of Au-Ag alloys in fractures in limonite at the Albany and Florence deposits show that the metal of these occurrences is compositionally indistinguishable from

unremobilized gold in the freshest sulfide ores of the same deposits.

Supergene minerals identified in the vein deposits are listed in Table 19. In all the deposits, chalcopyrite and bornite are replaced by limonite + secondary Cu sulfides, usually without net Cu enrichment. The alteration of chalcopyrite shown in Figure 21C is typical. The Albany deposit reportedly had a rich body of covellite (Curry, 1959), and in a few samples from the Keystone mine, a limited amount of Cu enrichment is reflected by digenite (Cu_9S_5) replacements of pyrite. In many deposits, some of the chalcopyrite oxidizes directly to limonite $\pm$ native copper, cuprite (Cu_2O), tenorite (CuO), and the carbonates malachite and azurite without intermediate formation of Cu sulfides. In this direct oxidation process, most of the Cu passes directly into solution and is lost.

Several secondary sulfate minerals were found in oxidized material from the Sunset mine and prospects along the carbonate-poor Sunset vein. The sulfates include antlerite [$Cu_3SO_4(OH)_4$], chalcanthite ($CuSO_4 \cdot 5H_2O$), and carphosiderite [$Fe_3(SO_4)_2(OH)_5 \cdot 2H_2O$], the latter occurring as a constituent of limonite. Strengite ($FePO_4 \cdot 2H_2O$) was also identified in earthy brown limonite from the Sunset deposit. Traces of brochantite [$Cu_4SO_4(OH)_6$] are associated with malachite at the Keystone mine.

Table 19. Supergene minerals of the vein deposits. Symbols as follows: O, identified optically by standard microscopic techniques; X, identified by X-ray powder diffraction; R, reported and reasonably inferred to be present.

	Albany Mine	"Anonymous" Mine	Bear Mine	Black Mine	Cuprite Mine	Duchess Mine	Florence Mine	Gold Crater Mine	Golden Key Mine	Independence Mine	Keystone Mine	Lake Creek Mine	Prospect, Sec.7, T.14 N., R.78 W.	Prospect, Sec.18, T.14 N., R.78 W.	Prospect, Sec.34, T.15 N., R.80 W.	Prospect, Sec.35, T.15 N., R.80 W.	Sunset Mine
Chalcocite	O		O		R		O	O		O	O	O	O	O	O		O
Digenite	O	O	O	O		O	O	O	O	O	O	O	O	O	O		O
Covellite	O	O	O	O		O	O	O	O	O	O	O	O	O	O	O	O
Copper	O				R		O	O				O					O
Cuprite	O				R		O	O		O	O	O					O
Tenorite	O							O			O						O
Antlerite	X																X
Brochantite											O						
Chalcanthite																	X
Malachite	O	O	O	O	O	O	O	O	O	O	O	O	O	O	O	O	X
Azurite						O				O					O		X
Smithsonite															O		
Chrysocolla	O		O	O		O	O	O		O	O	O	O	O	O	O	X
Shattuckite	X																
Anglesite															O		
Cerussite															O		
Pyromorphite															O		
Strengite																	X
Carphosiderite																	X
Hematite	X			O						O	O						X
Goethite	X	O	O	O	O	O	O	O	O	O	O	O	O	O	O	O	X
Calcite	O						O	O		O	O				O		
Quartz	O							O		O	O						O

At the Pb-Ag-Cu prospect, galena is replaced *in situ* by anglesite ($PbSO_4$) and subordinate amounts of cerussite ($PbCO_3$), and pyromorphite [$Pb_5(PO_4)_3Cl$] is common as greenish crusts lining fractures in vein quartz. A small amount of dull brownish smithsonite ($ZnCO_3$) accompanies Cu carbonates in decomposed sphalerite-friebergite ore. Secondary Ag minerals were sought in ore from this deposit, but none were seen.

Hydrothermal Wallrock Alteration Associated with Vein Deposits

Since the significantly mineralized portions of shear zones and fractures are in virtually every case obscured by natural cover or by debris from the mining operations, samples studied for effects of hydrothermal alteration were collected mainly from mine waste dumps. However, in a few cases it was possible to collect samples *in situ* from weakly mineralized veins and immediately enclosing wallrocks at exposures in prospect pits.

Alteration Zones in Structures Cutting the Keystone Quartz Diorite

The regularities of alteration zoning are more easily recognized in the Keystone quartz diorite than other lithologic units in the study area due to its relative homogeneity. As discussed in an earlier section, at localities in which

the quartz diorite was investigated in connection with vein mineralization, weak cataclastic effects and retrograde metamorphism are pervasive. These are evidenced mainly by granulation and recrystallization along grain boundaries of quartz and feldspars and by development of epidote, sphene, magnetite, and secondary olive-green biotite as partial replacements of hornblende (Fig. 22A). Metamorphic foliation in the quartz diorite is principally due to subparallel alignment of secondary biotite plates. The association blue-green hornblende + epidote + biotite + andesine represents the epidote amphibolite grade of metamorphism.

HYDROTHERMAL ALTERATION EFFECTS IN WALLROCKS OF VEIN DEPOSITS

Since the significantly mineralized segments of shear zones and fractures are in virtually every case obscured by natural cover or by debris from the mining operations, samples studied for effects of hydrothermal alteration were collected mainly from mine waste dumps. In a few cases it was possible to sample alteration zones in situ at exposures of small veins in prospect pits and adjacent outcrops.

The principal Au-Cu deposits have developed via multiple episodes of fault reactivation and hydrothermal activity in regimes of changing temperature, pressure, and fluid chemistry.

These complexities and the poor sample control--the original spatial relations of dump samples are of course unknown--leave some ambiguities concerning the spatial and temporal relationships among wallrock mineral assemblages and the conditions under which they formed. However, sufficient facts are available from limited outcrops and large dump samples to permit confident delineation of the general aspects of alteration facies distribution.

Metamorphism at Epidote Amphibolite Grade and Associated Mineralization

As discussed in a preceding section, country rocks throughout the district are affected by extensive weak cataclasis and retrograde metamorphism to epidote amphibolite grade. In the gneiss-schist complex and the Keystone quartz diorite, these effects are evidenced by grain boundary granulation with recrystallization of quartz and feldspars and by development of epidote, sphene, magnetite, and secondary biotite as partial replacements of hornblende. Figure 22A shows effects of this type in Keystone quartz diorite. Retrograde metamorphic effects on mafic rocks are analogous (Fig. 23A).

It was noted earlier that segments of mafic dikes have undergone local pegmatitic recrystallization and/or limited chemical reconstitution (bleaching of amphiboles) at epidote amphibolite grade under fault-localized volatile-rich

conditions. At the Cuprite mine, this was accompanied by formation of andesine/oligoclase-quartz-microcline pegmatite lenses alongside portions of the pegmatitic metagabbro dike and at intersections of the dike/fault with small northeast-trending fractures. Two larger northeast-trending lenses of quartz-microcline-tourmaline(schorl) pegmatite occur as isolated bodies in quartzo-feldspathic gneiss within a few hundred feet of the Cuprite dike/fault. These felsic pegmatites appear to have shared the general time and circumstances during which the gabbro recrystallized and very coarse-grained pyrite-magnetite-tourmaline-microcline-quartz-epidote veins developed locally along the main fault. (The carbonate-rich vein and wallrock assemblages at the Cuprite mine belong to a later episode of fault reactivation and mineralization.)

Elsewhere in the district, vein deposits show few or no indications of significant development under conditions approaching epidote amphibolite grade, and major mineralization effects appear to be superposed diachronously on the epidote amphibolite grade wallrocks.

Wallrock Alteration Zones in Felsic Wallrocks Adjacent to Ore Veins

Wallrock alteration accompanying a 5- to 12-inch wide quartz-chalcopyrite[1] and quartz-ankerite compound (multi-generation) vein of the Gold Crater system was investigated in prospect pit and outcrop exposures over a 75-foot lateral interval. The alteration effects developed in the meta-quartz diorite host rock are exemplary to varying degrees of alteration in felsic-intermediate composition rocks at most other vein deposits.

Hydrothermal alteration effects become apparent about six feet from the vein, and over the succeeding veinward interval essentially three alteration facies are developed in the meta-quartz diorite:

(1) A zone characterized mainly by secondary biotite, chlorite, and pyrite, with chloritization of all femic minerals on the inner part of this zone. In the outer portion of the zone, hornblende (already partly replaced by medium-grained biotite at epidote amphibolite grade) is variably altered to aggregates of extremely fine-grained matted olive-brown hydrothermal biotite together with a few coarser platelets of pale

---

[1]The ore mineral assemblage also includes minor bornite, pyrite, magnetite, hematite, sphalerite, galena, and electrum.

Fig. 22 A. Typical fresh quartz diorite from the Florence-Gold Crater vicinity. Hornblende (large striated grain, center; adjacent small light grain at left margin) is altered along grain margins and to a lesser extent in grain interiors to a fine-grained intergrowth of biotite + epidote + sphene + magnetite. Quartz (large black grain, at extinction, and adjacent lighter grains at bottom) is polygonized along grain margins. Andesine makes up the remainder of the photo. X40. Transmitted light. Crossed nicols.

B. Biotization alteration zone in quartz diorite. A large grain of former hornblende (central half of photo) is entirely replaced by an aggregate of extremely fine-grained matted biotite (lightly speckled, various shades of gray), subparallel chlorite platelets along former hornblende cleavage (light gray), and abundant pyrite (black) and sphene (dark gray). An earlier generation of coarser biotite and epidote are intergrown with quartz in the lower third of photo. Quartz makes up most of the remainder. Gold Crater mine. X40. Transmitted plane light.

C. K-feldspathization of quartz diorite. A large grain of andesine is extensively replaced by very fine-grained K-feldspar (variable gray, upper left). A little carbonate is intergrown with K-feldspar and replaces cataclastic portion of plagioclase grain (lower center). Black areas are voids. Keystone-Florence fault. X80. Transmitted light. Crossed nicols.

D. Former quartz diorite replaced by a mylonitic aggregate of chlorite (dark gray), matted sericite (speckled, upper right) and carbonate (striated wedge, center and light-colored grains below wedge and at top). Light grain in upper left is quartz. Florence mine. X40. Transmitted light. Crossed nicols.

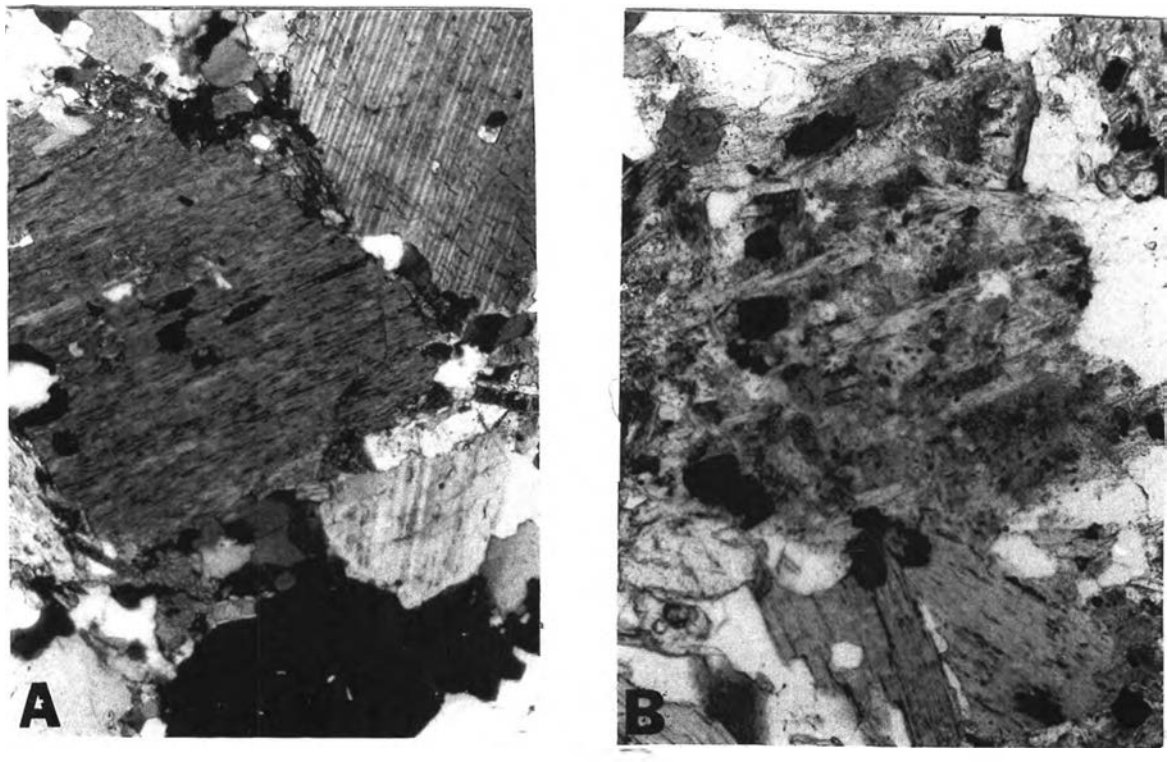

Figure 22

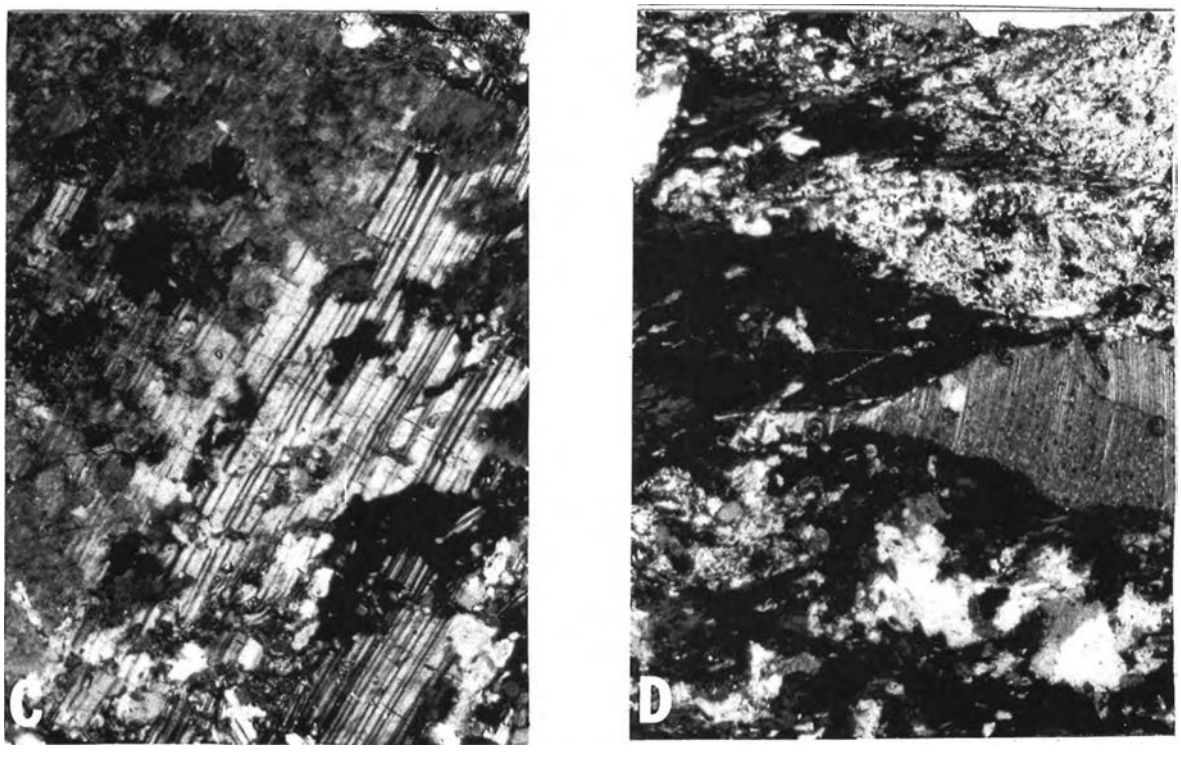

chlorite, and abundant disseminations of pyrite and sphene (Fig. 22B). Extremely fine-grained secondary K-feldspar and minor sericite make an appearance at the expense of andesine.

(2) A facies characterized in its outer part mainly by partial K-feldspathization of plagioclase (Fig. 22C) and on the inner side, over an eight-inch interval out from the vein selvage, by sericitization of everything but pyrite and primary quartz. K-feldspar survives to within a few inches of the selvage. The climax of sericitic alteration is represented by a weakly foliated porphyroblastic mass of felted sericite with scattered pyrite and relatively coarse relict quartz grains. No secondary quartz is visible, and all traces of epidote, chlorite, sphene, and feldspar are obliterated.

(3) A thin selvage developed from mylonitized quartz diorite consists of lenses of medium- to very fine-grained quartz intercalated with lenses of sericite; disseminations and lensatic segregations of black tourmaline and pyrite are present in amounts up to a few percent each.

A significant feature of the facies succession just described is the absence of secondary quartz over this six-foot alteration interval to within about a centimeter from the vein. Yet, as demonstrated in a following section, silica is liberated as a major by-product of silicate mineral reactions throughout the entire interval. Perhaps the silica liberated by wallrock reactions now resides in the vein.

At the Florence and Lake Creek mines many early, gold-bearing sulfide veins are bounded by quartz diorite that has undergone extensive K-feldspathization and silicification at the the selvage, with sericite ranging from minor to absent. At the Keystone and Black mines, wallrock at the selvage of gold-bearing sulfide veins consists of sericite-pyrite or quartz-sericite-pyrite assemblages, but much of this facies is obscured by overprinted events. Corroded sericite rock breccia and quartz-sericite-pyrite rock breccia fragments are commonly embedded in a very fine grained hornfels-textured matrix comprised mainly of carbonate, quartz, and pyrite, with or without sericite, albite, and tourmaline.

Alteration of Felsic Rocks Adjacent to Gold-Poor Veins

Carbonate-rich wallrock alteration assemblages are much in evidence at most vein deposits, but the spatial and temporal relations among carbonate-rich and carbonate-absent wallrock and vein assemblages within a given deposit are difficult to unravel with information only from dump material. However, in most deposits, crosscutting relations place much of the carbonate deposition as following the principal stages of carbonate-absent quartz-K-feldspar-sericite alteration. (This does not apply to the "Anonymous" deposit, in which carbonate apparently is pervasive throughout, nor to the Sunset mine

and several prospects in which carbonates are entirely absent.)

The following example of alteration zoning adjacent to intermediate-stage quartz-ankerite-sulfide veins at the Florence mine is typical of many veins at the Keystone, Black, Albany, Bear, Duchess, and Lake Creek mines, and sheds significant light on mineralization processes. A typical quartz-calcite-pyrite-chlorite vein in quartz diorite at the Florence mine is accompanied by the following veinward succession of three alteration facies:[1]

(1) A zone in which medium-grained metamorphic biotite is replaced pseudomorphously by pale chlorite and a little magnetite and pyrite; hornblende is altered to aggregates of fine-grained chlorite + calcite + leucoxene + magnetite and a little pyrite; metamorphic epidote/clinozoisite is partly replaced by calcite; in the outer portion of this zone andesine is pseudomorphously albitized (An_8), but in the inner portion, albite has undergone rim replacement by exceedingly fine-grained K-feldspar and relict albite cores are lightly dusted with sericite.

---

[1] Similar alteration accompanies late bornite- and sphalerite-bearing carbonate-rich veins and quartz-carbonate-Fe oxide veins at the Florence and other deposits, but in all deposits studied, gold is very rare in veins carrying carbonates or having conformable carbonate-rich wallrock alteration.

(2) The chloritization-K-feldspathization zone passes into a zone of complete sericite-carbonate replacement. Along the inner edge of the zone, chlorite, epidote, K-feldspar, and relict albite are entirely replaced by an assemblage of fine-grained sericite and calcite, with a little disseminated magnetite, pyrite, and primary quartz. Tourmaline is rare. Secondary quartz is absent.

(3) Within about a centimeter or less from the edge of the vein is an assemblage comprised of fine- to medium-grained carbonate, abundant black-green penninite (in thin section bright green with extremely anomalous birefringence), a little quartz and pyrite, and disseminated grains of absolutely fresh, medium-grained, twinned, anhedral albite pseudomorphous after andesine.

The most significant features of this facies series are the absence of secondary quartz in the outer two zones, and the presence of two zones of chlorite and albite stability (though chlorite compositions differ). The outer zone is a conventional propylitic association, but the inner zone is more difficult to interpret. The succession clearly differs, however, from the "classic" facies series developed by hot, reactive fluids diffusing outward from a vein conduit, with maximum hydrolysis adjacent to the vein and progressive neutralization of fluids along a reaction path into the wallrock.

In the Florence deposit, silica apparently has been mobilized toward the vein, and the inner zone of albite and chlorite stability might be accounted for by veinward advance of the hydrolytic alteration front, with loss of leaching potency just short of the vein being an effect of a pressure decrease at the fissure wall.[1]

The sericitic zone--the zone of peak hydrolysis--is not always developed as strongly as in the preceding example. Not uncommonly (e.g., at the Keystone and Black mines) this facies is represented by the equilibrium association carbonate + sericite + albite, in which the latter is precipitated in moderate abundance as fine-grained, euhedral to anhedral, untwinned grains, and locally penninite coexists with sericite (Fig. 22D). At the Black mine, euhedral albite is also a gangue constituent in some galena- and sphalerite-bearing quartz-carbonate veins. Figures 23C and D illustrate analogous carbonatization alteration in intermediate-composition schists at the Keystone mine.

---

[1]The fluid pressure regime in the mineralizing environment is discussed in a following section. The effects of pressure on the solvent properties of hot water and dissociational eqilibria in aqueous electrolyte solutions have been discussed by Helgeson (1969) and Ellis (1967). The effect of a substantial pressure drop is to induce association of ionized electrolytes, resulting in neutralization of pH and diminished activities of reactive free ions in solution.

Fig. 23 A. Fresh metagabbro from the dike along the Albany-Cuprite fault, near Cuprite mine. The photo is comprised entirely of a granoblastic intergrowth of medium- to fine-grained hornblende, calcic andesine, and epidote. X40. Transmitted light. Crossed nicols.

B. Hydrothermally decomposed metagabbro from same dike as shown in Fig. 23A. The main constituents are chlorite (penninite, dark gray) and carbonate (mostly lighter gray, speckled texture). A quartz veinlet cuts obliquely across the upper two-thirds of photo. Sphene (very dark gray, resembles chlorite in tone) is abundant in and along the margins of the quartz veinlet. Cuprite mine. X80. Transmitted light. Crossed nicols.

C. Nearly fresh quartz-andesine-biotite-hornblende-epidote schist. The elongate gray laths are mostly chlorite after biotite. The irregular dark gray clot in upper right is epidote. Remainder is mostly quartz and plagioclase, with a few scattered small grains of biotite and hornblende. Keystone mine. X40. Transmitted light. Crossed nicols.

D. Former schist analogous to that of Fig. 23C that is hydrothermally decomposed to a very fine-grained aggregate of carbonate, sericite, albite, and quartz. Very fine-grained quartz is more abundant near the large carbonate veinlet. Black is pyrite. Keystone mine. X16. Transmitted plane light.

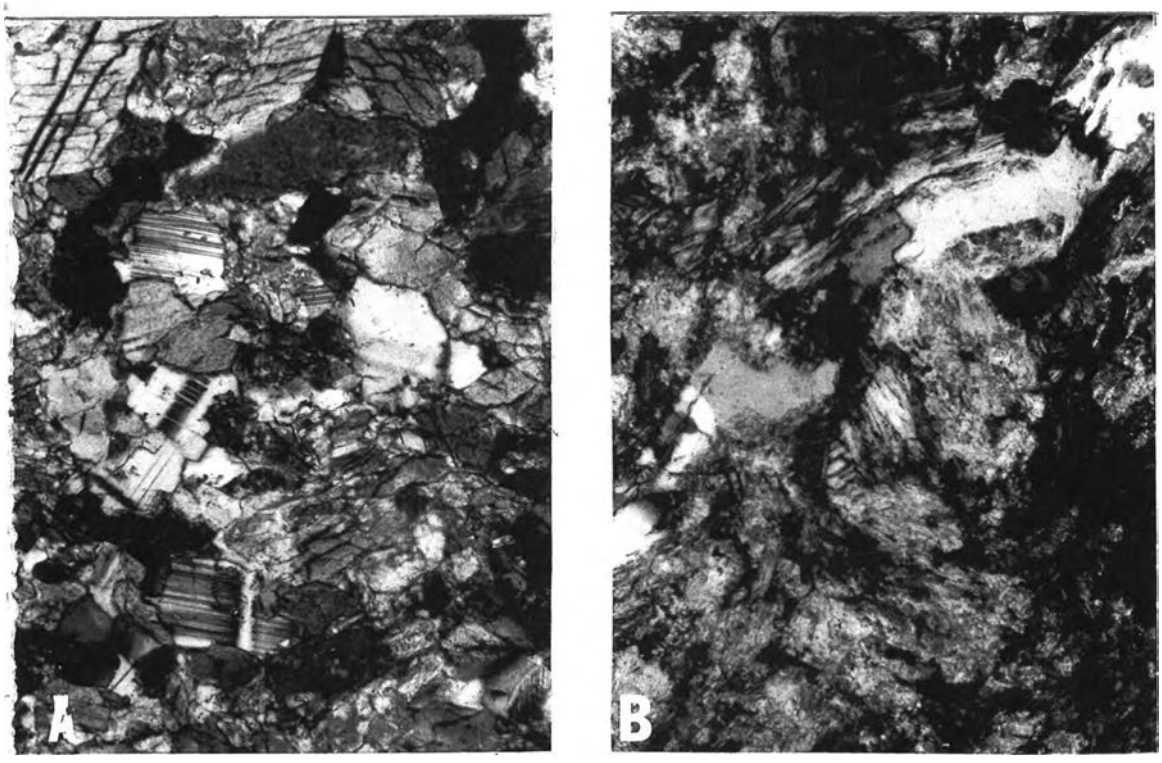

FIGURE 23

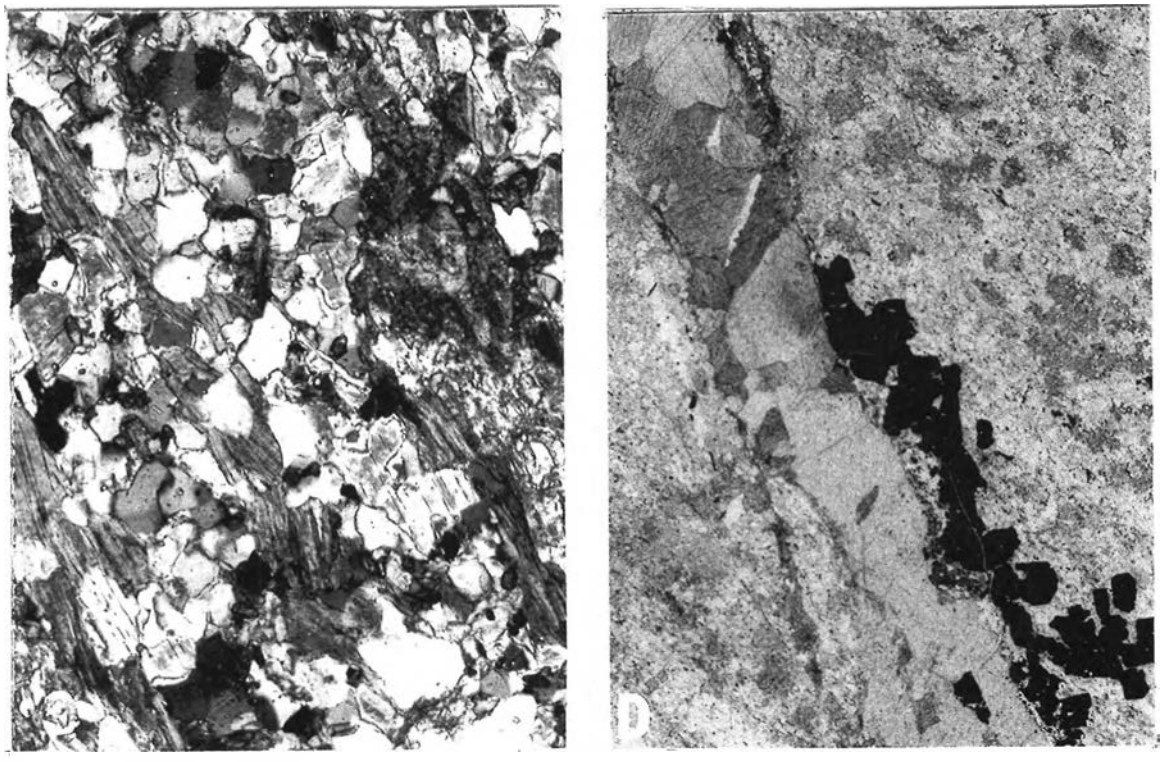

Alteration Effects in Mafic Rocks

The character of hydrothermal alteration of mafic dikes has been alluded to in preceding discussions. In the vicinity of the veins at the Florence, Keystone, Black, Independence, Albany, Cuprite, Bear, Duchess, and Lake Creek mines, the narrow metapyroxenite to meta-andesite dikes and lenses are altered over their full widths to schists comprised of calcite, sericite, albite, and commonly chlorite, with accessory hematite or pyrite, magnetite, sphene or leucoxene, and highly variable amounts of quartz. Hematite is in some cases the only opaque mineral in altered mafic rocks and is particularly conspicuous at the Florence and Keystone mines. Pyrite predominates in altered mafic rocks at most other localities. The significance of the prevalence of hematite and magnetite in mafic rocks associated with Au-rich deposits is discussed in a following section. Figures 23A and B illustrate typical alteration effects in the metagabbro dike at the Cuprite mine.

Discussion

Spatial and temporal relations between hydrothermal alteration affecting mafic and felsic rocks presents problems requiring special comment. The available evidence indicates that the richest ore veins at the Florence, Keystone, Lake Creek, Albany, Independence, Black, and Gold Crater mines have carbonate-absent alteration envelopes and are enclosed

in felsic-intermediate composition rocks; yet, heavily carbonated mafic rocks are much in evidence in dump material or nearby outcrops at each of these deposits. At each deposit, the mafic dikes have been sheared out to form discontinuous lenses along the faults. Since alteration of the strongly reactive mafic rocks necessarily must have proceeded contemporaneously with alteration of felsic-intermediate rocks along the same fault, it can be inferred that carbonate-sericite-albite(-chlorite) assemblages present in virtually all mafic lenses must have developed simultaneously with the early sericite + pyrite + quartz (carbonate-absent) assemblages in felsic rocks elsewhere along the fault. Except where felsic rocks directly enclose mafic pods, the very common crosscutting relations of carbonates clearly demonstrate that carbonate-rich wallrock and vein assemblages in felsic rocks belong to mineralization-alteration events postdating development of simple sericite pyrite-quartz wallrock assemblages and associated ore veins. Multiple generations of calcite veinlets and carbonatized breccia are not uncommon in mafic rocks, but the successive generations of alteration are all of the same general type.

It is reasonable to infer from these relations that solutions reacting with mafic rocks were buffered by hornblende-epidote-calcic plagioclase assemblages to relatively higher

pH's and activities of dissolved Ca, which together promoted early stability of carbonates in and immediately adjacent to mafic lenses. Where the faults cut only felsic rocks, solutions were locally buffered by wallrock mica-feldspar assemblages to lower pH's and relatively low Ca activities, so that in felsic wallrocks carbonate stability was delayed until chemical factors in the fluids evolved that were appropriate for stabilization of carbonate minerals. (The nature of these factors is discussed in a following section.) Since gold has not been detected by assay in significant amounts or seen in any carbonate-bearing veins, even in gold-rich deposits, it is apparent that environments suitable for carbonate deposition were generally unfavorable for precipitation of gold; where these conditions prevailed gold was mobile in hydrothermal solutions.

With the apparent exception of the "Anonymous" deposit, all the investigated mineralized veins in the central Medicine Bow Mountains are associated with mafic metaigneous rocks that have undergone intense cataclasis and hydrothermal alteration along mineralized shears and fractures. The persistence of this association suggests an important role of mafic rocks as contributors of ore metals to the vein deposits.

Evidence for Mobility of Metallic Elements in Wallrocks during Alteration

Sample control is insufficient to permit quantitative comparisons of chemical gains and losses over successive alteration facies. However, in an effort to evaluate qualitatively the hypothesis that ore- and gangue-forming elements underwent redistribution during wallrock alteration and might have supplied most of the necessary components for vein mineralization, concentrations of selected major and trace elements were compared for unsheared mafic dike rocks and quartz diorite of epidote amphibolite grade versus their sheared and intensely chloritized, sericitized, and carbonatized counterparts. (Lithologies of the gneiss-schist complex are too compositionally variable over short intervals to provide meaningful data on element redistributions accompanying hydrothermal alteration and so were not analyzed.)

Chemical data for analyzed groups of rocks are presented in Table 20. The data for each group are few, and the results for most elements do not show simple trends toward consistent enrichment or depletion in altered representatives, but it is certainly significant that Cu, Au, and Pd (the only tabulated metals that have strong propensities to form chloride complexes in solution) consistently tend to be upgraded in intensely altered rocks adjacent to the veins; Ni and Fe are in most

cases significantly enriched in the near-vein altered wallrocks, and Ca, Mg, and Mn are depleted in altered mafic rocks and enriched in carbonatized and chloritized quartz diorite, apparently due to metasomatic introduction from bordering sheared mafic dikes. (Unfortunately, representatives of non-carbonated altered quartz diorite were not analyzed.)

The general trend to enrichment of the principal ore-forming metals adjacent to veins might be interpreted in two ways: 1) dissolved metals and other mobile constituents introduced along flow channels in the faults diffused outward into wallrocks, causing hydrothermal alteration and buildup of metal concentrations in near-vein wallrocks; or 2) metals and other mobile constituents released from country rocks during regional tectonic activity diffused over lateral and vertical pressure gradients, with accumulations of mobile elements in and adjacent to fissures. Although there was probably a complex interplay of both factors locally, it will be argued that migration of components from wallrocks toward faults was probably by far the predominant process.

Relevant to this discussion are data presented by Wedepohl (1972, p.30-G-5) regarding leaching of tholeiites by acidic weakly chlorinated hot springs (73-97^{o}C) at Hveragerdi, Iceland (Cl concentration about 200 ppm in drill hole test at depth--Ellis, 1967, Table 11.5). Over a distance of a few meters from

Table 20. Contents of selected elements in unsheared, unaltered rocks and in sheared counterparts that have undergone intense carbonate-sericite-chlorite hydrothermal alteration accompanying vein mineralization. Values for Fe, Mg, and Ca in wt percent; all others in ppm. Numbers in parentheses indicate the number of samples analyzed in each group. ND = not detected; NA = not analyzed. Au, Pd, Pt by fire assay-emission spectrography--analysts: R.R. Carlson, E.F. Cooley, T.A. Doerge; Au and Cu by atomic absorption--analysts: R.B. Carten, C.A. Curtis, J.G. Frisken, J. Mitchell, R. M. O'Leary, J.A. Roybol, J. Sharkey, J.G. Viets; B, Ca, Co, Cr, Fe, Mg, Mn, Ni, V by semiquantitative D.C. arc spectroscopy--analysts: R. Babcock, L.B. Breeden, E.F. Cooley, K.J. Curry, G.W. Day, J. Domenico, W.D. Goss, D.J.Grimes, J. Haffty, R. Hopkins, L.B. Riley, D. Siems (all of U.S. Geological Survey).

	Fe	Mg	Ca	Mn	B	Au	Co	Cr	Cu	Ni	Pd	Pt	V
Fresh hornblendite (2)	15	7	7	2500	35	.005	70	250	40	200	.002	.004	400
Altered hornblendite (3)	13	7	7	1800	27	.007	70	670	150	430	.045	.051	270
Fresh metagabbro (3)	10	7	9	2000	16	.007	57	233	73	150	.001	.006	300
Altered metagabbro (7)	13	5	4	1643	60	.014	51	155	281	91	.002	---*	220
Fresh metadiorite (2)	12	5	7	3500	15	.009	60	65	50	60	.002	ND	300
Altered metadiorite (4)	14	3	4	1900	15	.010	38	50	64	90	.002	ND	350
Fresh quartz diorite (3)	6	1.5	3	800	37	NA	20	43	50	25	ND	ND	120
Altered quartz diorite (3)	9	6	4	850	1500	.003	33	80	267	93	.001	ND	233

* In 5 of 6 samples analyzed for Pt, it was not detected at a detection limit of .002 ppm; one sample contained .006 ppm.

the spring, 50 to 90 percent of the Zn (90-100 ppm Zn in fresh basalt), 80 to 95 percent of the Cu (about 180 ppm Cu in fresh rock), and a large proportion of the Fe were leached by the thermal waters.

In hydrothermal leaching experiments on a natural andesite, Ellis (1968, p.1359) leached 93 percent of the Cu from the andesite (initial Cu, 70 ppm) by reaction with 2 M. NaCl at 360-400°C in runs of 4 to 5 weeks duration. In the same experiments, 80 percent of the Pb was removed from the andesite (10 ppm Pb initially). Changes in Ni, Co, Cr, and V were not detectable within the limits of analytical uncertainty.

In a study of hydrothermal effects in ocean ridge tholeiites due to hot basalt-seawater interaction, Keays and Scott (1976) found that SiO_2, S, Ag, and Au are depleted in the altered interiors of basalt pillows relative to their fresh cores, and that S, Ag, and Au are enriched in the glassy margins of the pillows relative to fresh interiors by factors of 7.5 for Au and Ag and 2.5 for S. They conclude from their study that Au sited in igneous sulfide phases in basalts is particularly susceptible to remobilization and that the mobility of Au during hydrothermal alteration is consistent with the hydrothesis that basalts could have served as suitable source rocks for metamorphic-hydrothermal gold mineralization in Precambrian greenstone terranes.

Chemical Mechanisms of Wallrock Alteration

Table 21 presents generalized chemical reactions representing the principal mineralogical changes observed in successive wallrock alteration zones. These reactions demonstrate the ability of processes of this type to liberate large amounts of silica and base cations to pore solutions in the weakly to strongly cataclastic country rocks. Elements such as Cu, Ni, Au, Ag, S, and other trace impurities in ferromagnesian minerals can be expected to enter the fluids in a manner analogous to Fe, Ca, Na, and Cl which are shown. The low tolerance of sericite and calcite crystal lattices for such elements as Au, Ag, Cu, Ni, and Zn suggests that intense sericitization and carbonatization of wallrocks may have resulted in nearly wholesale expulsion of such elements from zones thus affected. As written, the reactions release some aluminum in order to account for precipitation of feldspars and chlorite in and along the selvages of some veins. In Table 21, part A, fluids reacting with more or less micaceous, felsic-intermediate composition rocks are shown as having higher activities of H^+ than reactions involving carbonate deposition (part B). The latter are written schematically (ignoring redox reactions) to liberate oxygen rather than consume additional hydrogen ions and liberate water in order to dramatize a mechanism for producing in weakly acidic or neutral solutions the relatively high oxygen

Table 21. Generalized chemical reactions representing typical wallrock alteration processes associated with vein deposits. (Redox equilibria not considered.)

A. Early alteration reactions in simple bodies of felsic-intermediate composition rocks.

(1) hornblende $\longrightarrow$ biotite + chlorite + sphene + pyrite

$$4[\overset{\text{hbld}}{NaCa_2(Mg_2Fe^2_2Fe^3_{.5}Ti_{.5})(Al_2Si_6O_{22})(OH)_{1.5}Cl_{.5}}] + 8H_2S + 2K^+ + 20\,H^+ \longrightarrow 2[\overset{\text{biot}}{K(Mg_2Fe^2)(AlSi_3O_{10})(OH)_{1.5}Cl_{.5}}] +$$

$$\overset{\text{chl}}{(Mg_4Fe^2Al)(AlSi_3O_{10})(OH)_8} + \overset{\text{spn}}{2CaTiSiO_5} + \overset{\text{py}}{4FeS_2} + 4Na^+ + 6Ca^{2+} + Fe^{2+} + 2Fe^{3+} + 4Al^{3+} + Cl^- + 14SiO_{2(aq)} + 16H_2O$$

(2) biotite + plagioclase (An_{33}) $\longrightarrow$ chlorite + K-feldspar + pyrite

$$2[\overset{\text{biot}}{K(Mg_2Fe^2)(AlSi_3O_{10})(OH)_{1.5}Cl_{.5}}] + \overset{\text{plag}}{Na_2CaAl_4Si_8O_{24}} + K^+ + 2H_2S + 3H^+ \longrightarrow \overset{\text{chl}}{(Mg_4Fe^2Al)(AlSi_3O_{10})(OH)_8} + \overset{\text{ksp}}{3KAlSi_3O_8} + \overset{\text{py}}{FeS_2} +$$

$$2Na^+ + Ca^{2+} + 2Fe^{2+} + Al^{3+} + Cl^- + 2SiO_{2(aq)} + H_2O$$

(3) epidote + chlorite + K-feldspar $\longrightarrow$ sericite + pyrite

$$\overset{\text{epid}}{Ca_2Fe^3Al_2Si_3O_{12}(OH)} + \overset{\text{chl}}{(Mg_4Fe^2Al)(AlSi_3O_{10})(OH)_8} + \overset{\text{ksp}}{2KAlSi_3O_8} + 2H_2S + 8H^+ \longrightarrow 2[\overset{\text{ser}}{KAl_3Si_3O_{10}(OH)_2}] + \overset{\text{py}}{FeS_2} + 2Ca^{2+} + 4Mg^{2+} +$$

$$Fe^{3+} + 6SiO_{2(aq)} + 9H_2O$$

B. Carbonitization reactions representing alteration of mafic rocks and bordering felsic-intermediate composition rocks.

(1) hornblende $\longrightarrow$ chlorite + calcite + sphene + hematite

$$2[\overset{\text{hbld}}{NaCa_2(Mg_2Fe^2_2Fe^3_{.5}Ti_{.5})(Al_2Si_6O_{22})(OH)_{1.5}Cl_{.5}}] + 2H_2CO_3 + 9H^+ \longrightarrow \overset{\text{chl}}{(Mg_4Fe^2Al)(AlSi_3O_{10})(OH)_8} + \overset{\text{ct}}{2CaCO_3} + \overset{\text{spn}}{CaTiSiO_5} + \overset{\text{hem}}{1/2\ Fe_2O_3} +$$

$$2Al^{3+} + 2Na^+ + Ca^{2+} + 3Fe^{2+} + Cl^- + 8SiO_{2(aq)} + 4H_2O + 3/4\ O_2$$

(2) epidote + biotite $\longrightarrow$ chlorite + sericite + calcite

$$\overset{\text{epid}}{Ca_2Fe^3Al_2Si_3O_{12}(OH)} + 4[\overset{\text{biot}}{K(Mg_2Fe^2)(AlSi_3O_{10})(OH)_2}] + 2H_2CO_3 + 5H^+ \longrightarrow 2[\overset{\text{chl}}{(Mg_4Fe^2Fe^3_{.5}Al_{.5})(AlSi_3O_{10})(OH)_8}] + \overset{\text{ser}}{KAl_3Si_3O_{10}(OH)_2} +$$

$$\overset{\text{ct}}{2CaCO_3} + 2Fe^{2+} + 3K^+ + 6SiO_{2(aq)} + 1/2\ O_2$$

(3) plagioclase (An_{40}) $\longrightarrow$ albite + sericite + calcite

$$\overset{\text{plag}}{Na_3Ca_2Al_7Si_{13}O_{40}} + H_2CO_3 + K^+ \longrightarrow \overset{\text{ab}}{NaAlSi_3O_8} + 2[\overset{\text{ser}}{(K,Na)Al_3Si_3O_{10}(OH)_2}] + \overset{\text{ct}}{2CaCO_3} + 2Ca^{2+} + Na^+ + 4SiO_{2(aq)}$$

fugacities evidenced by the dearth of secondary pyrite or other sulfides and prevalence of iron oxides in many altered mafic rocks. Furthermore, recent experimental data indicate that oxygen fugacity may be an important variable regulating mobilization and aqueous transport of gold (Henley, 1973).

Considerations Regarding Conditions of Formation and Origin of the Vein Deposits

The field facts suggest that the vein systems are not connected by any system of master channelways to a magmatic fluid source. The vein deposits display rather remarkable homogeneity of type throughout the 125 square mile region considered here, and eight additional Cu- and Au-bearing veins lying several miles to the north, south, and southwest of the area covered in this report have received cursory inspection by the writer and were found to have mineralogy and structural and lithologic associations differing in no significant respects from veins of the central Keystone district. None of these deposits displays any obvious spatial connection with magmatic activity. With the possible exception of Sherman-type granite, which is exposed only well outside the area of principal mineralization, all exposed igneous rocks in the district are older than the regional retrograde metamorphic event, whereas all vein

mineralization postdates the peak of this metamorphism.[1] In view of these and other considerations, it will be argued in this section that metamorphic-hydrothermal processes accompanying regional cataclasis are directly responsible for formation of the vein deposits.

Temperatures of Vein Mineralization

Clues to the temperatures of vein formation are scant and mostly qualitative in character. Indications of high temperature of wallrock alteration and vein mineralization are present in several deposits. In a sample from the Black mine, diffuse quartz-pyrite veinlets containing appreciable black tourmaline and euhedral albite are enclosed in mafic

---

[1]The peculiar PGE-rich, titaniferous magnetite-sulfide lens in Sec. 15, T. 14 N., R. 78 W., near Albany--which obviously formed at near magmatic temperatures in response to intrusion of Sherman-type granite--indicates that the host fault was active immediately after emplacement of the pluton. At the American mine, about seven miles south of the area covered in this report, a Cu-rich quartz vein of the type common in the study area is enclosed in a sheared diabase dike emplaced in Sherman granite. If this vein is a contemporary of analogous veins in the Keystone district, then district-wide mineralization of this type is at least in part younger than Sherman magmatism. But due to the multiple-mineralization history of many deposits, the age of earliest mineralization with respect to the age of Sherman intrustion in the Medicine Bow region is unknown. The epigenetic mineralization, cataclastic tectonism, and latest metamorphism in the district may generally correlate in time with Sherman magmatism, with all being expressions of the same regional thermal-tectonic event.

hornblende-biotite-andesine schist altered to an apparently equilibrium assemblage of calcite + iron-poor epidote/clinozoisite + fibrous actinolite after hornblende, fine-grained amber phlogopitic biotite after primary green biotite, albite + calcite after andesine, and disseminated tourmaline, pyrite, and quartz. The presence of secondary biotite, iron-poor epidote, and actinolite indicate formation of this vein-wallrock assemblage under greenschist facies conditions, i.e., at temperatures in the vicinity of 400°C or higher (e.g., see Winkler, 1974, p.64, 69, 73). In other samples from the Black mine, variations on this assemblage in more pelitic rocks include non-replacement coexistence of sericite and chlorite with light brown biotite, and associated veins include galena and sphalerite and sometimes a little chalcopyrite (though most chalcopyrite and gold occur in quartz-sericite wallrocks).

The magnetite-pyrite-microcline-epidote-quartz-tourmaline veins (containing up to a few percent tourmaline) at the Cuprite mine have probably also formed at high temperatures, as discussed earlier.

The assemblage bornite + pyrite + chalcopyrite has been observed at the Sunset mine (Fig. 18A). Experimental work in the Cu-Fe-S system by Sugaki et al. (1975) has shown that these minerals do not coexist in equilibrium at temperatures of 350°C or below due to replacement of the high-temperature pyrite-

bornite tie line by one from chalcopyrite to idaite at some undetermined temperature above 350°C. Metastable low-temperature persistence of the pyrite-bornite association due to the difficulty of nucleating idaite in experimental studies has led to uncertainty regarding the temperature of the tie line change. In a review of data on Cu-Fe-S phase relations, Craig and Scott (1974, Fig. CS-30) show the pyrite-bornite association as being stable at 400°C. Of additional interest to this line of inquiry is the abundance of exsolved chalcopyrite in bornite of the bornite-chalcopyrite-hematite association of the same deposit. At 228°C low-temperature tetragonal bornite inverts to a cubic structure, and with increasing temperature the cubic polymorph is capable of dissolving considerable amounts of chalcopyrite (Craig and Scott, 1974, p.CS-71). The large proportion of exsolved chalcopyrite in bornite from the Sunset (Fig. 18B), Gold Crater, and Lake Creek deposits suggest such bornite solid solutions crystallized well above the inversion temperature. More exact temperature estimates cannot be made from the proportions of phases in the exsolution mixture because the experimental composition data apply to bornite-pyrite-chalcopyrite or bornite-idaite-chalcopyrite assemblages, not to oxide-bearing systems.

Ramdohr (1969, p.792) notes that auriferous pyrite (Fig. 20D) is "mostly formed at high temperatures," and further

reports (p.915) that magnetite of hydrothermal vein parageneses (major in some Florence and Cuprite veins and abundant at many other deposits) "is generally an indicator of high temperature and considerable depth." As used by Ramdohr, "high temperature" implies temperatures above about 300°C.

At the Keystone mine, paragenetically late ankerite enclosing irregular grains of metallic bismuth does not show crystal faces against bismuth or lattice disruption against bismuth as might be anticipated if the bismuth had been trapped as a liquid. The melting point of bismuth is about 269°C, and it expands on freezing, often inducing rupture in brittle host minerals (Ramdohr, 1969, p.376).

Hydrothermal goethite has been encountered in the latest stages of the vein parageneses at the Keystone and "Anonymous" mines and at the Pb-Ag-Cu prospect (Fig. 17C). A useful estimate of maximum formational temperature of hypogene goethite is provided by a pertinent P-T curve for hematite-goethite equilibrium computed by Garrels and Christ (1965, p.338-341). At pressures in the range 350-500 bars the highest formational temperatures for goethite are 147° to 154°C, and a maximum of 175°C applies to pressures as high as 1000 bars.

In summary then, observational data indicate that vein mineralization in the district spans a broad range of temperatures from about 400° to 150°C or below, and the mineral

parageneses of some complex deposits, e.g., the Keystone, Florence, and "Anonymous" mines, appear to span virtually this entire range. The principal gold and sulfide mineralization occurred at temperatures approximately in the interval 400°-300°C; ankerite-bearing veins are of somewhat lower temperature origin, and late calcite-Fe oxide veins have formed at low temperatures.

Aspects of the Chemistry of Mineralizing Fluids and Mechanisms of Metal Transport

Phyllosilicate minerals of the wallrock alteration assemblages require moderate hydrogen metasomatism for their development (Meyer and Hemley, 1967; Table 21). Absence of argillization effects indicate the solutions were not strongly acidic, and the presence of alkali feldspars near and in some sulfide-bearing veins suggests the ore fluids were nearly neutral. At the Keystone, Sunset, and Lake Creek mines, the deposition sequence pyrite + chalcopyrite $\pm$ high bornite $\longrightarrow$ hematite + chalcopyrite + high bornite is observed within individual veins, and pyrite occasionally is seen in direct contact with hematite. The absence of magnetite as an intermediate product in this succession requires that these ore fluids were acidic. Development of this magnetite-absent succession at temperatures in the range 250°-350°C also requires

that concentrations of dissolved sulfur in the ore solutions were in excess of 0.1 m. At lower sulfur concentrations, the pyrite stability field shrinks such that magnetite intervenes as a stable phase between pyrite and hematite fields at pH values above 2 or 3 (e.g., see Ohmoto, 1972, p. 559-561 for Fe-S-O phase relations as functions of sulfur concentration, temperature, oxygen fugacity, and pH). Vein feldspars have not been recognized at the Keystone and Sunset mines (sericitic wallrock schlieren are present in ore veins), but deposition of abundant pink microcline (and barite) from at least mildly acidic fluids in ore veins at the Lake Creek deposit implies rather high ionic strengths, i.e., concentrations of dissolved K^+, and it thereby can be inferred that these ore fluids tended to be of a rather "concentrated" character. In most other vein deposits, e.g., the Florence, Gold Crater, Albany, and "Anonymous" mines, the assemblage magnetite + chalcopyrite appears at an intermediate stage, indicating these ore fluids either contained less sulfur or were at somewhat higher pH than magnetite-absent deposits. Carbonates are rather more prevalent in the wallrocks and later veins of magnetite-bearing deposits, which seems to favor slightly higher pH as the principal regulatory factor (though at moderate to high ionic strength, carbonates are stable in weakly acidic solutions at elevated temperatures).

The generally mild acidities suggested by the above data may be accounted for in large part by aqueous carbonate equilibria, as dissociation reactions of the type $H_2CO_3^o \longrightarrow H^+ + HCO_3^-$ and $HCO_3^- \longrightarrow H^+ + CO_3^-$ may continually regenerate the H^+ supply as it is consumed in wallrock reactions. The indicators of weak acidities and large amounts of dissolved CO_2 suggest that strong acids such as HCl or H_2SO_4 were of relatively minor significance.

Abundant data have been accumulated in recent years indicating that most hydrothermal solutions involved in transport and deposition of ore constituents are dominantly alkali chloride brines (e.g., Roedder, 1972; White, 1974). Results of Helgeson's (1969) thermodynamic calculations of the relative stabilities of various solution complexes of ore metals indicate that in acidic solutions at elevated temperatures Ag, Cu, Zn, and Pb are most effectively transported as chloride complexes. (Experimental data indicate that sulfide complexing is significant only in alkaline solutions--e.g., Barnes and Czamanske, 1967). Fuchs and Rose (1974) have shown that Pd and to a lesser extent Pt are most effectively transported as chloride complexes in acidic solutions. It was noted in the discussion of wallrock alteration data of Table 20 that the metals showing the greatest tendency to veinward enrichment are precisely those having the greatest tendency to form

chloride complexes in solution. Henley (1973) proposes that Au may commonly be transported in chloride systems as an oxidized auric chloride complex. He reports that results of high-temperature Au solubility experiments can be described by reactions of the type

$$Au + 3/4\ O_2 + 6HCl \longrightarrow H_3AuCl_6 + 3/2\ H_2O.$$

In natural systems the oxygen regime is buffered by iron silicates and oxides, and the distribution of ubiquitous chloride is controlled by silicates.

The development of secondary hematite and magnetite in preference to pyrite in mafic rocks associated with gold-rich deposits (most notably at the Florence and Keystone deposits) was noted earlier. This feature indicates that ambient oxygen fugacities during alteration at these localities were significantly higher than in penecontemporaneous K-feldspar/sericite-pyrite(-quartz) alteration zones in felsic rocks. Such variations in redox conditions in fluids along a given fault may have promoted leaching of Au from wallrocks in a relatively oxidizing environment and its precipitation upon migration into a less oxidized regime.

The influence of temperature on the solubility of gold is apparent from Henley's (1973) experimental data in an aqueous HCl-quartz-muscovite-K-feldspar-hematite-magnetite system which show that gold solubility rises very sharply from about 10 ppm

Au at 300°C to about 1000 ppm at 500°C. Fyfe and Henley (1973) conclude that if water moves out of rocks undergoing amphibolite grade metamorphism and if chloride is present, then most of the Au will move with water in solutions undersaturated with respect to Au, and major dumping should occur in the greenschist facies. Such enrichment of Au in greenschist grade rocks relative to epidote amphibolite and amphibolite grade counterparts have been documented by Moiseenko et al. (1971) and Petrov et al. (1972) in metamorphic terranes in the U.S.S.R. In regions where suitable structures were available for collection or focusing the flow of metamorphic solutions, this process has been suggested as responsible for formation of a number of major gold deposits in greenstone terranes, e.g., the Morro Velho district, Brazil (Fyfe and Henley, 1973); gold-quartz lodes in the Rhodesian and Kapvaal cratons, southern Africa (Anhaeusser, 1976); the Yellowknife district, N.W.T. (Boyle, 1960); and the Kalgoorlie goldfield, Western Australia (Travis et al., 1971).

If the ore solutions affecting the Keystone district had a significant vertical component to their migration paths, then metal solubilities may have been influenced along the migration route by thermal influences of the type discussed above.

Physico-Chemical Influences on the Mineralization Process

Several features of the vein deposits clearly point to pressure variations in space and time as being a major factor regulating the mineralization process. Observations from field studies are necessarily constrained to the horizontal dimension (i.e., the ground surface). Obvious hydrolytic alteration appears to be restricted to widths little greater than the faults themselves, but consideration of the vertical dimension suggests the volume of the slab of rocks affected by desilication and base leaching may have been quite large, in which case vertical pressure gradients may have influenced the flow of ore solutions.

An order of magnitude estimate of the possible influence of horizontal pressure gradients on fluid migration can be gained by considering the difference in lithostatic versus hydrostatic pressures ambient at the depth of ore deposition. It has been established that the veins formed in the approximate temperature range 400°-150°C, with major gold deposition restricted to the upper part of this interval. If the reasonable assumption is made that ore fluids were essentially in thermal equilibrium with enclosing wallrocks, then considerable depths of vein formation are implied, even assuming high geothermal gradients. For example, a geothermal gradient of 60°C/km would yield a temperature of 350°C at about 6 km depth. At

that depth, the lithostatic load would be about 1650-1750 bars and the hydrostatic load about 500-600 bars. Considering the extreme case, if following episodes of tectonic activity, the fluid pressure within fault zones approached hydrostatic conditions, then such events could have set up instantaneous fluid pressure gradients in wallrocks in excess of 1000 bars over lateral intervals of a few feet. If the geothermal gradient were less, or the considered temperature higher than 350°C, then pressure differentials would be correspondingly greater at the appropriate depth. Clearly, large pressure gradients are likely to have been present in wallrocks, and under these conditions, large volumes of country rock could have been tapped for metamorphic pore fluids and fluid inclusion material liberated by lattice disruptions during regionally pervasive weak cataclasis.

That hydrostatic conditions did not prevail at all points along a fault at a given depth is indicated by the fact that mineralization is principally confined in dilatant structures. Under the influence of pressure gradients along faults, such sites served as efficient collectors of ore solutions.

Since water is a reactant in the silica solution process ($SiO_2 + 2H_2) \longrightarrow H_4SiO_4$), silica solubility is largely dependent on the molecular concentration of water, i.e., the density (Ellis, 1967, p.471). Data given by Lovering (1972, p.38) for

silica solubility at 400°C show that the pressure-SiO_2 solubility curve undergoes a rather sharp inflection in the pressure range 500-700 bars (the approximate temperature and hydrostatic pressure in the regime considered here), and SiO_2 solubility drops rapidly with decreasing pressure. The implications for a silica-laden fluid entering such a pressure regime are obvious. Data for silica solubility variation with temperature at 300 bars show a solubility maximum at about 360°C and rapid decline with decreasing temperature (Lovering, 1972, p.38). These data do much to account for the observed strong removal of silica from wallrock alteration zones at relatively high temperatures and pressures and its precipitation in veins.

Consideration of the conditions requisite for deposition of late-stage vein carbonates (calcite, ankerite, siderite) suggests that carbonate deposition was pressure-regulated. The generally late position of carbonate-bearing veins in the parageneses of complex deposits is attested to by the facts that (1) carbonate and quartz-carbonate veins are seldom cataclastic; (2) they commonly crosscut brecciated quartz-sulfide (-gold) veins; (3) in some complex sulfide-bearing veins (e.g., in the Keystone deposit) euhedral quartz crystals jutting into calcite-ankerite matrix are strongly corroded at contacts with interstitial carbonate; and (4) the presence of hydrothermal goethite in some carbonate veins indicates low-temperature formation.

In a system in which ambient temperatures are controlled mainly by the geothermal gradient, temperature decreases of the magnitudes indicated between mineralization events in a given deposit imply substantial time lapses between episodes of fault reactivation and additional vein formation, with cooling attributable to wane of the geothermal gradient and/or erosional unloading.

Holland (1967) has discussed parameters regulating solubility of hydrothermal carbonate minerals. He points out (p.404-405) that at any given concentration of dissolved Ca, precipitation of calcite (or ankerite) is promoted by increasing temperature and/or decreasing partial pressure of CO_2 in the vapor phase. At any given temperature, release of CO_2 may trigger deposition of Ca-carbonates, but they cannot be deposited in response to cooling of hydrothermal solutions.

In the situation at hand, vein carbonate deposition has occurred in spite of, not because of, cooling of hydrothermal solutions. The simplest explanation for this phenomenon that is compatible with the cataclastic history of the deposits might be that, since solubility of gases in water is pressure dependent, decompression and degassing of fluids occurred during fault reactivation and migration of fluids into newly formed fissures. Since a vapor phase could not likely be present at the depths and pressures implied for early mineralization

events, decompression of fluids in the deep zone pressure interval would likely have minor effect on carbonate solubility, and their presence or absence would be largely a function of the local concentration of dissolved calcium (e.g., early carbonate alteration of mafic rocks). If during later periods of fault reactivation, the site of the deposit was by that time at lesser depths, degassing of solutions and escape of some CO_2 could induce carbonate deposition.

The appearance of iron oxides, especially hematite, in increasing amounts in the later stages of vein parageneses in nearly all vein deposits is probably attributable to cooling. Simple cooling at constant f_{O_2} can stabilize iron oxides relative to pyrite (e.g., see Ohmoto, 1972, p.556-561 for Fe-S-O phase relations as functions of temperature, f_{O_2}, and pH). The oxidative effect of simple cooling of residual solutions probably accounts adequately for (1) the transition from pyrite-chalcopyrite(-gold) to chalcopyrite-hematite (gold-absent) assemblages in quartz veins at the Sunset, Gold Crater, Lake Creek, Independence, and Keystone mines and several prospects, and to chalcopyrite-magnetite (gold-poor to gold-absent) assemblages and the Florence and Albany mines; (2) for the late replacement of chalcopyrite by bornite in many deposits (due to increase in Cu^{2+}/Fe^{2+} as Fe^{2+} is oxidized in solution); and (3) for the very late oxidation of Fe-carbonates and magnetite

to hematite/martite at the Albany, Cuprite, Florence, Keystone, and "Anonymous" mines and several prospects.

Conclusions Regarding Formation of the Vein Deposits

The formation of many deposits is seen as a long and complex process accompanying multiple episodes of fault reactivation and occurring over a broad temperature range spanning roughly the interval 400°-150°C or less.

The hydrothermal fluids are believed to have originated as metamorphic pore fluids and fluid inclusions liberated by pervasive regional cataclasis and collected in fault zones by diffusion over relatively steep wallrock pressure gradients following initiation of faulting activity. Adjacent to fractures, buildup of H_2O and CO_2 induced hydrolysis reactions in wallrocks. This process liberated substantial amounts of silica, base cations--including ore-forming metals--and mobile elements such as S, B, and Cl. The chemical analytical data of Table 20 demonstrate that the epidote amphibolite grade country rocks contain the principal ore-forming metals in concentrations that appear adequate to account for the metal contents of the veins when it is considered that the narrow mineralized quartz veins are separated by diaphthoresis/hydrothermal alteration. The ore solutions migrated along shear zones and faults under the influence of pressure gradients and were

collected in relatively low-pressure dilatant structures. Since the mafic dikes are generally sheared out along faults to form highly discontinuous pods and lenses, the dilatant structures along fault zones not infrequently occurred within felsic wallrocks where the local redox and/or pH conditions were suitable for destabilization of gold complexes in solution and deposition of gold in veins. As residual fluids cooled slowly in the fissures, the oxidative effects of cooling led to precipitation of increasingly oxidized sulfide-oxide, gold-poor and gold-absent vein mineral assemblages. Episodes of fault reactivation were accompanied by redistribution of fluids residing in the faults, with formation of additional generations of ore veins and lenses. Such events occurring late in the history of regional mineralization induced widespread formation of carbonate veins, probably under considerably lower conditions of total pressure than prevailed during formation of early ore veins. Subsequent cooling of residual static solutions in carbonate vein sites led to low-temperature oxidation of vein carbonates and magnetite.

The sporadic development and small size of gold deposits in the Medicine Bow Mountains lend this region little economic significance, but these very limitations attest to the sensitivity of the gold mineralization process to several crucial factors that enable this district to serve as a natural

laboratory for evaluating the influence of critical agents in processes of gold mineralization in metamorphic terranes in general. The specifics of this case that illuminate the general are linked to the lithologic diversity of the district, the varied character of wallrock alteration accompanying the various types of hydrothermal deposits, and the wide range in oxidation state of ore mineral assemblages.

Epigenetic gold deposits in metamorphic terranes are the second most important source of gold production in the world (after the Witwatersrand placers). The history of the controversy over the origin of these lodes has been reviewed by Anhaeusser (1976). Virtually all major deposits of this class are spatially associated with voluminous mafic metaigneous rocks, usually of volcanic origin. However, most such mafic terranes also host felsic intrusions, and a close association between gold lodes and granitoid rocks was recognized by Emmons (1937) and widely interpreted as a consanguineous link. This idea has carried sufficient weight to lead some investigators to hypothesize invisible granitoid intrusives as sources of the fluids and metals where evidence for the intrusives is scant (e.g., Knopf, 1929--the Mother Lode district; Bartram and McCall, 1971--the Kalgoorlie Goldfield). The concept of the mafic source bed for origin of the gold was advanced by Macgregor (1951), based on his experience with Rhodesian gold lodes, and

the concept received substantial support from exhaustive geochemical and geologic evidence presented by Boyle (1961) in a study of the Yellowknife district, Canada (where the distribution of metamorphic facies in greenstones is related to a large granodiorite intrusion). As pointed out by Viljoin et al. (1970), the volcanic and other source rocks have in many instances been modified to such a degree that the fundamental mafic volcanic-mineralization relation has become blurred, and granitic intrusion--whose only role may have been producing heat energy requirements for the migration of gold and other ore-forming constituents--has often been held solely responsible for the mineralization.

The investigated hydrothermal deposits of the Medicine Bow Mountains occur in a region of considerable lithologic diversity. The deposits are hosted by pelitic and intermediate-composition schists, granitoid gneisses, and quartz dioritic, granitic, and gabbroic plutonic rocks. However, of the 20 epigenetic Au-, Cu-, and PGE-bearing deposits encountered within the area covered by this report, 18 are visibly associated intimately with mafic metaigneous rocks,[1] and of an additional eight deposits visited briefly within a few miles of the

---

[1]The remaining two are the "Anonymous" deposit and the PGE-Ni-Cu-rich prospect in Sec. 7, T.14 N., R.78 W.; an invisible mafic source for the metals in the latter deposit is extremely likely.

principal study area, all are immediately associated with mafic dikes or plutons or amphibolites in gneissic terranes. The inescapable conclusion is that mafic rocks were the principal source of the Au, PGE, and Cu in these hydrothermal deposits and were an essential factor in the mineralization scheme.

A further statistic of considerable significance is that mafic rocks associated with veins having significant Au contents are in every case carbonatized, whereas those deposits without associated carbonatization of wallrocks are uniformly poor in gold, e.g., the Sunset mine, the Cu prospects in Sec. 35, T.15 N., R.80 W. and Sec.18, T.14 N., R.78 W., the PGE-Ni-Cu prospect in Sec.7, T.14 N., R.78 W., and PGE prospect in Sec.15, T.14 N., R.78 W., and the Blanche and New Rambler mines. Note that whereas each of the nine deposits containing more than about 3 ppm Au is associated with carbonatization, four of the four PGE-rich deposits are not.

The association with abundant carbonates is typical of gold-quartz lodes in greenstone terranes throughout the world. Anhaeusser (1976, p.79) suggests, with reference to Precambrian gold-quartz veins in southern Africa, that gold transport and deposition may have been influenced by very high partial pressures of CO_2 in auriferous fluids, as suggested by fluid inclusion data. Keays and Kirkland (1972) and Keays and Davison (1976) have investigated a number of Australian deposits

associated with carbonatized greenstones, and Keays (pers. comm., 1976) has expressed the opinion that CO_2 must have been a very important factor in genesis of the gold concentrations. Data from the vein deposits in the Medicine Bow Mountains leave little doubt that CO_2 plays a critical role. However, there are no data available on the hydrothermal solubility of Au in CO_2-rich solutions, and the role of CO_2 is unknown. This would seem to be a fruitful topic for future research.

The vein deposits of this district can readily attest to the influence of yet another variable regulating gold mineralization--the oxidation state of the mineralizing solutions and its implications regarding solution complexing of gold.

Two principal mechanisms are currently thought to be responsible for solution and transport of gold in most hydrothermal systems--gold-thio complexes and gold-chloride complexes. Seward (1973) has investigated the solubility of gold in aqueous sulfide systems in the pH range 4 to 9.5 and the temperature range 160° to 300°C. It was found that at pH 6 gold solubility reaches 40 to 230 ppm in this temperature interval. In acid solutions, the principal gold solution species was $Au(HS)^{\circ}$, whereas $Au(HS)_2^-$ and $Au_2(HS)_2S^=$ were found to predominate in neutral and alkaline solutions, respectively. Henley (1973) studied gold solubility in mildly acidic chloride systems with oxygen fugacity buffered by the magnetite-hematite pair. Gold

solubility was found to increase from 10 ppm at 300°C to about 1000 ppm at 500°C, with solubility attributed to formation of an oxidized auric-chloride complex.

Observational and chemical analytical data for richly mineralized samples from vein deposits in the Medicine Bow Mountains indicate, for comparisons within individual complex deposits and amongst the various deposits, that gold concentrations are uniformly very low in chalcopyrite-hematite(-bornite) assemblages, low in chalcopyrite-magnetite(-pyrite) assemblages, and all high gold concentrations occur with oxide-absent sulfide assemblages.[1] If gold were transported in these solutions as gold-thio complexes of the type discussed by Seward (1973), one should expect maximum solubility in reduced regimes. The reverse appears to be the case--gold has obviously been precipitated under relatively reduced conditions and has remained in solution under more oxidized circumstances. The influence

---

[1]Of the 20 epithermal deposits surveyed here, assay data of Table 11 show nine contain significant gold (i.e., more than 3 ppm); eight of the remainder are devoid of carbonate alteration. The remaining three--the Bear, Lake Creek, and Cuprite mines--are associated with carbonate-rich wallrock alteration, but all vein samples collected from the Bear and Lake Creek mines have hematite-bearing assemblages; most samples from the Cuprite mine are also hematite-rich, with the remainder being a few fragments of high-temperature pyrite-magnetite vein material. Copper-rich ore veins from the Cuprite mine reportedly carried up to 2.56 ounces Au per ton (Curry, 1965, p.8), but sulfides of any kind are exceedingly sparse on the well-cleaned mine dump. No copper-bearing material representative of the ore veins was encountered, so this ore is not represented in Table 11.

of oxidation state of the fluids on gold mobility is further attested to by the fact that carbonatized mafic rocks associated with the two richest gold deposits in the district--the Keystone and Florence mines (average grade of ore veins: about 120 and 300 ppm Au, respectively)--have hematite or hematite + magnetite as their sole or principal opaque Fe-minerals. At the Black, Gold Crater, Albany, Independence, Duchess, and "Anonymous" mines, carbonatized wallrocks carry pyrite or pyrite + magnetite as their opaque minerals, and although the early sulfide veins in these deposits have appropriately low oxidation states, their gold contents, while significant at a few to a few tens of ppm, are on average lower by about a factor of ten than corresponding generations of sulfide veins at the Florence and Keystone mines. These data are ample confirmation that gold may be effectively transported in natural hydrothermal solutions as an oxidized complex such as that proposed by Henley (1973).

THE DOUGLAS Zn-Cu-Pb-Co DEPOSIT

The Douglas mine is located in a gneiss-schist complex in Sec.9, T.14 N., R.79 W. Almost all surface evidence of the mine workings was destroyed when the present road was constructed along the west bank of upper Douglas Creek, but part of the mine dump remains. The deposit was investigated for this study by brief geologic reconnaissance in the immediate vicinity of the

mine and collection of materials from the mine dump for laboratory study.

History and Development of the Douglas Deposit

The claim was originally located as the Morning Star in 1870, when it was worked for gold ore reportedly valued at $25 per ton (Anonymous, 1901, p.7). The property lay idle for a period, but was relocated as the Douglas in 1898 and was worked for a few years on a small scale as a copper deposit.

Curry (1959, p.53) states that a 1903 report by the Medicine Bow Mines Co. gave an account of the mine developments up to that time. According to this report, the deposit was explored by an inclined shaft that in 1903 was 150 feet deep, with 80 feet of drifts and crosscuts. The Medicine Bow Mines Co. reported that "considerable" ore was shipped from the property, but no production figures are available.

The Douglas Orebodies

According to a short and vague contemporaneous report (Anonymous, 1901, p.9), the orebodies encountered at an early stage of mine development consisted of several narrow sulfide seams or lenses a few feet apart dipping along the gneissic foliation. Anonymous (1901, p.9) states that the four "leads" exposed in the mine to that date had widths of 6 inches to 2 feet, 2 to 3 feet, 1 foot, and 7 feet, each terminating along

strike by gradual fadeout and complex interdigitation with silicate gneiss folia. The ore was essentially massive sulfide, described as "the counterpart of that found in the Rambler" (Anonymous, 1901, p.6). Cu carbonates, native copper, chalcocite, chalcopyrite, and "a considerable quantity of cobaltite" were reported as present in amounts of commercial interest.

Mineralogy of the Douglas Deposit

Seventy samples of ore and wallrock were collected from the mine dump and sliced for visual inspection. Thirteen were selected for detailed study by ore microscopy, and seven thin sections of local gneisses and schists were evaluated. Eight ore specimens were assayed by the U. S. Geological Survey by routine analytical methods described previously. Assay data are summarized in Table 22.

Metallic Minerals

The principal primary metallic minerals are magnetite, pyrite, sphalerite, chalcopyrite, and ilmenite, present in the samples studied in variable but generally subequal amounts; in order of decreasing abundance, galena, pyrrhotite, cobaltite, and molybdenite occur as minor components. No precious minerals were seen. Supergene chalcocite, digenite, and covellite replace sphalerite and chalcopyrite to some degree in most specimens.

The metallic minerals occur as monomineralic polycrystalline masses, polymineralic aggregates, granular disseminations, and as intergranular films in a gangue comprised of various combinations of garnet, hornblende, cummingtonite, tremolite, diopside, plagioclase, carbonate, epidote, and quartz (Fig. 21D). No vein quartz or carbonates were seen on the mine dump, and the mineralogy and textures of the ore and gangue indicate the Douglas is not a vein-type deposit.

In polished section, most pyrite has a ragged and pitted appearance, contains scattered specks of pyrrhotite and magnetite, and locally shows well preserved relict cleavage derived from pyrrhotite. Over 95 percent of the pyrite seen in the specimens studied is derived from pyrrhotite by supergene replacement. Fresh pyrrhotite is preserved as common small globules in sphalerite, possibly exsolved, and to a lesser extent as irregular primary grains armored by chalcopyrite. Some ore specimens are essentially medium-grained banded sulfide-oxide-silicate gneisses in which bands rich in pyrite (ex-pyrrhotite) and hornblende are coarsely intercalated with seams comprised of subequal amounts of almandine, sphalerite, magnetite, and ilmenite. Primary pyrite has been observed as fine- to medium-grained euhedra included in massive chalcopyrite.

Table 22. Contents of some precious and base metals in eight assayed ore samples from the Douglas mine. Au determined by fire assay-emission spectrography in seven of eight samples--analysts: R.R. Carlson, E.F. Cooley, T.A. Doerge; one Au and all Cu by atomic absorption--analysts: C.A. Curtis, J.A. Roybol, J. Sharkey, J.G. Viets; Ag, Co, Fe, Mo, Ni, Pb, Ti, Zn by six-step semiquantitative D.C. arc spectroscopy--analysts: R. Babcock, L.B. Breeden, E.F. Cooley, K.J. Curry, G.W. Day, J. Domenico, W.D. Goss, D.J. Grimes, J. Haffty, R. Hopkins, L.B. Riley, and D. Siems, all of U.S. Geological Survey. Elements analyzed but not detected at detection limits shown in parentheses are: Pt (.005 ppm) and Pd (.002 ppm), except one Pd determination of .005 ppm--analysts: Carlson, Cooley, and Doerge, by fire assay-spectrography; and As (200 ppm) and Bi (10 ppm) by semiquantitative spectrochemical analysis, analysts as above. Values for Cu, Fe, and Zn in wt percent; all others in ppm.

	Mean	Range
Ag	33	6-70
Au	2.9	0.2-16
Co	108	70-150
Cu	2.8%	0.3-12%
Fe	17%	15-20%
Mo	12	2-30
Ni	14	10-20
Pb	584	70-2000
Ti	3500	1500-10,000
Zn*	>1%	.15->1%

* The upper determination limit for Zn by semiquantitative spectroscopy is 1 wt percent. Comparison of modal proportions of chalcopyrite and sphalerite suggests the average Zn content of the ore is between 5 and 10 wt percent.

Sphalerite is the most abundant economic mineral. It typically contains extremely abundant rows and randomly disseminated specks of exsolved chalcopyrite (Fig. 21D). The sphalerite is dark maroon-brown, almost black in hand specimen, and has deep red-orange internal reflections, indicating a high Fe content.

Chalcopyrite was the mineral of principal economic interest during mining. Exsolved sphalerite bodies in chalcopyrite have been noted rarely, but most is free of exsolution features of any kind. Chalcopyrite, like sphalerite, shows local evidence of remobilization along cataclastic partings in amphiboles and fractures in garnet, usually without evidence of replacement.

Magnetite is the most abundant metallic mineral, comprising about 5 to 20 volume percent of typical disseminated ore. It occurs mainly as medium-grained, anhedral, equant grains commonly intergrown with ilmenite in polycrystalline clusters, and magnetite locally contains coarse exsolution lamellae of ilmenite. Disseminated specks of magnetite, as well as sulfides, are very common in amphiboles and garnets. Magnetite is particularly prevalent in the mafic almandine-amphibole gneisses that contain most of the disseminated sulfide ore. Primary magnetite is sparse to absent in the few available specimens of essentially massive sulfide. Minute magnetite

granules of apparent supergene origin are sporadically distributed in secondary pyrite.

Ilmenite associates with magnetite in disseminated ores and host rocks and comprises several percent of most disseminated ore samples. Its most typical occurrence is as equant grains intergrown with magnetite in polycrystalline aggregates and intergrown granularly with silicates, occasionally as well formed rhombohedrons. Magnificent myrmekites of ilmenite and almandine occur locally, and hairlike ilmenite rods oriented along cleavage directions in hornblende are not uncommon.

Galena appears in moderate to trace amounts in about a third of the samples studied, usually as granular intergrowths with other sulfides and locally as angular interstitial fillings in aggregates of pegmatitic hornblende. Qualitative microprobe analysis of galena showed no detectable levels of Ag or other foreign elements.

Cobaltite was observed as a few large euhedral grains in nearly massive chalcopyrite-primary pyrite ore and in one instance as a partial replacement of tremolite. Qualitative microprobe analysis of cobaltite show a moderate Fe content, but no significant Ni.

A small amount of molybdenite is present in two of the samples examined, occurring as thin kinked flakes usually enclosed in chalcopyrite or along chalcopyrite-silicate grain contacts.

Mineralogy of the Gangue and Host Rocks

The principal rock types present on the mine dump are garnet amphibolites, calc-silicate gneisses and marbles, and biotite-hornblende-plagioclase-quartz gneisses. Only the garnet amphibolites and calc-silicate rocks seem to be intimately associated with ores.

Typical garnet amphibolites are banded to foliated granoblastic rocks containing subequal amounts of almandine and hornblende or almandine and cummingtonite; apatite is a major accessory ($\pm$ 5 percent), and in some samples quartz is present in moderate amounts. These rocks may contain from a few to 60 percent or more opaque minerals, and in some cases, sulfides and hornblende occur as small veinlets crosscutting gneissic foliation. Hornblende is fine- to medium-grained, equant to prismatic, and blue-green, especially along grain margins. Cummingtonite takes the place of hornblende in a few almandine-quartz amphibolites, occurring as neutral-colored, prismatic grains with characteristic polysynthetic twinning. The garnet is pale pink in thin section, and occurs as medium-grained equant poikiloblastic anhedra with more or less abundant inclusions of opaques.

The calc-silicate units include: 1) granoblastic, massive, medium-grained rocks composed entirely of tremolite, diopside and a full complement of the common opaque minerals; 2) schists

comprised of tremolite-actinolite (weakly colored), calcite, oligoclase-albite, epidote, and chlorite in subequal amounts, with accessory apatite and abundant oxide and sulfide minerals; and 3) calc-silicate marble with major calcite and tremolite-actinolite, subordinate quartz and epidote, accessory apatite, and 10 to 60 percent or more of clustered and disseminated opaques. Epidote and tremolite are exceedingly poikiloblastic with inclusions of quartz, calcite, and ore minerals. The latter two calcite-bearing assemblages display upper greenschist facies compatibilities; the diopside-tremolite and mafic gneisses belong to epidote amphibolite and incompletely retrograded almandine amphibolite metamorphic facies.

The country rocks near the Douglas deposit are gneisses comprised mainly of quartz, andesine/oligoclase, biotite, hornblende, and epidote in slightly varying proportions. The gneisses are similar in character to those enclosing the Keystone and "Anonymous" deposits, but generally of a rather more felsic character.

Considerations Regarding Origin of the Douglas Deposit

A small fault trends generally westward toward the vicinity of the Douglas mine (Fig. 2), but the fault is not apparent in surface exposures near the mine (McCallum, unpub.). The ore is in some instances enclosed in greenschist facies rocks,

and local veinlets and pegmatitic clusters of amphibole suggest metamorphic recrystallization under volatile-rich conditions, but there is no evidence of hydrothermal alteration in the ordinary sense of the term. Although silicates (especially garnet) and oxides show weak fracturing locally, none of the ore or enclosing rock examined from the Douglas mine shows strong cataclastic effects.

With the exception of exsolution textures and local evidence of late remobilization of chalcopyrite, sphalerite, and hornblende, there is comparatively little evidence of a crystallization sequence in intergrowths of metallic minerals with each other and with silicates. All the major metallic and silicate minerals in the ore show mutual inclusion relations. Local evidence of paragenetic diachronism is seen rarely as chalcopyrite rims on and replacements of pyrrhotite, and chalcopyrite and cobaltite replacements of tremolite-actinolite. The general lack of a recognizable deposition sequence, the generally high metamorphic grade of the silicate mineral assemblage enclosing the ore minerals, and the prevalence of (ex-) pyrrhotite and virtual absence of primary pyrite (except where pyrite cubes are thickly armored by chalcopyrite) are strong evidence that the ores were metamorphosed at garnet amphibolite grade along with their enclosing rocks. (The epidote-amphibolite and greenschist facies assemblages appear

to represent superposed retrograde effects.) The Douglas deposit is therefore at least as old as the ± 1.75 m.y. orogeny and is the oldest of the investigated mineral deposits in the district.

These considerations and the fact that the ore is associated with very iron-rich and calcic lithologies that are apparently local in extent and atypical of the gneissic complex suggest that the Douglas deposit may be a small metamorphosed exhalative massive sulfide body. The major ore metal assemblage--Zn-Cu-Pb--and primary ore mineralogy--magnetite, pyrrhotite, sphalerite, chalcopyrite, ilmenite, galena, and pyrite, in about that order of abundance--are totally unlike any other known deposits in the district, and are compatible with a metamorphosed massive sulfide hypothesis.

The general characteristics of syngenetic stratabound massive sulfide deposits have been reviewed by Fryer and Hutchinson (1976) and Mannard (1973). Sedimentary terranes containing massive sulfide deposits consist mainly of siltstones, shales, and graywackes, and, with a few notable exceptions, the sedimentary hosts to the massive sulfides contain at least a minor volcanic component. One of the most important results of investigations of massive sulfide deposits in recent years has been the recognition that most of these ores are closely associated, both spatially and genetically with siliceous, calcic (sulfate

or carbonate), and iron-rich (exhalative iron formation) chemical sediments. In many cases the ores and chemical sediments overlie mafic volcanics.

Effects of thermal metamorphism on pyritic volcanogenic massive sulfide ores have been discussed by Bachinski (1976) with reference to the cupriferous iron sulfide type deposits in Newfoundland. Bachinski (1976) found that pyritic ores in the low-grade greenschist facies are represented by pyrrhotite- and magnetite-bearing ores in the hornblende-hornfels facies. Originally pyritic ores have undergone desulfurization with resultant conversion of pyrite to pyrrhotite. The sulfur released by this process has remained in the system and reacted with Fe-bearing silicates of the gangue. At low metamorphic grades, the gangue minerals associated with sulfides are relatively rich in Fe and poor in Mg, but the reverse is true in high grade rocks. Magnetite and pyrrhotite are important reaction products during prograde metamorphism of the Fe-rich silicates present in low-grade facies (Bachinski, 1976, p.443).

There are few indications that reaction products of high grade metamorphism in the Douglas deposit have developed in situ, and it seems likely that sulfur and chalcophile metals have undergone significant short-range redistribution. Very abundant magnetite and pyrrhotite inclusions in amphiboles and garnet may be evidence of the latest effects of prograde

decomposition and sulfurization of originally Fe-rich silicates. One can perhaps speculate not too unreasonably that rocks comprised largely of magnetite, almandine, cummingtonite, and quartz may be metamorphosed equivalents of cherty iron formation; garnet-hornblende amphibolites may be metamorphic representatives of mafic volcanics, and calc-silicate-sulfide rocks may represent calcic chemical sediments of fumarolic origin.

In a general survey of characteristics of Precambrian mineralization in the Sourthern Rocky Mountains, Giles (1976) discusses the occurrences of dozens of small Zn-Pb-Cu sulfide deposits--in a number of cases with associated iron formation--distributed throughout the metasedimentary-metavolcanic terranes of central New Mexico and central and northern Colorado. Giles (1976, p.129) expresses the opinion that the majority of these Zn-Pb-Cu occurrences display features consistent with interpretation as metamorphosed volcanogenic massive sulfide deposits.

The absence of exposed plutonic igneous bodies in the immediate vicinity of the deposit and the fact that the calcic lithologies associated with the ore are apparently not widespread do not lend support to a contact metasomatic origin of the deposit by igneous intrusion into lime-rich sediments.

Although not conclusive, the available evidence lends strong support to the interpretation that the Douglas deposit formed by metamorphism of an exhalative sedimentary massive sulfide deposit.

CONCLUSIONS

(1) All investigated epigenetic deposits in the central Medicine Bow Mountains are thought to have formed during a single, protracted, regional thermal-tectonic disturbance.

(2) Ore-forming solutions are believed to be derived from metamorphic fluids collected in shear/fault zones by diffusion out of wallrocks over pressure gradients that were initiated during episodes of regional cataclastic activity. Petrographic and chemical analytical evidence support the interpretation that mineral matter now in these deposits had its ultimate source in the wallrocks, although much of it may have migrated for some distance vertically and laterally along fault channels before collecting and precipitating in dilatant portions of shear zones and fault intersections.

(3) Critical variables regulating the development of specific ore mineral assemblages in these diverse deposits are seen to be:

(a) The lithologies of the host rock environment, with PGE, Au, Ag, Cu, Ni, Zn, and Fe being contributed principally by mafic source rocks, and Pb (and significant Zn) being derived mainly from granitic igneous rocks and pelitic schists.

(b) Variations in pH and fugacities of CO_2 and O_2 in ore solutions, as reflected by presence or absence of carbonatization alteration of associated mafic rocks and oxidation state of ore and altered wallrock mineral assemblages. Gold is present in significant concentrations only in those deposits in which source rocks are hydrothermally carbonatized. Au has been mobile in CO_2-rich, oxidized solutions and precipitated from reduced ore fluids. Wallrocks associated with PGE-rich deposits do not show carbonitization alteration, and PGE have been precipitated from reduced ore solutions. Those deposits devoid of significant Au or PGE contents have oxidized hypogene ore mineral assemblages, regardless of the character of wallrock alteration.

(4) The high concentration of platinum-group elements in the New Rambler deposit is testimony to the effectiveness of hydrothermal systems in transport and concentration of these metals, a fact of general significance that is receiving belated recognition.

(5) In various stages of the New Rambler deposit's evolution, partitioning of platinoid metals according to their disparate solubilities has been apparent. The relative proportions of PGE in the ore compared to those in metagabbroic host indicates strong solubility fractionation during leaching of host rocks; relative to mafic host rocks, Pd has been

upgraded in sulfide ore by a factor of about 7500, Pt by 400, and other platinoids by probably less than 100. Contrast in geochemical character is well displayed in the weathering regime by the variation of Pd/Pt from approximately 17 to 16 to 3.1 to 2.7 in the chalcopyrite-secondary pyrite, supergene Cu sulfide, oxide ore, and gossan horizons, respectively. The distribution of metal values in the weathered profile reflects appreciable leaching of Pd in the strongly oxidized levels. A more than two-fold enrichment of Pt in oxide relative to sulfide ore and nearly ten-fold enrichment of Rh in oxide relative to sulfide ore may reflect supergene solution activity. Ir and Ru values rise significantly at the weathered outcrop.

(6) Platinum and palladium in the New Rambler deposit are believed to occur in sulfide ore principally as discrete platinoid minerals. A significant proportion of the Pt occurs in solid solution in Pd minerals, mainly merenskyite and michenerite. Rh, Ru, Ir, and Os are probably tied up mostly as trace substituents in Pt and Pd minerals.

(7) Zn-Cu-Pb mineralization at the Douglas mine occurs as massive sulfide lenses and granular sulfide disseminations in garnet amphibolites and calc-silicate rocks. The occurrence of titaniferous magnetite and pyrrhotite as the major metallic iron minerals and the general lack of a

crystallization sequence in the ore, as evidenced by mutual inclusion relations between all major metallic and silicate minerals, are strong evidence that the ore was metamorphosed to almandine amphibolite grade along with its enclosing rocks. Evidence that the deposit is a metamorphosed syngenetic, exhalative, sedimentary massive sulfide body is in part the characteristic Zn-Cu-Pb metal assemblage, but more importantly the association of the ore with very Fe-rich and calcic lithologies atypical of the gneissic complex, and apparently limited in spatial extent to the vicinity of the orebody. These unusual rock types are interpreted as the metamorphosed equivalents of Fe-rich and calcic chemical sediments of the types characteristically associated with stratabound massive sulfide ores.

(8) Mineragraphic and electron investigations of ore deposits in the central Medicine Bow Mountains have resulted in the discovery of at least six new minerals and recognition of two species (villamaninite and temagamite) known previously only from a single locality. The new minerals include unnamed $(Cu,Fe,Ni,Co)_2S_2$, unnamed $(Cu,Ni,Fe,Co)_6S_7$, unnamed $Pd_5(Te,Bi,Sb)_2$, unnamed (Pd,Pt)(Te,Bi,Sb), and unnamed $Pd(Bi,Te)O_3$(?) or $Pd_2BiTeO_4 \cdot 2H_2O$(?), all from the New Rambler mine, and an unnamed Fe-Cr-Ni alloy or intermetallic compound from a quartz vein occurrence at the Black mine. Further study of previously

unrecognized compositional and structural complexities in merenskyites may result in definition of at least two additional closely related mineral species.

APPENDIX

Analytical Techniques Used in Electron Microprobe Analyses

All electron microprobe analyses were performed by the writer on an Applied Research Laboratories instrument in the laboratory of G. A. Desborough, U. S. Geological Survey, Denver, Colorado. Desborough also gave helpful instruction in performing the analyses and methods of data correction.

All mineral grains analyzed are contained in their natural matrix; no artificial concentration methods were employed. Grains to be analyzed were selected during examination of polished ore specimens by reflected light microscopy. Approximately one-third of the polished sections analyzed were mounted in fused bakelite. The remainder were mounted in cold-setting epoxy resin. Samples mounted in fused bakelite showed no visible artificial thermal effects, and gave analytical results consistent with those of samples mounted in cold setting resin. Excellent polished surfaces were obtained by final polishing with 1 micron diamond paste on cloth-covered laps followed by very light-pressure buffing with a suspension of chrome oxide powder in water on a felt-covered lap. All samples were freshly buffed in this manner prior to analysis.

All platinum-group minerals and other minerals of questionable identity were first analyzed using the energy dispersive multi-channel analyzer accessory to the electron microprobe. This instrument gives simultaneous qualitative determinations for all elements present in more than trace elements. Microprobe analyses of platinoid minerals were performed at an accelerating voltage of 10 KV and at a constant beam current of 15 nanoamperes. Pt, Pd, Te, Bi, Sb, and As were analyzed simultaneously, and in the case of temagamite (Pd_3HgTe_3), Hg and Pt were determined in separate passes using wavelength dispersive analysis to avoid Mα peak interferences. Ni was analyzed at 15 KV in about 20 grains of Pd-Bi-Te minerals, but was not detected in any (Ni detection limit $\pm$ 0.1 wt percent). Some sperrylites were analyzed in two passes, for the above listed elements on the first pass, and for Pt, Rh, and As on the second pass. Five to eight point analyses with a counting interval of 13 seconds each were made on each grain.

Standards used in microprobe analyses of platinoid minerals were synthetic $PtTe_2$ (moncheite), $(Pd,Ni)Te_2$ (merenskyite), PdBiTe (michenerite), $PdBi_2$, $(Pd,Cu)Sb_5$, and $Pd_5(As,Sb)_2$, supplied by L. J. Cabri; and synthetic HgTe, Pt-Rh and Ir-Rh alloys, and analyzed natural (Sudbury) sperrylite ($PtAs_2$), orpiment (As_2S_3), stibnite (Sb_2S_3), and cinnabar (HgS), all supplied by G. A. Desborough. The standards used are

sufficiently similar in composition to most minerals analyzed that corrections for absorption are unnecessary. Data were corrected by hand for background and atomic number, using graphical interpolation between count data of appropriate standards to obtain correction factors.

Microprobe analyses of Cu-Ni-Fe-Co-S minerals from the New Rambler mine were performed at an accelerating voltage of 15 KV, constant beam current of 10 nanoamperes, and a focussed beam of 1-2 microns diameter. Ni and Co were determined simultaneously with Ni or Co on each pass. An average of seven 12-second point analyses were made on each grain on each pass, except villamaninite, which, due to minute grain size, was analyzed at three to five points per grain. Standards employed were analyzed natural pyrite, chalcopyrite, and millerite (NiS), and synthetic Co_9S_8, Ni_3S_2, (Fe,Ni)S with 6 and 10 wt percent Ni, and (Fe,Co)S with 4 wt percent Co. The standards used are sufficiently similar in composition to the samples that corrections for absorption were not necessary, as indicated by the satisfactory totals of the analyses. Raw data were corrected by hand for background and atomic number as described above.

Au-Ag-Cu alloys were analyzed at 15 KV, with a constant beam current of 15 nanoamperes, with five to eight point analyses per grain. Standards used were synthetic alloys

prepared by G. A. Desborough, consisting of pure Au and Ag; Au-Ag alloys containing 5.74, 27.65, 45.10, and 83.13 wt percent Ag; and Au-Ag-Cu alloys containing 0.66 and 14.37 wt percent Ag, and 0.99 and 16.17 wt percent Cu. No data corrections are required.

The Fe-Cr-Ni-Co metal from the Black mine was analyzed qualitatively using the multichannel analyzer, followed by quantitative analysis at 15 KV and constant beam current at 15 nonoamperes. Standards used were pure Fe Ni metals, Fe-Ni alloys containing 29.30 and 7.50 wt percent Ni, synthetic Fe_3O_4, Co_9S_8, (Fe,Co)S containing 4.09 and 0.53 wt percent Co, and natural (Stillwater) chromites containing 33.66 and 25.04 wt percent Cr. Corrections for background and atomic number were done by hand. The calculated results are preliminary, and the data need additional corrections for absorption and fluorescence.

Analyses of cobaltite, gersdorffite, and pyrites containing Ni, Co, and As were done in two passes at 15 KV and a beam current of 10 nanoamperes. Fe, Ni, As, and S were determined simultaneously in one pass, and Fe, Co, As, and S on the second pass. Standards for cobaltite and gersdorffite were As_2S_3 for As and S, and synthetic (Fe,Co)S with 4.09 wt percent Co and synthetic Ni_3S_2 as standards for Fe, Co, and Ni, respectively. Associated pyrite was analyzed using an

analyzed pure natural pyrite as standards for Fe and S, and the above standards for As, Co, and Ni. The data were corrected by hand for background. Corrections for atomic number, absorption, and fluorescence were done by computer using the program EMPADR VII of Rucklidge and Gasparrini (1969).

Bournonite was analyzed qualitatively for foreign elements by multichannel analyzer and none were found. The quantitative analysis was done at 15 KV using synthetic bournonite as a standard. No data corrections are required.

Wittichenite was analyzed qualitatively by multichannel analyzer, and only Cu, Bi, and S were detected. The analysis was done at an accelerating voltage of 15 KV and beam current of 20 nanoamperes. Standards were analyzed natural stibnite (Sb_2S_3) for S, synthetic $AgBiS_2$ for Bi, and synthetic $PbCuSbS_3$ for Cu. Data were corrected for background by hand, and for atomic number, absorption, and fluorescence by the computer program Magic IV of Colby (1972).

Tetrahedrite and friebergite were analyzed qualitatively on the multichannel analyzer and quantitatively in two passes. Cu, Fe, and Zn were determined in one pass at 15 KV and 10 nanoamperes, and Ag, Sb, As, and S were determined on the second pass at 7 KV and 20 nanoamperes. Reduced accelerating voltage was used on the second pass to minimize absorption effects. Standards used for Zn and Fe were synthetic (Zn,Fe)S

containing 26.98 wt percent Fe and synthetic $PbCuSbS_3$ for Cu. Sb_2S_3 was used for Sb and S, As_2S_3 for As, and Ag_2S for Ag. Data were corrected for background by hand, and for atomic number, absorption, and fluorescence using the computer program Magic IV of Colby (1972).

REFERENCES

Anhaeusser, C. R., 1976, The nature and distribution of Archean gold mineralization in southern Africa: Minerals Sci. Eng., v.8, p.46-84.

Anonymous, 1896, Albany County, Wyoming, mineral resources: The Laramie Mining and Stock Exchange, Laramie, Wyo., 51p.

Anonymous, 1900, Great mineral belt encircling Laramie, Wyoming: Laramie, Wyo., 9p. (copy in Geol. Survey, Wyo. files).

Bachinski, D. J., 1976, Metamorphism of cupriferous iron sulfide deposits, Notre Dame Bay, Newfoundland: Econ. Geol., v.71, p.443-452.

Barnes, H. L., and Czamanske, G. K., 1967, Solubilities and transport of ore minerals, in Barnes, H. L., ed., Geochemistry of Hydrothermal Ore Deposits: New York, Holt, Rinehart and Winston, p.334-381.

Bartram, G. D., and McCall, G. J. H., 1971, Wallrock alteration associated with auriferous lodes in the Golden Mile, Kalgoorlie: Geol. Soc. Australia Spec. Pub. 3, p.191-199.

Beeler, H. C., 1905, The Gold Crater mine: Unpub. Rept. of the Wyoming State Geologist, no.64, 6p. (Geol. Survey Wyo. files).

_____, 1906, Mineral and allied resources of Albany County, Wyoming and vicinity: Laramie, Wyoming, The Laramie Republican Company, 80p.

_____, 1907, The Hamilton mine: Unpub. Rept. of the Wyoming State Geologist, no.93, 4p.

Boyle, R. W., 1961, The geology, geochemistry and origin of the gold deposits of the Yellowknife District: Geol. Survey of Canada Mem. 310, 193p.

_____, Alexander, W. M., and Aslin, G. E. M., 1975, Some observations on the solubility of gold: Canada Geol. Survey Paper 75-24, 6p.

Cabri, L. J., 1972, The mineralogy of the platinum-group elements: Minerals Sci. Eng., v.4, p.3-29.

_____, Hall, S. R., Szymanski, J. T., and Stewart, J. M., 1973, On the transformation of cubanite: Can. Mineral., v.12, p.33-38.

Cameron, E. N., and Desborough, G. A., 1964, Origin of certain magnetite-bearing pegmatites in the eastern part of the Bushveld Complex, South Africa: Econ. Geol., v.59, p.197-225.

Colby, J. W., 1972, Magic IV--A computer program for quantitative electron microprobe analysis: Papers with Program, Electron Probe Analysis Soc. American Tutorial Sess., 7th Natl. Conf. on Electron Probe Analysis, San Francisco, July 1972, p.Ba1-Ba16.

Cooley, E. F., Curry, K. J., and Carlson, R. R., 1976, Analysis for platinum group metals and gold by fire-assay emission spectrography: Applied Spectroscopy, v.30, p.52-56.

Cotton, F. A., and Wilkinson, Geoffrey, 1972, Advanced Inorganic Chemistry, 3d ed.: New York, John Wiley and Sons, 1145p.

Cousins, C. A., 1973, Notes on the geochemistry of the platinum group elements: Geol. Soc. South Africa Trans., v.76, p.77-81.

_____, and Vermaak, C. F., 1976, The contribution of southern African ore deposits to the geochemistry of the platinum group metals: Econ. Geol., v.71, p.287-305.

Craig, J. R., and Scott, S. D., 1974, Sulfide phase equilibria, in Ribbe, P. H., ed., Mineral. Soc. America short course notes, sulfide mineralogy, v.1, p.CS-1 to CS-110.

Crocket, J. H., 1969, Platinum metals, in Wedepohl, K. H., ed., Handbook of Geochemistry, v.II/1: Berlin, Springer-Verlag, p.78-1 to 78-0-2.

_____, 1974, Gold, in Wedepohl, K. H., ed., Handbook of Geochemistry, v.II/4: Berlin, Springer-Verlag.

Curry, D. R., 1959, Geology of the Keystone area, Albany County, Wyoming: Unpub. Master's Thesis, Univ. Wyoming, 64p.

_____, 1965, The Keystone gold-copper prospect area, Albany County, Wyoming: Wyoming Geol. Survey Prelim. Rept. 3, 12p.

Desborough, G. A., and Czamanski, G. K., 1973, Sulfides in eclogite nodules from a kimberlite pipe, South Africa, with comments on violarite stoichiometry: Am. Mineral., v.58, p.195-202.

Eales, H. V., 1961, Fineness of gold in some southern Rhodesian mines: Trans. Instn. Min. Metall., v.71, p.49-73.

El Gorsey, A., and Kullerud, G., 1969, Phase relations in the system Cr-Fe-S, in Millman, P. M., ed., Meteorite Research: Dordrecht, Holland, D. Reidel Pub. Co., p.638-647.

Ellis, A. J., 1967, The chemistry of some explored geothermal systems, in Barnes, H. L., ed., Geochemistry of Hydrothermal Ore Deposits: New York, Holt, Rinehart, and Winston, p.465-514.

_____, 1968, Natural hydrothermal systems and experimental hot-water/rock interaction: Reactions with NaCl solutions and trace metal extraction: Geochim. Cosmochim. Acta, v.32, p.1356-1363.

Emmons, S. F., 1903, Platinum in copper ores in Wyoming: U. S. Geol. Survey Bull. 213, p.94-97.

Emmons, W. H., 1937, Gold Deposits of the World: New York, McGraw-Hill.

Ewers, W. E., 1972, Nickel-iron exchange in pyrrhotite: Proc. Aust. Inst. Min. Met., no.241, p.19-25.

Fryer, B. J., and Hutchinson, R. W., 1976, Generation of metal deposits on the sea floor: Can. Jour. Earth Sci., v.13, p.126-135.

Fuchs, W. A., and Rose, A. W., 1974, The geochemical behavior of platinum and palladium in the weathering cycle in the Stillwater Complex, Montana: Econ. Geol., v.69, p.332-346.

Fyfe, W. S., and Henley, R. W., 1973, Some thoughts on chemical transport processes, with particular reference to gold: Minerals Sci. Eng., v.5, p.295-303.

Genkin, A. D., 1959, Conditions of occurrence and features of the composition of minerals of the platinum group in ores of the Noril'sk deposit: Geol. Rudn. Mestorezhd., no.6, p.74-84 [in Russian].

_____, 1968, Minerals of the platinum metals and their associations in copper-nickel ores of the Noril'sk deposit: Moscow, Nauka, 106p. [in Russian].

_____, Distler, V. V., Laputina, I. P., and Filimonova, A. A., 1973, Geochemistry of palladium in copper-nickel ores: Geochemistry Internat., v.10, p.1007-1013.

Giles, D. L., 1976, Precambrian mineralization in the Southern Rocky Mountain region, in Woodward, L. A., and Northrop, S. A., eds., Tectonics and mineral resources of south-western North America: New Mexico Geol. Soc. Spec. Pub. no.6, p.127-131.

Ginzburg, V. L., and Rogover, G. B., 1961, Regularities in the distribution of nonferrous and precious metals in principal ore minerals and silicates of the Noril'sk deposits: Internat. Geology Rev., v.3, p.917-926.

Goldstein, J. I., Axon, H. J., and Yen, C. F., 1972, Metallic particles in the Apollo 14 lunar soil: Proc. Third Lunar Sci. Conf. (Suppl. 3, Geochim. Cosmochim. Acta), v.1, p.1037-1064.

Häkli, T. A., Hänninen, E., Vuorelainen, Y., and Papunen, Heikki, 1976, Platinum-group minerals in the Hitura nickel deposit, Finland: Econ. Geol., v.71, p.1206-1213.

Hedge, C. E., Peterman, Z. E., and Braddock, W. A., 1967, Age of the major Precambrian regional metamorphism in the northern Front Range, Colorado: Geol. Soc. America Bull., v.78, p.551-557.

Helgeson, H. C., 1969, Thermodynamics of hydrothermal systems at elevated temperatures and pressures: Amer. Jour. Sci., v.267, p.729-804.

_____, 1970, A chemical and thermodynamic model of ore deposition in hydrothermal systems: Mineral. Soc. America Spec. Pap. 3, p.155-186.

Henley, R. W., 1973, Solubility of gold in hydrothermal chloride solutions: Chem. Geol., v.11, p.73-87.

Hess, F. L., 1926, Platinum near Centennial, Wyoming: U. S. Survey Bull. 780-C, p.127-135.

Hills, F. A., Gast, P. W., Houston, R. S., and Swainbank, I. G., 1968, Precambrian geochronology of the Medicine Bow Mountains, southeastern Wyoming: Geol. Soc. America Bull., v.79, p.1757-1783.

Hoffman, Eric, and MacLean, W. H., 1976, Phase relations of michenerite and merenskyite in the Pd-Bi-Te system: Econ. Geol., v.71, p.1461-1468.

Holland, H. D., 1967, Gangue minerals in hydrothermal deposits, in Barnes, H. L., ed., Geochemistry of Hydrothermal Ore Deposits: New York, Holt, Rinehart, and Winston, p.382-436.

Houston, R. S., and others, 1968, A regional study of rocks of Precambrian age in that part of the Medicine Bow Mountains lying in southeastern Wyoming--with a chapter on the relationship between Precambrian and Laramide structure: Geol. Survey Wyoming Mem. 1, 167p.

Hurlbut, C. S., 1971, Dana's manual of mineralogy, 18th ed.: New York: John Wiley and Sons, 579p.

Kasteler, J. I., and Frey, Eugene, 1949, Diamond drilling at the Rambler copper mine, Albany County, Wyo.: U. S. Bur. Mines Rept. Inv. 4544, 6p.

Keays, R. R., and Crocket, J. H., 1970, A study of precious metals in the Sudbury nickel irruptive ores: Econ. Geol., v.65, p.438-450.

_____, and Davison, R. M., 1976, Palladium, iridium, and gold in the ores and host rocks of nickel sulfide deposits in Western Australia: Econ. Geol., v.71, p.1214-1228.

_____, and Kirkland, M. C., 1972, Hydrothermal mobilization of gold from copper-nickel sulfides and ore genesis at the Thomson River copper mine, Victoria, Australia: Econ. Geol., v.67, p.1263-1275.

_____, and Scott, R. B., 1976, Precious metals in ocean-ridge basalts: implications for basalts as source rocks for gold mineralization: Econ. Geol., v.71, p.705-220.

Kemp, J. F., 1904, Platinum in the Rambler mine, Wyoming: U. S. Geol. Survey Mineral Resources of the U. S., 1902, p.244-250.

Kingston, G. A., 1966, The occurrence of platinoid bismuthotellurides in the Merensky Reef at Rustenburg platinum mine in the western Bushveld: Mineral. Mag., v.35, p.815-835.

Knight, S. H., 1942, Known mineral resources of Albany County, Wyoming, Part I, The metallic minerals: Unpub. report prepared for the Albany County Council of Defense, 24p. (copy in Geol. Survey Wyo. files).

Knopf, A., 1929, The Mother Lode system of California: U. S. Geol. Survey Prof. Paper 157, 88p.

Kullerud, Gunnar, Yund, R. A., and Moh, G. H., 1969, Phase relations in the Cu-Fe-S, Cu-Ni-S, and Fe-Ni-S systems, in Wilson, H. D. B., ed., Magmatic ore deposits: Econ. Geol. Monogr. 4, p. 323-343.

Lindgren, Waldemar, 1905-06, Metasomatic processes in the gold deposits of Western Australia: Econ. Geol., v.1, p.530-544.

Lovering, T. G., 1972, Jasperiod in the United States --its characteristics, origin, and economic significance: U.S. Geol. Survey Prof. Paper 710, 164p.

Macgregor, A.M., 1951, The primary source of gold: S. Afr. Jour. Sci., v. 47, p. 157-161.

Mannard, G.W., 1973, The syngenetic massive sulfide deposits: A. I. M. E. preprint no. 73-S-53, paper presented at 1973 A. I. M. E. Annual Meeting, 31p.

Mason, Brian, and Graham, A.L., 1970, Minor and trace elements in meteoritic minerals: Smithsonian Contrib. Earth Sci., no. 3, 17p.

McCallum, M.E., 1964, Petrology and structure of the Precambrian and post-Mississipian rocks of the east-central portion of the Medicine Bow Mountains, Albany and Carbon Counties, Wyoming: Unpub. Ph.D. thesis, Univ. Wyoming, 164p.

_____, 1968, The Centennial Ridge gold-platinum district, Albany County, Wyoming: Wyoming Geol. Survey Prelim. Rept. 7, 13p.

_____, and Orback, C.J., 1968, The New Rambler copper-gold-platinum district, Albany and Carbon Counties, Wyoming: Wyoming Geol. Survey Prelim. Rept. 8, 12p.

_____, 1974, Dedolomitized marble lenses in shear zone tectonites, Medicine Bow Mountains, Wyoming: Jour. Geology, v.82, p.473-487.

_____, Loucks, R.R., Carlson, R.R., Cooley, E.F., and Doerge, T.A., 1975, Platinum metals associated with hydrothermal copper ores of the New Rambler mine, Medicine Bow Mountains, Wyoming [abs.]: SEG International Platinum Symposium, Denver.

_____,1976, Platinum metals associated with hydrothermal copper ores of the New Rambler mine, Medicine Bow Mountains, Wyoming: Econ. Geol., v. 71, p.1429-1450.

McKinstry, H.E., 1948, Mining Geology: Englewood Cliffs, N.J., Prentice-Hall, 680p.

Mertie, J.B., Jr., 1969, Economic geology of the platinum metals: U.S. Geol. Survey Prof. Paper 630. 120p.

Meyer, Charles, and Hemley, J.J., 1967, Wallrock alteration, in Barnes, H.L., ed., Geochemistry of Hydrothermal Ore Deposits: New York, Holt, Rinehart, and Winston, p. 166-235.

Mihalik, P., Jacobsen, J.B.E., and Hiemstra, S.A., 1974, Platinum-group minerals from a hydrothermal environment: Econ. Geol., v.69, p.257-262.

Mitcham, T.W., 1974, Origin of breccia pipes: Econ. Geol., v.69, p.412-413.

Moiseenko, V.G., and Mikhailov, M.A., 1970, Redistribution of gold during sediment accumulation and metamorphism: Vopr. Geol. Geokhimii Metallogenii Sev.-Zap. Sektora Tikhookean Posaya, p.198+ [in Russian].

Naldrett, A.J., Craig, J.R., and Kullerud, Gunnar, 1967, Pentlandite exsolution in iron-nickel sulfide ores (abs.): Geol. Soc. America Spec. Paper 101,p.149.

_____, and Cabri, L.J., 1976, Ultramafic and related rocks: their classification and genesis with special reference to the occurence of nickel sulfides: Econ. Geol., v.71, p.1131-1158.

Ohmoto, Hiroshi, 1972, Systematics of sulfur and carbon isotopes in hydrothermal ore deposits: Econ. Geol., v.67, p.551-578.

Orback, C.J., 1958, Geology of the New Rambler mine area, Albany County, Wyoming: Wyoming Geol. Survey open file rept., 14p.

Page, N.J., Riley, L.B., and Haffty, Joseph, 1972, Vertical and lateral variation of platinum, palladium, and rhodium in the Stillwater Complex, Montana: Econ. Geol., v.67, p.915-923.

Petrov, B.V., Krendelev, F.P., Bobrov, V.A., and Tsimbalist, V.G., 1972, Behavior of radioactive elements and gold during metamorphism of the Patmosk highland sedimentary rocks: Geokhumiya, v.8, p.947.

Ramdohr, Paul, 1960, Ore Minerals and Their Intergrowths: London, New York, Pergamon Press, 1174p.

Ramirez, Octavio, 1971, Petrology and structure of the Precambrian metaigeneous sequence in the Savage Run Creek area, Carbon County, Wyoming: Unpub. M. Sc. Thesis, Colorado State University, 117p.

Roedder, Edwin, 1972, Data of Geochemistry, Chapter JJ, Composition of fluid inclusions: U.S. Geol. Survey Prof. Paper 440-JJ, 164p.

Rucklidge, J.C., and Gasparrini, E.L., 1969, Electron microprobe and analytical data reduction (EMPADR VII): Dept. Geology, Univ. Toronto, Ontario.

Seward, T.M., 1973, Thio complexes of gold in hydrothermal ore solutions: Geochim, Cosmochim-Acta, v. 137, p.379-400.

Stumpfl, E.F., 1974, The genesis of platinum deposits: further thoughts: Minerals Sci. Eng., v.6, p.120-141.

Sugaki, A., Shima, H., Kitakaze, A., and Harada, H., 1975, Isothermal phase relations in the system Cu-Fe-S under hydrothermal conditions at 350°C and 300°C: Econ. Geol., v. 70, p.806-823.

Taylor, L.A., 1969, Low temperature phase relations in the Fe-S system: Carn. Inst. Wash. Yb. 68 (1968-1969), p. 259-270.

Theobald, P.K., Jr., and Thompson, C.E., 1968, Platinum and associated elements of the new Rambler mine and vicinity, Albany and Carbon Counties, Wyoming: U.S. Geol. Survey Circ. 607, 14p.

Till, Roger, 1974, Statistical Methods for the Earth Scientist: New York, Wiley & Sons, 154p.

Toulmin, Priestly, III, and Clark, S.P., Jr., 1967, Thermal aspects of ore formation, in Barnes, H.L., ed., Geochemistry of Hydrothermal Ore Deposits: New York Holt, Rinehart and Winston, p. 437-464.

Travis, G.A., Keays, R.R., and Davidson, R.M., 1976, Palladium and iridium in the elevation of nickel gossans in Western Australia: Econ. Geol., v.71, p. 1229-1243.

_____, Woodall, R., and Bartum, G.D., 1971, The geology of the Kalgoorlie gold field: Geol. Soc. Australia Spec. Pub. 3, p. 175-190.

U.S. Bureau of Mines, 1942, Rambler Mine, Albany County, Wyoming: U.S. Bur. Mines War Minerals Rept. 17,7p.

Vermaak, C.F., 1976, The Merensky Reef--thoughts on its environment and genesis: Econ. Geol., v.71, p. 1270-1298.

Viljoen, M.J., Bernasconi, A., van Coller, N., Kinlock, E., and Viljoen, R.P., 1976, The geology of the Shangani nickel deposit, Rhodesia: Econ. Geol., vol. 71, p.76-95.

Viljoen, R.P., Saager, R., and Viljoen, M.J., 1970, Some thoughts on the origin and processes responsible for the concentration of gold in the early Precambrian of southern Africa: Mineral. Deposita, v.5, p.164-180.

Watmuff, I.G., 1974, Supergene alteration of the Mt. Windarra nickel sulfide ore deposit, Western Australia: Mineral. Deposita, v.9, 0.199-221.

Wedepohl, K.H., 1972, Copper, section 29-F, Behavior in magmatogenic processes, in Wedepohl, K.H., ed., Handbook of Geochemistry, v. III/2: Berlin, Springer-Verlag, p. 29-F-1 to 29-F-3.

_____, 1972, Zinc, section 30-G, Behavior in hydrothermal processes, in Wedepohl, K.H., ed., Handbook of Geochemistry, v. II/2: Berlin, Springer-Verlag, p.30-G-1 to 30-G-7.

Wiessburg, B.G., 1970, Solubility of gold in hydrothermal alkaline sulfide solutions: Econ. Geol., v.65, 1970, p. 551-556.

White, D.E., 1974, Diverse origins of hydrothermal ore fluids: Econ. Geol., v. 69, p. 954-973.

Winkler, H.G. F., 1974, Petrogenesis of Metamorphic Rocks, 3d ed., New York, Springer-Verlag, 320p.

Yund, R.A., and Kullerud, Gunnar, 1966, Thermal stability of assemblages in the Cu-Fe-S system: Jour. Petrology, v.7, p.454-588.

Yushko-Zakharova, O. Ye., Ivanov, V.V., Razina, I.S., and Chernyayav, L.A., 1967, Geochemistry of platinum metals: Geochemistry Internat., v.4, p.1106-1118.

Zak, S.I., and Proskuryakov, V. V., 1971, Some problems of formation of metamorphic Cu-Ni-Fe-S ores in the Allarechensk region, U.S.S.R.: Geol. Rudn. Mestorezhd., v.13, no.4, p.30-40 [in Russian] .